Heterologous expression of the *Helicoverpa armigera stunt virus* in *Saccharomyces cerevisiae*

Thesis submitted in fulfillment of the requirements for the degree of

Doctor of Philosophy

at

Rhodes University

by

Philip Arno Venter

December 2001

Opgedra aan my ouma,

Aletta Johanna Heyns
18 Okt 1901 – 31 Aug 1999

Abstract

Lepidopteran insects like *Helicoverpa armigera*, more commonly known as the cotton bollworm, are economically important pests of a wide variety of crops throughout the world. The *Helicoverpa armigera stunt virus* (HaSV), a tetravirus with a bipartite single-stranded positive-sense RNA genome, has great potential as a biological pesticide against *H. armigera.* The larger genomic strand of this virus (RNA1) encodes the viral replicase, while the other (RNA2) encodes the 71 kDa capsid protein precursor (p71). 240 copies of p71 assemble into a procapsid with the concomitant encapsidation of the viral RNA. This is followed by a complex maturation event that is characterized by the autoproteolytic cleavage of p71 into the 64 kDa capsid protein (p64) and a 7 kDa peptide (p7). The rearrangements that occur during maturation results in the formation of mature HaSV capsids that can thereupon deliver RNA to other susceptible host cells.

The principal objective of the research described in this study was to demonstrate that this virus could be assembled in *Saccharomyces cerevisiae*.

S. cerevisiae expression vectors were constructed for the production of p71. This protein was detected in cell lysates from two different strains of *S. cerevisiae*, both containing either chromosomal or episomal copies of an expression cassette for *P71*. A number of factors relating to the expression of *P71* (e.g. strains used, expression loci and expression rate) and the preparation of protein extracts from *S. cerevisiae* (e.g. the presence of various protease inhibitors and salt concentrations) were examined to attain optimal levels of soluble p71. A small fraction of the optimized soluble p71 was shown to be in the form of virus-like particles (VLPs), with a yield of $\leq 10^7$ VLPs from a 1.5 *l* culture of $P71^+$ cells. These particles were exclusively in the procapsid form, had a similar buoyant density to that of wild-type HaSV and could undergo maturation when the pH was reduced to 5.

S. cerevisiae vectors were constructed for the episomal expression of the HaSV genomic RNAs. These vectors directed the transcription of RNA1 and RNA2 transcripts, which had similar sizes to those of the HaSV genomic RNAs.

Mature HaSV particles were purified from cells, transgenic for *P71*, *RNA1* and *RNA2*, by way of two different virus purification protocols that were developed during this study. RT-PCR analyses on RNA-extracts from these particles demonstrated that RNA transcripts, which were produced in *trans* with p71, could be encapsidated by HaSV capsids in *S. cerevisiae*. A

droplet-feed bioassay on *H. armigera* larvae demonstrated that the *S. cerevisiae*-derived HaSV particles caused impaired larval development. This response was correlated with the detection of HaSV RNA2 in RNA extractions from larvae that were used in this bioassay.

The results that were generated through the course of this study, provided proof for the concept of the non-host production of infectious HaSV particles from *S. cerevisiae*. This work could serve as a foundation for future research on the development of an expression system for the large-scale production of this virus as a biopesticide.

Table of Contents

List of Figures

List of Tables

List of Abbreviations

Viruses:

BBV	*Black beetle virus*
BMV	*Brome mosaic virus*
BmNPV	*Bombyx mori nuclear polyhedrosis virus*
CaMV	*Cauliflower mosaic virus*
CCMV	*Cowpea chlorotic mottle virus*
DtV	*Darna trima virus*
FHV	*Flock House virus*
HaSV	*Helicoverpa armigera virus*
NβV	*Nudaurelia capensis β virus*
NOV	*Nodamura virus*
NωV	*Nudaurelia capensis ω virus*
TaV	*Thosea asigna virus*
ToRSV	*Tobacco ringspot virus*

General:

A_{280nm}	absorbance at 280nm
AEBSF	4-(2-aminoethyl)-benzenesulfonyl fluoride
ARS	autonomous replication sequences
bp	base pair
BSA	bovine serum albumin
B.t. toxin	*Bacillus thuringiensis* toxin
CEN	yeast centromeric sequences
cryoEM	cryoelectron microscopy
ddH_2O	double-distilled water
DEPC	diethyl pyrocarbonate
DNA	deoxyribonucleic acid
DNase	deoxyribonuclease
ds	double stranded
dsDNA	double stranded DNA
DTT	dithiothreitol
EDTA	ethylenediaminetetraacetate
GC	gas chromatography
HC ribozyme	hairpin cassette ribozyme
HDV ribozyme	hepatitis deltavirus ribozyme
hpi	hours post induction
HPLC	high-performance liquid chromatography
IgG	immunoglobulin G
Ig-like	immunoglobulin-like

M_R	relative molecular mass
mRNA	messenger RNA
NaAc	sodium acetate
nt	nucleotide
OD_{600nm}	optical density at 600nm
ORF	open reading-frame
P_{35S}	*Cauliflower mosaic virus* 35S promoter
P_{ADH2}	*Saccharomyces cerevisiae ADH2* promoter
PCR	polymerase chain reaction
PEG	polyethylene glycol
P_{GAL1}	*Saccharomyces cerevisiae GAL1* promoter
PMSF	phenylmethyl-sulfonyl fluoride
PNK	polynucleotide kinase
RNA	ribonucleic acid
RNase	ribonuclease
ROS	reactive oxygen species
RT	reverse transcribing
RT-PCR	reverse transcription polymerase chain reaction
SAP	shrimp alkaline phosphatase
SDS	sodium dodecyl sulphate
SDS-PAGE	sodium dodecyl sulphate polyacrylamide gel electrophoresis
SMM	synthetic minimal medium
ss +RNA	single stranded, positive sense RNA
ss	single stranded
TCA	trichloroacetic acid
T_{CYC1}	*Saccharomyces cerevisiae CYC1* terminator
TEM	transmission electron microscopy
Tris	tris(hydroxymethyl)aminomethane
tRNA	transfer RNA
VLPs	virus-like particles
vps	virus particles
YIp	yeast chromosomal integration plasmid

Acknowledgements

My sincere thanks to the following people:

- My supervisor, Dr. Rosemary Dorrington, whose enthusiasm about, and interest in, science in general and this project in particular was a major source of inspiration. Without her guidance and assistance this project would not have been possible.
- My co-supervisor, Prof. Don Hendry, for always being willing to lend a helping hand and offering valuable advice throughout the course of this project.
- My parents, for their constant love and support. Especially to my father, whose passion for all things scientific inspired me in this direction.
- My girlfriend, Abi, for loving and supporting me no matter what the situation.
- My friends and fellow postgraduate students in Lab 417, both past and present, for creating a stimulating and pleasant work environment.

I would like to express my gratitude to the following people for their critical reading of this thesis, which led to valuable advice and criticisms:

- Dr. Rosemary Dorrington, Prof. Don Hendry, Dr. Carol Hartley, Fritha Hennessy and Abi Murton.

My sincere thanks for technical and intellectual support from the following people:

- At Rhodes, Val Hodgson and Meesbah Jiwaji, who helped with plasmid constructs and *P71* expression optimization in *Saccharomyces cerevisiae* cells.
- At the CSIRO Division of Entomology, Terry Hanzlik and Karl Gordon, who supplied me with the initial HaSV constructs and offered stimulating discussions on the data; Peter Christian, who guided and helped with the bioassays and Michelle Williams and Amir Masoumi for their technical support.
- At Syngenta (formerly ZENECA), Rachel Blaine, for her many plasmid constructs; Andrew Dinsmore, who generated the antibodies used in this study and John Windass for support and encouragement.

This research was funded by grants and scholarships from the National Research Foundation, Syngenta (1997 – 1998) and Shimoda Biotech. (Pty.) Ltd. (2000 – 2001).

1 Literature review

1 Literature review

In 1993 Terry N. Hanzlik and his co-workers at the CSIRO Division of Entomology in Canberra (Australia) reported on the isolation of a small RNA virus, the *Helicoverpa armigera stunt virus* (HaSV), from diseased insects in their laboratory colony of *Helicoverpa armigera*. Lepidopteran insects like *H. armigera* (more commonly referred to as the cotton bollworm) are economically important pests of a wide variety of crops throughout the world. The discovery of HaSV, which belongs to the virus family *Tetraviridae* (Figure 1.1), raised the possibility that this virus could be used as a biological pesticide against these insects. One of the major hurdles for such an application for HaSV was the lack of a system for the large-scale production of this virus. This led to the work described in this thesis, which had the ultimate goal of developing a non-host production system for this virus in Brewer's yeast (*Saccharomyces cerevisiae*).

A brief discussion on the potential of HaSV as a biological pesticide against *H. armigera* is presented in the following section. This is followed by a description of tetraviruses with particular reference to the principles relating capsid structure to biological function. The chapter is concluded by a discussion on the suitability of *S. cerevisiae* for the expression of viruses and virus-like particles (VLPs).

1.1 Biotechnological application

It was estimated in 1997 that, on a global scale, $4 billion (US) was spent per year to control lepidopteran insect pests with chemical pesticides (Hanzlik and Gordon, 1997). Biological control efforts against these insects have been dominated by the application of an entomopathogen from the bacterium *Bacillus thuringiensis*, called *B.t.* toxin, and by certain members of the virus family *Baculoviridae* (Christian *et al.*, 1993) (Figure 1.1). The application of HaSV as a biological pesticide would hold many advantages over existing means of control for this insect pest.

First, unlike chemical pesticides, viral insecticides are not harmful to the environment. The application of HaSV would result in the specific eradication of the pests, because this virus displays a narrow host range that is limited to a range of species within the lepidopteran family *Noctuidae* (Christian, P., Dorrian, S.D., Gordon, K.H.J., Hanzlik, T.N., unpublished results). Second, HaSV would be more effective, i.e. have a more rapid rate of kill, than baculoviruses (Christian *et al.*, 1993). Third, the replication of HaSV in its host results in its ability to mutate in order to overcome host resistance to an extent (Christian *et al.*, 1993). A

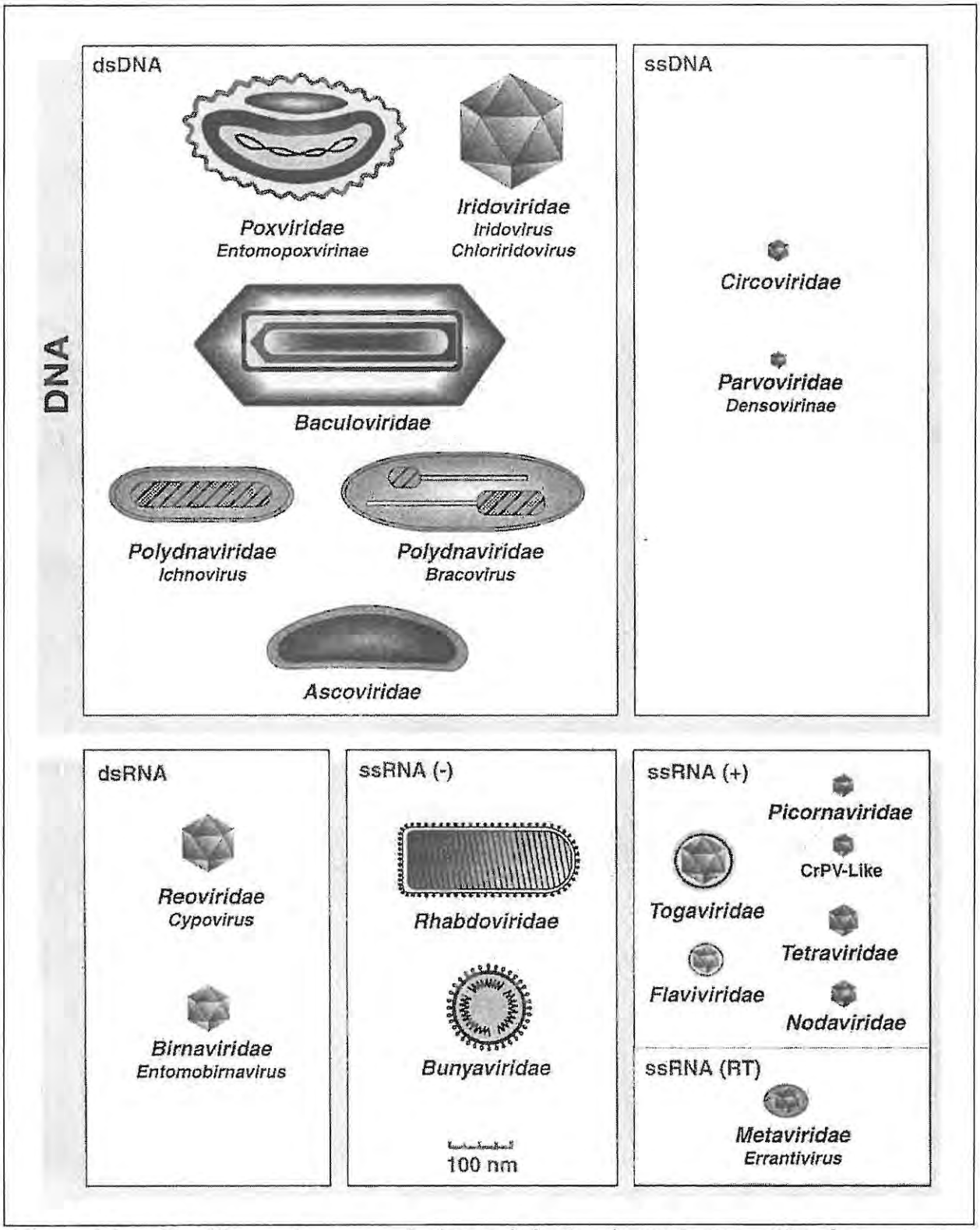

Figure 1.1 Families and genera of viruses infecting invertebrates. The frames separate viruses containing double stranded (ds) and single stranded (ss) genomes, while the horizontal gray boxes separate taxa of viruses having DNA or RNA genomes. Taxa containing reverse transcribing (RT) viruses and the negative (-) and positive (+) ssRNA genomes are also indicated (van Regenmortel *et al.*, 2000).

constant feature of chemical control efforts is the target pests' acquisition of resistance to a particular chemical pesticide that necessitates its replacement by a different one. Selection for resistance against *B.t.* toxin upon its indiscriminate usage is also a common occurrence (Christian *et al.*, 1993). For instance, several thousand acres of *Bt* cotton crops (transgenic cotton plants that were engineered to express *B.t.* toxin) were infested by cotton bollworms when these crops were planted for the first time in Georgia and Texas in the USA (Macilwain, 1996). Another property of HaSV that makes it very suitable as a biological pesticide against *H. armigera* is that it is highly pathogenic to these insects (Christian, P., Dorrian, S.D., Gordon, K.H.J., Hanzlik, T.N., unpublished results). Ingestion of as little as 1000 – 5000 virus particles by neonate larvae is sufficient to cause severe stunting and death.

The major drawback to the application of single stranded positive sense (ss +RNA) viruses, like HaSV, as insecticides is the lack of a large-scale production system for these viruses. This is why there are only a few documented instances where ss +RNA viruses have been successfully used as insect control agents. An example comes from the efficient control of *Setothosea asigna* and *Darna trima* (two oil palm pests) in Malaysia (Tiong and Munroe, 1977). 86 – 99% mortality was achieved in areas that were sprayed with aqueous extracts of insect cadavers infected with *Darna trima virus* (DtV, a tetravirus) and a possible insect picornavirus. This result led to the application of similar extracts for the protection of oil palm and coconut plantations in West Africa and South America (Philippe *et al.*, 1997).

At present, the only reliable means of producing HaSV requires its preparation from HaSV-infected *H. armigera* larvae within laboratory colonies. Bawden *et al.* (1999) screened thirteen insect cell lines using both infection with HaSV and transfection with HaSV RNA. Not one of these cell lines allowed for the propagation of this virus, indicating the lack of certain intracellular factors required for replication within these strains. The simplicity of the HaSV genome, which consists of two RNAs of 5.3kb and 2.5kb each, presented an intriguing prospect for the mass production of HaSV in transgenic organisms. This led to a research project, headed by Karl Gordon and Terry Hanzlik (both from the CSIRO Division of Entomology in Canberra, Australia), with the objective of producing transgenic HaSV-plants that would be resilient to *H. armigera*. Results from this project showed that infectious HaSV particles were assembled in tobacco (*Nicotiana plumbaginifolia)* protoplasts, as judged by the stunting of *H. armigera* larvae that were fed on a diet containing these protoplasts (Gordon *et al.*, 2001). The presence of non-host produced HaSV was confirmed by detection of HaSV genomic RNA in RNA extracts from stunted insects. However, the engineering of transgenic HaSV-tobacco plants proved to be far more problematic. Preliminary tests showed that a number of these plants were able to induce

stunting in *H. armigera* (Service, 1996). Despite this initial success, failure to repeat these experiments and the lack of detectable HaSV RNAs in plant tissues in subsequent analyses led to the suggestion that the expression of the HaSV components in plants was hindered by gene silencing (Gordon, K.H.J., personal communication).

The development of transgenic HaSV-plants is still an exciting possibility for the biological control of *H. armigera*. However, currently and in the foreseeable future, the negative public perception regarding genetically modified crops would hamper their release into the environment. Of major concern is an increased incidence of recombination events between insect and plant viral gene pools (Aaziz and Tepfer, 1999). This could result in the rapid evolution of viruses with altered properties that could bring about alarming consequences, including switching of host species and altered pathogenicity. A second problem associated with HaSV-plants is that their distribution throughout less developed countries would not be economically viable. This is especially important when one considers the enormous variety of crop cultivars that are cultivated by less sophisticated farmers. It would therefore be ideal to provide farmers with an inexpensive source of HaSV for application to their crops.

1.2 Tetraviridae

Viruses that infect invertebrates are currently divided into nineteen families (Figure 1.1) and four of these families exclusively infect arthropods (van Regenmortel *et al.*, 2000). These include three families with double stranded DNA (dsDNA) genomes (baculo-, asco- and polydnaviruses) and one family with an ss +RNA genome (tetraviruses).

Baculovirus virions aggregate into protein bodies, called occlusion bodies, within infected cells. The visualization of these occlusion bodies by a light microscope in diseased silkworms (*Bombyx mori*), led to the first scientific reports on an insect virus in 1856 (Smith, 1973). This virus, the *Bombyx mori nuclear polyhedrosis virus* (BmNPV), was later classified as a member of the nucleopolyhedrovirus genus of the baculovirus family. The baculovirus family, which includes the nucleopolyhedrovirus and granulovirus genera, has since then become one of the best-studied insect virus families. This is partly due to the fact that these viruses can be propagated in cell culture and the relative ease with which their large dsDNA genomes can be manipulated.

The situation is, however, different for asco-, polydna- and tetraviruses. The lack of cell culture systems for virus propagation has complicated studies on various properties of these virus families (Hanzlik and Gordon, 1997; Miller, 1998; Webb, 1998). Polydnaviruses, which are

non-infectious and have been shown to have a symbiotic relationship with their wasp host, cannot replicate outside the wasp cells, probably because genes that are essential for virus replication are expressed from the wasp genome (Webb, 1998). The development of a wasp cell line, which could sustain the replication of polydnaviruses, would therefore be useful for studies on these viruses. Cell culture lines for the propagation of ascoviruses would be useful for the molecular analysis of viruses of this newly recognized virus family, which also appear to have symbiotic relationships with their lepidopteran hosts (Miller, 1998). The advent of molecular biological studies on tetraviruses has also been hampered by the lack of cell culture systems for the production of these viruses (Bawden *et al.*, 1999). A considerable amount of molecular information has, however, been derived from tetraviruses isolated from their insect hosts (Hanzlik and Gordon, 1997).

1.2.1 History and Taxonomy

Viruses belonging to the *Tetraviridae* family are exclusively pathogenic to insects and have icosahedral capsids with $T = 4$ symmetry that encapsidate a ss +RNA genome (Hendry and Agrawal, 1994). The *Tetraviridae* form one of four families of ss +RNA viruses with nonenveloped capsids that infect invertebrates (Figure 1.1). The first tetravirus was isolated from diseased larvae of the pine tree emperor moth (*Nudaurelia cytherea capensis)* in South Africa (Struthers and Hendry, 1974). These larvae were found to be infected by at least five structurally distinct viruses, designated γ, δ, α, ε and β (Juckes, 1970). Of these, the *Nudaurelia β virus* (NβV) was characterized biophysically as the type-member of a new virus group known as *Nudaurelia* β-like viruses (Juckes, 1979; Mathews, 1982). This virus group was renamed *Tetraviridae* in the fifth report of the International Committee on Taxonomy of Viruses (ICTV) (Francki *et al.*, 1991) due to the $T = 4$ quasi-symmetry of its members' shell.

In 1985 Hendry *et al.* reported on the identification of another virus from *Nudaurelia* larvae, designated NωV. This virus was shown to be serologically distinct from NβV and contained a bipartite genome, as opposed to the monopartite genomes of all the previous members of this family. Based on this, NωV became the type-member of a second genus (ω-like tetraviruses) within the tetravirus family with β-like tetraviruses being the other genus (Murphy *et al.*, 1995). In the latest ICTV report (van Regenmortel *et al.*, 2000) these two genera have been renamed *Betatetravirus* and *Omegatetravirus* containing eight and two species, respectively. The *Helicoverpa armigera stunt virus* (HaSV) is the second species within the *Omegatetravirus* genus (Table 1.1).

Table 1.1 Species in the *Betatetravirus* and *Omegatetravirus* genera (Adapted from van Regenmortel *et al.* (2000)

Virus name	Abbreviation	Host family	Genome sequence accession number
Genus: *Betatetravirus*			
Nudaurelia capensis β virus	NβV	*Saturniidae*	AF102884
Antheraea eucalypti virus	AeV	*Saturniidae*	
Darna trima virus	DtV	*Limacodidae*	
Dasychira pudibunda virus (*Calliteara pudibunda virus*)*	DpV/CpV	*Lymantriidae*	
Philosamia cythia x virus	PxV	*Saturniidae*	
Pseudoplusia includens virus	PiV	*Noctuidae*	
Thosea asigna virus (*Setothosea asigna virus*)*	TaV/SaV	*Limacodidae*	AF062037**
Trichoplusia ni virus	TnV	*Noctuidae*	
Genus: *Omegatetravirus*			
Nudaurelia capensis ω virus	NωV	*Saturniidae*	RNA2, S43937
Helicoverpa armigera stunt virus	HaSV	*Noctuidae*	RNA1, U18246 RNA2, L37299

* Alternative names are placed between brackets
** Sequence information for a 2484 base region that includes the capsid gene

1.2.2 Host-pathogen interactions

Tetraviruses can be transmitted horizontally, by means of oral ingestion, and vertically, from parent to progeny (Hanzlik and Gordon, 1997). The host range of tetraviruses is limited to lepidopteran insects and their midgut cells are the primary sites of infection (Figure 1.2). There are four main types of cells in the midgut regions of these insects, differentiated columnar and goblet cells, and the basally situated undifferentiated regenerative cells and endocrine cells (Davies, 1988). Turnover of cells within the midgut occurs by the sloughing (detachment from basal membrane) of differentiated cells and subsequent replacement by regenerative cells. Brooks *et al.* (1998) demonstrated that an increase in the rate of sloughing occurs in the midguts of HaSV-infected larvae, resulting in the depletion of cells. This increased rate of rejection is possibly a defense response that has the purpose of clearing the midgut of infected cells. Cross-sections of the midgut regions of these larvae, which were stained by an immunogold labeling technique, revealed that the columnar, goblet and regenerative cells contained large quantities of HaSV (Figure 1.2). The degeneration of an infected insect's midgut is therefore enhanced by a

decreased ability to replace the sloughed differentiated cells by regenerative cells (Hanzlik and Gordon, 1997).

Figure 1.2 Cross-sections of the midgut regions of *H. armigera* larvae, which were stained by an immunogold labeling technique. HaSV (visible as black aggregations) was only detected in the columnar and goblet cells exposed to the lumen (below) (Hanzlik and Gordon, 1997).

Recent studies on HaSV demonstrated that it is highly pathogenic, which makes it favorable as a control agent against its heliothine hosts (Christian, P., Dorrian, S.D., Gordon, K.H.J., Hanzlik, T.N., unpublished results). Ingestion of as little as 1000 – 5000 virus particles by neonate (first instar) larvae is sufficient to cause a rapid cessation of feeding and development, severe stunting and ultimately death. Conversely, infection of older larvae (fourth and fifth instar) failed to elicit any response to high doses of HaSV. This could reflect a superior ability of the older larvae to rid their midguts of infected cells by sloughing (Brooks, E.M., Gordon, K.H.J., Dorrian, S.J., Hines, E. and Hanzlik, T.N., unpublished results).

1.2.3 Tetraviral genomes

i Genome organization

The genome organization of NβV, based on the complete sequence of its genome, was recently described by Gordon *et al.* (1999). The 6.6 kb genomic RNA was shown to contain a 5'proximal ORF that encodes the viral replicase (215 kDa) and a 3' proximal ORF that encodes the capsid protein precursor (70 kDa). The latter protein is expressed by means of a 2.6 kb subgenomic RNA that is encapsidated, along with the genomic RNA, by NβV capsids (Hanzlik and Gordon,

1997). The capsid protein precursor is cleaved between Asn-536 and Gly-537 to produce 62 kDa and 8 kDa proteins that make up the capsid shell. The sequence of the capsid protein gene of the *Thosea asigna virus* (TaV) indicated that this protein is cleaved at two positions, as compared to one for NβV (Pringle *et al.*, 1999). Two of these proteins are the TaV capsid proteins (58.3 kDa and 6.8 kDa), but the third N-terminal protein (17 kDa) could not be detected in virions.

For omegatetraviruses, nucleotide sequences are available for the larger genomic strand (RNA 1) of HaSV (Gordon *et al.*, 1995) and for the smaller genomic strands (RNA2) of HaSV (Hanzlik *et al.*, 1995) and NωV (Agrawal and Johnson, 1992) (Appendix 1, Figures A1.1 and A1.2). HaSV RNA1 (5312 nt) carries a large ORF that encodes the 187 kDa viral replicase, and three smaller ORFs at its 3'end (Figure 1.3). It is uncertain if these three ORFs are expressed in HaSV-infected cells, and if so, what the functions of the resultant proteins would be. According to Hanzlik and Gordon (1997), a subgenomic RNA template would be required for translation from these ORFs. HaSV RNA2 (2478nt) has two overlapping ORFs, the first encoding a protein (p17) of unknown function, while the second encodes the capsid protein precursor (p71) (Figure 1.3). Two possible functions have been ascribed to p17. The formation of hexagonal tube-like structures upon its expression in *Escherichia coli* has led to the proposal that it could function as a movement protein that allows the virus to migrate to adjoining cells (Hanzlik *et al.*, 1995). Hanzlik and Gordon (1997) also proposed that, since expression of p71 appears to favor replication of RNA2 compared to RNA1, it could play a role in the regulation of replication. p71 is cleaved between Asn-575 and Phe-576 into the 64 kDa and 7 kDa coat proteins designated p64 and p7, respectively (Hanzlik *et al.*, 1995).

There is a high level of sequence identity (67%) and an even higher level of sequence similarity (76%) between the coat protein sequences of HaSV and NωV (Agrawal and Johnson, 1992, Hanzlik *et al.*, 1995) (Figure 1.4). Two domains of high similarity and three smaller domains of lower similarity have been identified by sequence alignments. The latter domains are located at the N-terminal (40% identity) and C-terminal (53% identity) regions, and in the center of each protein (37% identity). The NβV and NωV capsid precursor proteins are, however, less similar. The sequence identity between specific domains of these two proteins varies from 21 to 29% (Gordon and Hanzlik, 1998) (Figure 1.4). A similar Asn/Phe cleavage site on the NωV α-protein (70 kDa) yields 62 kDa and 8 kDa proteins designated β and γ, respectively. The NωV sequence published by Agrawal and Johnson (1995) did not show the presence of an overlapping ORF comparable to p17. However, according to Hanzlik and Gordon (1997), *in vitro* translation studies on NωV RNA2 resulted in the expression of a protein with similar properties to that of p17.

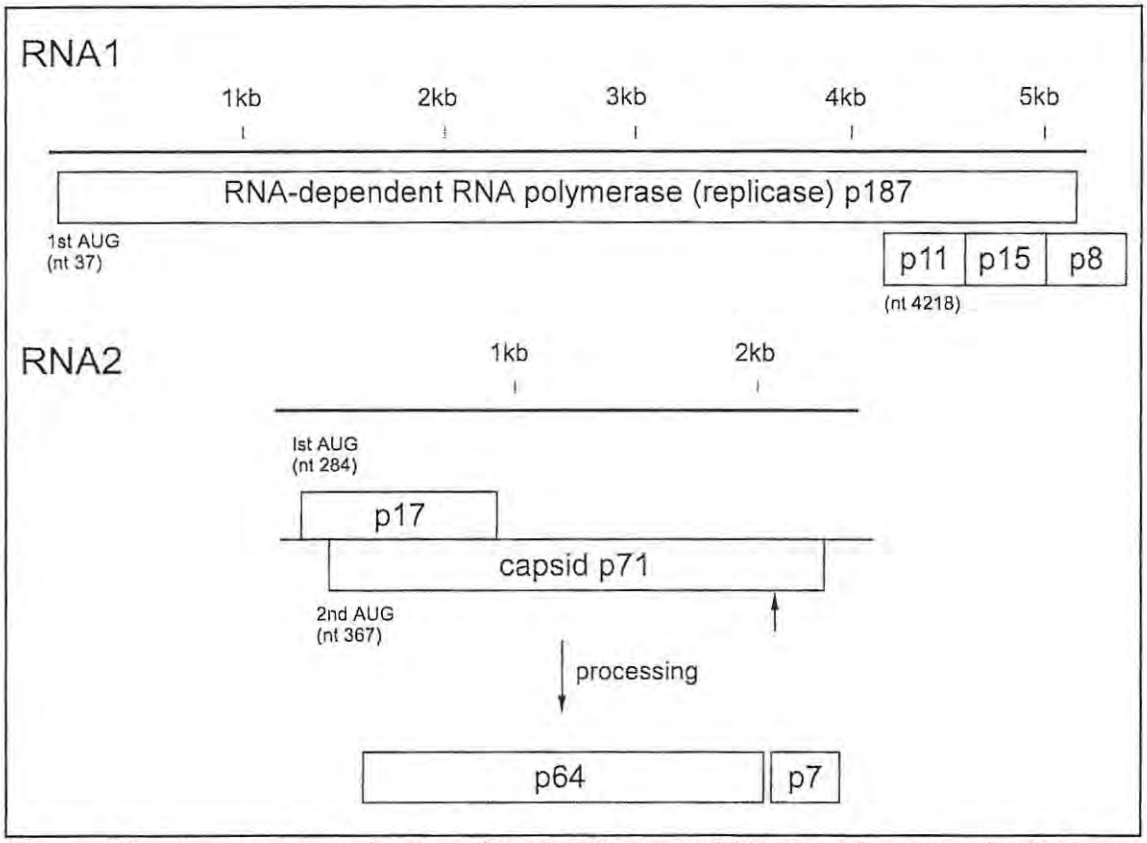

Figure 1.3 Genome organization of HaSV RNA1 and RNA2. The genomic RNAs are represented to the same scale, with their ORFs indicated. Adapted from Hanzlik and Gordon (1997).

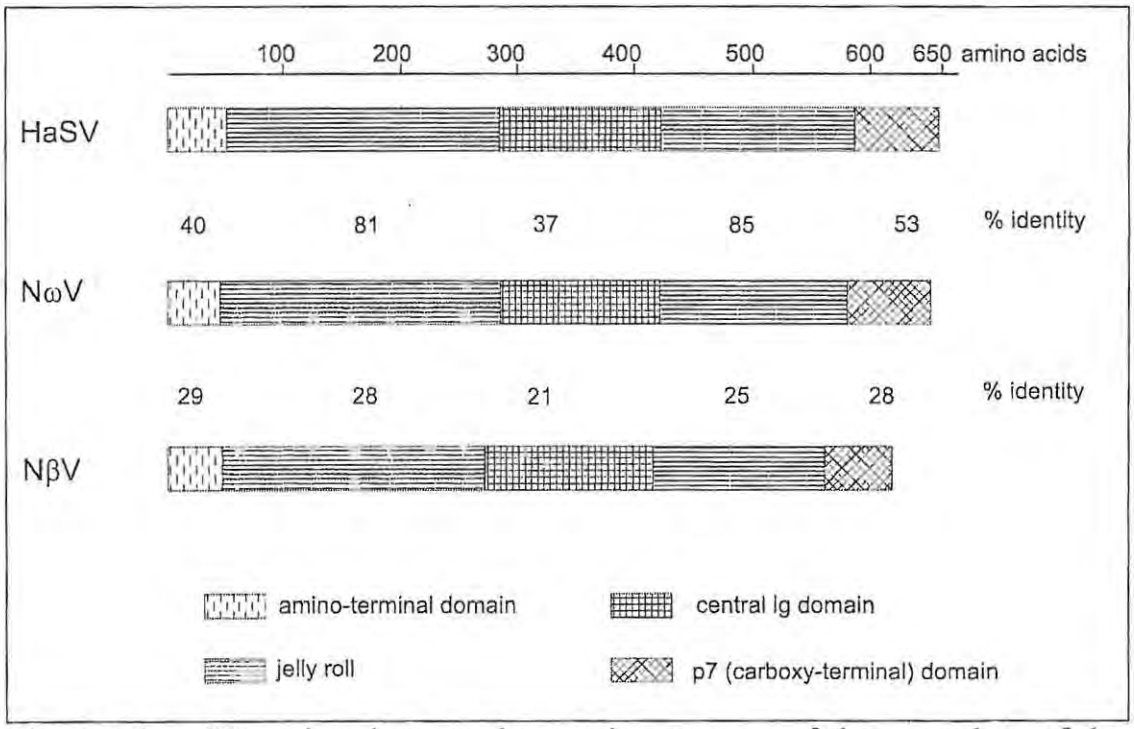

Figure 1.4 Comparison between the protein sequences of three members of the *Tetraviridae* family. The percentage sequence identity in four different domains determined for pair-wise sequence comparisons (NωV – HaSV and NωV – NβV) is provided (Gordon and Hanzlik, 1998).

ii RNA secondary structure

HaSV, NβV and NωV have tRNA-like structures at the 3' ends of the viral RNAs (Gordon *et al.*, 1995; Gordon *et al.*, 1999; Hanzlik *et al.*, 1995) (Figure 1.5). With the exception of these viruses, these structures are solely associated with RNA from plant viruses. There are two possible functions for these structures (Hanzlik and Gordon, 1997). They could protect the viral RNA from exonucleolytic degradation or play a role in viral replication, or both. The first suggestion is based on the absence of poly-A tails at the 3' ends of tetraviral RNAs, which protect cellular mRNAs from degradation (Hanzlik *et al.*, 1993; Hendry and Agrawal, 1994). The second suggestion is derived from roles in the replication of RNA for similar structures in plant virus RNAs (Gordon *et al.*, 1999).

In addition to the 3'terminal tRNA-like structures, the HaSV genomic RNAs have another secondary structure in common. Both RNAs form hairpin structures downstream of the cap site and contain the hexamer sequence GGUAAA (corresponding to nucleotides 19 – 24 and 24 – 29 for RNA1 and RNA2, respectively) in the loop (Gordon *et al.*, 1995; Hanzlik *et al.*, 1995) (Figures A1.1 and A1.2, Appendix 1). Roles in RNA replication have been suggested for these stem-loop structures (Gordon and Hanzlik, 1998).

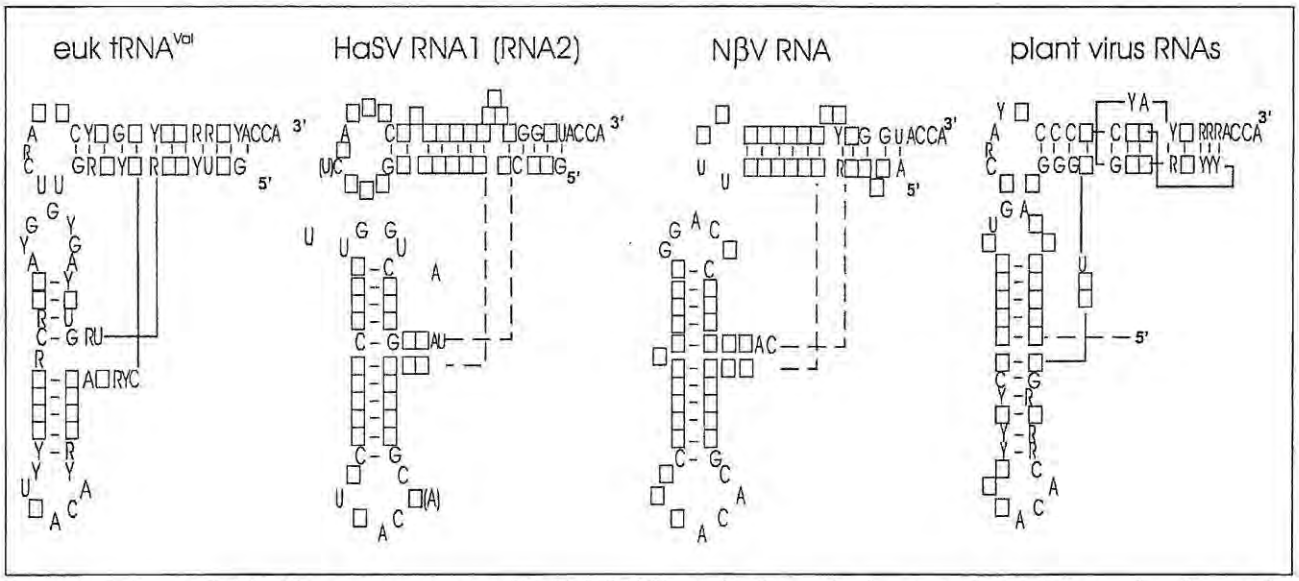

Figure 1.5 tRNA-like structures on HaSV, NβV and plant viral genomic RNA, and eukaryotic $tRNA^{Val}$. Only conserved residues are specified for $tRNA^{Val}$, while residues corresponding to the conserved ones in tRNA are specified. HaSV residues shown in parentheses refer to RNA2 (Gordon and Hanzlik, 1998).

1.2.4 Structure of the tetravirus capsid and procapsid

Viruses belonging to the *Tetraviridae* and *Nodaviridae* families (Figure 1.1) are the only ss +RNA viruses with quasi-equivalent protein shells. Because of the many structural

similarities between these two families (Munshi *et al.*, 1996), comparisons will be made between the two throughout this section where relevant.

i Virus structure – the theory of quasi-equivalence

The arrangement of subunits within spherical viruses is explained by the quasi-equivalence theory of Caspar and Klug (1962), which refers to the axes that relate different subunits within the quasi-equivalent shells. This theory will be explained in the following section, with special reference to the structures of tetra- and nodaviruses.

The constraint of T = 1 symmetry

The simplest virus particles have 60 identical subunits that are arranged in the symmetry of an icosahedron (Johnson, 1996) (Figure 1.6 panel A). In such a particle each one of the subunits is in an identical environment. These subunits are related by fivefold (vertices), threefold (faces) and twofold (edges) symmetry (named 532-symmetry). This form of symmetry represents the largest possible shell in which all the subunits lie in identical environments. The subunits of simple viruses generally are composed of 200-400 amino acids, but the internal cavity created by a shell formed by 60 subunits of this size would be too small to package the viral genome. The principles by which icosahedral virus particles are constructed with more than 60 subunits are explained by the quasi-equivalence theory. This theory states that the number of identical subunits organized in an icosahedral lattice is limited to $60T$, and that T is equal to 1, 3, 4, 7, etc. For T values > 1 the subunits are chemically identical, but are structurally quasi-equivalent due to T different environments (Caspar and Klug, 1962).

T = 3 particles

Nodavirus particles, like most RNA spherical viruses with nonenveloped capsids, have 180 subunits and are therefore arranged with $T = 3$ lattice symmetry (Figure 1.6, panel B). The trapezoids A, B and C correspond to the same gene product located in three slightly different environments within one icosahedral asymmetric unit (the central triangle). The rhombic triacontahedron geometry of these $T = 3$ particles relate A-subunits by true fivefold symmetry at the icosahedral fivefold axis (solid pentagon), and B- and C-subunits by quasi-sixfold symmetry at the icosahedral threefold axis (solid triangle). A trimer of BC dimers is related by true threefold symmetry around the latter axis (Johnson, 1996).

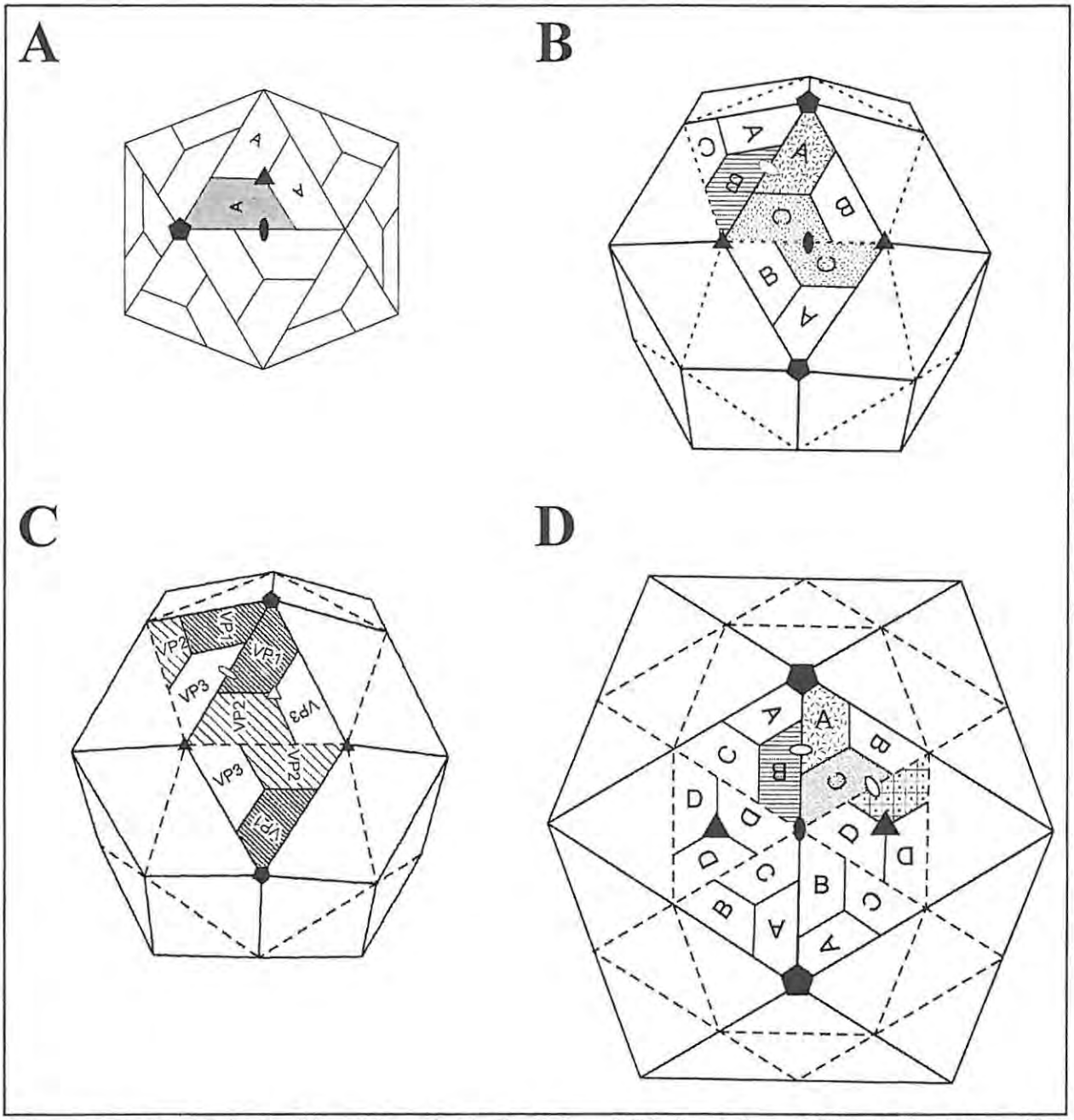

Figure 1.6 Comparison of $T = 1$ (panel **A**), $T = 3$ (panel **B**), $P = 3$ (panel **C**) and $T = 4$ (panel **D**) capsid shells. Solid eclipses, triangles and pentagons, indicate icosahedral twofold, threefold and fivefold symmetrical axes, respectively; while empty eclipses and triangles indicate quasi-twofold and quasi-threefold axes, respectively. The trapezoids labeled A, B, C and D in panels **B** and **D** correspond to the same gene product located in different environments within the respective icosahedral asymmetric units. The $T = 1$ capsid in panel **A** is also made up of identical gene products, but they are all located in the same environments within the shell. Conversely, the icosahedral asymmetric units of a picornavirus $P = 3$ shell (panel **C**) is made up of three different gene products (VP1, VP2 and VP3) which are located in different environments. The schematic in panel **A** was adapted from Johnson (1996), and those in panels **B**, **C** and **D** were adapted from Johnson and Reddy (1998).

The geometry of the $T = 3$ structure is the result of a difference between the icosahedral twofold axis (solid eclipse), which relates two C-subunits, and a quasi-twofold axis (open eclipse), which relates A- and B- subunits (Johnson, 1996). The C-subunits lie in the same plane, but the A- and B-subunits are in planes with an angle of 144°. These flat or bent contacts are formed by a process called molecular switching, which is required for the generation of quasiequivalent shells from identical subunits (Cheng *et al.*, 1994). So-called molecular switches are present at the C – C contacts, but absent at the A – B contacts, resulting in the different dihedral angles of the particle. The icosahedral asymmetric units of picornaviruses consist of three different gene products (VP1, VP2 and VP3) in a pseudo $T = 3$ ($P = 3$) lattice (Figure 1.6, panel C). The VP2 - VP2 interface and VP1 – VP3 interface have different protein surfaces that are placed side by side and there is thus no need for a molecular switch (Schneemann *et al.*, 1998).

T = 4 particles

Capsids with $T = 4$ structure have the geometry of a standard icosahedron. The name of this geometrical shape is derived from the Greek words "*eikosi*" (twenty) and "*hedra*" (seat or base) (Hanzlik and Gordon, 1997). The quasi-equivalent surface lattice of a $T = 4$ icosahedral structure therefore consists of twenty triangular faces, each of which are made up of four smaller trimers (Figure 1.6, panel D). The icosahedral asymmetric units of this structure consists of four identical gene products (designated A, B, C and D), three located in an outer trimer (A, B and C) and one in a central trimer (D) (Olson *et al.*, 1990).

Similar to the $T = 3$ structure, the A-subunits are related by true fivefold symmetry at the icosahedral fivefold axis (solid pentagon). The D-subunits show true threefold symmetry around the icosahedral threefold axis (solid triangle). Unlike the $T = 3$ structure, the $T = 4$ structure contains one type of icosahedral twofold axis (solid eclipse) and two types of quasi-twofold axes (open eclipses). B-, C- and D-subunits are related by quasi-sixfold symmetry and BCD dimers are related by true twofold symmetry at the icosahedral twofold axis. The one quasi-twofold axis relates subunits C and D in the same plane, while the other relates subunits A and B5 in different planes with a dihedral angle of 138°. This indicates that a molecular switch, similar to the one at the C – C contact in the $T = 3$ structure (Figure 1.6, panel B), is present at the C - D contact (Johnson and Reddy, 1998).

ii Tetravirus capsid structure

Tetraviruses are the only nonenveloped, icosahedral viruses discovered to date that have capsids organized in a $T = 4$ lattice symmetry. The only other known virus family with $T = 4$ symmetry is the *Togaviridae* (Figure 1.1). Viruses in this family, e.g. *Sinbis virus* and *Semliki Forest virus*, have nucleocapsids with $T = 4$ symmetry that are surrounded by a lipid envelope containing

heterodimeric glycoprotein spikes (Fuller, 1987). These spikes are organized in a $T = 4$ lattice for members of the *Alphavirus* genus of the *Togaviridae* family (van Regenmortel, 2000).

The first step towards the elucidation of this characteristic structure was made by Polson *et al.*, (1970) who estimated a value of approximately 16.3×10^6 for the molecular weight of NβV. Using this data, and the approximate molecular weights of each capsid protein (61 000) and the genomic RNA (1.8×10^6), Struthers and Hendry (1974) calculated that the capsid consisted of 240 subunits, which suggested a $T = 4$ arrangement according to the theory of quasi-equivalence. This was confirmed by three dimensional image reconstructions from electron micrographs of negatively stained NβV (Finch *et al.*, 1974). These reconstructions, and others from frozen-hydrated NβV (Figure 1.7, panel A), showed that each of the twenty triangular faces of the icosahedral shell was composed of twelve protein subunits clustered into four Y-shaped trimeric aggregates (Olson *et al.*, 1990). The arrangement of these subunits into icosahedral asymmetric units according to the quasi-equivalence theory is illustrated in Figure 1.7 (panel B) (Olson *et al.*, 1990).

Each one of the triangular faces of NβV was shown to be nearly planar and was separated from neighboring faces by deep grooves (Olson *et al.*, 1990). Apart from their planar appearance, a characteristic feature of the icosahedral faces of NβV was the presence of three prominent pits between the trimers of each face (Olson *et al.*, 1990). Image reconstructions of frozen-hydrated NωV (Figure 1.8, right hand side of panel A) revealed that the triangular faces of this virus were less planar than those of NβV and did not contain the pits (Hendry and Agrawal, 1994).

At present, the majority of structural information for tetraviruses is derived from the NωV X-ray structure at 2.8Å resolution (Munshi *et al.*, 1996). It is possible that other tetraviruses have similar structural features to that of NωV because: a) their protomers undergo similar autocatalytic cleavage events, b) their capsids are arranged with $T = 4$ symmetry, c) electron micrographs and cryoEM reconstructions of tetraviruses have revealed structural relatedness (Hendry and Agrawal, 1994), d) NβV and NωV have similar solution X-ray scattering patterns (Johnson *et al.*, 1994) and e) phylogenetic analysis of available tetraviral capsid protein sequences indicated that omegatetraviruses and betatetraviruses are closely related (Hanzlik and Gordon, 1997). This presumption is especially valid for HaSV due to the high amino acid sequence similarity between NωV and HaSV (Figure 1.4).

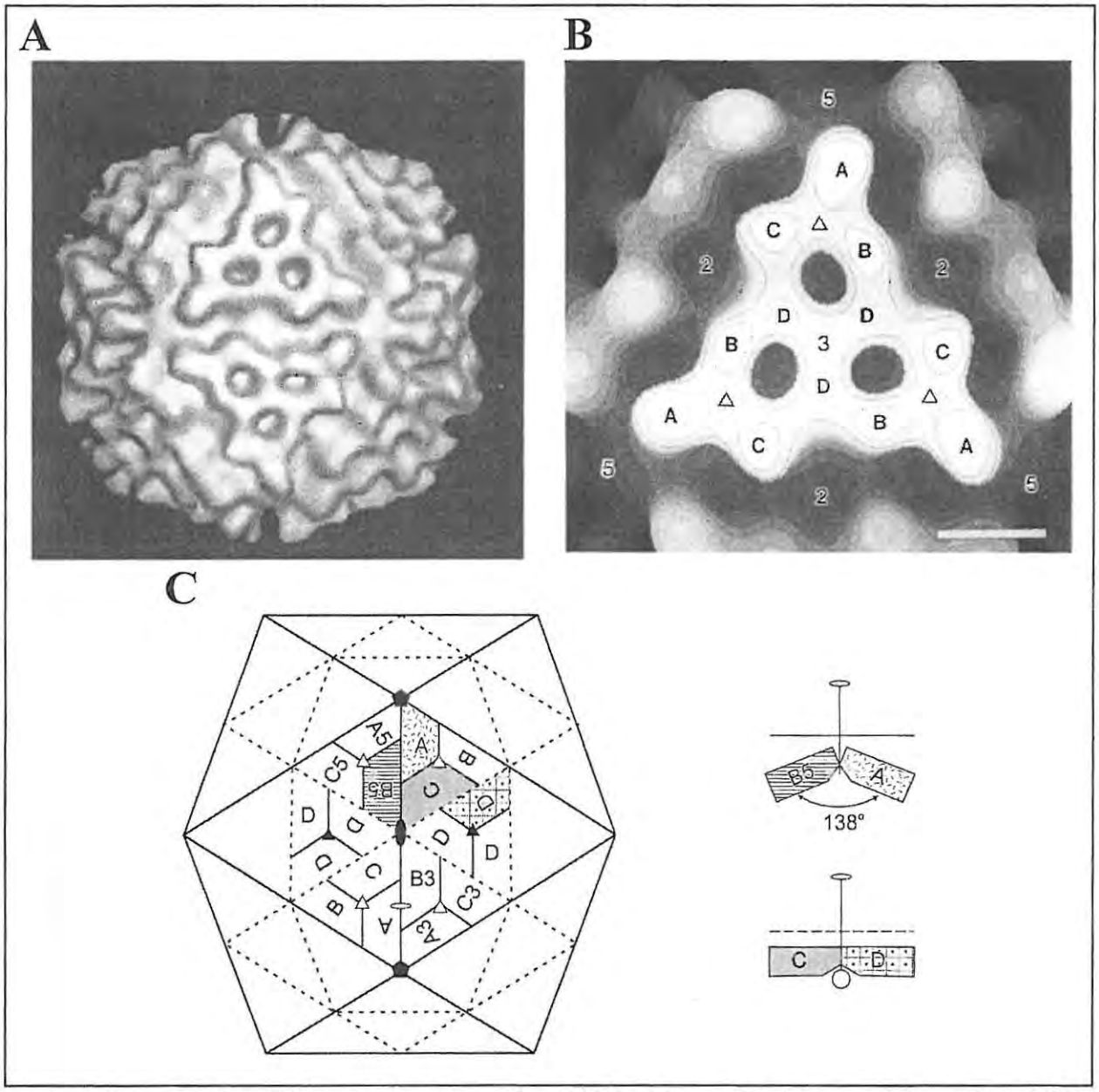

Figure 1.7 (**A**) CryoEM reconstruction of an NβV virion. (**B**) Close-up view of an NβV icosahedral face showing the twofold (**2**), threefold (**3**) and fivefold (**5**) symmetrical axes. The letters A, B, C and D denote the quasi-equivalent subunits that make up each of the three asymmetric units in an icosahedral face. The empty triangles denote the quasi-threefold axes, and the bar represents 5nm. (**C**) Diagrammatic representation of quasi-equivalent surface lattice for $T = 4$ tetraviruses. Solid eclipses, triangles and pentagons, indicate the icosahedral twofold, threefold and fivefold symmetrical axes, respectively; while empty eclipses and triangles indicate quasi-twofold and quasi-threefold axes, respectively. $T = 4$ shells have two types of quasi-twofold axes. At one type of quasi-twofold axis, an extended chain and a helix form a wedge that forces a flat contact along the line with B- and C-subunits on one side and two D-subunits on the other (bottom right of panel **C**). At the other type of quasi-twofold axis, these protein segments are disordered, resulting in a bent contact (138°) along the line with A and C on one side and A5 and B5 on the other (top right of panel **B**). The images in panels **A** and **B** were taken from Olson *et al.* (1990). The schematic representation (**C**) was taken from Johnson and Reddy (1998).

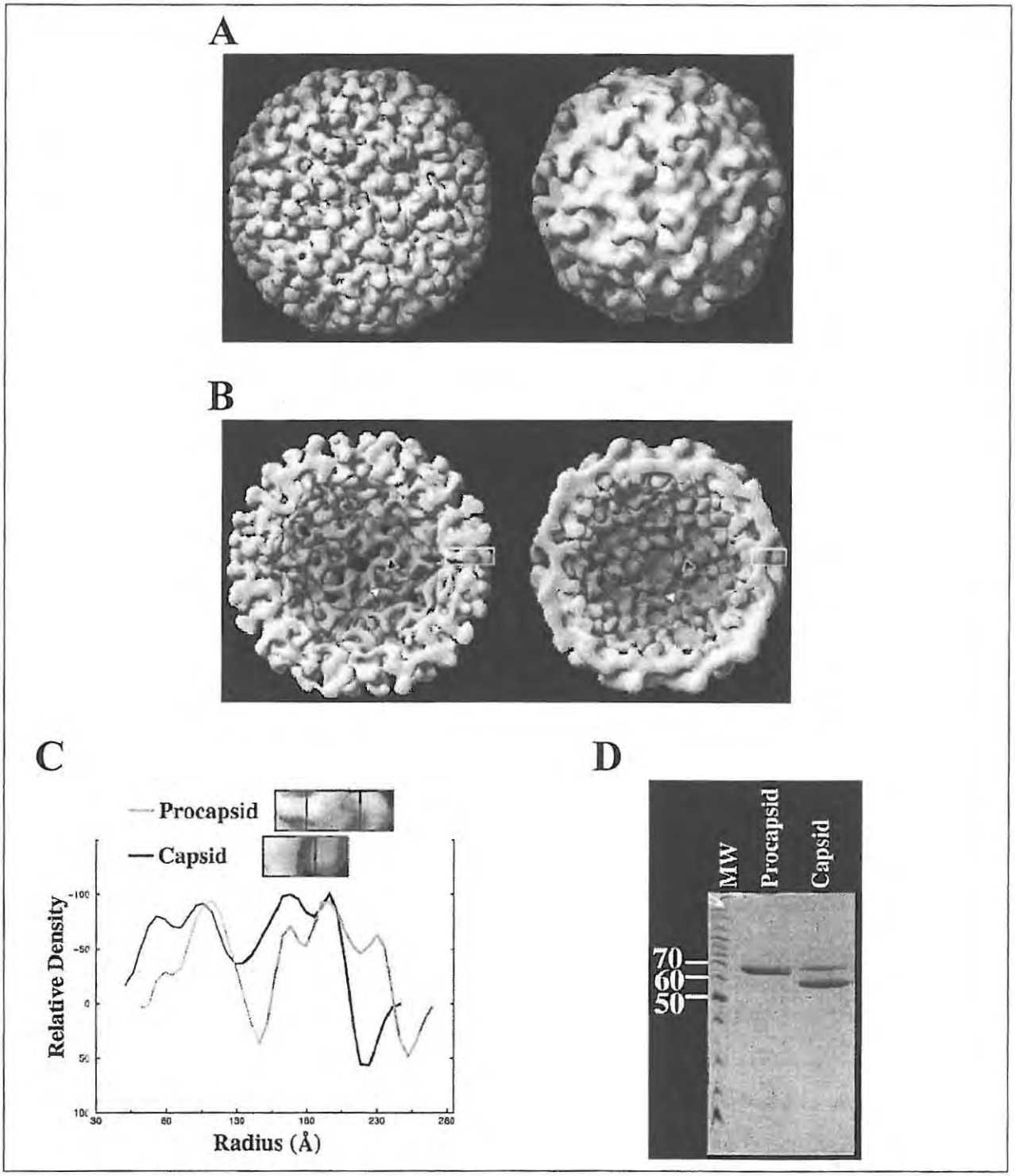

Figure 1.8 (**A**) Three-dimensional, surface shaded NωV procapsid (left) and mature capsid (right). (**B**) Sectioned views of NωV procapsid (left) and capsid (right). The threefold and quasi-threefold axes are indicated by black and white triangles, respectively. A triskelion-shaped internal domain is visualized at each of these icosahedral axes. (**C**) Radial density plots for the procapsid and capsid shells in panel **B**. These plots revealed that the capsid shell spanned 62 Å with two domains, while the procapsid shell spanned 83 Å with three domains. (**D**) An SDS-PAGE gel demonstrating that the 70 kDa α-protein (in lane labeled "procapsid") is cleaved into the β- and γ-proteins (in lane labeled "Capsid") upon a drop in the pH to 5. The latter two proteins have molecular weights of 62kDa and 8kDa, respectively. All these images were taken from Canady *et al.* (2000).

Subunit tertiary structure

The NωV protomer undergoes an autocatalytic cleavage event at an Asn – Phe peptide bond in NωV and HaSV, and an Asn - Gly peptide bond in NβV (Gordon and Hanzlik, 1998). Cleavage of the 70kDa capsid protein precursor (α) of NωV at Asn-570 – Phe-571 yields 62kDa and 8kDa proteins, designated β and γ, respectively (Agrawal and Johnson, 1992). The NωV α-, β- and γ-proteins are analogous to HaSV capsid proteins p71 (71kDa), p64 (64kDa) and p7 (7kDa), respectively.

The stereoribbon diagram of an NωV C-subunit in Figure 1.9 (panel A) illustrates that three domains are distinguishable for this protein: an internal helical domain, a central β-sandwich domain and an external immunoglobulin-like domain. Residues sequentially preceding (helix I and II) and following the β-sandwich (helix V, VI and VII) form the internal helical domain. This domain is therefore composed of the N- and C-terminal ends of the formerly uncleaved α-protein. Residues 1 – 43 and 591 - 607 do not adhere to icosahedral symmetry and are consequently not shown in this presentation. In addition, residues 608 - 644 are only ordered, and thus visible, in the C- and D-subunits. Helices VI (residues 571 – 590) and VII (residues 627 – 640) are located on the γ-peptide and will henceforth be referred to as γ_1- and γ_2-helices, respectively (Figure 1.9, panel B) (Munshi *et al.*, 1996).

Evidence for the interaction of the internal helical domain with genomic RNA comes from its abundance in positively charged residues (Agrawal and Johnson, 1995). The tetraviral γ-peptide has a net charge of +8 over the last twenty residues. These positively charged residues at the C-terminal end, and the net +11 charge of the first 40 residues at the N-terminal end, contribute to the positively charged character of the internal helical domain. These positively charged residues are sufficient to neutralize phosphate groups on over 50% of the genome (Agrawal and Johnson, 1995). Further evidence for interactions between the internal helical domain and the encapsidated RNA is based on a comparison between the amino acid sequences of the NωV and HaSV capsid precursor proteins, which reveals the presence of two low sequence homology domains at N- and C-termini of these proteins (Gordon and Hanzlik, 1998) (Figure 1.4). Therefore, the low homology between these domains probably reflects the prerequisite for different interactions with the genomes of these two viruses.

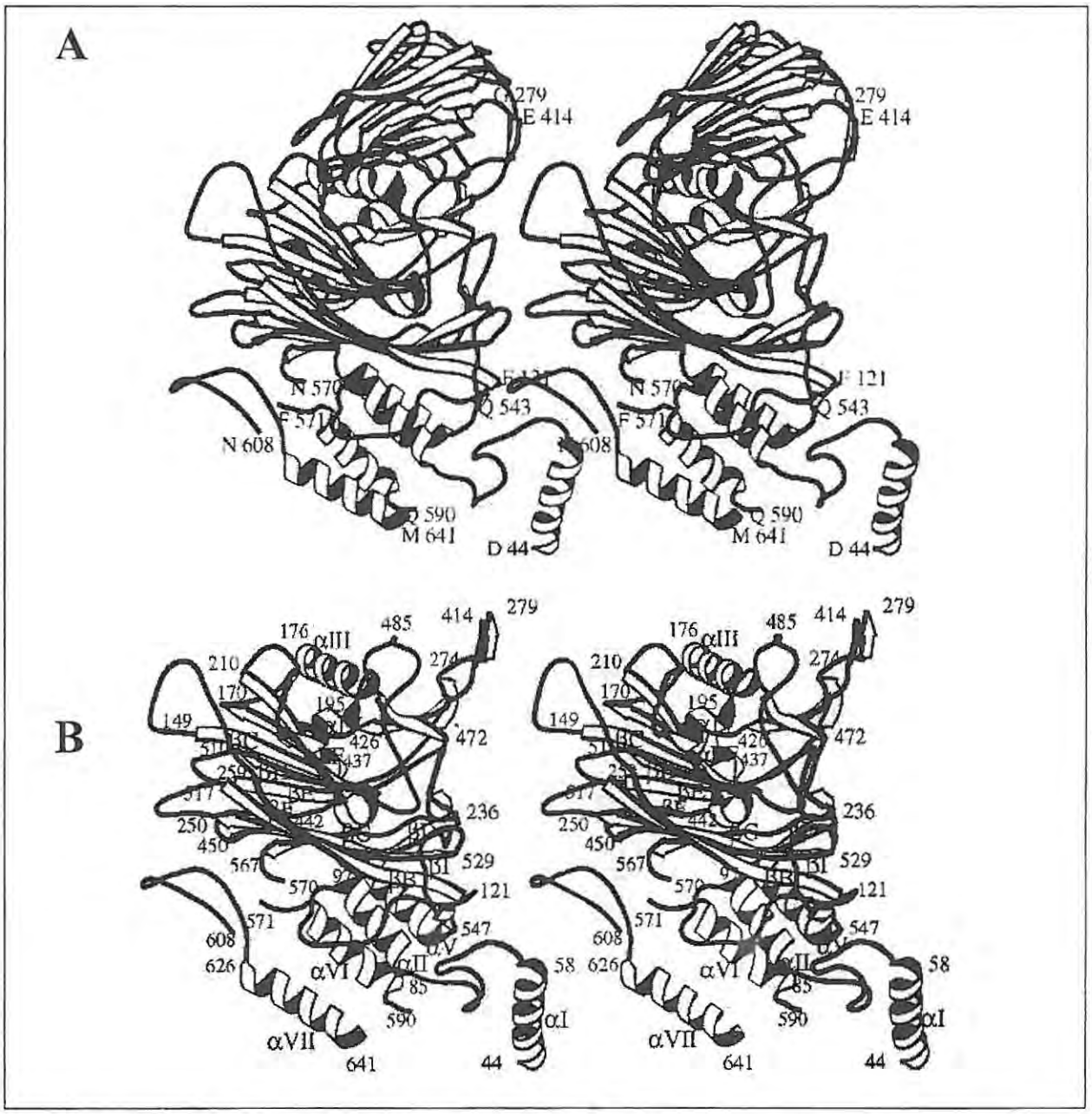

Figure 1.9 Stereo views of a single NωV protomer positioned in the C location in the diagram in Figure 1.7 (panel C). (**A**) Stereo view of NωV protomer in which labeled residues point to the approximated boundaries of the three domains (internal helical, β-sandwich and Ig-like) of this protein. Asp-44, Phe-121 and Gln-543 facilitate the demarcation of the internal helical domain, which consists of residues preceding (residues 44 - 120) and following (residues 544 –641) the β-sandwich (residues 121 – 543); and Gly-279 and Glu-414 point to the boundaries of the Ig-like domain (residues 280 – 413). The cleaved-off γ-peptide consists of residues 571 to 641. (**B**) Stereo view of only the internal helical and β-sandwich domains in which secondary structural elements and selected residues are labeled. βB, βC, βI, ... denote the various β strands, and αI, αII, αIII, ... denote the various α-helices. αVI and αVII are found on the cleaved-off γ-peptide and are referred to in the text as γ_1- and γ_2-helices, respectively. Both diagrams taken from Munshi *et al.* (1996).

The shell-forming β-sandwich, which is responsible for the two stretches of high amino acid sequence identity (81% and 85%) between NωV and HaSV (Figure 1.4), is composed of eight antiparallel strands (labeled βB, βC, ...βI) and two α-helices (labeled αIII and αIV). It contains β-sheets composed of strands B, I, D and G on one side and C, H, E and F on the other (Figure 1.9) (Munshi *et al.*, 1996).

The outermost protrusion of NωV, which forms the external domain of NωV, occurs as an insertion between the βE and βF strands. This protrusion is composed of 133 amino acids with an immunoglobulin-like (Ig-like) fold (Munshi *et al.*, 1996). The stretch of sequence corresponding to the external domain coincides with the domain of low sequence identity (37%) in the center of the capsid protein precursor sequences for NωV and HaSV (Figure 1.4) (Gordon and Hanzlik, 1998). The low sequence similarity of these domains is at least partly responsible for the specific binding of these two viruses to their respective host cells (Munshi *et al.*, 1996).

Quaternary structure

Quasi-twofold axes: Amino acid residues 608 – 644 in the NωV capsid, which are disordered for A- and B-subunits, form an extended chain (residues 608 – 626) and a helix (γ_2-helix) for C- and D-subunits (Figure 1.9, panel A). These residues function as a wedge that forces a flat contact along the line with B- and C-subunits on one side and two D-subunits on the other (Munshi *et al.*, 1996) (Figure 1.7, panel C). As a result of this, each of the triangular faces of the particle is planar. The disorder of these residues for A- and B-subunits results in a bent contact (138°) along the line with A and C on one side and A5 and B5 on the other (Munshi *et al.*, 1996). The molecular switch in NωV therefore consists only of protein as opposed to that of nodaviruses, which contains a polypeptide arm and duplex RNA (Fisher and Johnson, 1993). This exchange of roles between nucleic acid and protein is due to the NωV γ_2-helix fulfilling the same task as that of the nodaviral duplex RNA. Another significant difference between the nodavirus and NωV molecular switches is that the protein component of the nodavirus molecular switch is close to the N-terminus, while an equivalent polypeptide (residues 608 – 626) for NωV lies close to the C-terminus (Munshi *et al.*, 1996).

Threefold and quasi-threefold axes: The external domains of threefold- and quasi-threefold-related subunits interact with each other to give NωV its characteristic appearance in electron micrographs (Figure 1.8, right hand side of panel A). A surface representation of an NβV icosahedral face (Figure 1.7, panel B) demonstrates that the outside trimers have skew orientations about the quasi-threefold axes (empty triangles), as opposed to the inside trimer, which lies on equatorial lines between adjacent threefold and twofold axes (Olson *et al.*, 1990).

Twofold (quasi-sixfold) and fivefold axes: A-subunit γ_1-helices form pentameric helical bundles around the fivefold axes, which are similar to those described for nodaviruses (Cheng *et al.*, 1994) (Figure 1.10). γ_2-Helices, which are absent at the fivefold axes, completely change the interactions among B-, C-, and D-subunit γ_1-helices around the twofold axes. As a result, ten helices are grouped around these axes: six contributed by B-, C- and D-subunit γ_1-helices and four contributed by C- and D-subunit γ_2-helices (Munshi *et al.*, 1996) (Figure 1.11).

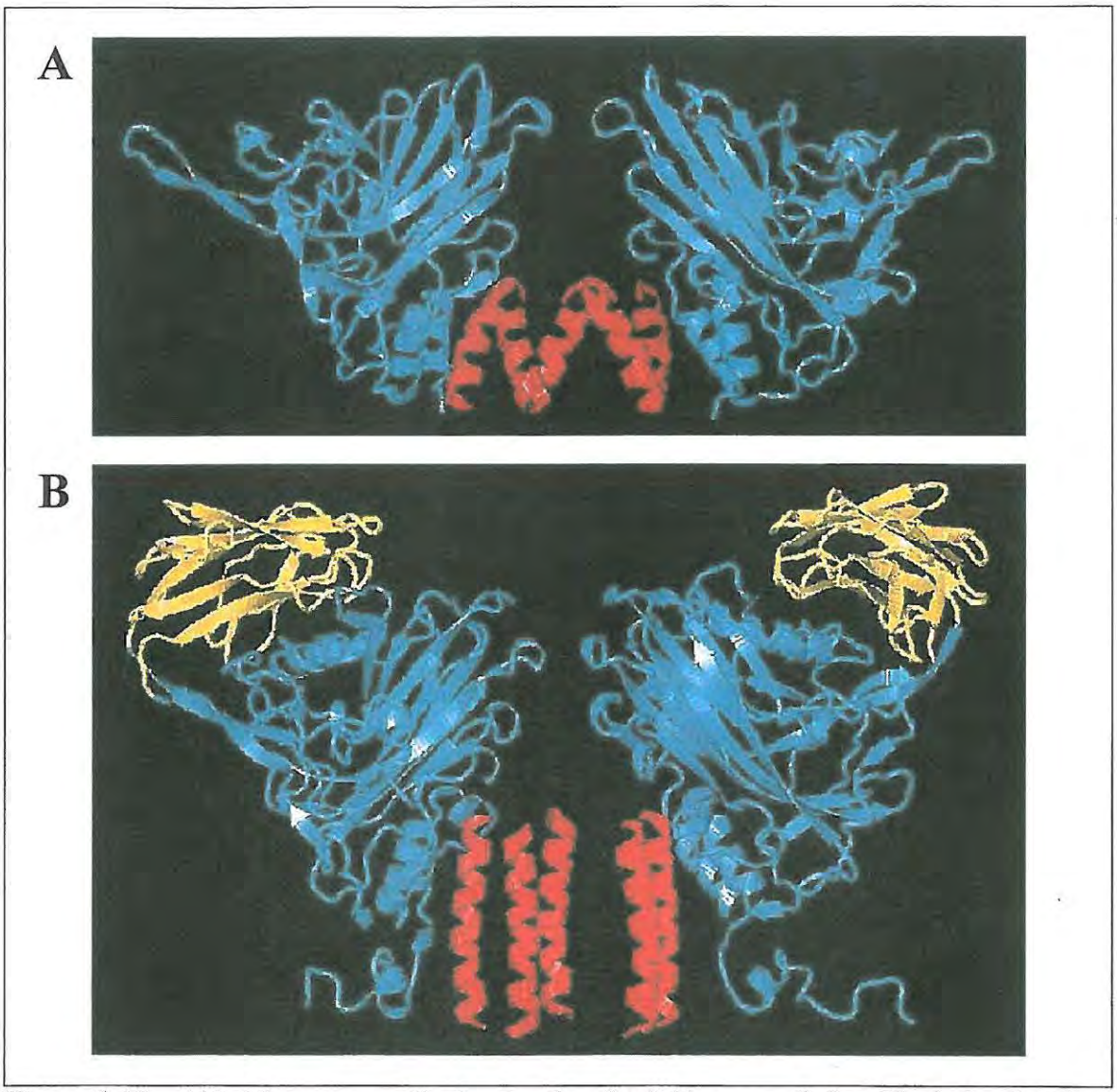

Figure 1.10 (**A**) View perpendicular to the fivefold axes of the *Black beetle virus* (BBV), a nodavirus. The residues in blue correspond with residues 55 to 363, and the residues in red represent the pentameric helical bundle consisting of fivefold-related γ_A-helices. For clarity, only two of the five A-subunits are represented. (**B**) View comparable to that of BBV (in panel A) for NωV. The portion in blue is nearly superimposable with that of BBV with no sequence similarity. The yellow portion, however, represents the Ig-like domain and is unique to NωV. Fivefold-related γ_1-helices form part of a pentameric helical bundle that is similar to that for BBV in panel A (Munshi *et al.*, 1996).

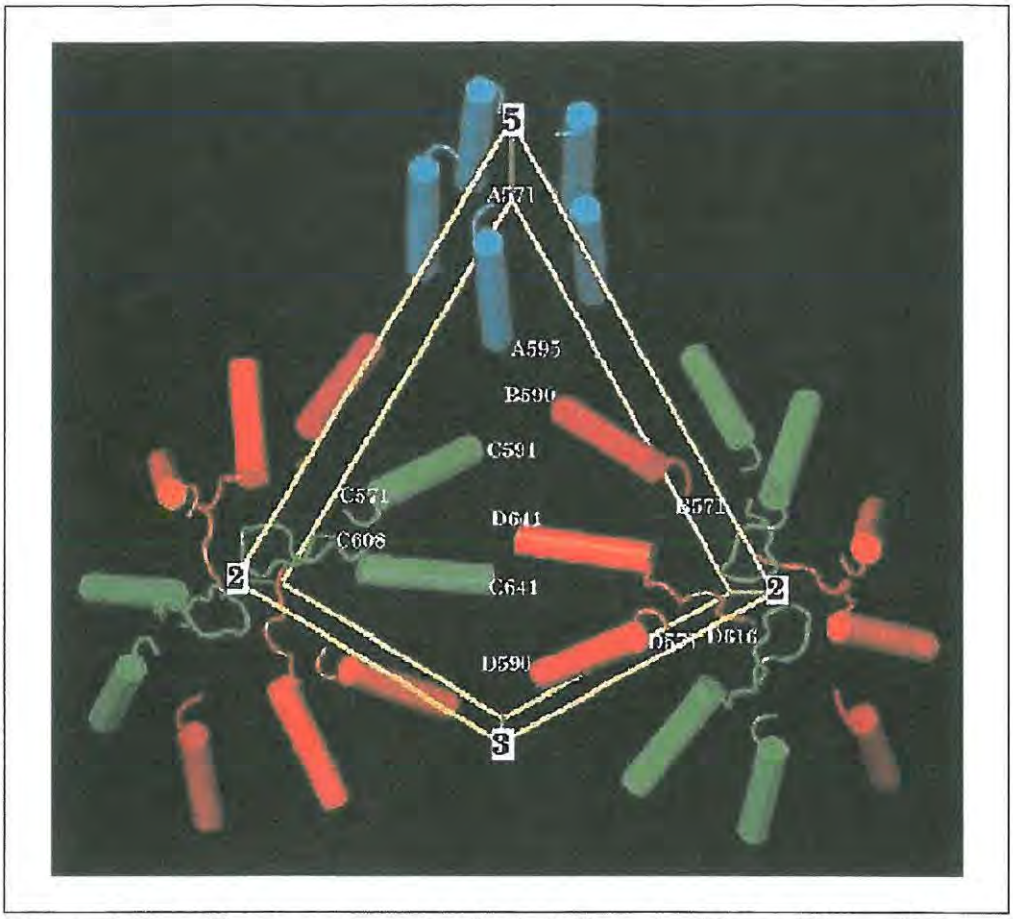

Figure 1.11 The arrangement of γ1 helices (residues 571 – 595) and γ_2-helices (residues 608 – 641) around the icosahedral twofold (**2**) and fivefold (**5**) axes. The positions of A-, B-, C- and D-subunit helices are represented as blue, red, green and orange cylinders, respectively (refer to the arrangement of A-, B-, C- and D-subunits into the quasi-equivalent shell in Figure 1. 7, panel C). At the fivefold axis, A-subunit-associated γ_2-helices are disordered, while γ_1-helices form a pentameric helical bundle. At the twofold axis, two γ_2-helices, which are associated with C and D subunits, are ordered. Ten helices are therefore clustered around the twofold axis: four C- and D-subunit associated γ2 helices, and six B-, C- and D-subunit associated γ_1-helices (two from each of these subunits) (Munshi *et al.*, 1996).

i Tetravirus procapsid structure

A fundamental difference between nodaviruses and tetraviruses is that, unlike nodavirus capsids, the structure of tetravirus capsids is distinct from that of their associated procapsids. This distinction translates into procapsid-associated biological functions that are different from those of nodavirus procapsids. Canady *et al.* (2000) revealed several of the differences between tetraviral procapsids and capsids through cryoEM and three-dimensional reconstructions of NωV procapsids. NωV procapsids were found to have an internal radius of 240 Å, as compared with 220 Å for mature capsids (Figure 1.8, panel A). The procapsids were porous and rounded, while the mature capsids were solid and isometric. Further, the procapsid exterior was made up of

dumbbell-shaped dimers, as opposed to the trimeric associations of protomer external domains described for capsids (Hendry an Agrawal, 1994) (Figure 1.8, panel A).

Sectioned views through the capsid and procapsid protein shells showed that the procapsid shells were thicker than those of capsids (Figure 1.8, panel B). Radial density plots revealed that this increased width of procapsid shells could be attributed to the presence of an additional (third) domain located on the inside of the shell (Figure 1.8, panel C). These domains were defined by the relative density of the capsid shell (Canady *et al.*, 2000) and should not be confused with the three domains of the capsid protomer, which are partitioned according to the nature of their tertiary structure (Munshi *et al.*, 1996).

Canady *et al.* (2000) proposed the pseudo-atomic model to describe the tertiary and quaternary structures of an NωV procapsid. In this model, which is described below, the NωV X-ray coordinates (Munshi *et al.*, 1996) were fitted into the cryoEM map of the procapsid.

Subunit tertiary structure

According to the pseudo-atomic model, conformational changes that occur during the maturation of procapsids into capsids do not result in dramatic changes in the association between the β-sandwich and external Ig-like domains, i.e. these two domains are shifted as a unit without significant hinging between them. The tertiary structures of these two domains are probably relatively similar for procapsid and capsid protomers. This implies that the additional procapsid domain, which is not present in capsids, is responsible for the changes in tertiary and quaternary structure during maturation (Figure 1.8, panel C). This domain corresponds with the internal helical domain of the protomer, which contains the γ_1- and γ_2-helices (Figure 1.9, panel B) (Canady *et al.*, 2000).

Each of these internal domains is associated with another two of its threefold-related and quasi-threefold-related equivalents to form trimers within the procapsid shell (Figure 1.8, left hand side of panel B). These trimers, each of which is in the shape of a triskelion, are found at the threefold (black triangle) and quasi-threefold (white triangle) axes (described further in the next section). The internal helical domains of all the procapsid subunits are most probably equivalent due to the threefold symmetry of each of these trimers and the similarity between threefold and quasi-threefold-related trimers. The combined effect of equivalent internal domains, as well as equivalent β sandwich and Ig-like domains, within the procapsid, suggests that all the procapsid subunits are similar (Canady *et al.*, 2000).

Quaternary structure

Threefold and quasi-threefold axes: The trimeric associations among threefold- and quasi-threefold-related internal helical domains are less obvious at the same axes of the mature capsids (Figure 1.8, panel A). This corresponds with the observation that the additional domains for procapsids were less distinct in cryoEM reconstructions of mature capsids (Figure 1.8, panel C). The arrangement of the internal domains in procapsids and capsids is, however, nearly reversed for their β-sandwich and external Ig-like domains. The Ig-like domains give the exterior of the capsid its trimeric appearance (Figure 1.8, right–hand side of panel A). The β-sandwich and Ig-like domains of procapsids, on the contrary, are arranged into dimers that consist of A and B, and C and D subunits, respectively. The Ig-like domains of these AB and CD dimers are responsible for the dumbbell-shaped protrusions on the exterior of the procapsid (Figure 1.8, left hand side of panel A) (Canady *et al.*, 2000).

Twofold (quasi-sixfold) and fivefold axes: The dimeric arrangement of the procapsid subunits results in the formation of ellipsoidal holes at the quasi-sixfold axes of the procapsid (Figure 1.12, panel A), which contribute to the porous appearance of the procapsid (Figure 1.8, left hand side of panels A and B). Such holes are less pronounced at the icosahedral fivefold axes of the procapsid (Figure 1.12, panel B) (Canady *et al.*, 2000).

Quasi-twofold axes: As described above, the pseudo-atomic model for the NωV procapsid demonstrates that the internal helical domains are found along the threefold and quasi-threefold axes of the procapsid. The positioning of the γ_2-helices and polypeptides (residues 608 – 626) of these domains at threefold and quasi-threefold axes of the procapsid therefore suggests that they cannot fulfil their functions as molecular switches in procapsids. This brings about the hypothesis that the absence of molecular switches at quasi-twofold-related C – D junctions result in the rounded, or so-called "truncated icosahedral", geometry of procapsids (Canady *et al.*, 2000). The γ_2-helices and polypeptides (residues 608 – 626), which are disordered around the bent A – B junctions in capsids (Munshi *et al.*, 1996), are most probably associated with the internal trimeric domains of procapsids in an orderly fashion (Canady *et al.*, 2000).

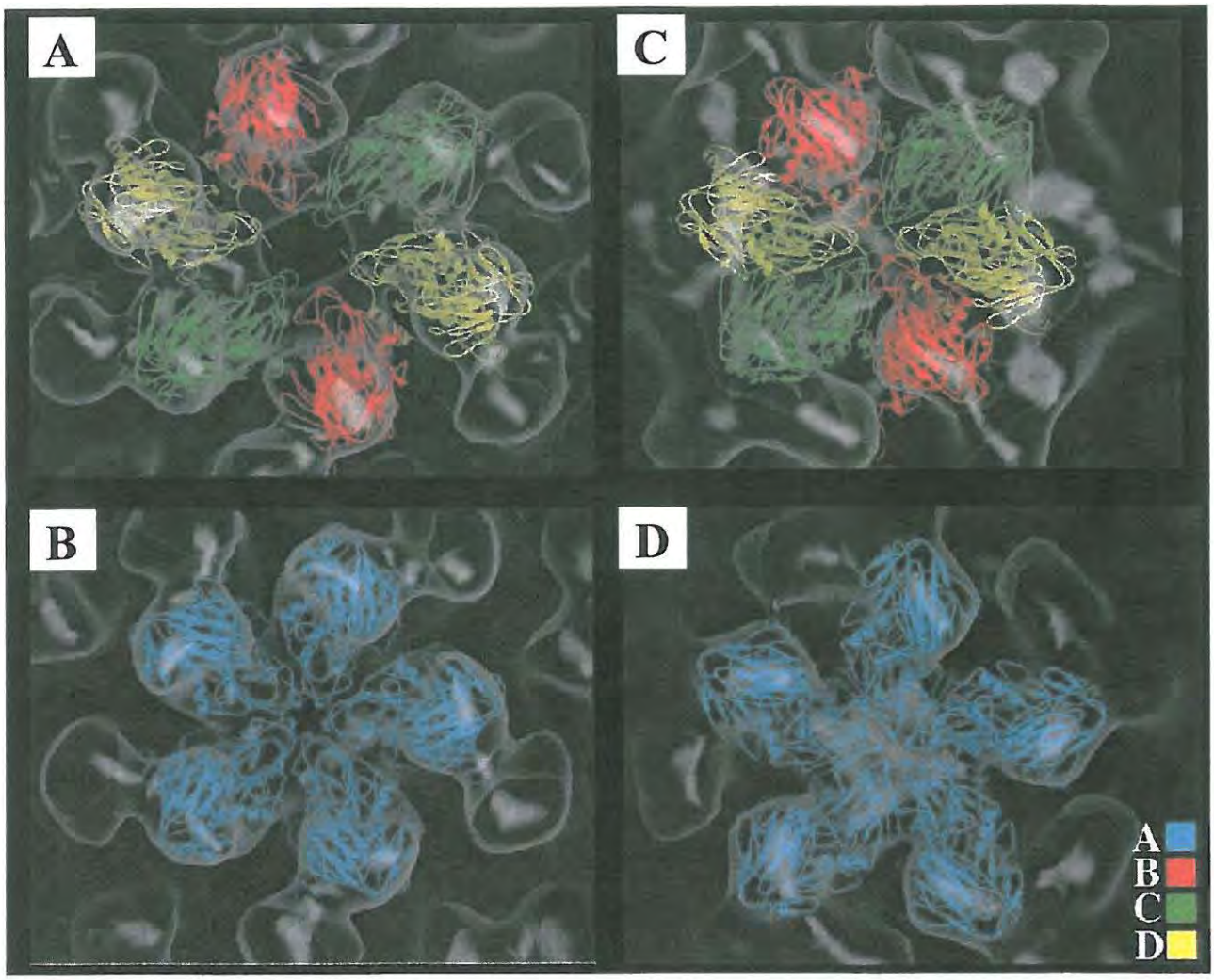

Figure 1.12 The arrangement of quasi-equivalent NωV subunits (key shown on right) around the quasi-sixfold (panels A and C) and fivefold (panels B and D) axes of a procapsid (panels A and B) or a mature capsid (panels C and D). The arrangements for the NωV procapsid were computed using a pseudo-atomic model (as described by Canady *et al.*, 2000), and demonstrated that there were ellipsoidal holes around the quasi-sixfold axes of procapsids (Canady *et al.*, 2000).

1.1.2 Functions of the procapsid and capsid during the tetraviral lifecycle

Compared to nodaviruses, much less work has been done to determine how the structural features of tetravirus capsids translate into their biological functions. However, mechanisms for autoproteolytic cleavage and RNA translocation are proposed to be nearly identical for these two virus families (Munshi *et al.*, 1996).

i Provirion assembly

Role of RNA in assembly:

As in nodaviruses, tetravirus RNA replication most probably occurs exclusively in the early stages in an infected cell, while capsid protein precursor synthesis and particle assembly occurs later (Bawden *et al.* 1999). RNA1 and RNA2 are probably present at high cellular levels, prior

to the synthesis of the capsid protein precursor, to ensure that the optimal amount of virions are assembled. As in nodaviruses, RNA1 is not required for the assembly of omegatetravirus capsids (Agrawal and Johnson, 1995; Schneemann *et al.*, 1993). Complete RNA2 strands are also not required, as judged by the expression of the HaSV and NωV capsid protein precursor genes in baculovirus-infected insect cell lines (Agrawal and Johnson, 1995; Hanzlik and Gordon, 1997). In both instances, the heterologous expression of these genes resulted in the production of VLPs that resembled intact virions. These VLPs furthermore incorporated their own mRNA at a high degree of specificity, indicating that specific encapsidation signal(s) exist within the ORF of the respective capsid protein precursor genes.

Tetraviruses do not contain structured RNA components, similar to those of nodaviruses, within their capsid shells (Munshi *et al.*, 1996). However, this does not imply that these capsids could assemble into normal virus particles in the absence of RNA, because the highly charged inner surface of these particles would almost certainly require some form of polyanion to allow capsid formation (Agrawal and Johnson, 1995).

Dimers are the building blocks of procapsid assembly:

The current model for the assembly of tetravirus procapsids is schematically represented in the top half of Figure 1.13 (Canady *et al.*, 2000). This model relies to a great extent on the evidence for the arrangement of subunits with equivalent structures into AB and CD dimers within the procapsid shell. The tight associations between the AB and CD dimers lead to the assumption that, similar to many plant viruses, the NωV procapsid is assembled from undifferentiated dimers (Canady *et al.*, 2000). In line with this assumption, the formation of a procapsid assembly intermediate for tetraviruses allows these dimers to assemble as nearly equivalent units.

Functions of internal helical domain in procapsid and capsid geometry:

The foundation for the construction of a polyhedral nodavirus capsid is most probably laid during the recognition phase of its assembly process and involves the interaction of two subunits with duplex RNA (Schneemann and Marshall, 1998). This interaction, and similar ones that occur throughout the propagation phase, mediate the generation of flat contacts between twofold-related subunits. As a result of these RNA – protein interactions, a nodaviral procapsid has a rhombic triacontahedral geometry that is similar to that of its capsid (Schneemann *et al.*, 1994).

In tetraviruses, RNA does not seem to play an important role in the assembly of procapsids. Crystallography studies have not revealed interactions, equivalent to those for nodaviruses, which assist in the construction of icosahedral geometry (Munshi *et al.*, 1996), resulting in the rounded shape of the tetraviral procapsid. This rounded, or truncated icosahedral particle is an unstable assembly intermediate that is stabilized by the internal helical domains, which act as

scaffolding proteins that allow AB and CD dimers to be associated as nearly equivalent units in the context of a virus particle. Upon the advent of maturation, which will be described in the next section, these domains migrate from the threefold and quasi-threefold axes and then reside at the quasi-twofold axes. The γ_2-helices and polypeptides (residues 608 – 626) of these domains, which are positioned between quasi-twofold-related C- and D-subunits, act as molecular switches, resulting in flat C – D contacts. On the other hand, these protein segments become disordered around the quasi-twofold-related A- and B-subunits, resulting in bent A – B contacts. Regions of the internal helical domains, which function as protein scaffolds for the rounded geometry of provirions, therefore also function as molecular switches for the icosahedral geometry of mature virions (Canady *et al*, 2000).

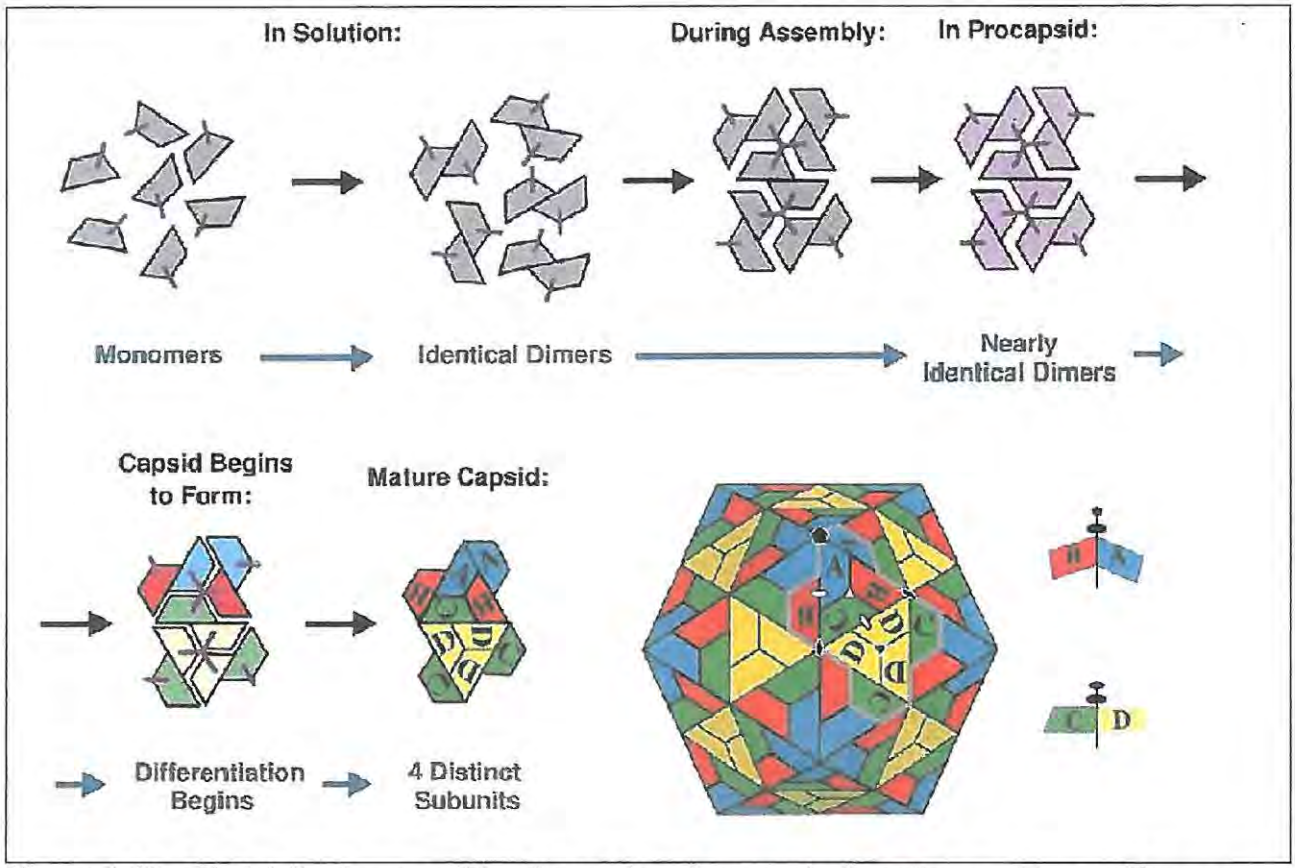

Figure 1.13 Model for the assembly of tetravirus from equivalent dimers. Trapezoids represent individual subunits and purple lines represent the internal helical domains of these subunits. The assembly of these domains to form the triskelion-shaped internal domains within the procapsid is illustrated in the top half of the figure. The colour-change of the trapezoids (from gray to purple) represents slight structural changes upon assembly into procapsids. The subsequent colour-change to blue, red, green and purple, with the concomitant loss of the purple lines represent the differentiation of nearly equivalent dimers (in the procapsid) into the four quasi-equivalent subunits of a $T = 4$ icosahedron. This differentiation is mediated by molecular switches (internal helical domains) that produce bent A – B, and flat C – D contacts (bottom right of the figure) (Canady *et al.*, 2000).

ii Maturation

The two phases of tetraviral maturation:

Quaternary interactions, which function in the stabilization of the NωV provirion, precede autoproteolytic cleavage (Canady *et al.*, 2000). These interactions are more extensive in tetraviruses as compared with nodaviruses (Schneemann *et al.*, 1993) because they mediate a significant transition in the geometry of the particle (Canady *et al.*, 2000). This transition can be instigated for NωV procapsids by the lowering of the pH to 5. It occurs rapidly, as judged by solution X-ray scattering, and is completed within seconds. The associated autocatalytic cleavage, however, is much slower and requires hours for completion. The pH-induced cleavage of NωV procapsids is illustrated in Figure 1.8 (panel D), where only the 70 kDa α-protein was detected for VLPs in a solution with neutral pH, while the 62 kDa β-protein and a low level of α-protein were detected upon lowering the pH to 5 (Canady *et al.*, 2000).

The interactions that bring about transition have not yet been elucidated. However, it is assumed that the residue(s), which become protonated at a pH of 6, are integral to this process. This is because X-ray solution scattering demonstrated that, upon a reduction of pH, the initial structural changes in the NωV procapsid occurred at a pH of ~6. It was proposed that some of the numerous arginine residues, which are found in the internal helical domain, could have abnormally low pK_a values due to their respective chemical environments. They would subsequently become positively charged at pH 6, causing the repulsion that is required for structural rearrangement (Canady *et al.*, 2000).

Unlike nodavirus procapsids, maturation of tetraviral procapsids does not occur automatically after assembly (Agrawal and Johnson, 1995; Gallagher and Rueckert, 1988). A drop in pH acts as an external signal for the structural rearrangement of the tetraviral procapsid, which results in the production of an intermediate with the same icosahedral geometry as that of the mature capsid. Hereafter autocatalytic cleavage, which is dependent on the formation of the icosahedral intermediate, occurs in a time-dependent manner (Canady *et al.*, 2000). The tetraviral maturation process could therefore be subdivided into two phases: (a) a transition phase in which structural rearrangements alter the geometry of the procapsid to yield an icosahedral intermediate (dissimilar to nodaviral maturation); and (b) a cleavage phase in which the α-proteins of an icosahedral intermediate undergo autocatalytic cleavage in a time dependent manner (similar to nodaviral maturation).

Equivalent dimers are differentiated during the transition phase:

Transition is mediated by the migration of internal helical domains from the threefold and quasi-threefold axes of the procapsid (where they fulfill a scaffolding role), to the quasi-twofold-axes of the icosahedral intermediate (where certain segments of these domains act as molecular switches). Both tertiary (movement of the α-helices) and secondary (disordering of the α-helices at the A – B contacts) structural changes lead to the strengthening of quaternary interactions among the subunits of the icosahedral intermediate. This disordering of the internal domains in the procapsid results in the differentiation of equivalent AB and CD dimers, which in turn results in bent contacts between AB dimers and flat contacts between CD dimers (Figure 1.13). Concurrent with this differentiation process, all four subunits migrate towards the center of the particle due to the degeneration of the protein scaffold. This process explains the smaller diameter of capsids, as opposed to that of procapsids. The A and B subunits undergo a rotation, due to the "shrinking" of the particle, which results in the trimeric associations among subunits within the icosahedral intermediate (Figure 1.13) (Canady *et al.*, 2000).

Similarities between tetraviral cleavage phase and nodaviral maturation:

Nearly identical dispositions of the cleavage sites of tetra- and nodaviruses suggest similar cleavage mechanisms (Figure 1.14) (Munshi *et al.* 1996). Zlotnick *et al.* (1994) proposed a mechanism for autoproteolytic cleavage of nodavirus particles (Figure 1.15). The bracketed numbers in this paragraph refer to the various steps shown in this figure. (1) The hydrophobic nature of the cleavage environment has the effect of raising the pK_a of Asp-75, which is in close proximity to the scissile peptide bond (Figure 1.15, panel A). (2) As a result, this residue is at least partially protonated at physiological pH, and forms a hydrogen bond with the carbonyl of the Asn-363 – Phe-364 peptide bond. This peptide bond is consequently susceptible to nucleophilic attack by water, (3) which results in the formation of a tetrahedral intermediate. (4, 5 and 6) This intermediate relaxes by the loss of the amine group, which constitutes the new N-terminus of the γ-peptide (Zlotnick *et al.*, 1994).

In tetravirus capsids, Glu-103 fulfils the same role as Asp-75, forming a hydrogen bond with the carbonyl group of the Asn-570 - Phe 571 peptide bond (Figure 1.14). Similar to the mechanism of cleavage of nodaviruses, the pK_a of Glu-103 is most probably raised by its environment, allowing it to be protonated at physiological pH (Munshi *et al.*, 1996).

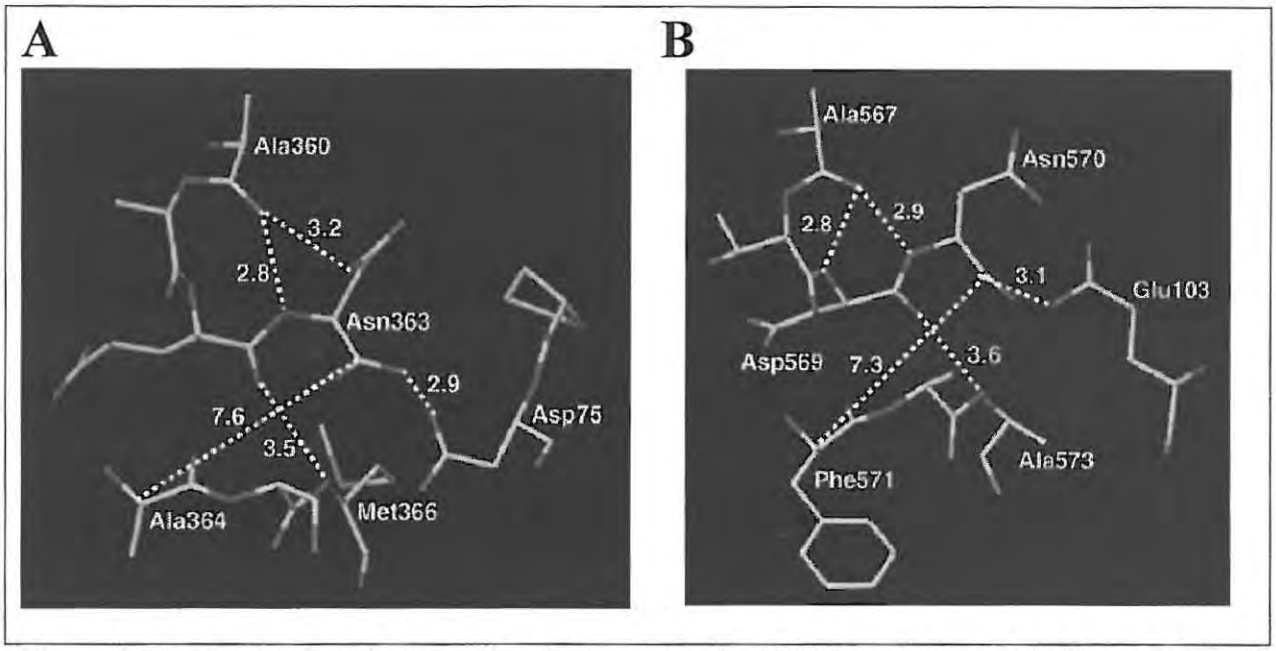

Figure 1.14 Comparison between the cleavage sites in BBV (panel **A**) and NωV (panel **B**). In BBV, the cleavage site is between Asn-363 and Ala-364 and Asp-75 appears to form a hydrogen bond with the carboxyl group of Asn-363. Similarly, in NωV, Glu-103 forms a hydrogen bond with the carboxyl group of Asn-570. The alanine residue at the C-terminal-side of the scissile in BBV is however replaced with Phe-571 in NωV (Munshi *et al.*, 1996).

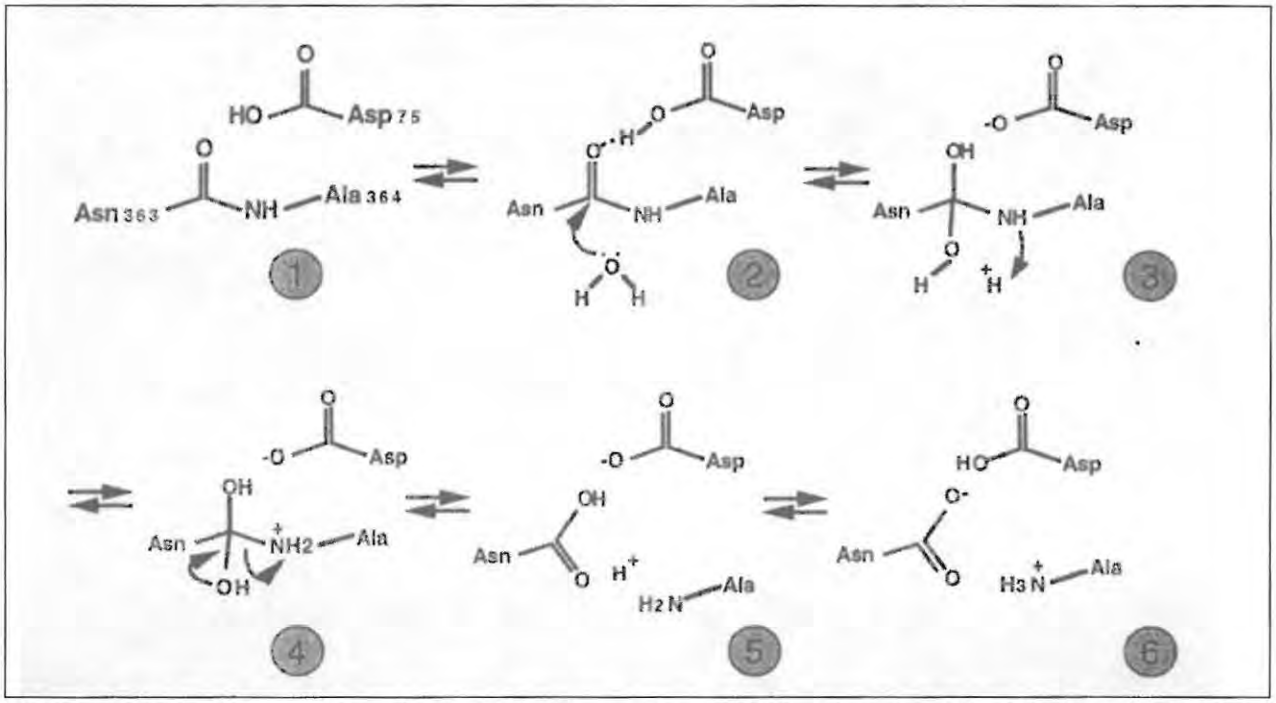

Figure 1.15 Proposed mechanism for the autoproteolytic cleavage of nodavirus α-proteins. Refer to the text for a description of the series of steps (1 - 6) involved in this mechanism (Johnson and Reddy, 1998).

There are, however, a number of other similarities, apart from the proposed cleavage mechanisms, tetraviral cleavage phase and nodaviral maturation: First, in both instances, cleavage occurs in a time-dependent manner (Canady *et al.*, 2000; Gallagher and Rueckert,

1988). To date, a kinetic model, similar to one of the two that has been proposed for nodaviruses (Zlotnick *et al.*, 1994), has not yet been proposed for tetraviral autoproteolysis. Second, there are probably no substantial structural differences between the uncleaved (tetraviral icosahedral intermediates and nodaviral provirions) and cleaved (mature virions) particles (Canady *et al.*, 2000; Schneemann *et al.*, 1993). However, for noda- and tetraviruses, N-termini of γ-peptide helices probably form a closer association around fivefold-axes upon cleavage, which results in the formation of pentameric helical bundles (Figures 1.10 and 1.11). Third, the cleavage sites for each of the subunits are located at similar geometrical interfaces in mature noda- and tetraviral particles. These sites lie close to the periphery of the three-membered trimeric asymmetric units and twelve-membered triangular faces of noda- and tetraviral particles, respectively (Figure 1.6, panels B and D) (Hosur *et al.*, 1987; Munshi *et al.*, 1996). Last, similar to nodaviruses, autoproteolytic cleavage also mediates the production of infectious tetravirus particles (Schneemann *et al.*, 1992). γ_1-helices are required to "escape" from the capsid protein, so that they can participate in the translocation of the viral genome across the host cell's membrane bilayer (Johnson and Reddy, 1998). This translocation process, which brings about infection, would therefore be impossible if the γ_1-helices were still covalently attached to the capsid shell.

Possible roles for RNA during the cleavage phase:

The proximity of RNA to the cleavage sites within nodaviral particles probably assists autocatalytic cleavage (Schneemann *et al.*, 1998). During the tetraviral cleavage phase, autocatalytic cleavage events with similar mechanisms occur at similar geometrical locations to those of nodaviruses (described above). It follows that it is very likely that there are close associations between RNA and the Asn – Phe cleavage sites at the interfaces between the tetraviral triangular faces. Therefore, even though a requirement for RNA was not implicated in the assembly and transition phases, non-specific RNA –protein interactions may play important roles in the cleavage phase.

iii RNA delivery

Analogous mechanisms for delivery of RNA by noda- and tetraviral capsids:

A-subunit γ_1-helices form pentameric helical bundles around the fivefold axes that are similar to those described for nodaviruses (Figures 1.10 and 1.11). The current model for tetraviral RNA delivery, which is solely based on the existence of these bundles, is assumed to be analogous to that for nodaviruses (Cheng *et al.*, 1994). The model predicts that, upon attachment, the tetraviral bundles migrate along the fivefold axes, towing the RNA with them via their C-terminal ends. Support for interactions between the C-terminal ends of these bundles and encapsidated RNA within the tetravirus particle was obtained from cryoEM representations of

NβV (Olson *et al.*, 1990). In these representations, high-density regions, which probably represented partially or highly ordered RNA, were detected at a radius of ~11.9nm at the fivefold axes of the virus. For NωV, similar RNA – protein interactions at these axes probably involve the structurally disordered C-terminal regions of the γ_A-peptides.

Proposed studies on the delivery of tetraviral RNA to the host cells:

Viral uncoating: It is unclear if the destabilization of tetravirus virions occurs in a manner that is similar to what was proposed for nodaviruses (Cheng *et al.*, 1994). It has been proposed that as yet unidentified "pocket factors" occupy hydrophobic cavities at the fivefold axes of nodaviral capsids. These factors have been identified as fatty acids for picornaviruses like *Poliovirus* and *Rhinovirus* 16 (Olson, *et al.*, 1993; Yafel *et al.*, 1993) and have been shown to play a role in the destabilization of picornavirus capsids for the delivery of genomic RNA to the host cell (Rossmann and Johnson, 1989). The pocket factors have a stabilizing effect on the capsids, but are lost upon attachment to the cellular receptor, membrane, or both, resulting in destabilization around the fivefold axis. It has been proposed that an ellipsoidal density, which has been observed at the fivefold axis on a cryoEM X-ray model difference map of the *Flock House virus* (FHV) capsid, is an as yet unidentified nodaviral pocket factor, and that this factor could perform a similar function to that of its picornavirus counterpart (Cheng *et al.*, 1994). In addition, Schneemann *et al.* (1994) demonstrated via *in vitro* assembly experiments that factor(s) other than viral RNA and protein are involved in the assembly of nodaviral capsids. Factor(s) required for assembly are therefore present in the nodavirus' host cell and it is possible that these factors could be pocket factors. The application of similar *in vitro* assembly experiments could test if tetravirus capsids are also dependent on cellular factors for assembly. Alternatively, analytical chromatographic techniques like HPLC and GC could be used for the detection of pocket factors in purified tetravirus capsids. The detection of these factors within tetravirus capsids would be indicative of similar mechanisms for the destabilization of tetra- noda- and picornavirus capsids during viral uncoating.

Membrane permeabilization: In the absence of helical wheel representations for γ_1-helices, it is logical to assume that amphipathic characteristics of these helices stabilize tetraviral pentameric helical bundles in a manner that is comparable to that of the nodaviral γ-helices (Bong *et al.*, 1999). It has been demonstrated that nodaviral γ-helices increase the permeability of the membrane bilayer for the translocation of the nodaviral genome into the cell (Bong *et al.*, 1999). The elucidation of this biological function for nodaviral γ-helices was attained through physicochemical characterization studies of *in vitro*-synthesized γ-peptides (Bong *et al.*, 1999;

Bong *et al.*, 2000). Similar studies for γ_1-helices could provide a valuable insight into the tetraviral RNA translocation mechanism.

Cotranslational disassembly: It has been proposed that cotranslational disassembly, which is an established mechanism for infection by plant RNA viruses e.g. CCMV (Roenhorst *et al.*, 1989), probably contributes to the translocation of nodaviral RNA across the lipid membrane (Ball and Johnson, 1998). Accordingly, a stretch of viral RNA containing the ribosome-binding site becomes available to the host cell's protein translation machinery. Translation would assist in viral uncoating and RNA translocation into the host cell. Hiscox and Ball (1997) provided evidence for the contribution of cellular factors in the uncoating process, demonstrating that some cytoplasmic factor in cell free extracts could destabilize a small fraction of FHV particles. This destabilization resulted in the release of viral RNA to the ribosomes for protein synthesis, supporting the possible involvement of cotranslational disassembly in viral entry. Similar studies on tetravirus particles could establish whether cotranslational disassembly contributes to the translocation of tetraviral RNA across the lipid bilayer.

1.2.6 Concluding remarks: structure/function comparison between tetravirus and nodavirus capsids

Capsids that are composed of multiple gene products facilitate viruses, like picornaviruses, to accomplish the biological functions that are required for their lifecycles. Differences in the tertiary structures of three different picornavirus coat proteins allow them to assemble into polyhedral virus particles without the need for molecular switches (Cheng *et al.*, 1994). Tetra- and nodaviruses accomplish the same biological functions as picornaviruses through the packaging of their identical gene products into quasi-equivalent shells. The assembly of these shells is, however, dependent on distinct molecular switching mechanisms which are significantly different for the two virus groups.

Nodavirus capsids are dependent on segments of genomic RNA as molecular switches for the assembly of polyhedral capsids (Fisher and Johnson, 1993). In the structurally more complex tetraviruses the assembly of structurally distinct procapsids, which undergo structural transitions to form polyhedral capsids, circumvents the requirement for RNA as molecular switches. These transitions form the first phase of the tetraviral maturation process. For a number of reasons listed in Section 1.2.5ii, the second phase, which involves the autocatalytic cleavage of precursor proteins, is very similar to the entire nodaviral maturation process. Based on this similarity, tetraviral maturation can be demarcated into transition and cleavage phases, and an analogy was made between a tetraviral polyhedral intermediate and the nodaviral procapsid (Section 1.2.5ii).

Another instance where the presence of multiple gene products assists capsid function is found during cellular binding and RNA delivery. In picornaviruses, the N-terminus of virus protein 1 (VP1) was shown to interact with the cellular membrane during RNA delivery, which implies that VP1 plays a distinct role at this stage of the lifecycle, as compared with VP2 and VP3 (Fricks and Hogle, 1990). Furthermore, the release of internally located VP4 chains from picornaviruses has been proposed to facilitate the uncoating process during RNA delivery (Rueckert, 1996). Quasi-equivalent capsid shells facilitate noda- and tetraviruses to accomplish these RNA delivery functions in ways that have been conserved between these two virus families. Similar autoproteolytic cleavage events within tetraviral polyhedral intermediates and nodaviral procapsids produce virions with structurally distinct quasi-sixfold and fivefold axes. Analogous to the picornaviral VP1 subunits, fivefold-related A-subunits are therefore sufficiently non-equivalent to the quasi-sixfold-related B, C and D subunits in tetraviral capsids. This enables A-subunits, like VP1 subunits, to interact with cellular membranes. In addition, release of the noda- and tetraviral γ-peptides during viral uncoating is highly reminiscent of a similar release of VP4 chains from picornaviruses.

To conclude, the constraints of a single capsid component have led to the allocation of numerous functions to individual structural elements within quasi-equivalent shells. The best example of this is the multi-functional tetraviral γ-peptides, which are most probably involved in the release of the RNA from the virion and the permeabilization of membrane bilayers for the translocation of the viral genome. These peptides also form part of protein scaffolds for provirions, where they stabilize these truncated icosahedral structures; and are hereafter transformed into molecular switches for $T = 4$ virions. It is also possible that γ-peptides could be involved in the specific encapsidation of viral RNA in a manner analogous to what has been described for the nodaviral γ-peptides (Schneemann and Marshall, 1998).

1.3 Heterologous expression in *S. cerevisiae*

The yeast *S. cerevisiae* is an excellent host for the expression of eukaryotic proteins because it has the potential to produce correctly folded proteins that are posttranslationally processed in a manner similar to that of higher eukaryotes (Eckart and Bussineau, 1996). It also has the ability to grow rapidly to high cell densities on simple media and it can be manipulated genetically almost as easily as *E. coli* (Romanos *et al.*, 1992). Extensive research in the molecular genetics of *S. cerevisiae*, which culminated in the complete sequence of its genome in 1998

(http://genome-www.stanford.edu/Saccharomyces), has led to the development of a great variety of promoter systems and methods for propagating foreign DNA.

1.3.1 Expression vectors

Yeast vectors can be introduced into *S. cerevisiae* by means of a number of different methods. These include electroporation (Meilhoc *et al.*, 1990) and methods in which cells are made competent by treatment with lithium acetate (Kaiser *et al.*, 1994) or dimethyl sulfoxide (Hill *et al.*, 1991). Selection of transformants can be achieved by two types of plasmid borne selectable markers: drug resistance genes and cloned yeast genes (Romanos *et al.*, 1992). The latter type, of which the *URA3*, *TRP1*, *LEU2* and *HIS3* genes are most commonly used, is transformed into *S. cerevisiae* cells that have a recessive mutation in the corresponding chromosomal copy of the cloned gene (Lundblad, 1997).

There are a number of different vectors for episomal and chromosomal expression in *S. cerevisiae*. These include the *ARS* vectors, 2μ-based vectors and yeast chromosomal integration plasmids (YIps): *ARS* vectors contain yeast autonomous replication signals (*ARS*) that function as origins of replication (Lundblad, 1997). These plasmids have been shown to be mitotically unstable due to a strong bias to segregate to the mother cell (Romanos *et al.*, 1992). The mitotic stability of *ARS* vectors can be increased by the incorporation of yeast centromeric sequences (*CEN*) into these vectors (Sikorski and Hieter, 1989). The presence of *CEN* sequences in *ARS/CEN* vectors ensures a copy number of 1 to 2 vectors per cell (Lundblad, 1997).

2μ-based vectors contain sequences of the endogenous 2μ circle of *S. cerevisiae* and are the most commonly used vectors for high-level expression in yeast (Romanos *et al.*, 1992). This is due to their mitotic stability and high copy number (20-50 copies) (Rose and Broach, 1990). Most 2μ-based vectors carry only the sequences that are required for their autonomous replication and depend on the yeast strain for the *REP1* and *REP2* encoded proteins (Kikuchi, 1983). The 2μ circle-encoded REP1 and REP2 proteins contribute to the segregation of 2-μ plasmids during cell division (Velmurugan *et al.*, 1998).

YIps are designed to integrate foreign DNA into the genome of *S. cerevisiae* by homologous recombination. These plasmids lack an origin of replication and therefore cannot replicate in yeast cells. They do, however, contain a fragment of yeast chromosomal DNA to target integration as well as a yeast selectable marker, a bacterial origin of replication and an antibiotic resistance gene. The yeast chromosomal DNA usually contains a unique restriction site that can be cleaved to produce a linear DNA fragment. Upon transformation into *S. cerevisiae* this fragment can be integrated through homologous recombination into the chromosomal target sequence, resulting in a duplication of the target sequence (which brackets the rest of the

plasmid) (Stearns *et al.*, 1990). This duplication can result in excisional recombination, where the integrant "pops out" from the chromosome (Lundblad, 1997). Chromosomal integration is nevertheless the most stable method for heterologous expression in *S. cerevisiae* and less than 1% of the vector is lost per generation in the absence of selection (Romanos *et al.*, 1992).

1.3.2 Expression of VLPs in *S. cerevisiae*

It has been demonstrated that *S. cerevisiae* cells are capable of the assembly of intracellularly expressed oligomeric proteins such as the α- and β-subunits of mammalian Na^+, K^+-ATPase (Horowitz *et al.*, 1990) and the functional a2b2 tetramers of the three human embryonic haemoglobins (Hofman *et al.*, 1995). *S. cerevisiae* has also been used for the expression of VLPs from viruses belonging to a wide range of virus families. The assembly of VLPs has been demonstrated upon the expression of structural genes belonging to *Brome mosaic virus* (*Bromoviridae*) (Price *et al.*, 1999), *Human papillomavirus* (*Papillomaviridae*) (Hofmann *et al.*, 1995), *Hepatitis delta virus* (Deltavirus genus) (Wu, *et al.*, 1997), *Poliovirus* (*Picornaviridae*) (Rombaut and Jore, 1997), and *Rabbit haemorrhagic disease virus* (*Caliciviridae*) (Boga and Alonso, 1997). However, the best-known application for the expression of VLPs in *S. cerevisiae* comes from the production of the first recombinant vaccine (hepatitis B surface antigen) for humans (Miyanohara *et al.*, 1983, Valenzuela *et al.*, 1982).

1.3.3 Expression of virus particles in *S. cerevisiae*

A recent patent by Price *et al.* (1999) described the only instances where virus particles have been expressed in *S. cerevisiae*. Proof for the assembly of these particles were presented by the detection of viral RNA, other than the mRNA of the capsid protein, in purified virus particles, and by demonstrating that the particles were infectious. In this patent, two types of encapsidation were described for the assembly of virus particles, i.e. replication dependent and replication independent encapsidation.

Evidence for replication dependent encapsidation was provided for FHV and *Brome mosaic virus* (BMV), two viruses that were shown to be capable of replication in *S. cerevisiae* cells (Janda and Ahlquist, 1993, Price *et al.*, 1996). For FHV, the transfection of yeast spheroplasts with FHV RNA1 and RNA2 resulted in the encapsidation of these RNAs, as demonstrated by plaque assays on *Drosophila* monolayers. For BMV, virus particles were formed in *S. cerevisiae* cells that expressed the viral replication proteins 1a and 2a, and replicated BMV RNA3. Northern blot analysis of RNA extracts from these particles demonstrated that the mRNA for proteins 1a and 2a, as well as RNA3, was encapsidated.

Alternatively, evidence for replication independent encapsidation was only provided for BMV (Price *et al.*, 1999). The co-expression of BMV capsid protein and RNA3 resulted in the

synthesis of virus particles that encapsidated capsid protein mRNA and RNA3, as demonstrated by Northern blot analysis.

1.4 Project proposal

At the onset of this project in 1996, a number of reports were available on the non-host production of HaSV. These included a report in 1995, which stated that *H. armigera* larvae became stunted upon ingestion of tobacco protoplasts that were engineered to express HaSV (Beckmann, 1995). This work, led to the generation of transgenic HaSV-tobacco plants, which were shown to induce stunting in *H. armigera* larvae in preliminary tests (Service, 1996).

The successful results for the expression of HaSV in plant cells were suggestive of a similar outcome for its expression in *S. cerevisiae*, because yeast cells provided a similar eukaryotic cellular environment for the assembly of HaSV virions. One of the main draw cards for the expression of HaSV in *S. cerevisiae* was its potential for the high-level production of this virus through a large-scale fermentation process (Romanos *et al.*, 1992).

Alternative expression systems for the non-host production of HaSV include *E. coli* and baculovirus expression systems. The former was not ideal for this project because no evidence for the assembly of VLPs was detected for the expression of the HaSV and NωV capsid protein precursor genes in *E. coli* (Agrawal and Johnson, 1995; Hanzlik *et al.*, 1995). Although a baculovirus expression system has been used for the production of tetravirus VLPs (Agrawal and Johnson, 1995; Pringle *et al.*, 2001), it is not nearly as commercially applicable as *S. cerevisiae* for this purpose. Cumbersome and time-consuming cell-culture techniques are required for the propagation of baculovirus-infected insect cells (O'Reilly *et al.*, 1992), while *S. cerevisiae* cells can be grown to high densities using convenient fermentation procedures (Romanos *et al.*, 1992). The use of *S. cerevisiae* for HaSV production would also be far more economical than a baculovirus expression system.

Thus, the principle objective of this project was to demonstrate that HaSV virions could be assembled in *S. cerevisiae* by using a similar strategy to the one that was employed in plant protoplasts (Gordon *et al.*, 2001). The ultimate goal was to develop a biotechnological process for the production of a sprayable formulation of HaSV, for application as a biopesticide against *H. armigera*.

The objectives for the research described in this thesis were as follows:

- Construction of DNA vectors for the expression of HaSV in *S. cerevisiae*. Constructs that direct the expression of genes for the production of the HaSV capsid protein precursor (p71) and the two genomic RNA transcripts are required.
- Analysis of *P71* expression in *S. cerevisiae* and optimization of the production of soluble capsid protein.
- To determine if the expression of *P71* leads to the assembly of HaSV VLPs in *S. cerevisiae*.
- Analysis of the expression of HaSV *RNA1* and *RNA2* in *S. cerevisiae*.
- To determine if infectious HaSV particles can be purified from *S. cerevisiae* cells that are transgenic for *P71*, *RNA1* and *RNA2*.

2 Strategies followed in constructing DNA vectors for the expression of HaSV in *S. cerevisiae*

2 Strategies followed in constructing DNA vectors for the expression of HaSV in *S. cerevisiae*

2.1 Introduction

Although the simplicity of the bipartite HaSV genome lends itself to its non-host production, a few problems that pertain to the novelty of a required expression system have to be addressed. The focal point of these problems lies in the requirement for a system that mimics the production of infectious virus particles in host cells. The criteria for such a system and a brief description of each are provided in the next few paragraphs of this section. The objective of this chapter is to demonstrate how a heterologous expression system for the assembly of HaSV in *S. cerevisiae* was designed to accommodate each of these requirements. From here on, *S. cerevisiae* will be referred to as yeast, since no reference is made throughout this thesis to any other types of yeast.

2.1.1 Capsid expression

Translation in yeast is very sensitive to the secondary structure of the leader sequence (Romanos *et al.*, 1992). Translation efficiency is also reduced by alterations to the consensus sequence for translation initiation (Kozak sequence) and runs of G's or U's in the untranslated leader (Cigan and Donahue, 1987; Kozak, 1989; van der Heuvel *et al.*, 1990). The first 48 bases of the 365 nucleotide leader sequence upstream of the *P71* ORF on HaSV RNA2 (Figure A1.2, Appendix 1) can be folded into a stem-loop structure with the hexamer sequence GGUAAA (nucleotides 24 to 29) (Hanzlik *et al.*, 1995). The presence of this structure, a foreign Kozak sequence and a run of U's at nucleotides 1-14 makes it unlikely that p71 translation would occur from RNA2 transcripts in yeast cells.

A second point of concern is that *P71* is the second ORF on a bicistronic RNA molecule (Hanzlik *et al.*, 1995) (Figure 1.3). In the viral host cells, the *P71* ORF is most probably translated by ribozymes leaking past the *P17* start codon, which is in poor context for translation initiation (Hanzlik *et al.*, 1993). However, a possible preference for an upstream start codon further reduces the likelihood of efficient translation in yeast. This presumption is consistent with the lack of detectable p71 levels from RNA2 transcripts in transgenic plant protoplasts (Gordon, *et al.*, 2001).

2.1.2 Expression of *RNA1* and *RNA2*

The HaSV RNA1 and RNA2 transcripts must be able to interact with the viral replicase, the host cell components and the capsid protein domains. Alterations to transcript sequences involved in these interactions could result in the loss or lack of infectivity. The presence of nonviral nucleotides or absence of viral nucleotides at the extremities of RNA transcripts could also greatly affect their infectivity. This is the result of the viral replicases' limited tolerance for the structures and/or sequences of the 5' and 3' ends (Boyer and Haenni, 1994).

i 5' terminal extensions

Viral RNA transcripts with accurate 5' ends can be produced from exact fusions between transcriptional promoters and the beginning of the viral sequence (Boyer and Haenni, 1994). Infectivity can be severely reduced by the addition of only a few nucleotides to the 5' ends, e.g. FHV RNA2 transcripts with only 1 or 2 additional 5' nucleotides resulted in a 10-fold decrease in replication efficiency by FHV replicase (Ball and Li, 1993). A similar scenario probably exists for HaSV, since *H. armigera* larvae were not infected when fed protoplasts producing HaSV RNA1 and RNA2 transcripts with an additional 22 and 26 nucleotides at their 5' ends, respectively (Gordon *et al.*, 2001).

The presence of cap structures at the 5' ends of HaSV genomic RNAs is very important because it gives the 5' ends a 3'-like character that protects them against the host cell's nucleases (Fraenkel-Conrat *et* al., 1988). This structure is also required for efficient translation initiation and the absence thereof could result in a reduced level or a complete loss of infectivity (Boyer and Haenni, 1994). The HaSV replicase catalyzes the capping of both genomic RNAs in the cytoplasm of the host cell (Gordon *et al.*, 1995). Conversely, in a DNA-templated expression system, either the cellular capping enzymes in the nucleus or the replicase in the cytoplasm could perform this reaction.

ii 3' terminal extensions

Viral RNA transcripts with accurate 3' termini can be transcribed from DNA templates by the accurate positioning of a *cis*-cleaving ribozyme immediately downstream of the viral sequence (Ball and Li, 1993; Ishikawa *et al.*, 1997). Replicases are generally more tolerant of 3' end extensions than 5' extensions, but long extensions mostly abolish replication (Ball, 1992; Boyer and Haenni, 1994). Ishikawa *et al.* (1997) demonstrated that BMV RNA3 transcripts with 0 or 3-nucleotide 3' extensions were replicated more efficiently than those with 19-nucleotide 3'

extensions. The 19-nucleotide 3' extensions were, however, still infectious, but transcripts with extensions of 42-nucleotides or longer inhibited BMV infectivity (Dzianott and Bujarski, 1989). Long 3' end extensions also seem to be detrimental to the replication for HaSV since RNA transcripts with >200 nucleotides at their 3' ends were not infective (Gordon *et al.*, 2001).

Another important consideration is that the HaSV genomic RNAs are not polyadenylated while, in yeast, poly-A tails are added to the 3' ends of all the primary transcripts (Egli and Braus, 1994). Poly-A tails could therefore jeopardize the infectivity of viral RNA transcripts that were expressed from DNA templates in yeast. According to Boyer and Haenni (1994) the general rule that increased 3' extension length results in decreased infectivity also seems to apply to extensions in the form of poly-A tails.

2.1.3 Assembly of HaSV virions

During the infection of an insect cell by HaSV, the viral genomic RNA is delivered directly to the cytoplasm, where it is replicated to high levels by the viral replicase and other viral and/or cellular proteins (Bawden *et al.*, 1999). The p71 monomers, which are translated from HaSV RNA2, associate with the genomic RNAs in the cytoplasm to produce HaSV virions. An entirely different process would occur for the successful expression of HaSV from DNA genes in yeast. In the cytoplasm, p71 monomers would be translated from mRNA that was transcribed from *P71* genes in the nucleus. These monomers would associate with RNA1 and RNA2, which were exported to the cytoplasm after transcription in the nucleus, to produce HaSV virions. A number of factors are required for the successful application of this process, which was used for the expression of HaSV in plant protoplasts (Gordon *et al.*, 2001).

First, it is very important that a powerful promoter system is used to drive the expression of the *RNA1*, *RNA2* and *P71* genes. Failed attempts to replicate HaSV in a variety of insect cell lines (Bawden *et al.*, 1999) makes it is highly unlikely that replication will take place in yeast cells. In addition, recent results by Gordon *et al.* (2001) demonstrated that replication was not detected upon the transfection of HaSV genomic RNA into plant protoplasts. The expression of the genes for the production of viral RNA transcripts and p71 should therefore be placed under the control of a powerful promoter, to ensure that these viral components are expressed at high levels in the cell.

Second, the RNA1 and RNA2 transcripts should be polyadenylated for efficient export from the nucleus to enable the assembly of HaSV virions in the cytoplasm, because poly-A tails play an

important role in the nucleocytoplasmic transport of mRNA (Huang and Carmichael, 1996). However, the presence of poly-A-tails at the 3' ends of the viral transcripts could reduce their infectivity (described above). Poly-A tails have also been implicated to play roles in mRNA stability (Caponigro and Parker, 1996) and translation (Jackson and Standart, 1990).

2.2 Materials and Methods

2.2.1 General recombinant DNA techniques

Unless otherwise stated, general recombinant DNA techniques were essentially as described by Sambrook *et al.* (1989). Restriction and DNA modifying enzymes were used according to the suppliers' instructions. In general, *Escherichia coli* DH5α (Hanahan, 1983) was used as host for recombinant plasmids and *E. coli* JM110 (Yanisch-Perron *et al.*, 1985) was used as host for plasmids carrying methylation-sensitive restriction sites. DNA sequencing was determined either by manual sequencing (SequiTherm EXCEL™ II DNA sequencing kit, Epicentre) or using an ABI automatic sequencer (model 373A). pDHVStuR1HC, pDHCStuR2HP and pDHVCAPB (Figures 2.1, 2.2 and 2.3, respectively), plant expression vectors for HaSV *RNA1*, *RNA2* and *P71*, were kindly provided by Karl Gordon and Terry Hanzlik (CSIRO Entomology, Canberra, ACT, Australia). DNA fragments encoding HaSV sequences were subcloned or PCR amplified from these plasmids for the construction of all the expression vectors used in this study.

2.2.2 Construction of a vector for the episomal expression of *RNA1*

The RNA1 expression vector pDHVStuR1HC carries an exact fusion between the *Cauliflower mosaic virus* (CaMV) 35S promoter (P_{35S}) and the 5' end of RNA1, and the hairpin cassette (HC) ribozyme from the satellite RNA of *Tobacco ringspot virus* (ToRSV) (Hampel *et al.*, 1990) directly downstream of its 3' end. To enable expression of RNA1 transcripts with precise 5' and 3' ends in yeast, P_{35S} was replaced with the *S. cerevisiae GAL1* promoter (P_{GAL1}) and the *RNA1*-encoding DNA fragment was inserted into the *ARS/CEN* vector pKG6 as follows:

A 6140 bp *Eco* RI DNA fragment, carrying P_{35S}, *RNA1*, the HC ribozyme and the CaMV terminator from pDHVStuR1HC, was inserted into pKG6 between P_{GAL1} and the *S. cerevisiae CYC1* terminator (T_{CYC1}) (Figure 2.1, Step I). The resulting construct (pAV8F) was used to generate pVH1, where a 6867 bp internal *Xba* I fragment has been deleted to reduce the plasmid size (Figure 2.1, Step II). pVH1 carries the truncated 5' end of HaSV *RNA1* separated from

P_{GAL1} by a 671bp DNA fragment. This 671bp DNA fragment was deleted by reverse PCR with primers AV4 (corresponding to nucleotides –1 to –25 of P_{GAL1}) and AV1 (corresponding to nucleotides +1 to 25 of *RNA1*) using the Expand™ High Fidelity PCR System (Roche) (Primers: Appendix 4, Thermal cycling programme: Programme 1, Appendix 5). The re-ligation of the amplified DNA fragment resulted in the construction of pVH4, and the fidelity of the P_{GAL1}-*RNA1* fusion was confirmed by DNA sequencing (Figure 2.1, Step III).

An 882 bp *Sal* I – *Xho* I pVH4 DNA fragment carrying the P_{GAL1}-*RNA1* fusion was excised from pVH4 and inserted into pKG6 to produce pAV10 (Figure 2.1, Step IV). A 5827 bp *Xba* I – *Afl* II DNA fragment, carrying the remaining 3' end of *RNA1* missing in pAV10 together with the downstream HC ribozyme, was excised from pDHVStuR1HC. The internal *Xba* I site downstream of the *Afl* II site in this restriction fragment was not digested because it was *dam*-methylated in *E. coli* strain DH5α. This *Xba* I – *Afl* II fragment was introduced into pAV10 to produce pAV13HC (Figure 2.1, Step V). This vector carried the P_{GAL1}–*RNA1*–HC ribozyme–T_{CYC1} expression cassette for the production of RNA1 transcripts with 5' and 3' ends identical to those of the HaSV genomic RNAs. The presence of the correct ribozyme sequence in pAV13HC was confirmed by DNA sequencing.

An error was discovered for the P_{GAL1}-RNA1 fusion in the RNA1 expression vector pAV13HC when these regions were sequenced (at ZENECA Agrochemicals Ltd., Jealott's Hill, UK) for a second time. The sequence results indicated that the first G nucleotide of RNA1 was not present in this construct (Table 2.2). Rachael Blaine (ZENECA Agrochemicals Ltd., Jealott's Hill, UK) repaired the PGAL-RNA1 fusion in this vector to produce pAV13HC (G+) (bracketed in Figure 2.1). Reference is made as to which of the two constructs were used in experiments described throughout the remainder of this thesis.

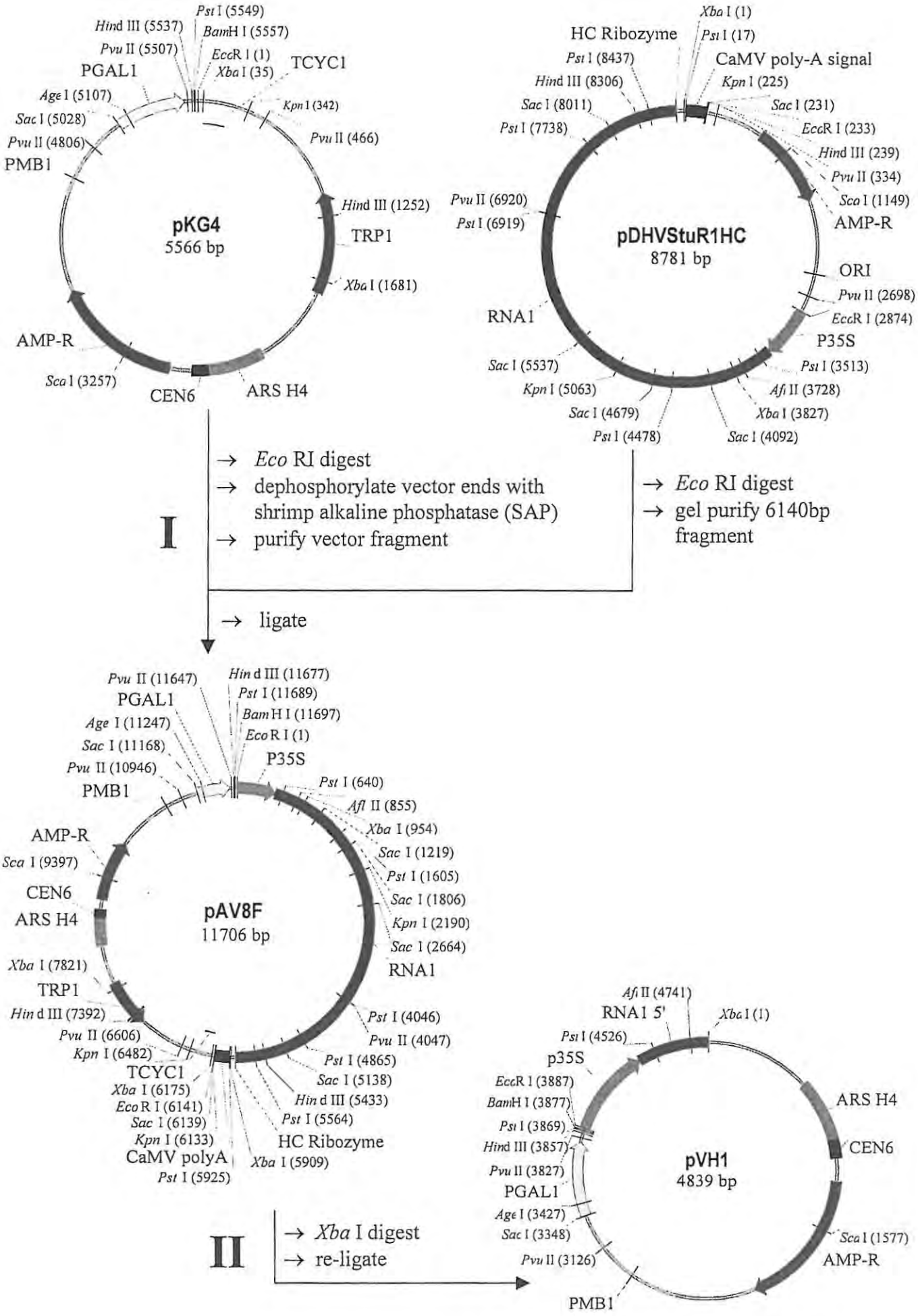

Figure 2.1 A flow diagram of the cloning steps for the construction of a vector for the episomal expression of HaSV *RNA1*.

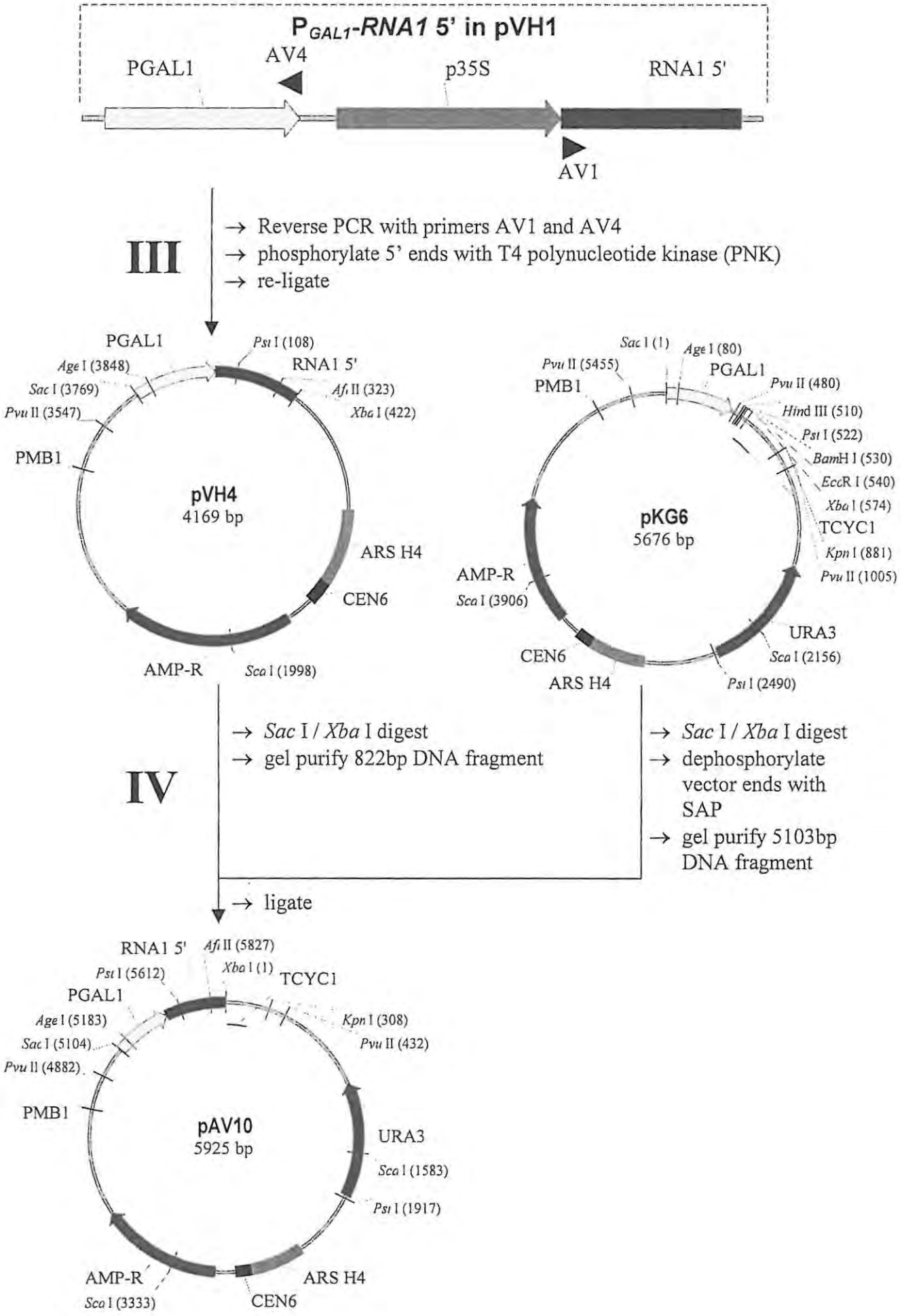

Figure 2.1 Continued...

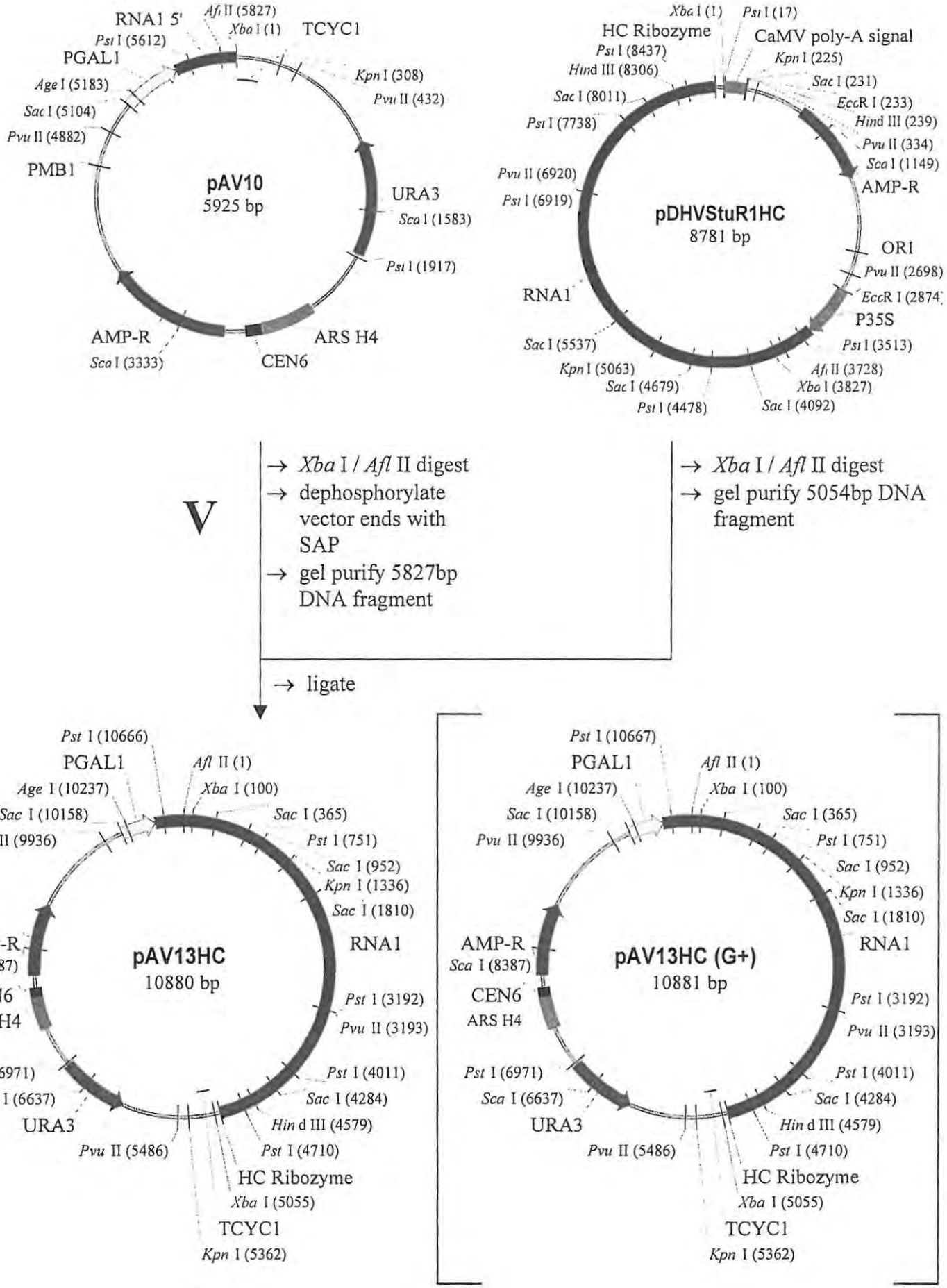

Figure 2.1 Continued...

2.2.3 Construction of a vector for the episomal expression of HaSV *RNA2*

pDHVR2HP is a plant expression vector that contains the 5' end of RNA2 flanked by a *Bam* HI site. A 2588 bp *Bam* H1 – *Xba* I DNA fragment carrying HaSV *RNA2*, the HC ribozyme and the CaMV terminator was excised from pDHVR2HP, and inserted into the *ARS/CEN* vector pKG5 (Figure 2.2, Step I). The resulting construct (pMLY2) was used to generate pMLY3, where a 4306 bp internal *Eco* RI fragment has been deleted to reduce the plasmid size (Figure 2.2, Step II). The P_{GAL1}-*RNA2* fusion was constructed in a manner similar to that described for *RNA1* expression module above. pMLY3 carries the truncated 5' end of HaSV *RNA2* separated from P_{GAL1} by an 133bp DNA fragment. This DNA fragment was deleted by reverse PCR with primers AV4 (corresponding to nucleotides –1 to –25 of P_{GAL1}) and AV2 (corresponding to nucleotides +1 to 25 of RNA2) using the Expand™ High Fidelity PCR System (Roche) (Primers: Appendix 4, Thermal cycling programme: Programme 1, Appendix 5). The re-ligation of the amplified DNA fragment resulted in the construction of pVH5, and the fidelity of the P_{GAL1}-*RNA2* fusion was confirmed by DNA sequencing (Figure 2.2, Step III).

A 993 bp *Sac* I – *Eco* RI DNA fragment, carrying the P_{GAL1}-*RNA2* fusion in pVH5, was inserted into the *ARS/CEN* vector pKG3 (Figure 2.2, Step IV). The truncated *RNA2* sequence in the resulting plasmid, pAV11 was repaired by the insertion of a 1951bp *Eco* RI – *Xba* I DNA fragment from pDHVStuR2HP to produce pAV14HP (Figure 2.2, Step V). The *HIS3* selectable marker on pAV14HP did not complement *his3* in the *S. cerevisiae* JRY188 strain (*MATα*, *his*3, *leu*2, *trp*1, *ura*3) (Table A6.1, Appendix 6). The P_{GAL1}–RNA2–HC ribozyme–T_{CYC1} expression cassette was therefore subcloned into pKG4, which carries the *TRP1* selectable marker (Figure 2.2, Step VI). The resulting plasmid, pAV14HPTrp, was used for the heterologous expression of RNA2 transcripts in yeast.

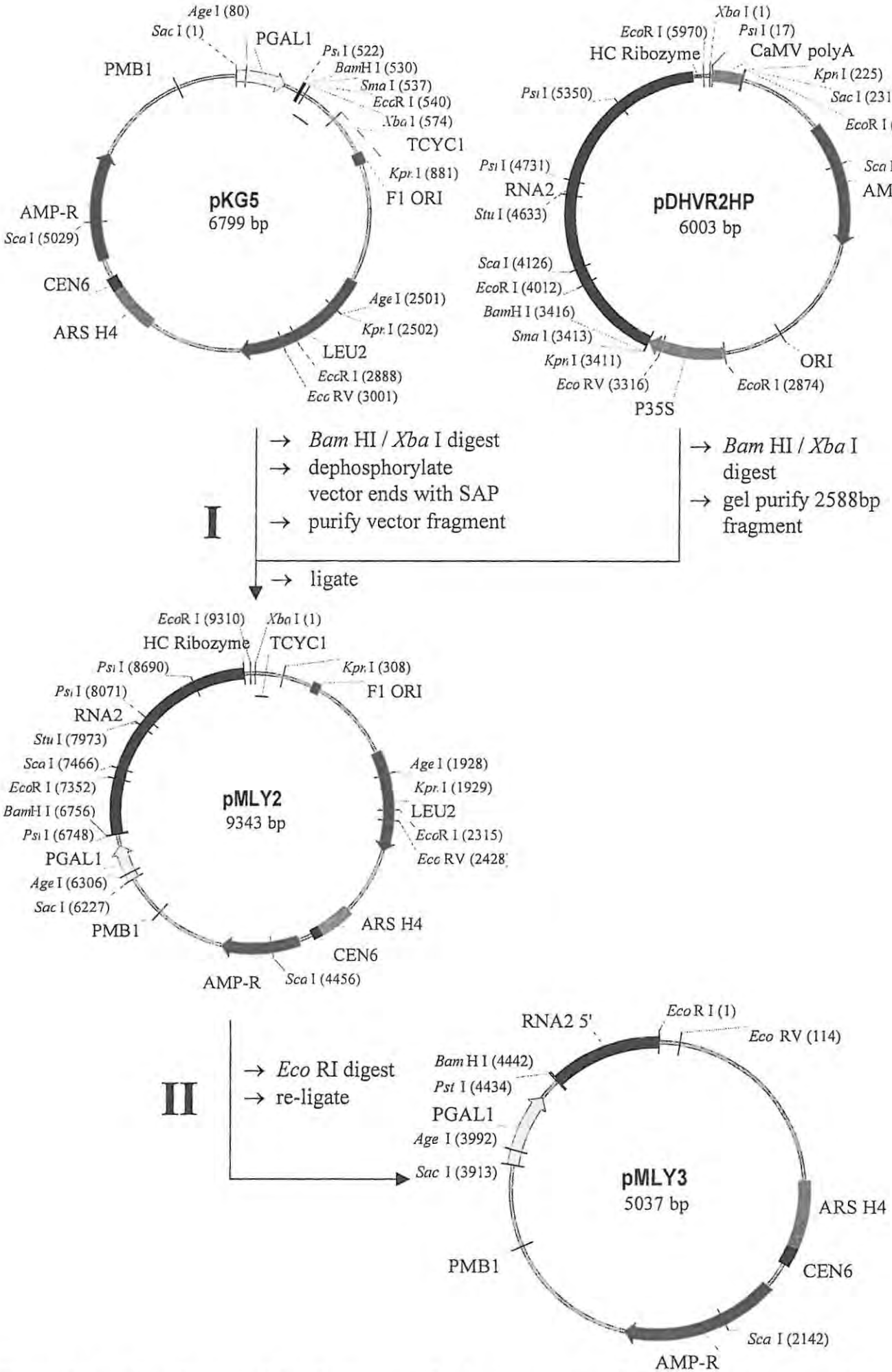

Figure 2.2 A flow diagram of the cloning steps for the construction of a vector for the episomal expression of HaSV RNA2.

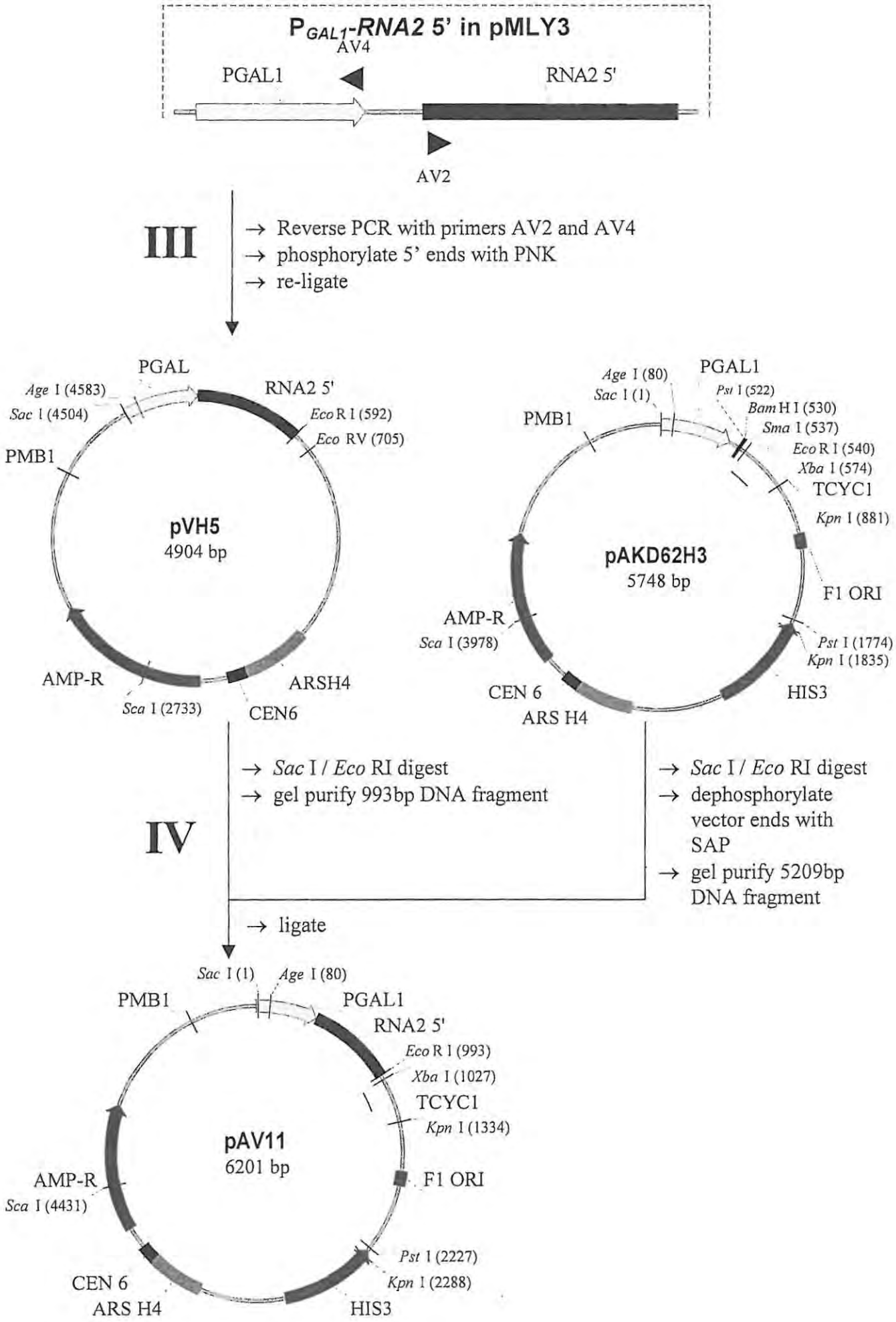

Figure 2.2 Continued...

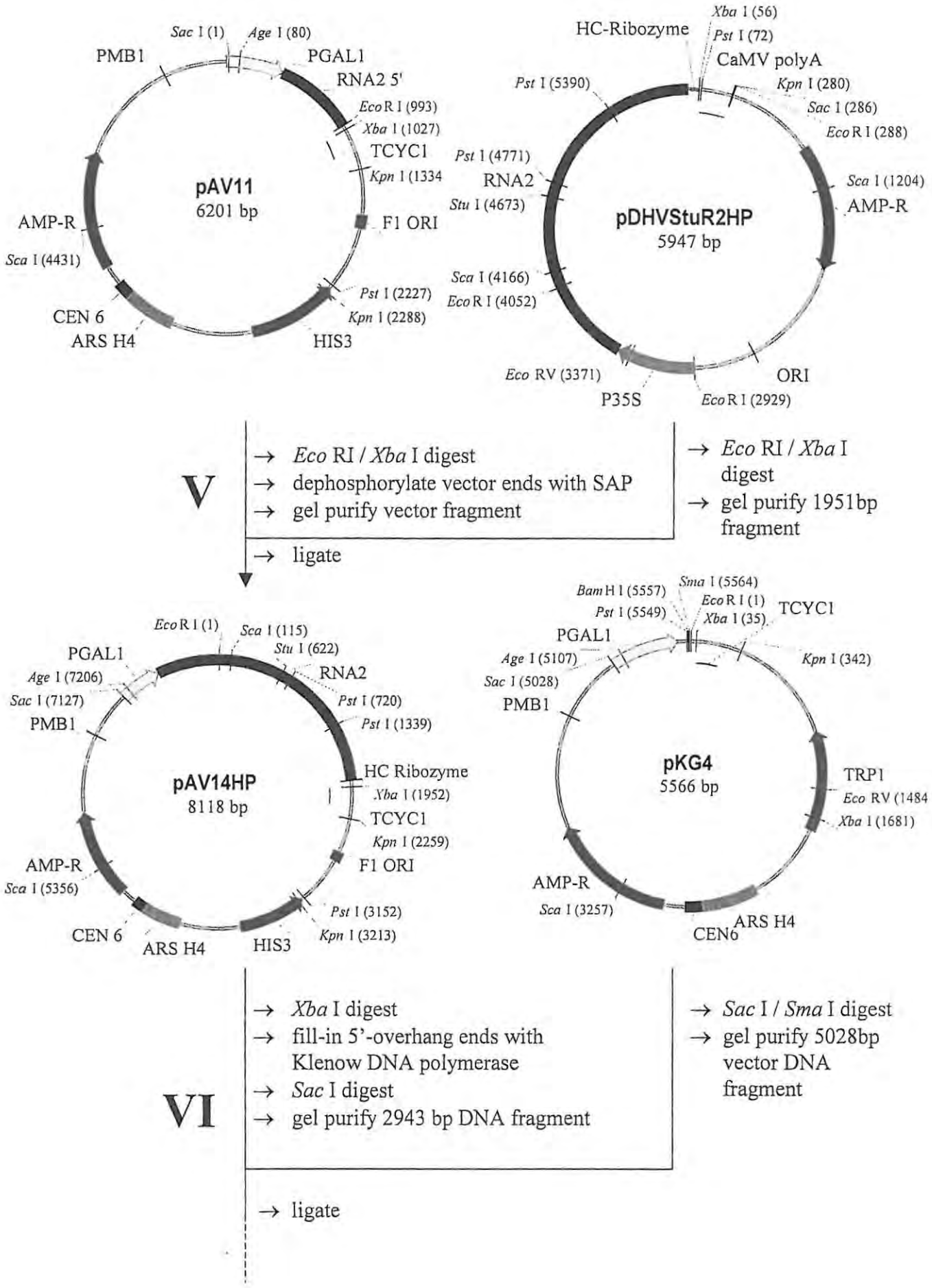

Figure 2.2 Continued

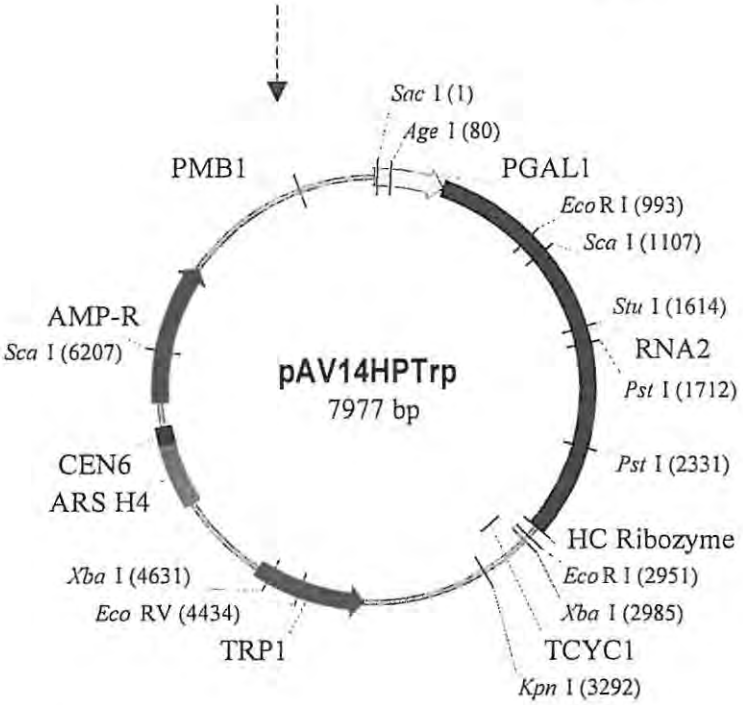

Figure 2.2 Continued...

2.2.4 Yeast expression vectors for *P71*

pAV3, a multi-copy yeast expression vector for *P71*, was constructed by inserting an 1954 bp *Bam* HI DNA fragment encoding the amino acid sequence of p71 in the plant expression vector pDHVCAPB (Gordon *et al.*, 2001) into the 2μ-based vector pYES2 (Invitrogen) (Figure 2.3). pAV3 carries the p71 coding sequence flanked by P_{GAL1} and T_{CYC1} together with a *URA3* selectable marker.

An integration vector for chromosomal expression of *P71*, YIpLacVCAPB320 (Figure 2.4, panel B), was constructed by Rachel Blaine (Syngenta, Jealott's Hill Research Station, Berkshire, UK) as follows: first, the P_{GAL1}-*P71*-T_{CYC1} expression module of pAV3 (Figure 2.3) was PCR-amplified using primers PGALFOR (5'-GCGCTCGAGACGGATTAGAAGCC GCCGAGC-3') and TCYCREV (5'-CGGGAGCTCGCAAATTAAAGCCTTCGAGCG-3') using VENT® polymerase (New England Biolabs) and inserted into the 3'T-overhang sites of the cloning vector pCR®2.1 (Invitrogen). Two *Sac* I sites, one introduced by TCYCREV adjacent to the 3' end of T_{CYC1} (underlined) and the other in the multiple cloning site of pCR®2.1, were used to subclone the expression module into the *Sac* I site of YIplac128 (Figure 2.4, Panel A). The P_{GAL1}-*P71*-T_{CYC1} cassette of the resulting plasmid, YIpLacVCAP320, was fully sequenced to confirm that no errors were introduced by PCR. An unique *Cla* I site within the *LEU2* selection marker can be used to create DNA fragments with *LEU2* flanking regions for the integration into the *leu2* chromosomal locus.

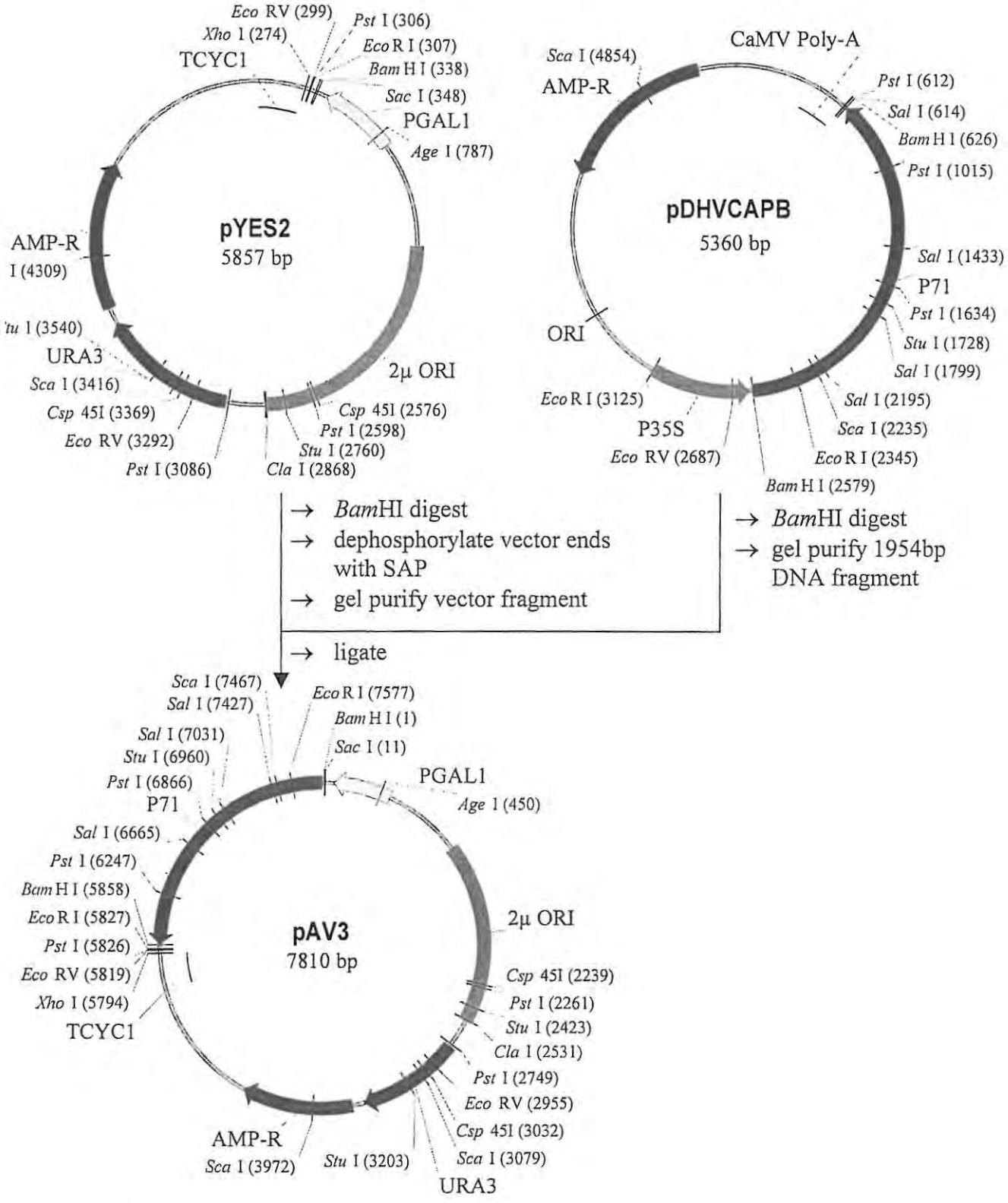

Figure 2.3 Diagrammatic representation of the construction of a multi-copy expression vector for HaSV *P71*.

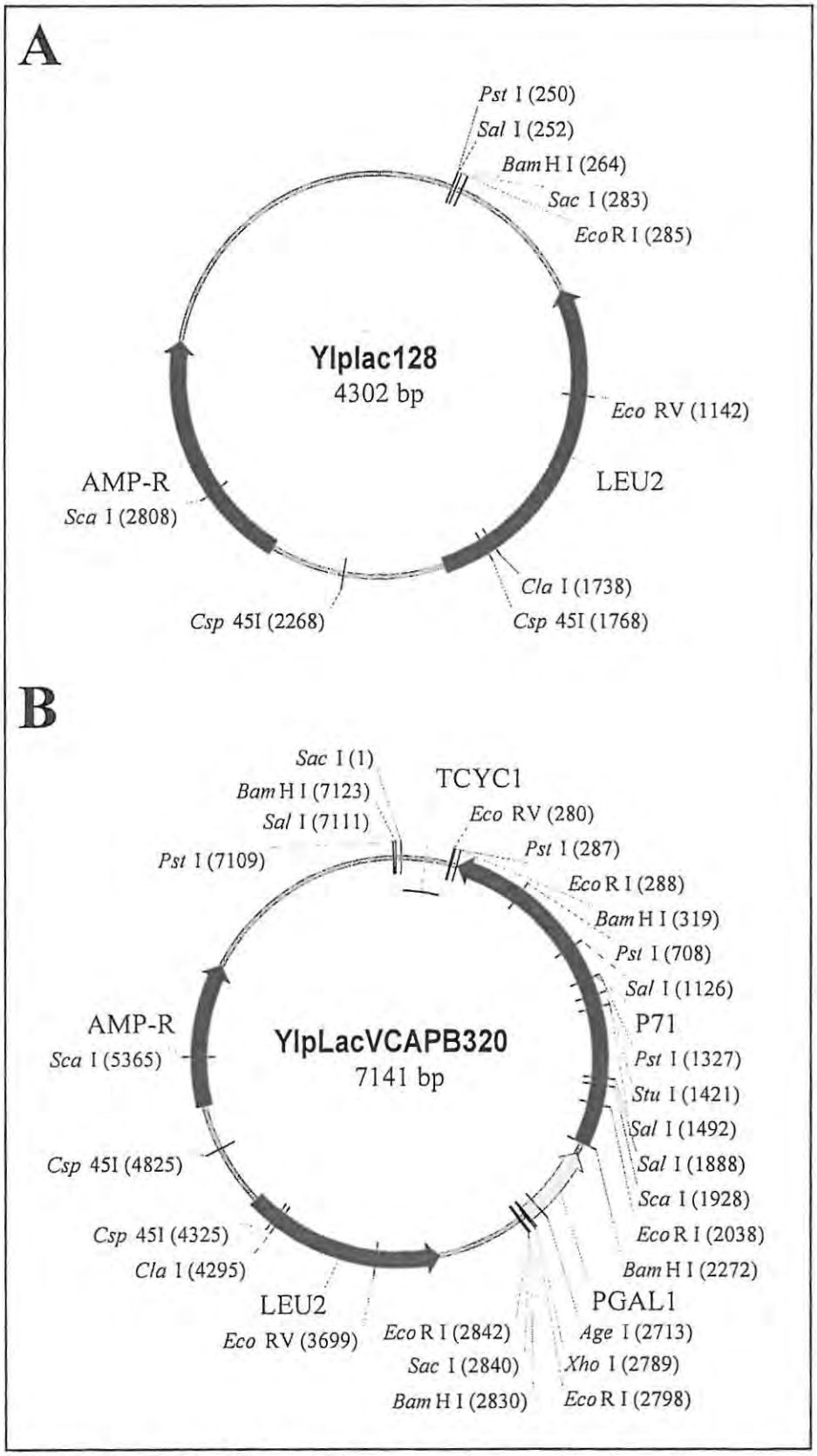

Figure 2.4 The YIpLac128 vector (panel **A**) for chromosomal integration into the *leu2* locus and the YIpLacVCAPB320 vector (panel **B**) for the integration of the P_{GAL1}-*P71*-T_{CYC1} cassette into the *leu2* locus of the yeast chromosome.

2.3 Results and Discussion

2.3.1 Separate expression vector for *P71*

The low probability of *P71* expression from RNA2 transcripts in yeast necessitated the construction of an independent expression cassette for the production of p71 (Figure 2.5). *P71* expression in yeast should result in *P71* mRNA with a 5' untranslated leader sequence that is mainly derived from pYES2 (Figure 2.3), a vector constructed for high-level protein expression in yeast. The leader therefore contains little secondary structure and no runs of G or U nucleotides. The 3 nucleotides directly downstream of the start codon are derived from the plant expression vector pDHVCAPB (Figure 2.3) and place the start codon into the plant consensus context for translation initiation (Gordon, *et al.*, 2001). The yeast and plant consensus sequences are fairly similar with an exception at the -2 position (Table 2.1). This alteration would most probably not have an adverse effect on the translation efficiency because the only alteration to the AUG context that seems to have such an effect is the lack of an A nucleotide at –3 (Romanos *et al.*, 1992).

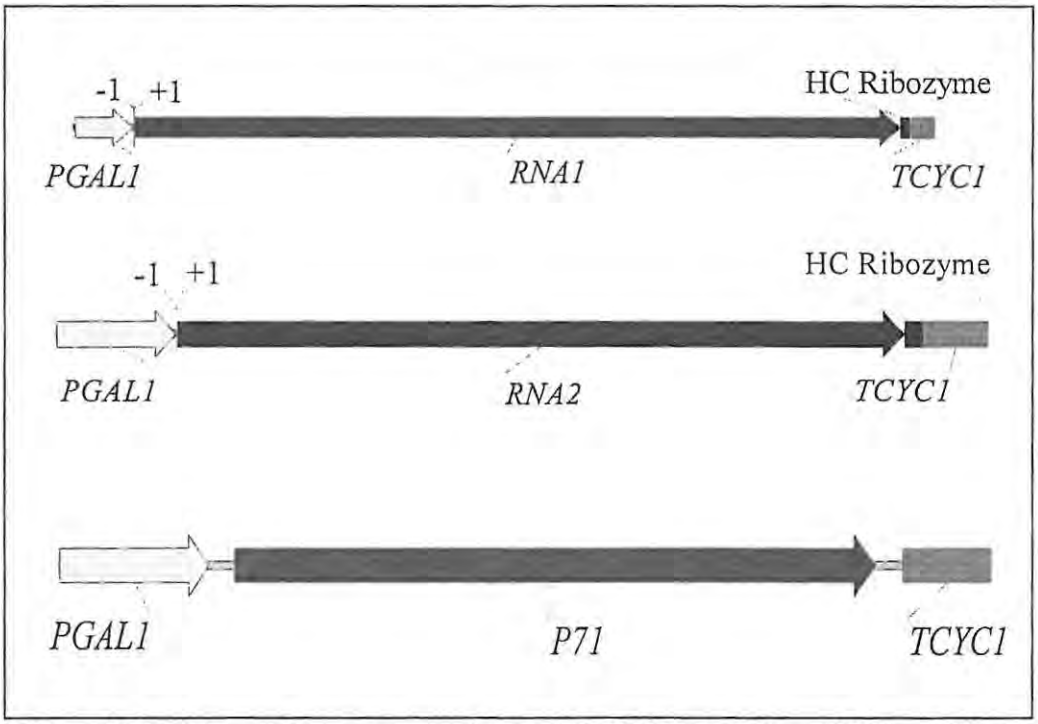

Figure 2.5 Expression cassettes for HaSV *RNA1*, *RNA2* and *P71*. (+1) and (-1) indicates the fusions between the –1 nucleotide of P_{GAL1} and the +1 nucleotides of *RNA1* or *RNA2*. The schematics are not drawn to scale.

2.3.2 Choice of promoter

The expression of *RNA1*, *RNA2* and *P71* was placed under the control of P_{GAL1}, since it is a powerful and tightly regulated promoter. P_{GAL1} is one of three promoters involved in the regulation of *GAL* gene expression that, collectively, drives the expression of 0.3 to 1.5% of

total cellular protein and 0.25 to 1% of total mRNA (Johnston, 1987). P_{GAL1}-driven transcription is also subject to dual control: it is induced by galactose and repressed by glucose. The presence of glucose in a culture medium causes a complete shutdown of expression through carbon catabolite repression (Gancedo, 1998). This allows one to avoid potential toxicity problems during biomass production prior to induction of protein (*P71*) expression.

Table 2.1 Comparison of sequences surrounding the start codons of HaSV RNA2 and *P71* mRNA (transcribed from pAV3) to that of the *S. cerevisiae* translation initiation consensus sequence.

Origin	Sequence around start codon	Leader length
	-4 -3 -2 -1 +1 +2 +3 +4 +5 +6	
S. cerevisiae consensus[1]	A A A A **A U G** U C U or or Y[3] U	~50[2]
P17 (HaSV RNA2)[4]	A U U U **A U G** A G C	282
P71 (HaSV RNA2)[4]	C A G G **A U G** G G A	365
P71 (pAV3)[5]	C A C A **A U G** G G A	134
	-4 -3 -2 -1 +1 +2 +3 +4 +5 +6	

Nucleotides that match *S. cerevisiae* consensus sequence are underlined.
[1] Cigan and Donahue (1987)
[2] Romanos *et al.* (1992)
[3] C/U
[4] Figure A1.2, Appendix 1
[5] Figure 2.3

2.3.3 RNA transcripts that mimic viral RNA

i Plasmids engineered to produce exact 5' termini

Val Hodgson (Department of Biochemistry and Microbiology, Rhodes University) produced exact fusions between P_{GAL1} and the HaSV RNA1 and RNA2 sequences by using reverse PCR. The primers that were used for reverse PCR directed the amplification of linear DNA fragments that should be able to re-ligate to produce plasmids carrying exact fusions between P_{GAL1} and the HaSV genomic RNA sequences. After the re-ligation step, the ligation reactions for the construction of P_{GAL1}-*RNA1* and P_{GAL1}-*RNA2* fusions were transformed into *E. coli* DH5α. Plasmid DNA preparations from the resultant colonies were screened by restriction digests for the absence of DNA fragments separating the P_{GAL1} -1 nucleotide, and RNA1 and RNA2 +1 nucleotides, on the plasmids pVH1 and pMLY3, respectively (pVH1: Figure 2.1; pMLY3:

Figure 2.2). For RNA1, a *Pvu* II / *Xba* I digest of a plasmid that contains the correct fusion would result in 3125 and 1044bp restriction fragments as compared to the 3125, 1013 and 701bp restriction fragments for pVH1 (Figure 2.6, panel A). Likewise, for RNA2 an *Eco* RI / *Pst* I digest would result in a 4904bp restriction fragment as compared to the 4433 and 604bp restriction fragments for pVH1 (Figure 2.6 panel B). Restriction digests of a number of the plasmids that were for screened for correct P_{GAL1}-*RNA1* and P_{GAL1}-*RNA2* fusions produced promising results (indicated by arrows in Figure 2.6).

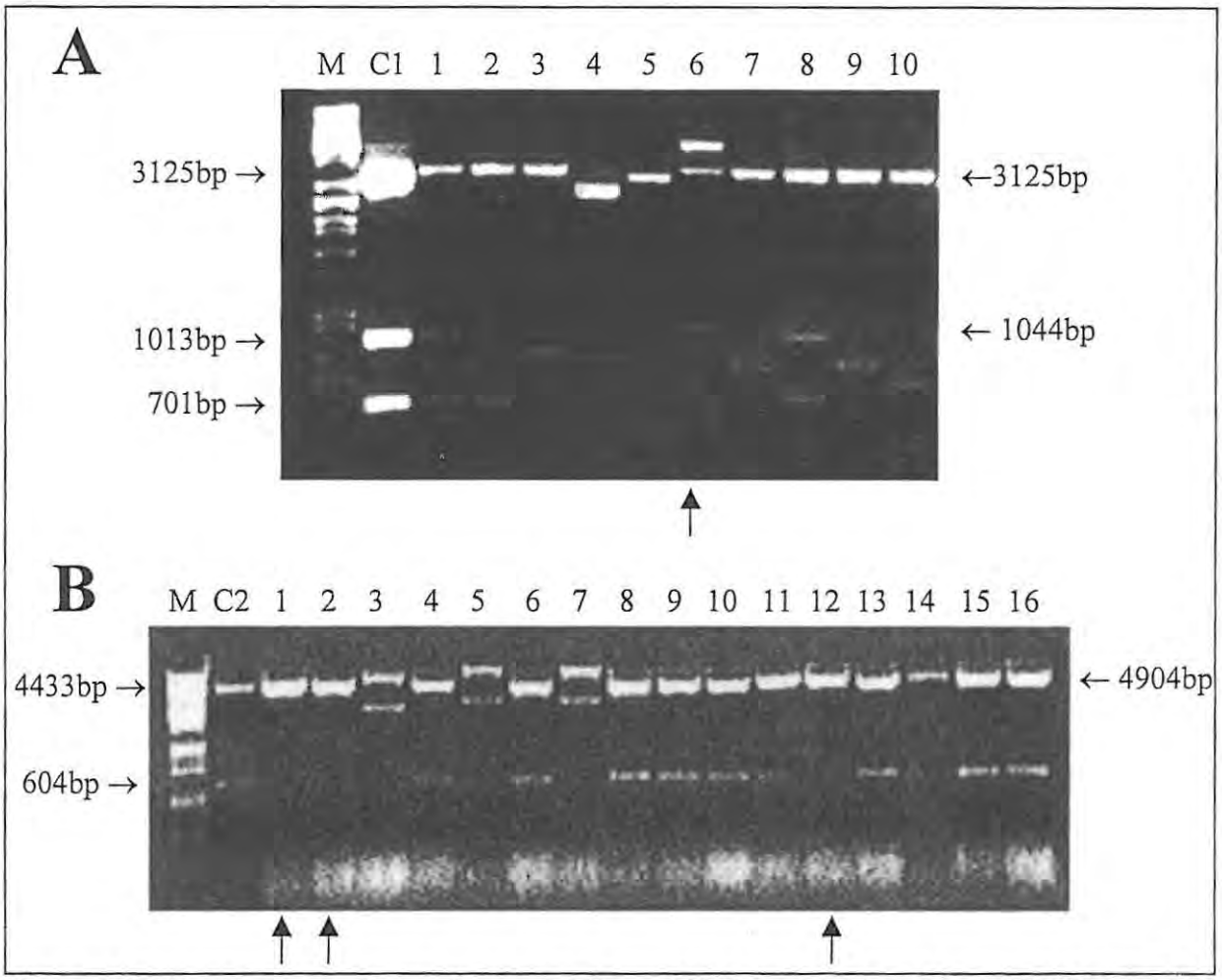

Figure 2.6 Restriction analyses of potential P_{GAL1}-*RNA1* (panel **A**) and P_{GAL1}-*RNA2* (panel **B**) fusion clones. The plasmids were either digested with *Pvu* II and *Xba* I (**A**) or *Eco* RI and *Pst* I (**B**). The restriction fragment sizes for restriction digests of pVH1 (**C1**) (Figure 2.1) and pMLY3 (**C2**) (Figure 2.2) are displayed on the left-hand side of each gel. The expected restriction fragment sizes for restriction digests of potential clones are displayed on the right-hand side of each gel. The up-arrows indicate potential clones. A *Pst* I digest of lambda-DNA was used as a molecular weight marker (**M**). These results were generated by Val Hodgson (Department of Biochemistry and Microbiology, Rhodes University).

The promoter-viral RNA fusion regions of these plasmids were sequenced to verify that the fusions were correct and to establish whether any mutations were introduced through PCR. Manual sequencing results showed that one out of two of the RNA1-derived plasmids that were selected contained the anticipated fusion (pVH4 in Figure 2.1). However, subsequent sequence

analysis of this fusion region in RNA1 expression vector pAV13HC (Figure 2.1) indicated that first G nucleotide of RNA1 was not present (Table 2.2). The erroneous PGAL-RNA1 fusion was prepared by Rachael Blaine (ZENECA Agrochemicals Ltd., Jealott's Hill, UK) (Table 2.2) to produce pAV13HC (G+) (bracketed in Figure 2.1). Automated sequencing results showed that one out of three of the RNA2-derived plasmids that were selected contained the anticipated fusion (pVH5 in Figure 2.2) (Table 2.2).

Table 2.2 Nucleotide sequences around the junctions between P_{GAL1} and the 5' ends of *GAL1*, HaSV *RNA1* and *RNA2*, BMV *RNA3* and FHV *RNA1*

mRNA species	Promoter-RNA junction
GAL1[1]	T G T A A T A A A A G T A T C A A C A A A
HaSV *RNA1* (pAV13HC)	T G T A A T A A A T T C T G C C T C C C C
HaSV *RNA1* (pAV13HC G+)	T G T A A T A A A G T T C T G C C T C C C
HaSV *RNA2*	T G T A A T A A A G T T T T T C T T T A C
BMV *RNA3*[2]	T G T A A T A A A A G T A C G T A A A A T
FHV *RNA1*[3]	T G T A A T A A A A G T A C T G C A G T T

Underline denotes the 5' ends of *GAL1* mRNA cDNA and viral RNA cDNA.
Dotted underline denotes the promoter - viral RNA linkages for BMV and FHV RNA.
Nucleotides in blue font denote transcriptional starts upon *in vivo* transcription in the absence of replication.
[1] Johnson and Davis, 1984
[2] Ishikawa *et al.*, 1997
[3] Price *et al.*, 2000

The transcription initiation sites in the P_{GAL1}-HaSV RNA fusions of pVH4 and pVH5 were designed to be the same as that published for the *GAL1* gene (Table 2.2) (Johnson and Davis, 1984). These fusions are however different to those used for the expression of replicative BMV and FHV RNA transcripts in yeast (Ishikawa *et al.*, 1997; Price *et al.*, 2000). In these studies, the promoter linkages consisted of an additional 5 and 9 nucleotides for BMV and FHV, respectively (dotted underlined nucleotides in Table 2.2). Expression of these fusion constructs in the absence of replication resulted in transcripts with incorrect transcription starts as determined by primer extension analyses (denoted by blue font in Table 2.2). These extended transcripts, however, served as templates for the replication of a much-increased amount of secondary transcripts with exact 5' ends in the presence of the respective viral replicase

enzymes. Other significant results from these experiments were that doublets were obtained at positions -2/-3 and –8/-9, and at positions –6/-7 and –12/-13 for BMV- and FHV-derived transcripts, respectively (Table 2.2). –1/+1 doublets were also obtained for both BMV- and FHV-derived transcripts expressed in the presence of the replicase enzymes. The first member of each of these doublets is most probably representative of a 5'-methylated cap.

It is therefore unlikely that the P_{GAL1}-viral RNA fusions used for the research described in this thesis would result in the exclusive production of RNA transcripts with precise 5' termini in the absence of an active replication system. It is more likely that a heterogeneous transcript population (similar to the ones describe above) would be produced, which would depend on a yeast - or insect-based replication system for the high-level production of secondary transcripts with exact 5' ends. The primary function of these fusions is therefore to produce transcripts with near-perfect 5' ends that would not inhibit replication to the same extent as longer 5' extensions.

ii Plasmids engineered to produce exact 3' termini

To generate transcripts with 3' ends identical to those of viral RNA a *cis*-cleaving ToRSV hairpin cassette (HC) ribozyme was placed directly behind the last nucleotide of viral sequence. This ribozyme was shown to cleave at an efficiency comparable to hammerhead and *Hepatitis delta virus* (HDV) ribozymes when tested *in vivo* (Chowrira *et al.*, 1994). The yeast expression cassettes for *RNA1* and *RNA2* (Figure 2.5) contained identical HaSV RNA - HC ribozyme constructs to the ones used for the expression of HaSV RNA transcripts in plant protoplast (Gordon *et al.*, 2001) (Figure 2.7, panel A). The ribozyme portions in these constructs were based on the minimal wild-type sequence as determined by Hampel *et al.* (1990). The constructs were shown, by means of RNase protection assays, to generate RNA1 and RNA2 transcripts with precise 3' ends in plant protoplasts (Gordon *et al.*, 2001).

An HC ribozyme contains two domains (A and B) that are necessary for its activity (Figure 2.7, panel A). Domain A contains the cleavage site and interacts side by side with domain B to create a buried active site, held together by tertiary contacts (Doherty and Doudna, 2000). This interaction aligns the cleavage site and should result in cleavage at the 5' phosphodiester bond between the 3' terminal nucleotide of HaSV RNA and the following nucleotide (James and Turner, 1995). During cleavage, the 2' hydroxyl of the 5' nucleotide acts as a nucleophile that attacks the adjacent phosphate in the RNA backbone, resulting in cleavage products with 2'3'-cyclic phosphate and 5' hydroxyl termini (Figure 2.7, panel B).

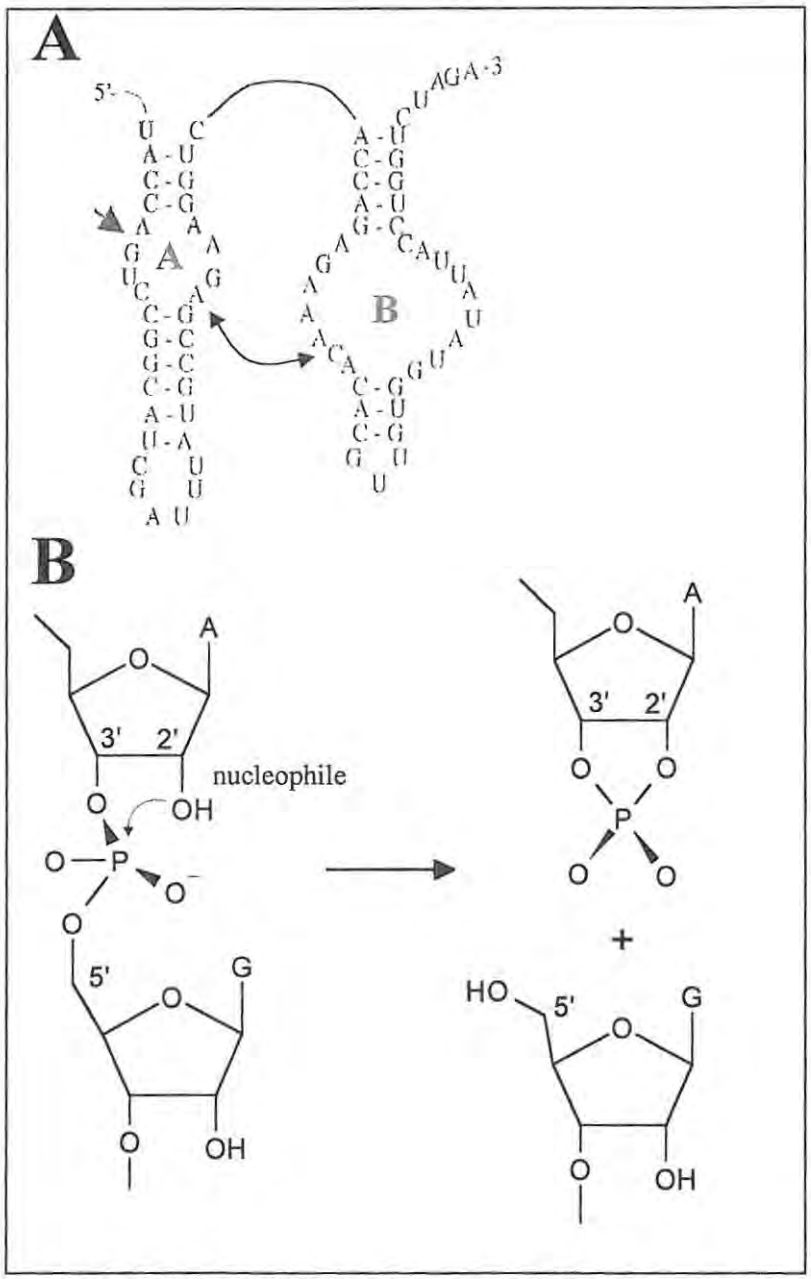

Figure 2.7 **(Panel A)** HC ribozyme used for the generation of HaSV RNA1 and RNA2 transcripts with precise 3' termini. The arrow indicates the site of cleavage and the double-sided arrow the tertiary folding that causes the stacking of domains A (A) and B (B). The viral sequence is indicated with bold script. Adapted from Doherty and Doudna, 2000. **(Panel B)** Mechanism of phosphodiester bond cleavage at the site of cleavage. Adapted from James and Turner (1995).

Combined evidence for successful implications of *cis*-cleaving ribozymes in yeast (Egli and Braus, 1994; Ishikawa *et al.*, 1997; Price *et al.*, 2000) makes it plausible to believe that the HaSV RNA – HC ribozyme constructs described above would be functional. The stability of the cleaved transcripts in yeast could most probably be increased by their 3' terminal tRNA-like structures. According to Hanzlik and Gordon (1997) these structures could have the purpose of replacing poly-A tails for protection against exonucleolytic degradation. Experimental evidence

suggests that *cis*-cleaving ribozymes could be used for the expression of stable RNA transcripts with a cytoplasmic locus in yeast. Ishikawa *et al.* (1997) used an HDV ribozyme for the expression of BMV RNA3 transcripts with precise 3' ends. These transcripts, which also contain 3' terminal tRNA-like structures, were exported to the cytoplasm since they were available for replication by the viral replicase. Price *et al.* (2000) obtained similar results for FHV RNA1 with an HDV ribozyme.

2.3.4 HaSV expression strategy

For the stable expression of HaSV RNA1 and RNA2 transcripts, their respective expression modules were cloned onto *ARS/CEN* vectors carrying the *URA3* and *TRP1* selectable markers (Figure 2.1 and 2.2). The *P71* expression module was cloned into a YIp carrying the *LEU2* selectable marker (Gietz and Sugino, 1988) (Figure 2.4). The *LEU2* selectable marker of this YIp has a unique restriction site that can be cleaved to produce a linear DNA fragment with *LEU2* flanking regions (Lundblad, 1997). This fragment can therefore be integrated via homologous recombination into the *leu2* locus of a mutant yeast strain to produce a $p71^+$ strain. The success of the expression strategy illustrated in Figure 2.8 is limited by the factors that have been considered in this chapter. In accordance with this strategy, chromosomal expression of *P71* and episomal expression of the viral RNAs (from expression modules depicted in Figure 2.5) should direct the assembly of virus particles in the cytoplasm.

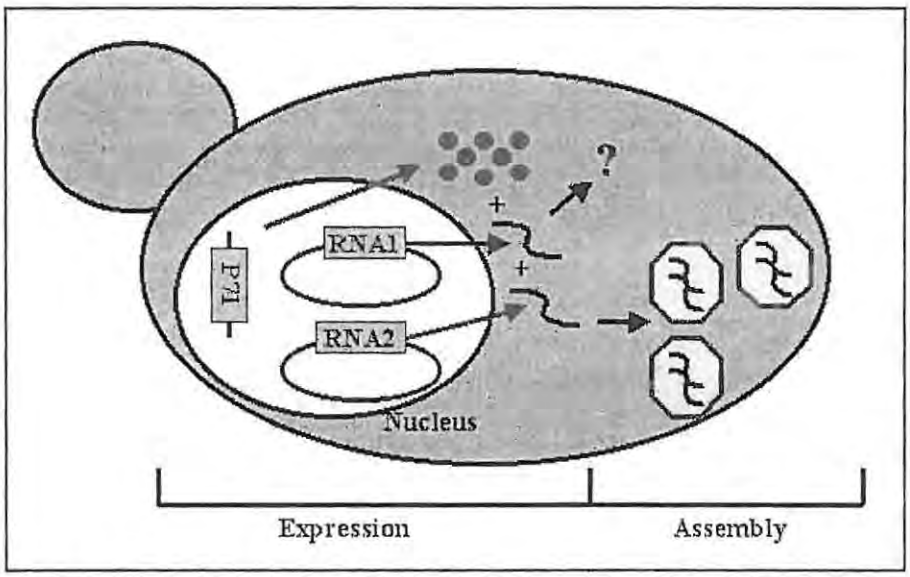

Figure 2.8 A generalized diagrammatic representation of the expression strategy for the non-host production of HaSV in yeast. The question mark symbolizes a potential role of the HaSV replicase in the amplification of RNA1 and RNA2 transcripts.

3 The expression of *P71* in *S. cerevisiae*

3 The expression of *P71* in *S. cerevisiae*

3.1 Introduction

In the previous chapter, it was proposed that mRNA transcribed from the *P71* expression cassette (Figure 2.5) would serve as an efficient template for the translation of this protein in yeast. Protein translation is, however, followed by a number of other steps that form part of the complex multi-step expression process. These steps include the folding and post-translational processing of the newly synthesized polypeptide. In addition to the potential problems relating to expression, certain properties of the final expression product could lead to its instability in yeast.

3.1.1 Polypeptide folding

In *E. coli*, the over-expression of foreign proteins often results in the formation of insoluble complexes, called inclusion bodies, which consist of only certain conformations of folding intermediates of the over-expressed protein (Speed *et al.*, 1996). The solubilization, denaturation and renaturation of these intermediates have proved to be an effective way to purify large quantities of different foreign proteins from *E coli* (Fischer *et al.*, 1993). In contrast with *E. coli*, few problems relating to the folding of over-expressed proteins have been experienced for yeast (Romanos *et al.*, 1992). Binder *et al.* (1991), however, demonstrated that the over-expression of catalase A induces inclusion body formation in yeast, and Weik *et al.* (1998) reported on the denaturation and refolding of yeast-expressed aliin lyase from inclusion bodies.

There is, however, another method for the production of a higher level of protein in its native conformation (apart from *in vitro* renaturation) in the event of an insoluble over-expressed protein. The over-expression of a protein places a high demand on factors required for protein folding to act on abnormally high levels of newly synthesized polypeptides. Inclusion bodies are formed when polypeptides fold incorrectly due to a lower than threshold concentration of these factors. Accordingly, expression conditions conducive to a decreased rate of translation (i.e. a lower growth temperature during induction or a reduced induction rate) could result in a cellular environment that is more favorable for the proper folding of a protein (Nilsson and Anderson, 1991). There are some examples where lower expression rates increased product solubility in yeast. The level of soluble pertactin (a bacterial membrane protein) was increased 10-fold as a result of a decreased expression rate in *Pichia pastoris* (Romanos *et al.*,

1991). In addition, a much greater proportion of hepatitis B surface antigen particles were purified from *P. pastoris* when produced in a strain that grew slowly during induction (Cregg *et al.*, 1987).

3.1.2 Post-translational processing

In yeast, all the different forms of posttranslational processing generally occur in a manner similar to that of higher eukaryotes (Romanos *et al.*, 1992). Two types of amino-terminal modifications occur: removal of the N-terminal Met residue (catalyzed by methionine aminopeptidase) and N-acetylation (catalyzed by N^{α}-acetyltransferase). There is a preference for Ser as the second residue in yeast proteins (Romanos *et al.*, 1992). This is indicative of the N-end rule for *S. cerevisiae* whereby certain "destabilizing" residues at the N-terminal ends of proteins targets them for degradation by the ubiquitin pathway (Finley, 1992). Destabilizing residues are penultimate amino acids that are either defined as charged (type I) or bulky (type II). This rule is however limited in its application, because methionine aminopeptidase only cleaves if the second residue is of the stabilizing kind. Accordingly, most cytosolic proteins have stabilizing N-terminal residues. It would therefore be expected that the N-terminal Met residue of p71 would be cleaved off, because a Gly residue, which is classified as a stabilizing type (type III), follows it (GGA codon for Gly in Table 2.1). It is unclear whether p71 will be N^{α}-acetylated in yeast. It is however safe to assume that it will be processed in a way that is similar to that in insect cells, because the rules governing acetylation seem to be conserved among eukaryotes (Romanos *et al.*, 1992).

3.1.3 Protein stability

Heterologously expressed proteins could be degraded endogenously through the ubiquitin pathway as a result of their instability (as defined by the N-end rule and other factors), toxicity to the cell, or tendency to form insoluble protein aggregates (or inclusion bodies) (Finley, 1992). In these instances, 76-residue ubiquitin molecules are covalently attached to specific lysine residues on these proteins. More ubiquitin molecules are thereafter linked to the Lys-48 residues of the attached ubiquitin molecules to form extended ubiquitin chains. The resulting "multi-ubiquinated proteins" are then the targets for the rapid proteolytic breakdown by yeast proteasome enzymes. According to Romanos *et al.* (1992) intracellular proteolysis could be reduced by (i) inducing at a lower temperature, (ii) harvesting at exponential growth phase, (iii) using protease inhibitors during extraction and (iv) using a rapidly induced promoter.

Vacuolar proteases do not pose a problem for foreign proteins within the cell, because they only degrade stable proteins ($t_{1/2}$ = approximately 160 hours) and there are endogenous protease inhibitors for them (Jazwinski, 1990). These proteases are predominately responsible

for the proteolytic activities in yeast protein extracts (Jones, 1991). According to Jazwinski (1990) there are three types of vacuolar proteases: A, B and C. Protease A is an acid-protease that could be inactivated to a great extent by maintaining the pH above 6. Proteases B and C are serine proteases and could therefore be inactivated by the presence of serine protease inhibitors. For optimal yields of a heterologously expressed protein it is however advisable to use as wide a range of protease inhibitors as possible.

The objective of the work described in this chapter was to develop a yeast expression system for the high-level production of HaSV capsid protein in its native form. This would, in turn, increase the likelihood for the assembly of HaSV VLPs. The effect of a number of factors, which could increase the production of native protein in a yeast expression system, will be described. These include expression conditions (e.g. strains used, expression loci and expression rate) and protein extract preparation (e.g. the presence of various protease inhibitors and salt concentrations).

3.2 Materials and methods

Recipes for the preparation of complex (YPD) and supplemented minimal media (SMM), which was used for selection of plasmid-containing yeast strains, are described in Appendix 7. All the yeasts strains that were used for this study are listed in Table A6.1 (Appendix 6).

3.2.1 Construction of YIps for *RNA2* and *P71*

To draw a comparison between the respective efficiencies for the production of p71 from *RNA2* and *P71* expression cassettes (Figure 2.5), YIps were constructed for the chromosomal expression of *RNA2* and *P71*.

***RNA2*:** The plasmid 5.66/5(G+) (constructed by Rachel Blaine from Syngenta, Jealott's Hill Research Station, Berkshire, UK) is an intermediate construct for the cloning of a YIp for RNA1 that directs the transcription of RNA1 molecules with precise 5' ends. A 2056bp DNA fragment harboring P_{GAL1} fused to the 5' end of *RNA1* was subcloned from 5.66/5(G+) into YipLac204 to produce YipLac204/5.66(G+) (Figure 3.1, Step I). An unique *Age* I restriction site within P_{GAL1} was used to swap an *Age* I – *Kpn* I fragment carrying the 3' end of P_{GAL1} fused to the 5' end of *RNA1* for a 3213bp *Age* I – *Kpn* I fragment carrying the *RNA2* expression module of pAV14HPTrp (Figure 3.1, Step II). The resulting plasmid, YipLac204/HaSVRNA2, was used for the chromosomal expression of *RNA2* in yeast.

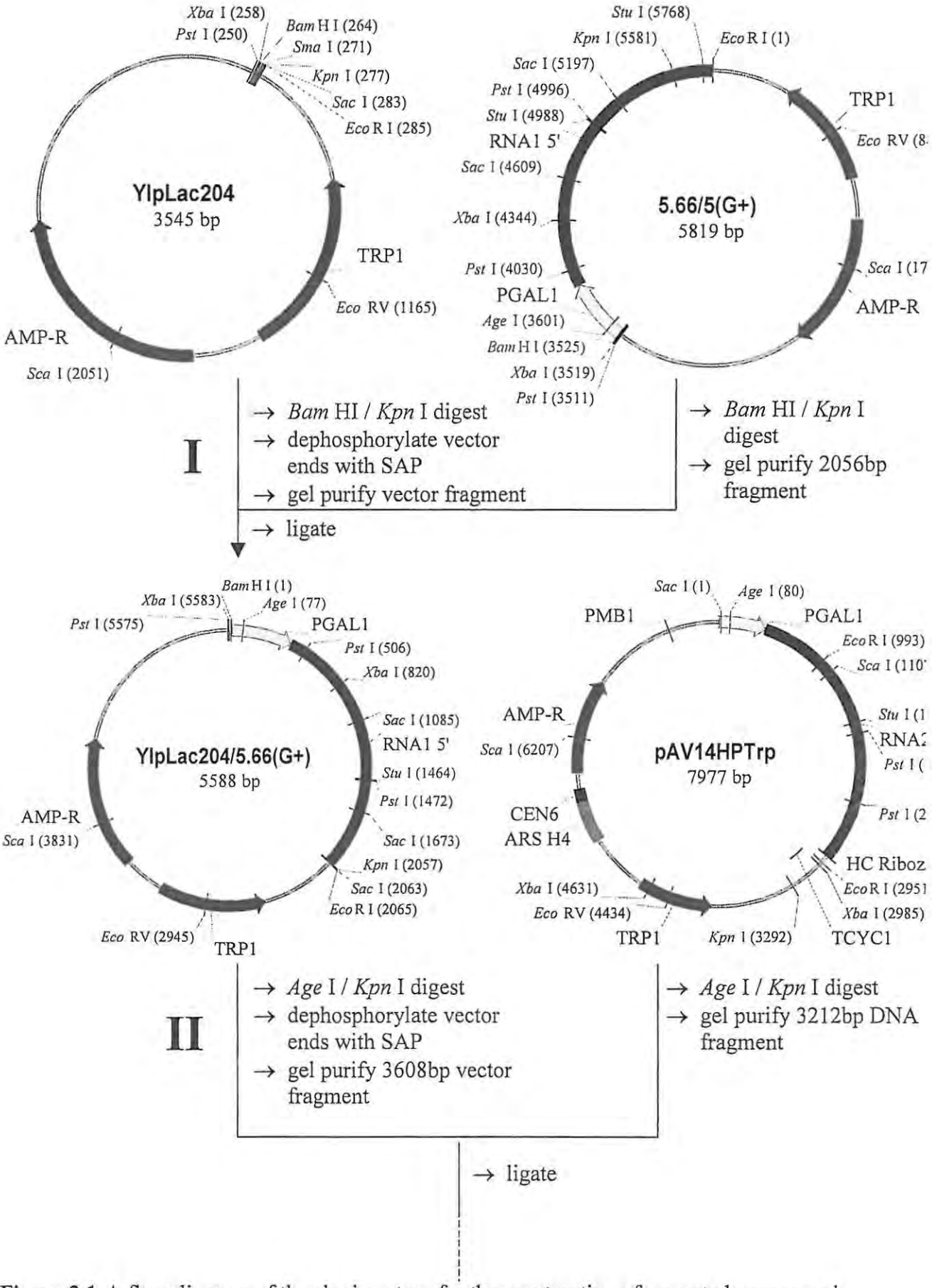

Figure 3.1 A flow diagram of the cloning steps for the construction of a yeast chromosomal integration vector for the expression of *RNA2*.

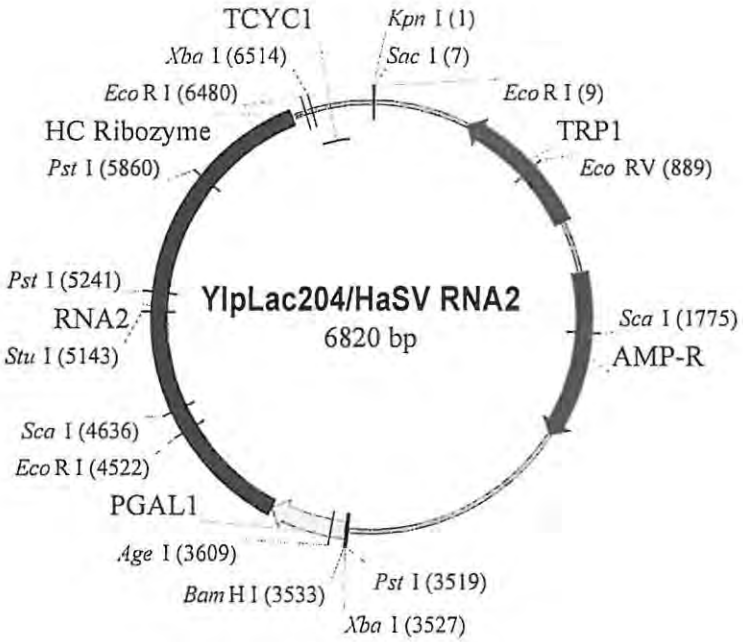

Figure 3.1 **Continued...**

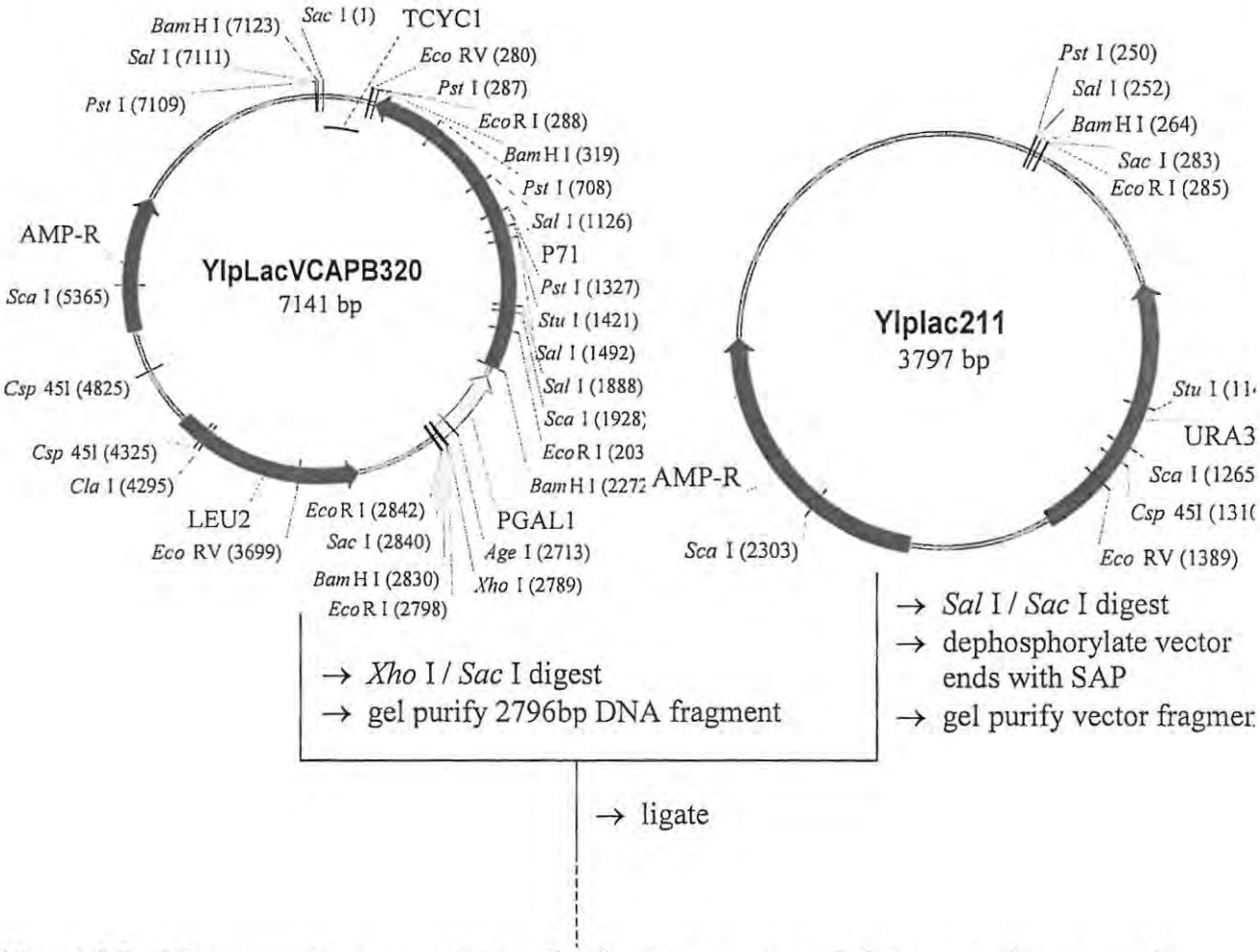

Figure 3.2 Diagrammatic representation for the construction of the yeast chromosomal integration vector pMJ2 for the expression of *P71*.

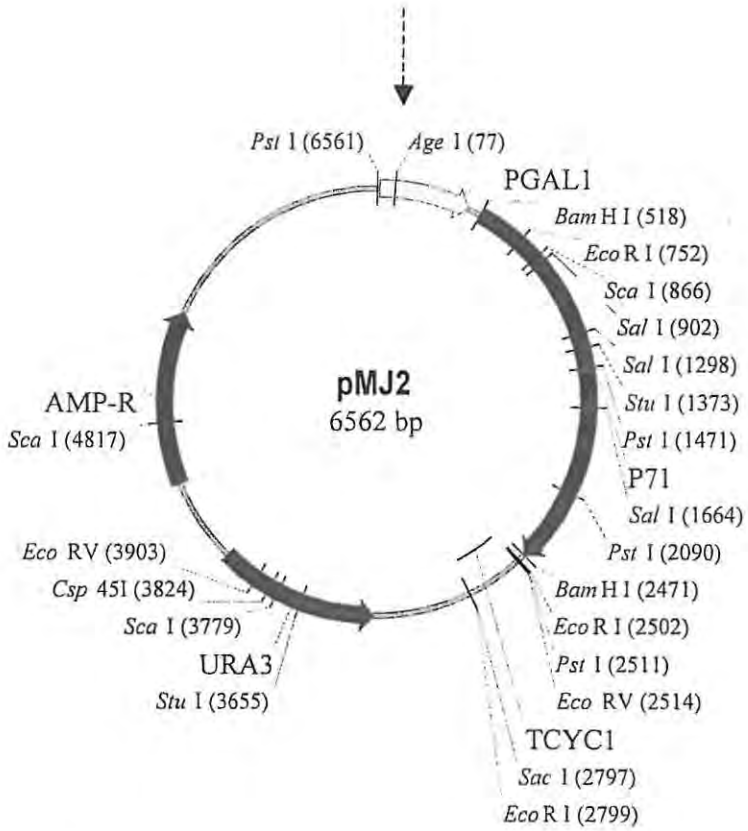

Figure 3.2 Continued...

P71: The P_{GAL1}-*P71*-T_{CYC1} cassette was subcloned from YIpLacVCAP320 into YipLac211, which carries the *URA3* selection marker, to produce pMJ2 (Figure 3.2). This plasmid can be linearized by a *Csp* 45I restriction digest for integration into the *ura3* chromosomal locus.

3.2.2 Yeast transformations

The yeast strains INVSc1 (Invitrogen) and JRY188 were used for the expression of *P71* (Table A6.1, Appendix 6). Plasmids were transformed into these strains using the Frozen-EZ Yeast Transformation II kit (Zymo Research). For the selection of transformants, amino acids or uracil were omitted from the SMM used to select for transformants

3.2.3 Generation of yeast strains for the chromosomal expression of *P71* and *RNA2*

YIps were digested at unique restriction sites within selection marker genes to produce DNA fragments that could integrate into the chromosomal mutant allele of the respective selection markers used. These fragments were transformed into INVSc1, JRY188 or strains that were generated during the course of this study. A list of these strains and their respective genotypes are displayed in Table A6.1 (Appendix 6). The YIps that were used for the generation of each of these strains are also listed. *Cla* I was used to linearize YipLac128 (Figure 2.4) and YIplacVCAP320 (Figure 2.4), while *Csp* 45I was used to linearize pMJ2 (Figure 3.2).

Eco RV was used to linearize all the other YIps that were used in this study. The presence of *P71* chromosomal expression modules in the strains INVSc1 3#20.1 and JRY188 3#20.1 was verified by Western analyses of protein extracts from cells induced for *P71* expression. The presence of *RNA2* chromosomal expression modules was verified using PCR amplification of yeast genomic DNA.

3.2.4 Growth characteristics of yeast in batch culture

INVSc1 cells were inoculated into 400ml SMM containing 2% glucose. The culture was incubated at 30 °C, shaking at a speed of 200rpm. 10ml aliquots were taken at various time intervals and the OD_{600nm} (UNICAM Helios Alpha spectrophotometer) and cell count (using a hemocytometer) of each aliquot was determined.

3.2.5 Confirmation of episomal expression of *P71*

Uracil was omitted from SMM when appropriate to maintain selection for pAV3 or pYES2. The cells were grown at 30°C in SMM containing 2% glucose up to mid log phase (OD_{600nm} of approximately 0.5), centrifuged for 10 min at 4000rpm in a Beckman JA20 rotor and resuspended in SMM containing either 2% galactose or 2% raffinose. The cells were then grown for a further 4h at 30°C and harvested as described above. Yeast protein extractions were carried out by vortexing in the presence of glass beads as described in Section A8.1 (Appendix 8).

3.2.6 Testing yeast strains for chromosomal expression of *P71*

Putative $P71^+$ strains were transferred from agar plates to Eppendorf tubes containing 1ml sterile ddH_20 and the OD_{600nm} values of these cell suspensions were determined. A volume of each of these suspensions was added to 5ml YPD medium to make the OD_{600nm} approximately 0.5. The strains were grown in YPD medium containing either 2% glucose or 2% galactose for 4 hours at 30°C. The cultures were then centrifuged as described above, and yeast protein extractions were carried out as described in Section A8.1 (Appendix 8).

3.2.7 Protein analysis

The protein concentration of samples was estimated using the Bradford protein assay (Smith, 1988). BSA was used as a protein standard and protein standard curves (with R^2 values of at least 0.99) were generated for each protein determination. Protein samples were subjected to SDS-PAGE in 7.5% polyacrylamide gels according to the procedure of Laemmli (1970). Electrophoretic transfer to Hybond-C+ membranes (Amersham) and immunoblot processing was according to Towbin *et al.* (1979). Premixed protein molecular weight markers from Roche were used for molecular weight estimation of bands visualized on gels (stained with

Coomassie Brilliant Blue R250 from Sigma) and membranes (stained with Ponceau-S, as described by Sambrook *et al.*, 1989). The Chemiluminescence Western Blotting Kit (Roche) was used for immunological detection.

The anti-HaSV antiserum used for preliminary experiments was obtained from Karl Gordon and Terry Hanzlik (CSIRO Entomology, Canberra, ACT, Australia). This antiserum interacted nonspecifically to yeast proteins and was preadsorbed with yeast cell lysates as follows. The yeast cell lysate was prepared from 250ml INVScI cells grown in SMM to an OD_{600nm} of 0.5. The cells were centrifuged for 10min at 3000rpm in a Beckman JA14 rotor and resuspended in 6ml 50mM Tris-HCl buffer (pH 7.4) with 1mM phenylmethyl-sulfonyl fluoride (PMSF) and 1mM DTT. The resuspended cells were transferred to a JA20 centrifuge tube and 6 g of 0.2mm acid-washed glass beads (Section A8.2, Appendix 8) were added. Cell disruption was carried out by vortexing for 30 sec periods with 30 sec intervals (on ice) and a total homogenization time of 5 min. The lysate was diluted 3.3-fold with Tris-HCl buffer and centrifuged at 12500rpm for 15 min at 4°C in a Beckman JA20 rotor. For preadsorption, the antiserum was incubated for 1 hour at room temperature in 1ml of the supernatant from the previous centrifugation step, which contained 0.25% total yeast protein. This mixture was thereafter diluted in 0.1M Tris-HCl (pH 7.6) containing 0.15 M NaCl, 1% BSA and 0.5% Tween 20, and added to the blot for the primary antibody immunodetection step.

Three antibody preparations, two polyclonal (HaSV-RB1 IgG and HaSV-RB2 IgG) and one monoclonal (HaSV-35), with little or no cross-reactivity with yeast proteins were obtained from Andrew Dinsmore (Syngenta, Jealott's Hill Research Station, Berkshire, UK).

3.2.8 Preparation of soluble protein fractions

After induction, 30µl of ice-cold 50mM Tris-HCl (pH 7.4) containing 1mM DTT and 1mM 4-(2-aminoethyl)-benzenesulfonyl fluoride (AEBSF) (Roche Molecular Biochemicals) were added to every 2 OD_{600nm} units of yeast cells. The cells were vortexed with 0.1g glass beads for 30 sec periods with 30 sec intervals (on ice) and a total homogenization time of 5 min. 20 to 40µl of the protein extracts were transferred to Eppendorf tubes and 2.3 volumes of 50mM Tris buffer were added to the remainder. The homogenates were briefly vortexed and then microfuged for 5 min. 5× SDS-PAGE loading buffer was added to each of the yeast protein extracts and supernatant fractions. An equivalent volume of 50mM Tris buffer to that of each supernatant fraction and 5 × SDS-PAGE loading buffer were added to the pellets. The protein extracts, supernatants (or soluble fractions) and pellets (or insoluble fractions) were separated on SDS-PAGE and transferred electrophoretically to nitrocellulose membranes for immunoblotting.

3.2.9 PCR analysis of genomic DNA

To verify that *RNA2* expression modules were integrated into yeast genomic DNA, approximately 1µg of yeast chromosomal DNA preparations (extracted as described in Section 8.3, Appendix 8) was used as a template for PCR with the primers RNA2F3 (corresponding to nucleotides 52 – 72 of RNA2) and RNA2R2 (complementary to nucleotides 530 – 550 of RNA2). The Expand™ High Fidelity PCR System (Roche) was used for these reactions and the parameters described for Programme 2 (Appendix 5) were used for thermal cycling.

3.3 Results

3.3.1 Growth of INVScI cells in batch culture in SMM

It was necessary to characterize growth of INVScI cells in SMM to determine when the cells were in exponential growth phase for induction of *P71* expression. This characterization would also provide the strain's generation time, which could be used to estimate the time required for a culture to reach mid-log phase. OD_{600nm} values were correlated with the number of cells per milliliter using a hemocytometer.

A growth curve for INVScI demonstrated that mid-log phase was reached at an OD_{600} value of approximately 0.5 (Figure 3.3, panel A). According to a correlation between OD_{600nm} and cell counts per milliliter (Figure 3.3, panel B), this equates to a concentration of 3×10^7 cells/ml. The generation time of this strain was estimated as 2.7hrs from the portion of the growth curve that represented exponential growth (which had an r^2 value of 0.965).

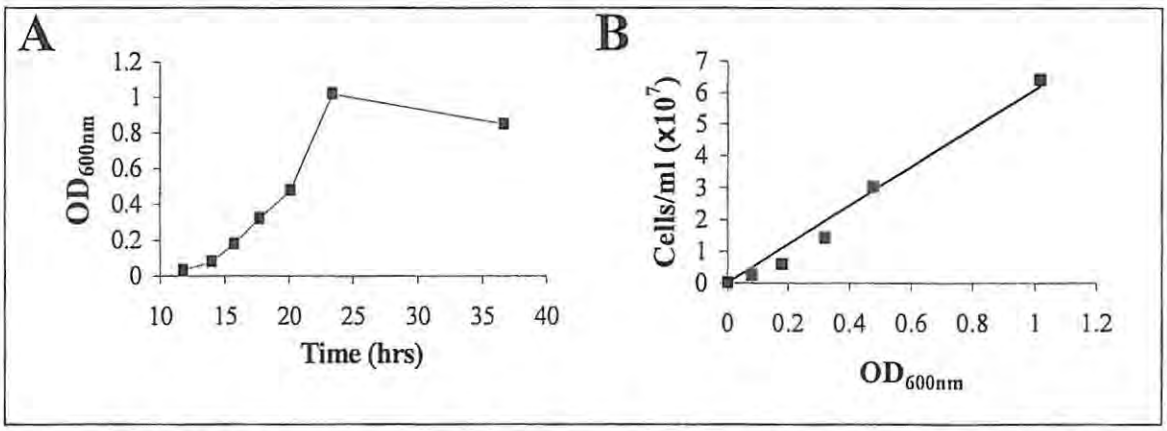

Figure 3.3 (**A**) Growth curve for the yeast strain INVScI in SMM. The growth conditions are described in Section 3.2.4. (**B**) Correlation between OD_{600nm} and the concentration of cells in the culture. ($r^2 = 0.975$)

3.3.2 Episomal expression of *P71*

To determine whether P_{GAL1} driven expression of *P71* was occurring, total protein extracts from induced and uninduced INVSc1 cells, transformed with either pYES2 (Figure 2.3) or pAV3 (Figure 2.3), were separated on 10% SDS-PAGE gels. Staining of one of these gels with Coomassie R-250 showed that the band intensities in the different lanes were equivalent, indicating that the same amount of protein was loaded in each lane (Figure 3.4, panel A). No protein bands of the expected sizes were however detected for cells that were induced for the expression of *P71*. The proteins were electroblotted to a nitrocellulose membrane and probed with anti-HaSV antiserum, which was preadsorbed with a yeast cell lysate to reduce cross-reaction with yeast proteins. This preadsorption technique did not eliminate cross reactivity, because a number of proteins with M_R-values smaller than 64 kDa were detected in extracts from cells that were not induced for the *P71* expression (lanes 1 – 3 in Figure 3.4, panel B). A protein that migrated at a M_R of 71kDa was, however, exclusively detected in induced INVSc1 cells transformed with pAV3 (lane 4 in Figure 3.4, panel B). In addition, a very low level of a protein co-migrating with p64 from wild-type virus was detected.

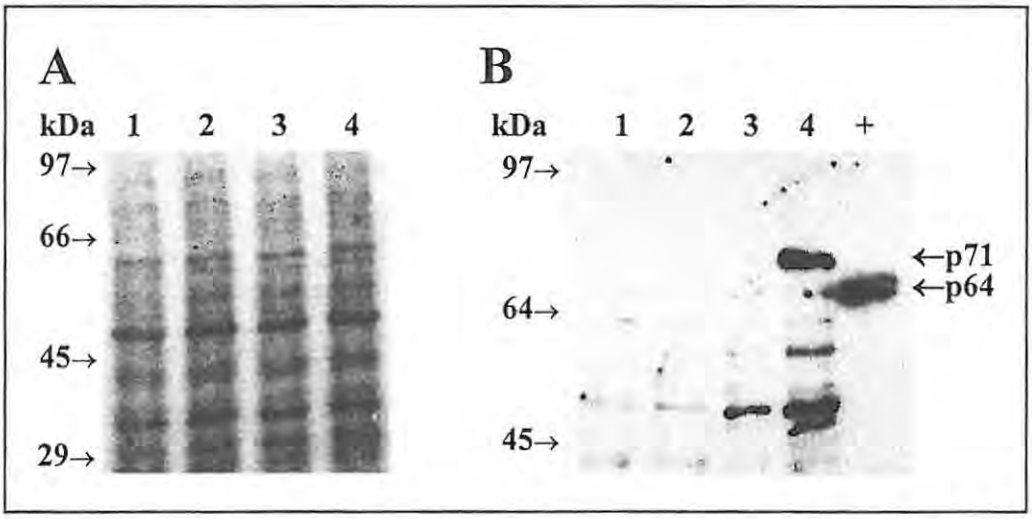

Figure 3.4 Coomassie-stained gel (panel **A**) and Western analysis (panel **B**) of total protein extracts from yeast cells. The blot in panel B was probed with anti-HaSV polyclonal antibodies preadsorbed with yeast cell lysate. INVScI cells were transformed with either pYES2 (lanes 1 and 2) or pAV3 (lanes 3 and 4), and grown in either raffinose (lanes 1 and 3) or galactose (lanes 2 and 4) during the induction phase. (+), 5ng wild-type HaSV.

3.3.3 Chromosomal expression of *P71*

After the transformation of linear YIplacVCAP320 (Figure 3.2) fragments into JRY188, four of the transformants (designated as strains 3#20.1, 2#37.1, 1#41.1 and 2#54.1) were tested for the presence of *P71* chromosomal expression modules. P_{GAL1}-dependent *P71* expression was either induced or repressed by the presence of galactose or glucose as the sole carbon source,

respectively. Protein extracts from these strains were run on 10% SDS-PAGE gels and examined for the presence of p71 by Western analysis (Figure 3.5). Two new anti-HaSV antibodies, which were specially selected as detection antibodies for yeast expression experiments, were also tested in this experiment. The blots were probed with either a polyclonal (HaSV-RB2 IgG) or a monoclonal (HaSV-35) antibody.

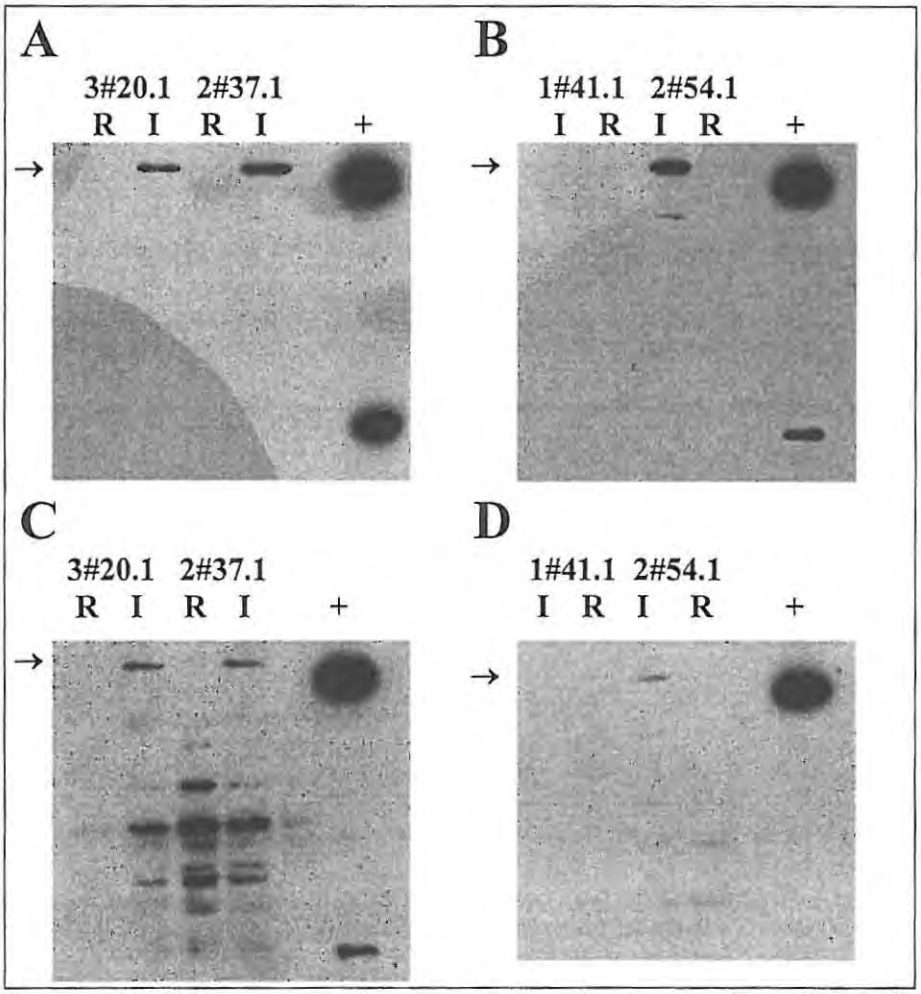

Figure 3.5 Western analysis of total protein extracts from JRY188 3#20.1, 2#37.1, 1#41.1, and 2#54.1 cells. *P71* expression was either galactose induced (**I**) or glucose repressed (**R**). The blots were probed with the antibodies HaSV-RB2 IgG (panels **A** and **B**) or HaSV-35 (panels **C** and **D**). The arrows identify bands that migrate at a similar molecular weight as p71. (+), 5ng wild-type HaSV. Taken from Venter (1998).

The cross-reactivity with yeast proteins for HaSV–35 (Figure 3.5, panels C and D) and absence thereof for HaSV-RB2 IgG (Figure 3.5, panels A and B) was unexpected. HaSV-35 interacted with several proteins that migrated at molecular weights lower than that of the HaSV capsid proteins in cell extracts from uninduced yeast cells. Both the antibodies, however, interacted with a protein that migrated at a molecular weight of approximately 71kDa for protein extracts from JRY188 3#20.1, 2#37.1 and 2#54.1 cells that were grown in

galactose during the induction stage. No p71 was however detected by either of these antibodies for the 1#41.1 strain. P_{GAL1}-directed expression of *P71* in the 3#20.1, 2#37.1 and 2#54.1 strains resulted predominately in the production of p71 since no p64 was detected for any of these strains. HaSV-RB2 IgG detected a smaller protein with an MR of approximately 55 kDa in extracts from the latter strains subsequent to growth in galactose (Figure 3.5, panels A and B). This protein, which was detected in all the other western analyses described in this chapter, was probably a proteolytic degradation product of p71.

This result is similar to that described above for the production of p71 in INVSc1 cells transformed with pAV3. HaSV-RB2 IgG was used for further Western analyses due to its superior specificity to yeast expressed p71. The JRY188 3#20.1 strain was in turn selected for subsequent expression experiments.

3.3.4 The effect of induction period on *P71* expression

The effect of induction period on p71 production was examined for JRY188 3#20.1 cells over 48 hours (Figure 3.6, panel A). Protein production increased with time, with maximal production at 12 hours post induction (hpi). No protein could, however, be detected after 12 hours.

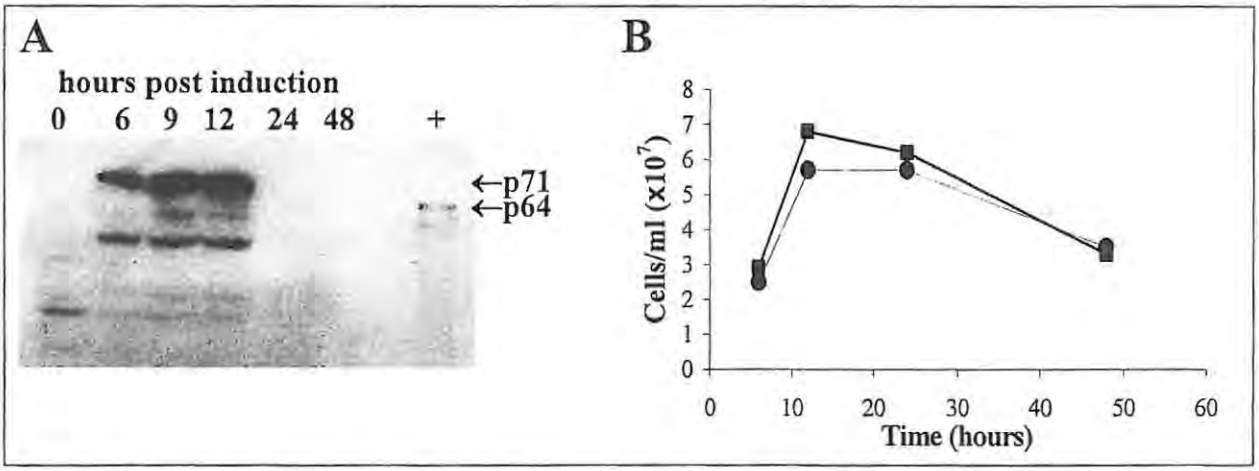

Figure 3.6 (**A**) Western analysis of protein extracts from JRY188 3#20.1 cells that were grown at 30°C in SMM containing 2% galactose for 0-48h for the induction of *P71* expression. (+), 1ng wild-type HaSV. (**B**) Graph comparing cell counts from JRY188 3#20.1 cultures that were either plated out on plates containing (■), or not containing (●), L-leucine during the 48 hour induction period for *P71* expression (Taken from Jiwaji, 1999).

Several possible explanations could account for the disappearance of *P71* from JRY188 3#20.1 cells at 12 hpi. Since integration of YipLac128 into the *LEU2* locus results in duplication of the *LEU2* sequence, selective pressure against *P71* expression could result in loss of the *P71* expression module through homologous recombination (Romanos *et al.*, 1992). After induction, cells were plated onto SMM either containing, or not containing, L-

leucine to look for the progressive loss of the Leu^+ phenotype during induction (Jiwaji, 1999). There was no significant difference in the number of colonies on both sets of plates, even at 48 hpi (Figure 3.6, panel B), indicating that no loss of *LEU2* occurred. The possibilities of lethality of *P71* expression or transcriptional repression were excluded since no difference in growth rate was detected between JRY188 and JRY188 3#20.1 in SMM containing galactose.

3.3.5 Optimization of soluble p71 levels

The growth conditions described for the preparation of yeast cell lysates (SMM containing 2% galactose and induction at 30°C for 4 hours) resulted in the expression of insoluble p71, as most of this protein was found in the pellet fractions when cell lysates were microfuged for 5 min (results not shown). Experiments were therefore designed to determine whether or not a decrease in the rate of *P71* expression would increase protein solubility. Two factors that would bring about reduced expression rate were tested: a reduction in the galactose concentration and a decreased incubation temperature during the induction period.

P_{GAL1}-driven expression was very sensitive to galactose concentration since p71 was detected at the lowest concentration tested (0.01%) (Jiwaji, 1999) (Figure 3.7). The amount of p71 produced reached a maximum at a concentration of 0.1%, and seemed to taper off at higher concentrations. 0.01% galactose was used for further expression experiments.

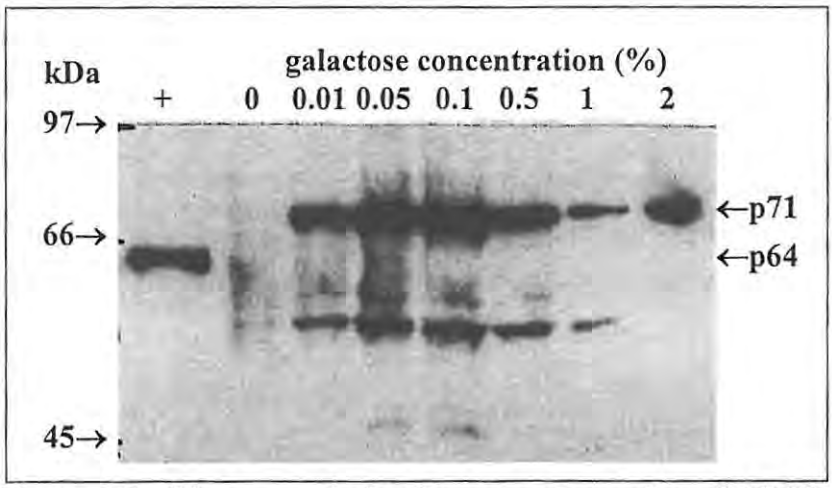

Figure 3.7 Western analysis of protein extracts from JRY188 3#20.1 cells that were grown in different galactose concentrations for 4 hours. (+), 1ng wild-type HaSV. Taken from Jiwaji (1999).

In the experiments described up to this point, cells were grown with 2% glucose prior to induction (according to the protocol in Section 3.2.5). After the addition of galactose, it takes 3 to 5 hours for the glucose to be depleted from these cells before expression was initiated (Johnston, 1987). An alternative is to grow the cells on a non-catabolite repressing source (5% glycerol and 0.1% glucose) before induction. There are two advantages for this strategy:

no centrifugation steps for the purpose of media changes are necessary and the cells become induced within 10 – 20 min after the addition of galactose (Johnston, 1987).

This was confirmed by the detection of p71 after only 1 hour when cells were grown on the optimal galactose concentration (0.1%) at 30°C (Jiwaji, 1999) (Figure 3.8, panel A). *P71* expression was at a maximum 2-4 hpi and decreased until nothing was detected 16 hpi. The disappearance of p71 after prolonged expression is in agreement with the results displayed in Figure 3.6 (panel A). The "window period" for p71 production was however shifted to a stretch of time that was closer to the onset of induction (Jiwaji, 1999). This shift is due to a reduced lag-period in which P_{GAL1}-dependent expression was repressed. The lag period increased upon decreasing the galactose concentration from 0.1 to 0.01% (Figure 3.8, panels A and B), and increased even further when the growth temperature was reduced (Figure 3.8, panels C and D).

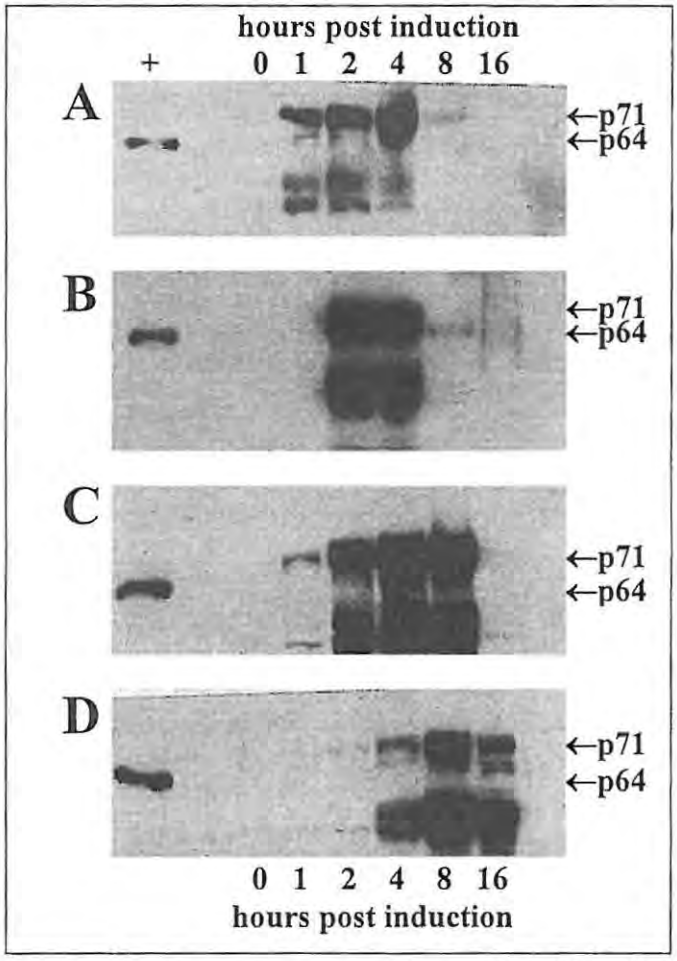

Figure 3.8 Western analysis of protein extracts from JRY188 3#20.1 cells that were grown in SMM containing 0.1% galactose at 30°C (panel **A**), 0.01% galactose at 30°C (panel **B**), 0.01% galactose at 25°C (panel **C**) or 0.01% galactose at 20°C (panel **D**) for 0-16 hours during induction. The cells were grown on 5% glycerol and 0.01% glucose at 30°C prior to the addition of galactose. (+), 1ng wild-type HaSV. Taken from Jiwaji (1999).

The solubility of the p71 production within the "window periods" for growth at 20°C and 25°C was tested (Jiwaji, 1999). Western analyses of protein extracts, soluble fractions and insoluble fractions of samples within the respective "window periods" demonstrated that proteins, which interacted with HaSV antibodies, were only detected in the soluble fractions for 8- and 16-hpi at 20°C (Figure 3.9). The 8-hpi fraction showed a more prominent protein band at 71kDa than at 64kDa, while the 16-hpi fraction showed a more prominent band at 64kDa. Numerous proteolytic-breakdown products were however detected for both these soluble fractions.

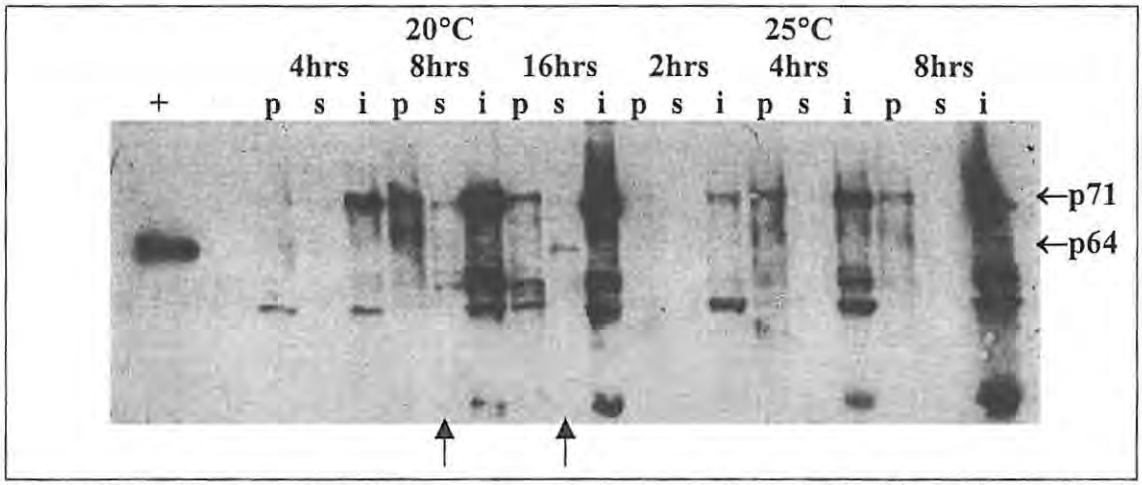

Figure 3.9 Western analysis of total protein extracts (**p**), soluble (**s**) and insoluble (**i**) fractions from JRY188 3#20.1 cells that were induced for different time periods at either 20°C or 25°C. The protocol described in Section 3.2.8 was followed for the preparation of these fractions. The arrows indicate lanes in which soluble HaSV capsid proteins were detected. (+), 1ng wild-type HaSV. Taken from Jiwaji (1999).

3.3.6 The effect of two different serine protease inhibitors on p71 production

The detection of numerous proteolytic breakdown products in p71 preparations led to the testing of an alternative protease inhibitor to the one that was used for the cell lysis at that point in time, being AEBSF. PMSF protected p71 during yeast cell lysis to a far greater extent than AEBSF and concomitantly a much higher level of p71 was detected in soluble fractions derived from JRY188 3#20.1 cells (Figure 3.10, panel A). Furthermore, there were fewer proteolytic breakdown products, compared to earlier attempts (Figures 3.8 and 3.9), for the protein extracts and soluble fractions in the presence of PMSF. However, a considerable amount of insoluble p71 was still obtained from cells that were lysed in the presence of PMSF. Similar results were also obtained for the production of p71 in the INVScI cells (Figure 3.10, panel B). The exposure time of the film during chemoluminescent detection was not sufficient for the detection of p71 in soluble fractions from both JRY188 3#20.1 and INVScI cells that were lysed in the presence of AEBSF (Figure 3.10). It was, however, detected in these fractions after longer exposure times (results not shown).

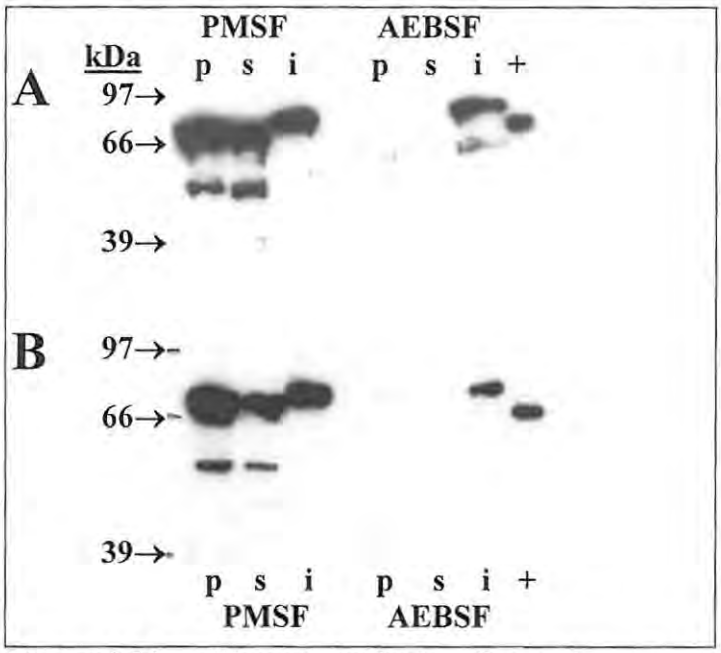

Figure 3.10 Western analysis of protein extracts (**p**), soluble (**s**) and insoluble (**i**) fractions that were prepared using cell buffers containing either PMSF or AEBSF (the protocol described in Section 3.2.8 was followed). These fractions were derived from JRY188 3#20.1 cells (panel **A**) and INVScI cells transformed with pAV3 (panel **B**). (+), 1ng wild-type HaSV.

These findings led to the re-examination of the effects of growth temperature and inducer concentration on the expression of soluble p71. The level of soluble p71 produced after the optimum induction periods for the high expression rate system (30°C, 0.1% galactose) was compared with that for the low expression rate system (20°C, 0.01% galactose). Protein determinations on the protein extracts used for this experiment showed that equivalent amounts of protein were loaded into each well. Western analysis of soluble fractions of these extracts showed that the minor effect of a decreased expression rate (shown in Figure 3.9) was surpassed by the much greater effect of the presence of PMSF in cell lysis buffers (Figure 3.11). The only difference between the soluble fractions from cells induced under these two conditions was that more proteolytic breakdown products were detected at 30°C. This observation, together with the slight effect on p71 solubility, let to the decision to continue with the lower expression rate system for further experimentation.

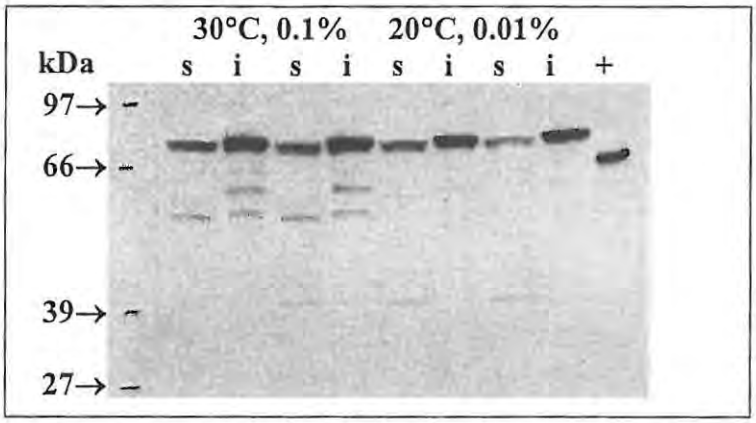

Figure 3.11 Western analysis of protein extracts of duplicate soluble (**s**) and insoluble (**i**) fractions that were prepared from JRY188 3#20.1 cells that were either induced for 4 hours at 30°C in 0.1% galactose or for 8 hours at 20°C in 0.01% galactose. These fractions were prepared using cell lysis buffers containing 1mM PMSF. (+), 1ng wild-type HaSV.

3.3.7 Additional optimization experiments

It was recently demonstrated that baculovirus-expressed NωV procapsids could be purified from an insect cell line (Canady *et al.*, 2000). A Tris-HCl buffer containing 250mM NaCl was used during this purification process, due to an apparent increased stability of these procapsids in buffers with a high ionic strength (M. Canady, personal communication). Experiments were performed to test whether high NaCl concentrations could increase the stability of yeast produced p71.

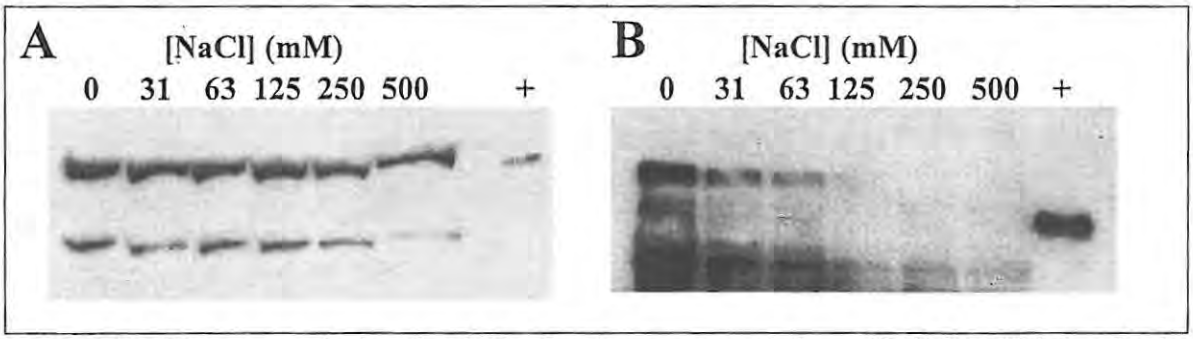

Figure 3.12 Western analysis of soluble fractions prepared from JRY188 3#20.1 cells by lysis in 50mM Tris pH7.4 containing different concentrations of NaCl, 1mM DTT and either 1mM PMSF (panel **A**) or 1mM AEBSF (panel **B**). +, 1ng and 2ng wild-type HaSV in panels **A** and **B**, respectively.

NaCl concentrations as high as 500mM did not seem to have any effect on the solubility of p71 when cells were lysed in the presence of PMSF (Figure 3.12, panel A). In contrast, when AEBSF was used as a protease inhibitor, a NaCl concentration as low as 31mM resulted in a decreased level of soluble p71 and no soluble protein was detected at a concentration of 250mM (Figure 3.12, panel B).

A comparison of the levels of soluble p71 production in JRY188 and INVSC1 from episomal and chromosomal expression modules demonstrated that the highest levels of p71 were detected in soluble fractions from INVSC1 cells transformed with pAV3, and JRY 188 3#20.1 cells (Figure 3.13, lanes 1 and 4). Low levels of *P71* expression were observed in JRY188 cells transformed with pAV3 (Figure 3.13, lane 2).

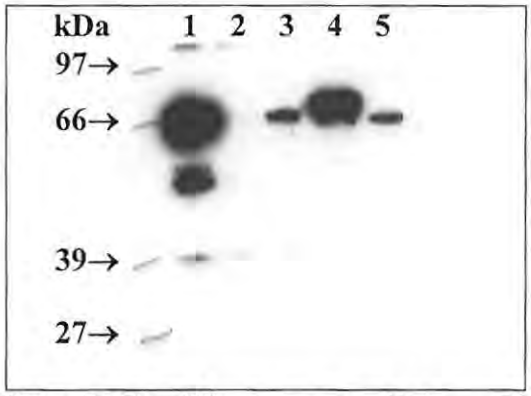

Figure 3.13 Western analysis of soluble fractions prepared from JRY188 3#20.1 cells (lane 1), JRY188 cells transformed with pAV3 (lane 2), INVSc1 3#20.1 cells (lane 3) and INVSc1 cells transformed with pAV3 (lane 4). Lane 5 contains 1ng wild-type HaSV.

3.3.8 Production of p71 from RNA2 transcripts

A direct comparison between the *P71* expression efficiencies of the *RNA2* and *P71* expression cassettes (shown in Figure 2.5) necessitated the transcription of *RNA2* mRNA from a chromosomal copy of the *RNA2* expression cassette. Accordingly, YIps for the expression of *RNA2* (YIpLac204/HaSVRNA2) and *P71* (pMJ2), as well as YIpLac128, YIpLac204 and YIpLac211, were transformed into INVScI cells to produce a variety of yeast strains, the genotypes of which are listed in Table 3.1 (YIpLac204/HaSVRNA2: Figure 3.1; pMJ2: Figure 3.2; YIpLac128: Figure 2.4; YIpLac204: Figure 3.1; YIpLac211: Figure 3.2). The YIps that were used for the generation of each of these strains are also listed in Table 3.1. YIplac128, YIpLac204 and YIpLac211 do not contain expression modules for *RNA2* and *P71*, and carry the *LEU2, TRP1* and *URA3* selectable markers, respectively.

Table 3.1 Yeast strains for the chromosomal expression of *P71* and *RNA2*

Yeast strain	Genotype*	Yip(s)
INVScI	*his3*, *leu2*, *trp1*, *ura3*	
INVScI R2	*his3*, *leu2*, ***R2::TRP1***, *ura3*	**YIpLac204/HaSVRNA2**
INVScI T+	*his3*, *leu2*, ***TRP1***, *ura3*	**YipLac204**
INVScI R2 L+	*his3*, ***LEU2***, ***R2::TRP1***, *ura3*	**YIpLac204/HaSVRNA2** **YipLac128**
INVScI L+ T+	*his3*, ***LEU2***, ***TRP1***, *ura3*	**YipLac128** **YIpLac204**
INVScI U+ T+ L+	*his3*, ***LEU2***, ***TRP1***, ***URA3***	**YipLac128** **YIpLac204** **YIpLac211**
INVScI CAP T+ L+	*his3*, ***LEU2***, ***TRP1***, ***P71::URA3***	**pMJ2** **YipLac128** **YIpLac204**
INVScI R2 U+ L+	*his3*, ***LEU2***, ***R2::TRP1***, ***URA3***	**YIpLac204/HaSVRNA2** **YipLac128** **YIpLac211**
INVScI CAP R2 L+	*his3*, ***LEU2***, ***R2::TRP1***, ***P71::URA3***	**pMJ2** **YIpLac204/HaSVRNA2** **YipLac128**

* Boldface text denotes dominant alleles generated via integration of YIps
Green text denotes plasmids and genes for the expression of *P71*
Blue text denotes plasmids and genes for the expression of *RNA2*

Proof for the presence of chromosomal copies of the *RNA2* expression cassette was obtained through PCR analysis of genomic DNA preparations from the putative $RNA2^+$ strains. (Figure 3.14). A 498bp PCR product was amplified by an RNA2-specific primer pair for strains that were transformed with YIpLac204/HaSVRNA2 (INVScI R2), while no product was detected for strains that were transformed with YIpLac204 (INVScI T+) (Table 3.1). INVScI R2 was used for subsequent transformation experiments that led to the generation of the INVScI R2 L+, R2 U+ L+ and CAP R2 L+ strains (Table 3.1). INVScI T+ was, in turn, used for subsequent transformation experiments that led to the generation of the INVScI L+ T+, U+ T+ L+ and CAP T+ L+ strains (Table 3.1).

The p71 production levels among $P71^+$ (Figure 3.15, lanes 2.1 and 2.2), $RNA2^+$ (Figure 3.15, lanes 3.1 and 3.2) and $P71^+/RNA2^+$ strains (lanes 3.15, lanes 4.1 and 4.2) were compared by Western analysis. Protein extracts from two of each of the (*TRP1, LEU2, URA3*)-strains were analyzed in an attempt to obtain a more accurate assessment. A very low level of p71 production was obtained from the $RNA2^+$ strains as compared with the $P71^+$ strains (bands co-migrating with p71 in lanes 3.1 and 3.2, Figure 3.15, were clearly visible on the original

autoradiography film, but did not reproduce well on subsequent copies). The co-expression of *RNA2* and *P71* did, however, not result in a detectable increase in the level of p71. A protein with an M_R of approximately 39 kDa, which was detected for extracts from all the strains that were tested (Figure 3.15), was probably from yeast origin and was detected due to a low level of cross-reactivity by anti-HaSV-RB2 IgG.

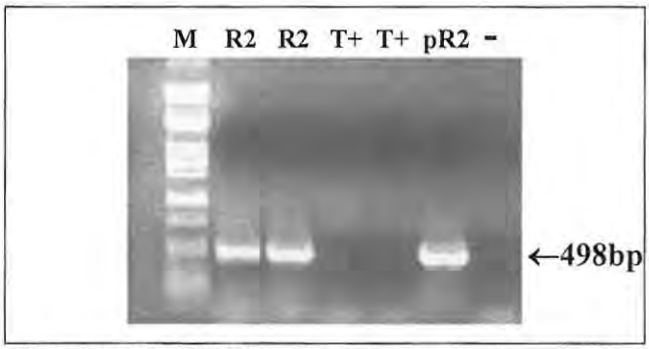

Figure 3.14 PCR of genomic DNA preparations from two RNA2$^+$ INVScI strains (**R2**) and two TRP$^+$ INVScI strains (**T+**) using the primers RNA2F3 and RNA2R2 (Appendix 4). The expected size of PCR products from HaSV RNA2 cDNA templates is indicated on the right-hand side of the gel. pAV14HPTrp (**pR2**) was used as a DNA template for a PCR positive control. The negative control (-) for these reactions contained all the required PCR constituents, except for a DNA template. A *Pst* I digest of lambda-DNA was used as a molecular weight marker (**M**).

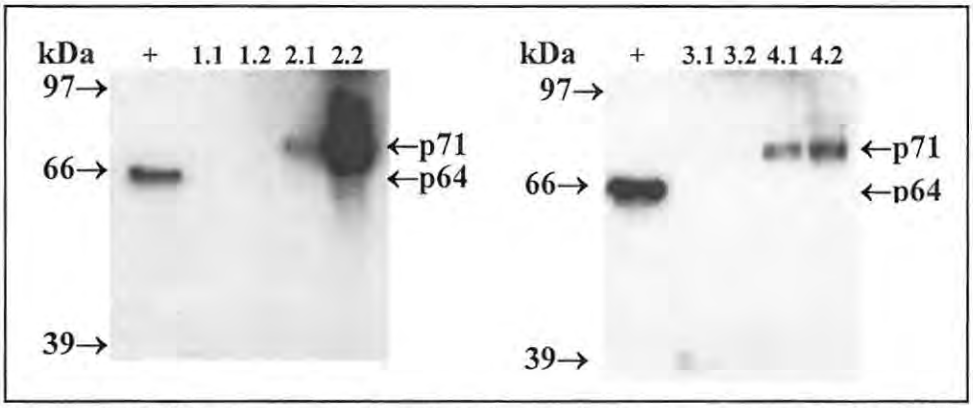

Figure 3.15 Western analysis of total protein in yeast extracts from the INVScI yeast strains U+T+L+ (**1.1&1.2**), CAP T+L+ (**2.1&2.2**), R2 U+L+ (**3.1&3.2**) and CAP R2L+ (**4.1&4.2**) (refer to Table 3.1). The expression and protein extraction methods that were followed are the same as those described in Section 3.2.6. (+), 1ng wild-type HaSV.

3.4 Discussion

3.4.1 Detection of p71 in yeast cell lysates

Evidence for the necessity of expression modules for *P71* independent from those for *RNA2* is provided in Figure 3.15. A much higher level of HaSV capsid protein was produced from these expression modules than from those for *RNA2*. These results differed from similar studies in plant protoplasts where no *P71* expression was detected from RNA2 transcripts (Gordon, *et al.*, 2001).

The experiments also demonstrated that a very low amount (if any) of p71 autocatalytic cleavage occurs under the expression conditions in yeast (Figures 3.4). This was not an encouraging result because the autocatalytic cleavage of capsid precursors could be used as evidence of assembly. This observation differs from that obtained for the expression of the NωV capsid precursor protein gene in insect cells by baculovirus vectors (Agrawal and Johnson, 1995). Crude protein preparations from these cells contained mixtures of processed and unprocessed capsid proteins.

3.4.2 Stability of yeast-expressed p71

Prolonged induction with galactose resulted in a disappearance of p71 in yeast cell lysates (Figure 3.6, panel A). This could have been due to a loss of the *P71* gene from the genome of yeast cells after 12 hours' growth in galactose. Evidence was provided that the disappearance of p71 was probably not the consequence of the excision of the *P71* expression module from the chromosome through homologous recombination (Figure 3.6, panel B) (Jiwaji, 1999). There was no difference in the number of colonies that were obtained when cells were plated onto SMM either containing, or not containing, L-leucine to look for progressive loss of the Leu^+ phenotype during induction (Jiwaji, 1999). This indicated that no loss of *LEU2* occurred, and therefore the *P71* expression module was not either likely to have been lost. It is, however, possible that recombination occurred at a position in the chromosomal selectable marker that led to the looping out of *leu2* together with the *P71* expression module. The possibility that the *P71* expression module was lost from the genome by homologous recombination could therefore not be ignored completely.

Furthermore, the repression of P_{GAL1}-driven transcription was most probably not responsible for the disappearance of p71. A reduced cell growth rate would have been expected for cells that could not catabolize galactose (their sole carbon source) due to the repression of the galactose utilization pathway. There was however no difference in cellular proliferation between cells expressing and those not expressing *P71*.

Alternative explanations for the disappearance of p71 are that it was either synthesized at a decreased rate or degraded at an increased rate. A decreased rate of protein synthesis could have been responsible for a reduction in p71 levels, but not for the complete depletion thereof. Proteolytic degradation was therefore to a certain extent responsible for the complete depletion of p71. Two main pathways of protein degradation occur in *S. cerevisiae*: vacuolar degradation and degradation by the ubiquitin pathway (Romanos *et al.*, 1992). The former is responsible for the degradation of long-lived proteins (t½ approximately 160 h), while short-lived proteins (t½ less than 2.5 h) are degraded by the latter (Finley, 1992).

The disappearance of p71 after 12 hours' growth demonstrated that this protein could be classified as a short-lived protein in yeast. It is therefore highly probable that p71 was targeted for degradation by the ubiquitin pathway. This hypothesis is supported by evidence for the production of insoluble p71 in yeast cells (Figure 3.10). The insolubility of p71 was most probably the result of the formation of p71-containing aggregates (or inclusion bodies) within the yeast cell. According to Finley (1992) the presence of these aggregates elicit a heat-shock response that results in the rapid degradation of the aggregated proteins by the ubiquitin pathway.

It was attempted to increase the yield of p71 by (i) determining the optimum time period for induction, (ii) reducing the rate of expression, and (iii) testing the effects of different protease inhibitors. The optimal induction periods for the expression of *P71* under conditions conducive to a reduced expression rate were determined (Figure 3.8). The solubility of p71 was slightly increased when cells were grown at 20°C in SMM containing 0.01% galactose (Figure 3.9). This effect was, however, minor compared to that of the serine protease inhibitor PMSF (Figure 3.10). This was quite an unexpected result because AEBSF, another sulfonyl fluoride-type serine protease inhibitor, did not provide any protection against this degradation. AEBSF has a reported range of protection similar to that of PMSF and has the added advantage in that it is much more stable than PMSF in aqueous buffers (Mintz, 1993).

It was demonstrated that cell lysis buffers with high NaCl concentrations did not have a significant effect on the levels of soluble p71 when cells were lysed in the presence of PMSF (Figure 3.12, panel A). Conversely, NaCl concentrations as low as 31 mM had a significant effect on the amount of p71 in soluble fractions from cells lysed in the presence of AEBSF (Figure 3.12, panel B). There are two possible explanations for this result: First, it is possible that the soluble p71 obtained from a decreased expression rate differed from the protein protected by PMSF in its stability at high ionic strength. In accordance, this protein probably represented unstable expression products that were "salted out" from solution (Englard and

Seifter, 1990). Second, it is possible that the protein obtained from a decreased expression rate was degraded by a salt-dependent AEBSF-insensitive protease.

3.4.3 Reasons for the formation of insoluble p71 protein aggregates: impaired folding or assembly?

The heterologous expression of insoluble protein is an indication of a cellular environment that is not suited for its proper folding (Speed *et al.*, 1996). This is generally the case for the expression of monomeric globular proteins, but could potentially be different for the expression of capsid proteins, which have the propensity to assemble into VLPs. If this assembly process is impaired, these proteins could form insoluble protein aggregates within the cell. As discussed in the previous paragraph, these proteins would be defined as unstable due to the relatively short half-lives of proteins that are incorporated into insoluble aggregates. This interpretation is in agreement with the minor effect (described in the previous paragraph) of a decreased expression rate on the levels of soluble p71 (Figure 3.11), and the infrequent occurrence of problems associated with the improper folding of polypeptides in yeast (Romanos, *et al.*, 1992)

The tendency of capsid proteins to form insoluble aggregates during assembly was demonstrated in experiments in which FHV particles were assembled *in vitro* from dissociated provirions (Schneemann *et al.*, 1994). In these experiments, a considerable fraction of the dissociated capsid proteins formed insoluble α-protein aggregates and was therefore not available for assembly. Impaired assembly could possibly also explain why the amount of NωV VLPs produced from a baculovirus expression system did not correlate with the high levels of α-protein that were detected in the insect cells (Agrawal and Johnson, 1995).

3.4.4 Chromosomal vs. episomal *P71* expression

Expression in two different yeast strains from either episomal or chromosomal expression modules was compared in order to maximize the amount of soluble p71 produced (Figure 3.13). In INVScI, *P71* expression from a 2μ-based vector (pAV3: Figure 2.3) produced a much higher level of p71 than chromosomal expression. These different levels were due to the much higher copy-number of the pAV3 (approximately 50) (Rose and Broach, 1990). The opposite was true for JRY188 where chromosomal *P71* expression produced equivalent (or higher) levels to that of pAV3 in INVScI, while episomal expression was barely detectable. This anomaly could be due to the lack of genes for the stable propagation of pAV3 in the genome of JRY188. Two 2μ-plasmid-borne genes (*REP*1 and *REP*2) in conjunction with a *cis*-acting locus (*STB*) contribute to the segregation of 2-μ plasmids during cell division (Velmurugan *et al.*, 1998). pAV3 carries the *ORI-STB* yeast selectable marker but depends on

a 2μ-host strain (like INVScI) that supplies *REP1* and *REP2* (Kikuchi, 1983). The much higher level of p71 production from JRY188 3#20.1, as compared to INVScI 3#20.1, most probably reflects differences in the regulation of galactose metabolism between these strains.

4 The assembly of HaSV procapsids in *S. cerevisiae* and the pH-dependent maturation of these particles

4 The assembly of HaSV procapsids in *S. cerevisiae* and the pH-dependent maturation of these particles

4.1 Introduction

Heterologous expression systems have been used to study the cellular and viral factors that are involved in the assembly of capsids from a variety of ss +RNA viruses (Agrawal and Johnson, 1995; Schneemann *et al.*, 1993). Non-structural virus proteins are often not a requirement for the non-host production of ss +RNA virus capsids. This seems to be the norm for simpler viruses like nodaviruses and omegatetraviruses, because the expression of FHV and NωV capsid protein precursors in baculovirus expression systems resulted in the assembly of VLPs (Agrawal and Johnson, 1995; Schneemann *et al.*, 1993). Exceptions are found in more complex viruses, like picornaviruses, where post-translational processing of capsid protein precursors by viral proteases is required. Jore *et al.* (1994) demonstrated that *Poliovirus* VLPs were assembled in yeast upon simultaneous expression of *P1* (capsid protein precursor gene) and *3CD* (nonstructural gene).

The presence of RNA has been shown to be a requirement for the assembly of the capsids of some ss +RNA viruses. It does not seem as if picorna- and caliciviruses require viral RNA for assembly, as judged by the production of empty *Poliovirus* (Jore *et al.*, 1994), *Hepatitis E virus* (Li *et al.*, 1997) and *Rabbit hemorrhagic disease virus* (Boga and Alonso, 1997) VLPs in heterologous expression systems. Conversely, an RNA component plays a very important role in nodavirus capsid assembly. Schneemann *et al.* (1994) demonstrated that dissociated FHV provirions could not re-assemble in the absence of an encapsidatable component. Re-assembly was however not solely dependent on FHV-derived RNA, because it also took place in the presence of heterologous RNA, ss DNA and polyanions, such as dextran sulfate.

Omegatetravirus capsids seem to encapsidate viral RNA with a high degree of specificity. Baculovirus expression of NωV capsid protein precursor genes resulted in the specific encapsidation of α mRNA (Agrawal and Johnson, 1995). This result demonstrated that the encapsidation signal for NωV resided within the capsid protein precursor ORF. In addition, the baculovirus expressed NωV VLPs consisted of mixtures of procapsids and capsids.

In the previous chapter Western analysis data showed that processing, in the form of the autoproteolytic cleavage, was not detected for yeast-produced p71. A similar result for the bacterial expression of the closely related NωV capsid protein precursor (α), led Agrawal and

Johnson (1995) to suggest that NωV VLP assembly did not occur. The main objective of the work described in this chapter is to demonstrate that the expression of *P71* is all that is required for the assembly of VLPs in yeast and that these VLPs are able to mature *in vitro*.

4.2 Materials and methods

4.2.1 Purification of VLPs

Two different protocols for the purification of HaSV VLPs from yeast cell pellets are summarized in Figure 4.1. In the first protocol, VLPs were sedimented through a 30% sucrose cushion; in the second, the particles were purified by centrifugation through a glycerol gradient (adapted from a method used by Agrawal and Johnson, 1995).

The cell pellets were obtained as follows: Shake flask cultures of $P71^+$ yeast cells in SMM containing 5% glycerol and 0.1% glucose up to a combined volume of 2 to 5*l* were grown to midlog phase at 30°C. 10% galactose was then added to these cultures to a final concentration of 0.01% and the cultures were grown at 20°C for a further 8 hours. The cells were centrifuged at 4000rpm for 10 min at 4°C in a Beckman JA10 rotor. Cell lysis by bead beating (Figure 4.1) was performed according to the instructions provided with the Bead-Beater (Biospec Products).

Glycerol and CsCl gradients were fractionated using an ISCO Model 640 density gradient fractionator, and refractometry was carried out using an ABBE-type refractometer (Bellingham and Stanley, Ltd., England).

4.2.2 Standardization of density gradient centrifugation techniques

For the determination of the glycerol concentration at a particular refractive index, the refractive indices of solutions with known glycerol concentrations were measured. The data from this experiment was used to construct a standard curve relating glycerol concentration to refractive index, which had an r^2 value of 0.998 (results not shown). The slope and y-intercept of this curve (0.130 ml g^{-1} and 1.339, respectively) were used for the calculation of glycerol concentration at a given refractive index.

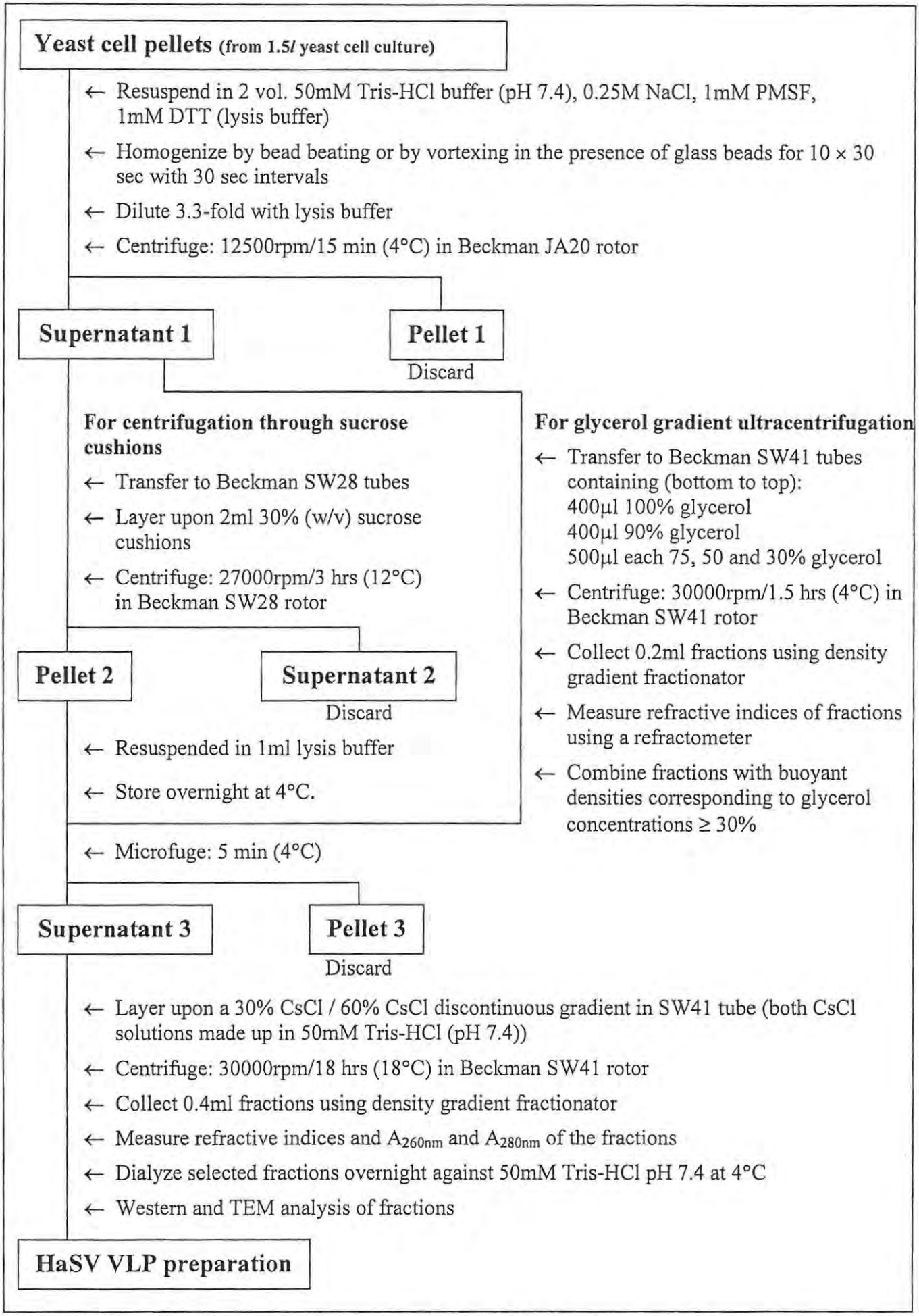

Figure 4.1 A flow diagram for the purification of HaSV VLPs from yeast by way of glass bead homogenization.

The data from Dawson *et al.* (1987) was used to construct a plot of CsCl concentration versus buoyant density. The slope of this curve was used to construct a density calibration curve ($r^2 = 0.999$) relating refractive indices of known CsCl concentrations to their respective densities (results not shown). The slope and y-intercept from the density calibration curve (0.096 ml g^{-1} and 1.237, respectively) were, in turn, used for the calculation of the buoyant densities of CsCl density gradient fractions. The presence of 50mM Tris-HCl did not interfere with the measured refractive index at a particular CsCl concentration (results not shown).

4.2.3 Electron microscopy

Yeast-derived VLP preparations were applied to carbon-coated copper grids and allowed to absorb for 1 - 2min. The grids were blotted dry with filter paper, stained with 1% phosphotungstic acid and viewed in a JEM100CX transmission electron microscope.

4.2.4 Maturation protocols

Three different experiments were attempted to demonstrate the pH-dependent maturation of HaSV procapsids. In one of these experiments, sucrose cushion pellets were microfuged for 5 min (as described in Figure 4.1) and loaded onto discontinuous sucrose gradients in Beckman SW41 tubes. The gradients consisted of 2.5ml each of 5, 10, 15, and 20% sucrose, which were made up in 70mM sodium acetate (NaAc) (pH 5 and 5.5), 70mM sodium citrate (pH 6 and 6.5) and 70mM Tris-HCl (pH 7 and 7.4). The buffers were selected for their pK_a values (within 1 pH unit of the desired pH values). The gradients were centrifuged at 30000rpm for 3hr at 4°C in a Beckman SW41 rotor. The pellets were then resuspended in equivalent volumes of 50mM Tris pH7.4 to that of the original resuspended sucrose cushion pellets. In other experiments, the pH of p71-containing HaSV VLP preparations (Figure 4.1) was dropped by overnight dialysis (at 4°C) against 70mM NaAc (pH 5), or by the addition of five volumes of the same buffer. In the latter instance, samples were left on ice for at least 2 hours after the addition of NaAc, prior to the next step of experimentation. pH measurements carried out subsequent to the addition of NaAc were used to ensure that the expected pH change (i.e. from 7.4 to 5) was achieved.

4.2.5 Analysis of encapsidated RNA

RNA was extracted by vortexing a mixture containing equal volumes of the sample and phenol (equilibrated with 2M NaAc, pH 4) for 1 min. The mixture was microfuged for 5 min and the resultant aqueous layer was washed twice with chloroform-isoamyl alcohol (24:1). 0.1 volumes of 3M NaAc (pH 5.2) and 2.5 volumes of ethanol were added to the aqueous layer and it was left at -20°C for at least 2 hours. The RNA precipitate was collected by

centrifugation for 10 minutes at 4°C in a microfuge. The pellet was air-dried and resuspended in a small volume of DEPC-treated water.

RNA extracts were used as templates for RT-PCR using the Titan™ One Tube RT-PCR System (Roche). The primers RNA2F6 (corresponding to nucleotides 502 – 522 of RNA2) and AV9 (complementary to nucleotides 1351 – 1368 of RNA2) were used for the detection of *P71* mRNA (primers: Appendix 4; thermal cycling programme: Programme 3 in Appendix 5). The RNA extracts were subjected to PCR (using the Expand™ High Fidelity PCR System from Roche) to ensure that amplified products were not the result of genomic DNA contamination.

4.3 Results

4.3.1 Establishment of techniques for determination of VLP buoyant density

Wild-type HaSV was subjected to CsCl density gradient centrifugation as described in Figure 4.1. Fractions were collected across the gradient and dialyzed overnight against 50mM Tris pH7.4. Western analysis of the dialyzed fractions showed that the largest amount of HaSV was detected in a fraction with a density of 1.290 g/ml (Figure 4.2), which is identical to that obtained for HaSV by Hanzlik *et al.* (1993). This result indicated that reliable buoyant density determinations could be obtained through the use of this technique.

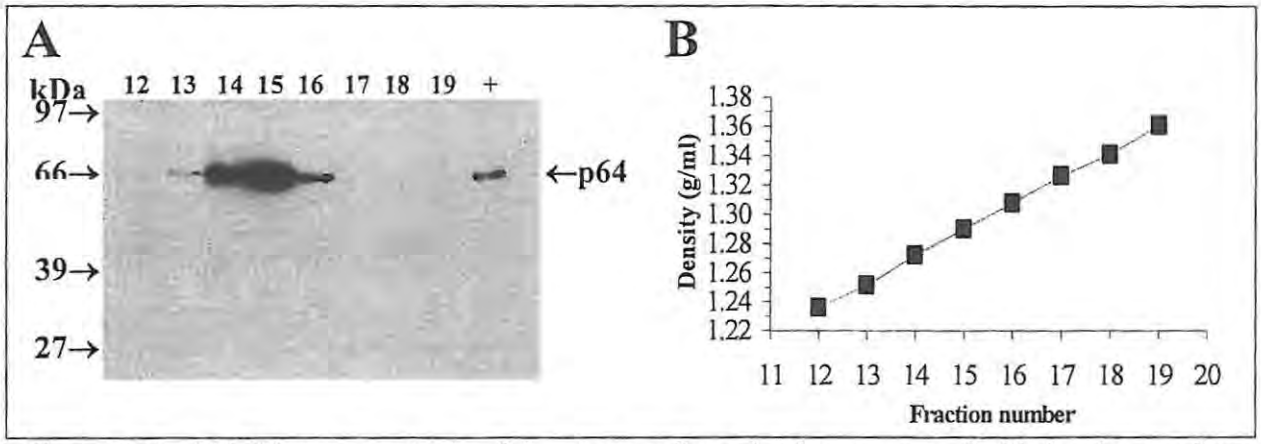

Figure 4.2 (**A**) Western analysis of fractions collected subsequent to CsCl density gradient centrifugation of wild-type HaSV. 100ng HaSV was loaded upon a discontinuous CsCl gradient, as described in Figure 4.1. 2µl of each fraction were separated by SDS-PAGE. (+), 1ng wild type HaSV. (**B**) Profile of the densities of these fractions.

4.3.2 Yeast VLP preparations

To determine whether HaSV VLP assembly occurs in yeast, VLP preparations were performed on INVScI cells (transformed with pAV3) and JRY188 3#20.1 cells, since these two combinations were shown to express the highest levels of soluble p71 (Figure 3.13; pAV3: Figure 2.3). Low expression rate conditions were used during the induction phase (as

described in Section 3.3.5) to optimize the production of correctly folded p71 molecules. 250mM NaCl was added to cell lysis buffers due to its reported stabilizing effect on procapsids (M. Canady, personal communication).

i Preparation of VLPs from INVScI cells (transformed with pAV3) using the sucrose cushion centrifugation procedure

In the previous chapter, it was shown that a fraction of the total p71 expressed in INVScI cells from pAV3 was soluble (Figure 3.10, panel B). If the p71 molecules in this fraction were monomeric proteins, they would remain in the supernatant when sedimented through a 30% sucrose cushion (as described in Figure 4.1). Alternatively, the sedimentation coefficient for omegatetravirus particles (S_{20w} = 194-217) dictates that these proteins should pellet under these conditions if they are associated with VLPs (van Regenmortel *et al.*, 2000). Equivalent amounts of yeast cell lysate (representative of total amount of p71 produced) and the resuspended pellet (after centrifugation through a 30% sucrose cushion) were separated on an SDS-PAGE gel for western analysis (Figure 4.3, panel B). A considerable portion of the total p71 produced in yeast was detected in the resuspended pellet, suggesting the presence of HaSV VLPs.

No distinct bands were, however, observed when the resuspended pellets were subjected to CsCl density gradient centrifugation. Fractions were collected across the CsCl gradients to determine whether p71 or p64 was present in these fractions at the expected buoyant density range for HaSV VLPs (Figure 4.3, panels A and B). Two protein species that contained p71 were separated by the CsCl gradient. The low-density type was found in fractions that contained the highest protein concentrations (as estimated from the UV-trace in Figure 4.3, panel D) and had buoyant densities ranging from 1.209-1.232 g/ml (Figure 4.3, panels A, fraction no. 10 - 12, and D). These p71 species were, however, found to be insoluble since it was found in pellet fractions when it was microfuged for 5 min (Figure 4.3, panel C). The high-density type contained much lower amounts of p71 and had a buoyant density of 1.267-1.287 g/ml (Figure 4.3, panels A, fraction no. 14 and 15, and D). At least a fraction of the p71-containing species in fraction 15 (with a density of 1.287 g/ml) remained soluble after being microfuged for 5 min, while no soluble p71 was detected for fraction 14 (Figure 4.3, panel C). As with previous experiments, no p64 could be detected, indicating very low levels, if any, of maturation.

The band detected for the 1ng HaSV positive control in the Western blot in Figure 4.3 (panel C) represents an approximate virus particle (vp) concentration of 10^9 vp/ml. It follows that if the band detected in fraction 15 (Figure 4.3, panel C) is estimated to represent $1/10^{th}$ of

that obtained for the positive control, then there would be at most 10^8 vp/ml in this fraction, which had a total volume of 400µl. This sample was prepared from a 0.5*l* yeast culture, which had an OD_{600nm} of 0.738 prior to cell lysis. From the standard curve in Figure 3.3 (panel B) it is therefore estimated that about 4×10^7 VLPs were purified from 2.5×10^{10} INVScI cells, equating to a very low maximum yield of approximately 2 VLPs from every 1000 yeast cells.

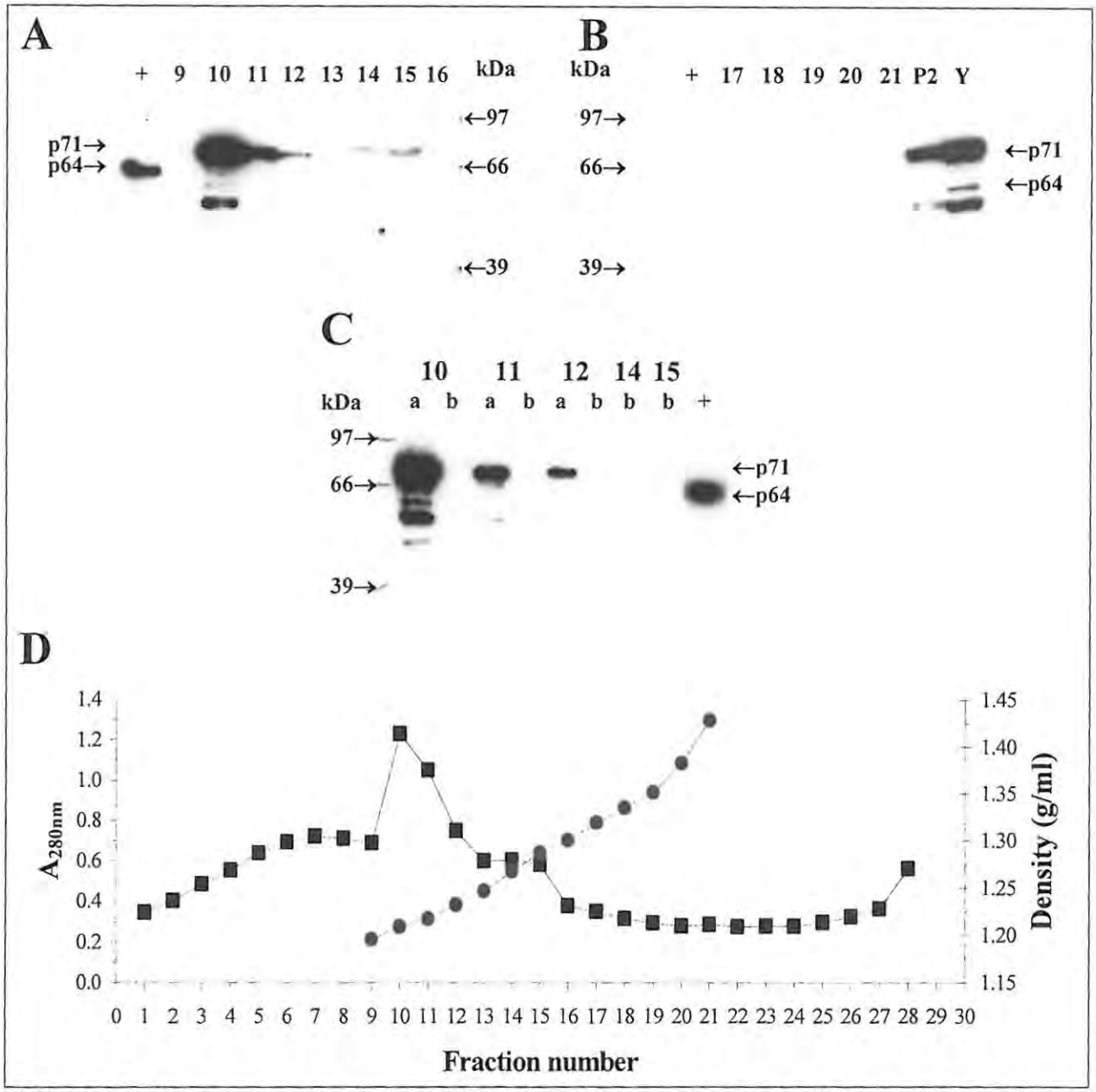

Figure 4.3 Vlp preparation from INVScI cell cultures with a total volume of 0.5*l*. Yeast pellets were subjected to the sucrose cushion centrifugation purification procedure described in Figure 4.1. 20µl of each of the dialyzed CsCl fractions were separated by SDS-PAGE. **Panels A and B:** Western analysis of fractions that were collected from the CsCl gradient. (**Y**) and (**P2**) denote yeast cell lysate and "Pellet 2" (in Figure 4.1), respectively. (+), 1ng wild type HaSV. **Panel C:** Western analysis of p71-containing fractions (**a**) and their respective supernatants (**b**) after centrifugation for 5 min in a microfuge. (+), 1ng wild type HaSV. **Panel D:** Profile of the A_{280nm} readings (■) and densities (●) of the fractions.

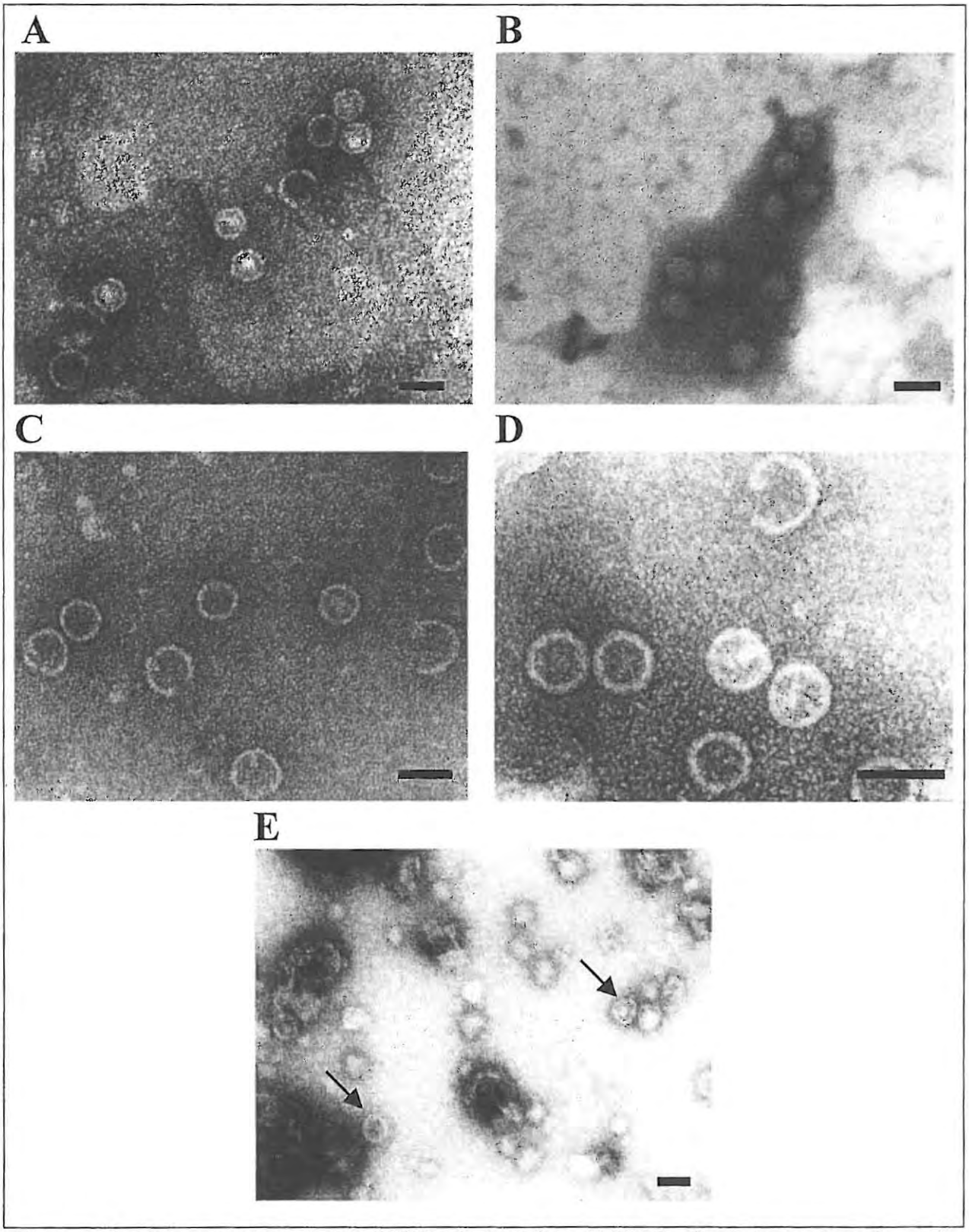

Figure 4.4 Electron micrographs of VLPs derived from INVScI cells that were transformed with pAV3 (panels **A** and **C**) and JRY188 3#20.1 cells (panels **D** and **E**), and wild-type HaSV (panel **B**). The VLPs in panels **A**, **B** and **D** were purified by centrifugation through sucrose cushions, followed by CsCl density gradient centrifugation (Figure 4.1). The particles in panel **E** (indicated by arrows) were prepared by glycerol gradient centrifugation (Figure 4.1). Bar represents 50nm.

In spite of this low yield of VLPs from INVScI, an attempt was made to visualize these particles by TEM analysis. Accordingly, fraction 15 was diluted in 50mM Tris pH7.4, spun down in an ultracentrifuge (27000 rpm for 3hrs in an SW41 rotor), and resuspended in 25µl of the same buffer. Vlps, with an approximate diameter of 40nm were detected in this concentrated sample at amounts that exceeded the estimated concentration of HaSV VLPs by at least one order of magnitude (Figure 4.4, panels A and C). A very high estimate for the VLP concentration in the concentrated fraction 15 would be in the region of 10^9 VLP/ml, while the abundance of VLPs that were observed under the electron microscope reflected a concentration of at least 10^{10} vp/ml. These particles appeared to be slightly larger and more rounded than HaSV (Figure 4.4, panel B), and their inner cores were less electron-dense. Some particles, however, appeared to contain single electro-dense spots in their viral cores. A second VLP preparation from INVScI cells (transformed with pAV3) produced similar results with no marked increase in the yield of fractions analogous to fraction 15 (results not shown).

ii Preparation of VLPs from JRY188 3#20.1 cells using the sucrose cushion centrifugation procedure

In Figure 4.5 (panel A), a typical Western blot of CsCl density gradient fractions derived from JRY188 3#20.1 cells is shown. There was a remarkable degree of similarity in the patterns that were obtained for the bands on the Western blots from three separate experiments (results not shown). Based on these results, three different protein species that interacted with anti-HaSV antibodies were categorized. Type I (Figure 4.5, panel A: fractions 10 - 11) is most probably similar to the low density-type that was obtained from INVScI cells (described above), because it had a similar buoyant density range with values of up to 1.245 g/ml (SEM ±0.002, $n = 3$). In addition, no VLPs were detected in any of the fractions that contained this protein species. Type II (Figure 4.5, panel A: fraction 12) consists of a protein that seemed to be slightly smaller than p71. Bands representative of this protein migrated on SDS-PAGE gels at a molecular weight of approximately 69kDa. This species had a characteristic buoyant density of 1.266 g/ml (SEM = 0.001, $n = 3$). No VLPs were detected, when these fractions were examined under TEM. Type III (Figure 4.5, panel A: fractions 13 - 15) had a buoyant density range of 1.278 – 1.310 g/ml (Figure 4.5, panel C). Vlps, identical to those described above, were visualized when these fractions were pooled, concentrated with PEG, and visualized by TEM (Figure 4.4, panel D).

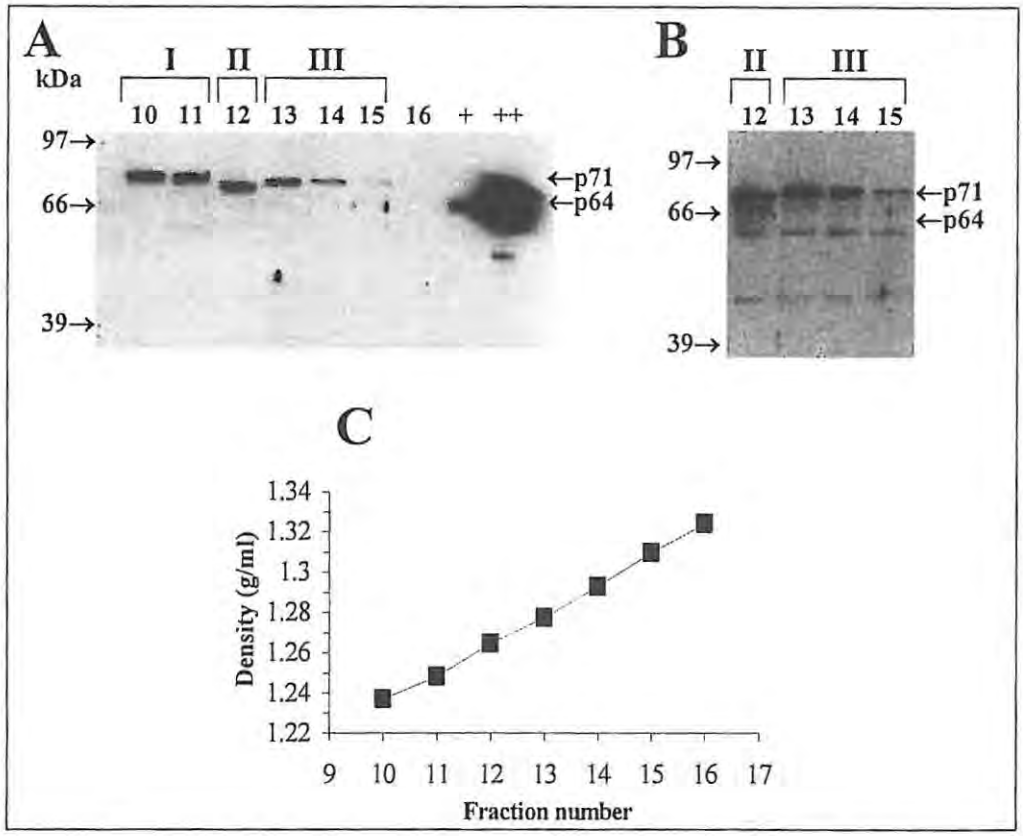

Figure 4.5 Vlp preparation from JRY188 3#20.1 cultures with a total volume of 1.5*l*. Yeast pellets were subjected to the sucrose cushion centrifugation purification procedure described in Figure 4.1. 20µl of each of the dialyzed fractions were separated by SDS-PAGE. (**A**) Western analysis of fractions that were collected from the gradient. **I**, **II** and **III** denote the three different proteins species described in the text, while (+) and (++) denote 0.1 and 1ng wild type HaSV, respectively. (**B**) Western analysis of fractions that were stored at 4°C for one week. (**C**) Profile of the densities of these fractions.

The yield of the Type III protein species was estimated from the blot in Figure 4.5 (panel A) by comparison with different known amounts of HaSV (0.1ng-1ng) that were run alongside the CsCl fractions on an SDS-PAGE gel. Within the limits of accuracy for this type of assessment, there was no significant increase in the levels of the higher density p71 fractions from JRY188 3#20.1 cells to that from INVScI cells transformed with pAV3. In line with the HaSV expression strategy discussed in Section 2.3.4, JRY188 3#20.1 was selected for further experimentation. Accordingly, a purification protocol for the preparation of an optimal amount of functional HaSV VLPs would be established using this *LEU2* strain (Table A6.1, Appendix 6). This strain would be transformed with the pAV13HC and pAV14HPTrp vectors bearing *URA3* and *TRP1* markers, respectively, for the co-expression of *P71*, *RNA1* and *RNA2*.

iii Preparation of VLPs from JRY188 3#20.1 cells using the glycerol gradient ultracentrifugation procedure

Western analysis of samples that were taken at the various steps of the sucrose cushion protocol (Figure 4.1) is shown in Figure 4.6. Equivalent aliquots were electrophoresed in an SDS-PAGE gel to ensure that a direct comparison could be drawn among these samples. This Western blot demonstrated that the level of p71 diminished with each successive purification step, and that a very small fraction of the p71 detected in the yeast cell lysate was available for CsCl density gradient centrifugation (lane 4 in Figure 4.6, panel B). This result also indicated that the majority of the p71 in sucrose cushion pellets was in an insoluble form, and did not form part of HaSV VLPs.

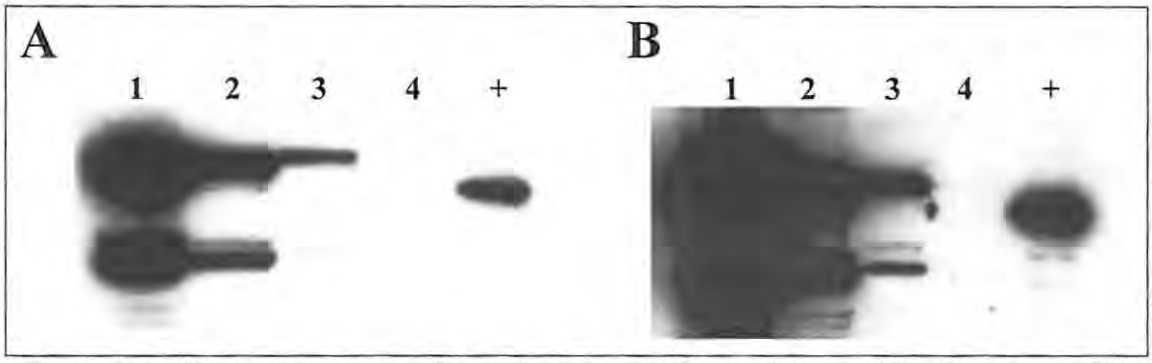

Figure 4.6 Western analysis of samples taken at the various purification steps of the sucrose cushion centrifugation procedure for the preparation of VLPs from JRY188 3#20.1 cells (Figure 4.1). Panels **A** and **B** represent 1 and 5 min periods for the exposure of films during chemoluminescent detection, respectively. Lane **1**, yeast cell lysate prior to 12500rpm centrifugation step, lane **2**, "Supernatant 1", lane **3**, resuspended "Pellet 2", and lane **4**, "Supernatant 3". (+), 2ng wild type HaSV.

Agrawal and Johnson (1995) reported an initial low yield of NωV VLPs from a baculovirus expression system when they attempted to purify these particles by means of centrifugation through a 30% sucrose cushion. It was suggested that this protocol was too harsh for the purification of the inherently unstable NωV procapsids. An improved yield was, however, obtained through the application of a milder glycerol gradient centrifugation protocol. This protocol (described in Figure 4.1) was used in an attempt to increase the yield of HaSV VLPs from yeast.

Following glycerol gradient centrifugation, the majority of p71 was found in the 50 – 75% glycerol layers (Figure 4.7, panels C and D). Coomassie stained gels furthermore showed an increase in the levels of a protein, which migrated at a molecular weight of approximately 71kDa, in lanes corresponding to these glycerol concentrations (Figure 4.7, panels A and B). This result is similar to what was reported for the baculovirus-expressed NωV VLPs (Agrawal and Johnson, 1995), with the exception that the processed form of the NωV capsid protein was

predominately detected. Only a small amount of a protein that co-migrated with p64 was detected in the 44-68% glycerol layers (Figure 4.7, panel C). Vlps similar to those described before, were visualized in these glycerol layers, but the preparation was much more heterogeneous than the CsCl density gradient fractions (Figure 4.4, panel E).

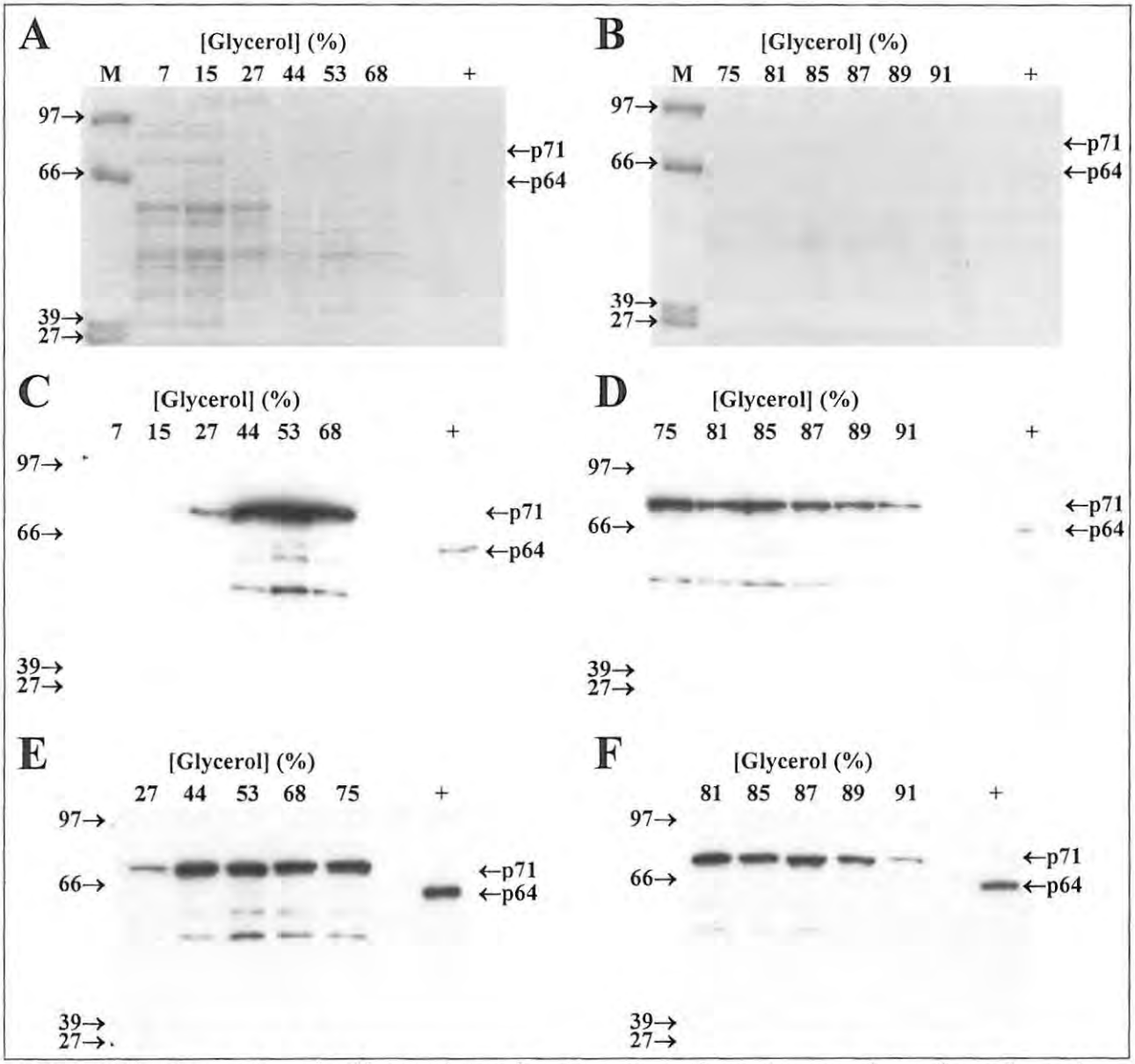

Figure 4.7 Separation of p71-containing fractions on a discontinuous glycerol gradient. A soluble fraction, derived from 0.5*l* of JRY188 3#20.1 cells, was subjected to glycerol gradient centrifugation as described in Figure 4.1. 20µl of the resultant fractions were separated on SDS-PAGE gels. **Panels A and B:** Coomassie blue-stained SDS-PAGE gels of glycerol gradient fractions. +, 200ng wild-type HaSV. **Panels C and D:** Western analysis of the SDS-PAGE gels displayed in panels A and B. +, 1ng wild-type HaSV. **Panels E and F:** Western analysis of these fractions after the addition of 5 volumes 70mM sodium acetate (pH5). The diluted samples were kept on ice for 2 hours, TCA precipitated and separated by SDS-PAGE. +, 1ng wild-type HaSV.

4.3.3 Maturation of procapsids

Similar to NωV procapsids (Canady *et al.*, 2000), the HaSV-derived VLP preparations did not mature upon storage. The Type II and Type III protein species (described for VLP preparations from JRY188 3#20.1 cells) did not undergo autocatalytic cleavage subsequent to a one week storage period at 4°C (Figure 4.5, panel B). Three strategies were used to determine if the yeast-derived HaSV procapsids could undergo acid-induced maturation: (a) sedimentation of VLP preparations through sucrose gradients that were buffered at a reduced pH, (b) dialysis of VLP preparations against a buffer with a reduced pH and (c) the addition of a buffer with a reduced pH to VLP preparations.

Resuspended sucrose cushion pellets (Figure 4.1) were spun through sucrose gradients made up in buffers with pH values ranging from 7.4 down to 5. The resulting pellets were thereafter separated on SDS-PAGE gels and assayed for the presence of p64 by Western analysis. No p64 was detected for any of the pH values that were tested (Figure 4.8, panel A). A drop in pH resulted in the precipitation of the p71-containing species within the solution, because a minimal amount of p71 remained soluble below a pH of 5.5 (Figure 4.8, panel B).

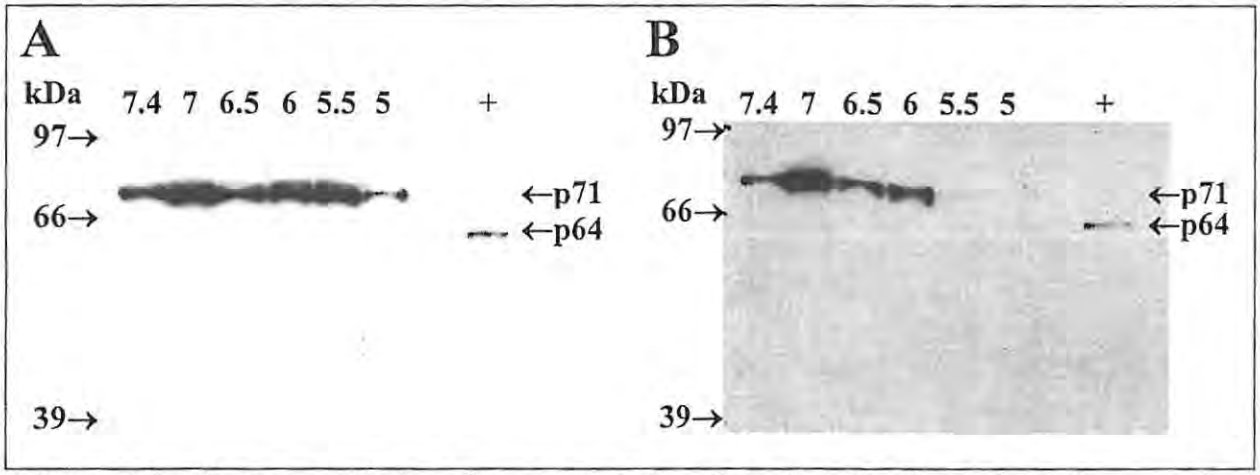

Figure 4.8 Western analysis of resuspended pellets (panel **A**), and their respective supernatants (panel **B**) upon centrifugation for 5 min in a microfuge, subsequent to centrifugation through sucrose gradients that were made up in buffers with different pH values. The protocol described in Section 4.2.4 was used for the preparation of these gradients at pH **7.4**, **7**, **6.5**, **6**, **5.5** and **5**. 10µl of each of the resuspended pellets, or supernatants, were separated on SDS-PAGE gels. +, 1ng wild-type HaSV.

No autoproteolytic cleavage was detected after a drop in pH for glycerol gradient fractions (Figure 4.7, panels E and F). In these experiments, the pH was reduced by the addition of 5 volumes of NaAc (pH5) to each of the glycerol gradient fractions. The possibility that the glycerol interfered with the maturation process was also ruled out. This was done by detecting no autoproteolytic cleavage in experiments in which these fractions were either dialyzed against lysis buffer (50mM Tris pH 7.4, 250mM NaCl), or 50mM Tris pH 7.4, prior to the

reduction in pH (results not shown). Furthermore, neither the protein concentration of the preparation nor the NaAc to sample ratio seemed to have an effect. This was because no autoproteolytic cleavage was evident upon a 10-fold dilution of the preparation, or upon the addition of 10 volumes of 70mM NaAc (pH 5) (results no shown).

Dialysis of an INVScI-derived VLP preparation (similar to fraction 15 in Figure 4.3, panel C) against 70mM NaAc (pH5) showed that a very faint protein band, which co-migrated with p64 in an SDS-PAGE gel, was detected upon lowering the pH of the sample (Figure 4.9, panel A). Similar results were obtained upon the addition of five volumes of NaAc (pH 5) to the Type III protein species described for a VLP preparation from JRY188 3#20.1 cells (Figure 4.5, panel A), which resulted in the appearance of a 64kDa protein in duplicate experiments (Figure 4.9, panel B). Not all the p71, however, underwent cleavage in the experiments described in this paragraph, as it was still present in the lanes in which p64 was detected.

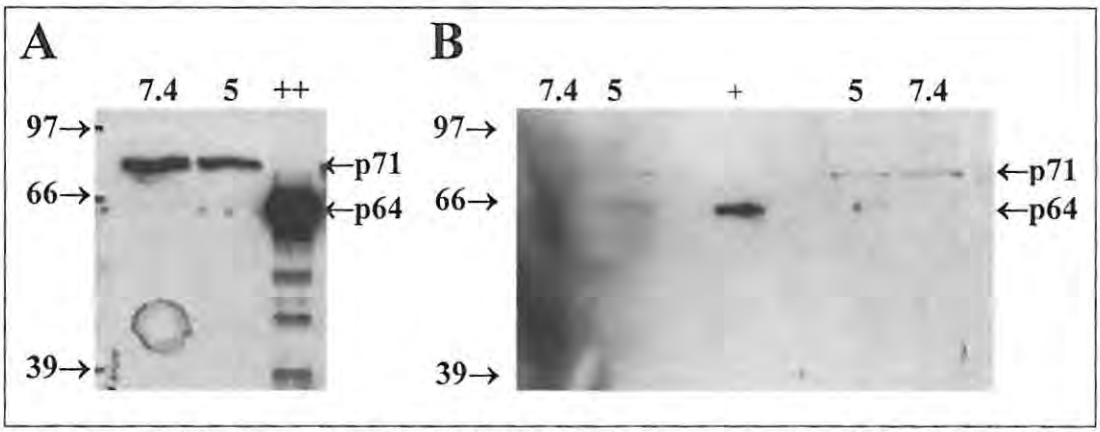

Figure 4.9 Western analysis of INVScI-derived (panel **A**) and JRY188 3#20.1-derived (panel **B**) VLP preparations that were tested for their ability to undergo pH-dependent maturation upon a reduction in pH from **7.4** to **5** (using the methods described in Section 4.2.4). The INVScI-derived samples (panel **A**) were either dialyzed against 70mM NaAc (pH 5), or 50mM Tris-HCl (pH 7.4). 40µl of each of the dialysates were separated by SDS-PAGE. The JRY188 3#20.1-derived samples (panel **B**) consisted of fractions 13, 14 and 15 (Figure 4.5, panel A), which were combined and concentrated sixteen-fold by means of dialysis against polyethylene glycol 20000. 20µl of 70mM NaAc (pH 5) or 50mM Tris-HCl (pH 7.4) were added to 4µl of each of the duplicate concentrated samples, all of which was separated by SDS-PAGE. (+) and (++) denote 0.1 and 1ng wild type HaSV, respectively.

Further evidence for the autoproteolytic cleavage of p71 was obtained upon CsCl density gradient centrifugation of pooled glycerol gradient fractions (with buoyant densities corresponding to glycerol concentrations ≥ 30%) (Figure 4.7, panels A - D). As expected, no p64 was detected in the CsCl density gradient fractions prior to the addition of 70mM NaAc (pH 5) (Figure 4.10, panel A). However, a lowering of the pH of fraction 17 (Figure 4.10,

panel B) resulted in the appearance of p64. This fraction had a buoyant density of 1.297 g/ml, which is close to the high limit in the buoyant density range for JRY188 3#20.1 Type III species (Figure 4.5). The relatively high level of p64 detected for fraction 17 (Figure 4.10, panel B) was unexpected, since a p71 band of comparable intensity to that of p64 was absent for the same fraction in Figure 4.10 (panel A).

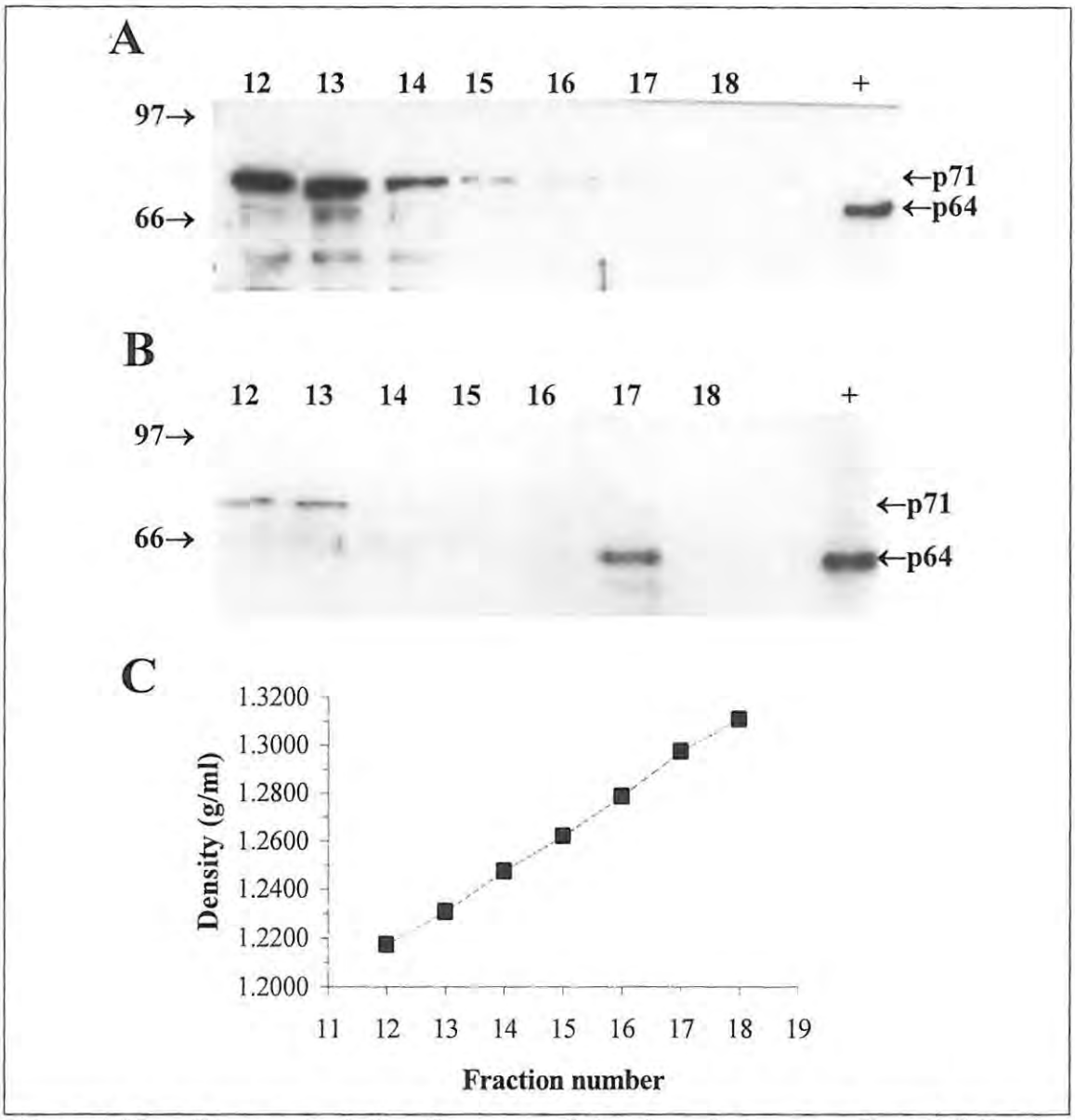

Figure 4.10 Western analysis of a range of fractions that were collected following CsCl density gradient centrifugation of combined glycerol gradient layers before (panel **A**), and after (panel **B**) the addition of five volumes 70mM NaAc (pH5) to each fraction. The diluted samples were kept on ice for 2 hours, TCA precipitated and separated by SDS-PAGE. A profile of the densities of these fractions is shown in panel **C**. (+), 0.1ng wild type HaSV.

4.3.4 RT-PCR analysis of encapsidated RNA

To determine whether *P71* mRNA was encapsidated by the yeast-derived VLPs, RNA was extracted from INVScI- and JRY188 3#20.1-derived VLP preparations. These RNA extracts

were subjected to RT-PCR analysis using primers that were specific for the amplification of an 866bp fragment from the *P71* ORF. RT-PCR analysis on extractions from INVScI-derived preparations showed no evidence for the presence of *P71* mRNA (results not shown). A faint band of 886bp was however present for RT-PCR analysis of an RNA extract from Type III protein species (described for a VLP preparation from JRY188 3#20.1 cells in Section 4.3.2ii) (Figure 4.11). Various non-specific bands were also detected for this extract. No convincing data identifying *P71* mRNA as the encapsidated RNA species was therefore obtained.

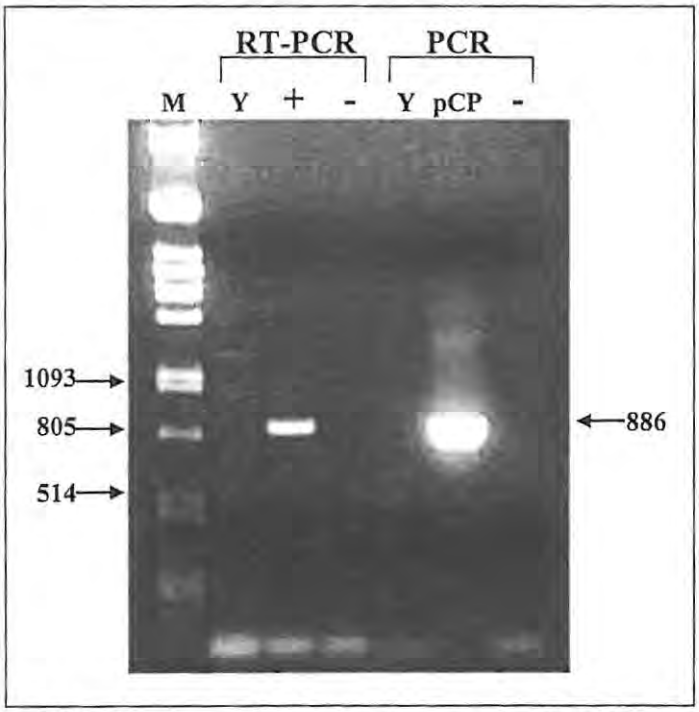

Figure 4.11 Agarose gel electrophoresis of RT-PCR and PCR analyses (indicated by square brackets) of RNA extracts from a JRY188 3#20.1-derived VLP preparation (**Y**) and wild-type HaSV RNA (+). pAV3 (**pCP**) was used as a DNA template for the PCR positive control (Figure 2.3). Negative controls (-) for RT-PCR and PCR contained all the required constituents, but an RNA or DNA template was left out, respectively. The expected size of a PCR product (in bp) with the RNA2F6/AV9 (Appendix 4) primer pair is indicated on the right-hand side of the gel. A *Pst*I digest of lambda-DNA was used as a molecular weight marker (**M**).

4.4 Discussion

4.4.1 Assembly of p71 into HaSV procapsids

Results from initial purification steps for the preparation of HaSV VLPs indicated that a detectable amount of VLP assembly occurred in yeast. Significant amounts of p71 were detected in pellets following centrifugation through 30% sucrose cushions for preparations from INVScI cells that were transformed with pAV3 (Figure 4.3, panel B: lane "P2") and from JRY188 3#20.1 cells (Figure 4.6, panels A and B, lane 3). Furthermore, the centrifugation of p71-containing particles through glycerol density gradients produced a similar result to that obtained for baculoviral-expressed NωV capsids (Agrawal and Johnson, 1995) (Figure 4.7, panels C and D). However, Western analyses of CsCl density gradient fractions from INVScI-derived (Figure 4.3, panel C) and JRY188 3#20.1-derived (Figure 4.5, panel A) preparations demonstrated that as little as 100 – 1000pg (equivalent to 10^7 – 10^8vps) of the p71-containing species had the expected buoyant density values for HaSV procapsids. In addition, TEM examination of yeast VLP preparations (Figure 4.4) showed virus particles at higher concentrations than indicated by Western analyses. This discrepancy suggests that VLPs other than HaSV VLPs may be present in the yeast cells. This possibility is supported by the following experimental evidence:

First, the capsid shells of these particles appear to be much narrower than 8.3nm, which is the width that was computed for NωV procapsids from the CryoEM reconstructions in Figure 1.8 (panel B). Second, the electron dense spots within the inner cores of these particles, which represent encapsidated nucleic acid, are uncharacteristic for tetravirus particles. According to Olson *et al.* (1990) a density distribution plot for a CryoEM reconstruction of NβV revealed that its genome is loosely packed within the particle. This most probably precludes the presence of electron dense areas inside NβV and other tetravirus capsids. Third, a number of the particles in Figure 4.4 appear to contain less electron dense cores, which is indicative of empty particles. The assembly of particles devoid of RNA is highly unlikely for tetravirus particles, because baculoviral expressed NωV particles were shown to contain RNA (Agrawal and Johnson, 1995). Furthermore, RNA is probably required to neutralize the highly charged inner surface of tetravirus capsids (Agrawal and Johnson, 1995).

In the light of the above evidence it is highly probable that the particles in Figure 4.4 represent endogenous yeast virus particles. Likely candidates are the *S. cerevisiae L-A viruses*, double-stranded RNA viruses with capsid shells that are 40nm in diameter (Wickner, 1996). The $T = 1$ capsids of these viruses consist of 76 kDa and 180 kDa capsid proteins. Proteins of

similar sizes were observed on Ponceau S-stained nitrocellulose membranes, subsequent to the electrophoretic transfer from SDS-PAGE gels on which yeast VLP preparations were separated (results not shown). In addition, electron micrographs of negative-stained L-A virus particles also depict electron-dense spots within their inner cores (Van Regenmortel *et al.*, 2000).

Techniques other than the generally used electron microscopic examination were therefore required to provide evidence for the assembly of HaSV procapsids in yeast. A particular functional property of tetraviral procapsids was used to provide proof for correct VLP assembly. Tetravirus procapsids differ from those of nodaviruses in the requirement for an external signal for the initiation of autoproteolytic cleavage (Canady *et al.*, 2000). In nodaviruses, cleavage occurs automatically, subsequent to the assembly of procapsids, with a $t_{1/2}$ of 2 days at 5°C (Gallagher and Rueckert, 1988). This, however, does not seem to be the case for p71-containing CsCl fractions, since no cleavage was detected after a one week storage period at 4°C (Figure 4.5, panel B). Yeast derived p71-containing particles could undergo pH-dependent maturation, analogous to what was recently demonstrated for baculoviral expressed NωV procapsids (Canady *et al.*, 2000) (Figures 4.9 and 4.10). This, in turn, provided evidence for the assembly of functional procapsids. The term "functional" in this context refers to the ability of these particles to carry out the biological function of maturation cleavage. The observation that maturation cleavage occurred exclusively for particles with an identical buoyant density to that of HaSV provided further support for this hypothesis (Figure 4.10, panels B and C).

Yeast-derived p64 was detected more readily than p71 the by anti-HaSV IgGs (Figure 4.10, panels A and B). A possible explanation for this is that the anti-HaSV antibodies bound more readily to p64 than to p71, because these antibodies were raised against mature wild-type HaSV (made up of p64 protomers). This disproportionate level of detection for p64 and p71 could therefore be suggestive of a serological distinction between capsid and procapsid monomers.

No conclusive data identifying *P71* mRNA as the encapsidated RNA species was obtained (Figure 4.11). It is uncertain whether this was due to the nonspecific encapsidation of yeast cellular RNA or insufficient levels of *P71* mRNA for detection by RT-PCR, the latter being most likely due to the very low level of functional procapsid production in these experiments.

4.4.2 Requirement for RNA for maturation cleavage

pH-dependent maturation was only detected for VLPs with a buoyant density identical to that of HaSV. Since the buoyant densities of virus particles are relative to their RNA contents, it appears as if a certain complement of RNA is required for the assembly of functional procapsids. Identical buoyant densities for procapsids and HaSV do, however, not imply that these particles require a complement of RNA equivalent to that of the viral genome for assembly, as is the case for nodavirus particles (Schneemann and Marshall, 1998). It is plausible to suggest that, within the limits of accuracy for buoyant density measurements, these procapsids could undergo maturation as a result of a certain amount of encapsidated RNA. In Section 1.2.5ii it was explained how, based on similarities between noda- and tetraviruses, RNA could play an important role in tetraviral maturation cleavage. The results discussed in this paragraph present evidence for such a requirement for the maturation of HaSV procapsids.

4.4.3 Low yields of HaSV VLPs

The results described in this chapter demonstrate that the expression of *P71* in yeast failed to produce a significant amount of VLPs. A possible explanation for this failure could be a shortage of sufficient amounts of RNA for encapsidation during VLP assembly. This explanation is highly probable for a number of reasons:

First, only a small fraction of the CsCl density gradient fractions that contained p71 had buoyant densities in the same range of that of HaSV (Figure 4.5, panel A, Figure 4.10, panel A), and an even smaller fraction of the preparations could undergo pH-dependent cleavage into p64 (Figure 4.10, panel B). This indicates that only a small amount of these p71-containing species contained significant complements of RNA.

Second, taken that capsid precursor protein mRNA is the predominate type of RNA encapsidated by omegatetravirus VLPs, the more successful expression of omegatetravirus capsids in baculovirus expression systems (Agrawal and Johnson, 1995) could possibly be the result of a much higher level of capsid precursor mRNA in the baculovirus-infected insect cells than yeast cells. The polyhedrin promoter, which was exclusively used for the expression of tetraviral capsid precursors in the latter expression experiments, directs the expression of 25 – 50% of the total cellular protein in baculovirus-infected cells (Miller, 1988). This is at least an order of magnitude greater that the expression levels expected for the P_{GAL1}-directed expression of *P71*, which makes up one of three *GAL* promoters that collectively drives the expression of 0.3 to 1.5% of the total cellular protein in yeast (Johnson, 1987).

A final indication for this hypothesis comes from evidence that the replication strategy for omegatetraviruses is similar to that of nodaviruses, in that genomic RNA is replicated to high levels prior to capsid protein synthesis (Bawden *et al.*, 1999). This indicates that a high cellular concentration of viral RNA is also required for the assembly of omegatetraviral VLPs and virions.

Based on this hypothesis for the lack of assembly into functional VLPs, it is possible that the majority of the p71 detected in yeast VLP preparations form part of abberant VLPs that are devoid of, or that contain insufficient amounts of RNA. Another possible reason for impaired assembly is the absence of as yet unidentified cellular factors that could be required for the assembly of omegatetraviral VLPs. These factors could be nucleation structures guiding accurate accumulation of assembly units (Schneemann *et al.*, 1994). They could also be as yet unidentified "pocket factors" that are required for capsid uncoating (Cheng *et al.*, 1994).

A number of characteristics of the p71-containing species, which did not form part of functional VLPs, were delineated in this chapter. First, these aberrant particles were shown to be very unstable. A large amount of p71 is lost subsequent to centrifugation through sucrose cushions (Figure 4.6). The milder glycerol gradient centrifugation technique might have yielded a larger amount of these unstable particles (Figure 4.7, panels C and D), but they still did not undergo any detectable signs of maturation (Figure 4.7, panels E and F). These particles were furthermore shown to precipitate at a pH below 5.5 (Figure 4.8, panel B). The following chapter will describe how this attribute was used to separate mature HaSV particles from these malformed VLPs.

5 The preparation of infectious HaSV particles from *S. cerevisiae*

5 The preparation of infectious HaSV particles from *S. cerevisiae*

5.1 Introduction

In the previous chapter, it was demonstrated that no p64 was detected in VLP preparations from yeast cells that were induced for the expression of *P71*. These data indicated that autoproteolytic cleavage neither occurred in the yeast cellular milieu, nor during the extraction and purification steps. An inability to produce mature HaSV capsids *in vivo* complicated the effort to produce infectious HaSV, due to the requirement for maturation cleavage in RNA release upon infection (Munshi *et al.*, 1996). A solution to this problem was, however, presented by Canady *et al.* (2000), demonstrating that autoproteolytic cleavage could be induced in NωV procapsids by a reduction in pH. In the previous chapter, it was demonstrated that this also applied for HaSV procapsids that were produced in yeast. This laid the foundation for the development of protocols for the purification of infectious HaSV from yeast, which are described in this chapter.

Apart from an ability to undergo maturation, proof for the infectious character of the yeast-expressed HaSV is reliant on experiments that demonstrate an ability to perform additional biological functions. These functions comprise the specific encapsidation of the viral nucleic acid and the specific attachment to, and delivery of this nucleic acid to the viral host cell. The main objective of this chapter is to demonstrate that yeast-derived HaSV could perform both of these functions.

5.2 Materials and methods

5.2.1 HaSV purification protocols

Yeast-derived HaSV particles were prepared from JRY188 3#20.1 cells that were transformed with either pAV13HC or pAV13HC (G+) (Figure 2.1), and pAV14HPTrp (Figure 2.2) as described in Section 3.2.2. Leucine, tryptophan and uracil were omitted from SMM for the selection of expression vectors. Flask cultures of these cells in SMM containing 5% glycerol and 0.1% glucose to a combined volume of 1.5*l* were grown to midlog phase at 30°C. 10% galactose was then added to these cultures up to a final concentration of 0.01% and the cultures were grown at 20°C for a further 8 hours. The cells were centrifuged at 4000rpm for

10 min at 4°C in a Beckman JA10 rotor and lysed by glass bead homogenization or zymolyase treatment.

i Preparation of mature HaSV particles by way of glass bead homogenization

A protocol that is similar to the one described in Figure 4.1 was used for the purification of mature HaSV virus particles from yeast, with the exception that a pH-reduction step was introduced prior to CsCl density gradient centrifugation. Accordingly, the pellets resulting from centrifugation through 30% sucrose cushions ("Pellet 2" in Figure 4.1) were resuspended in 2ml lysis buffer and stored overnight at 4°C. Hereafter, the resuspended pellets were dialyzed overnight against 50mM Tris-HCl pH 7.4 at 4°C. The pH of the resulting dialysate was dropped by the addition of five volumes of 70mM NaAc (pH5) and the preparation was kept on ice for at least 2 hours. Next, the preparation was concentrated down to a volume lesser than 1ml by means of dialysis against PEG 20000. The concentrated preparation was microfuged for 5 min at 4°C and the resulting supernatant fraction was layered upon a 30% CsCl / 60% CsCl discontinuous gradient as described in Figure 4.1. The rest of the purification protocol was as is described in Figure 4.1.

ii HaSV preparation by way of zymolyase treatment

A protocol that was adapted from one described by Dunn and Wobbe (1997) was used for the lysis of yeast by means of zymolyase treatment. In this protocol (Figure 5.1) cells were enzymatically converted to spheroplasts and then lysed by a combination of Dounce homogenization and osmotic shock. Subsequent to the osmotic shock treatment, the cell lysates were centrifuged at 12500rpm for 15 min at 4°C in a Beckman JA20 rotor and the protocol for centrifugation through sucrose cushions in Figure 4.1 was followed. The dialysis step subsequent to fractionation of CsCl density gradients was altered in some experiments. In these instances, fractions with buoyant densities ranging from 1.23-1.36g/ml were transferred to a SW41 tube and diluted by the addition of 50mM Tris pH7.4. The tube was filled up to 5mm from its rim, sealed with laboratory film, and mixed by inversion. The diluted fractions were centrifuged at 30000rpm for 3 hours at 4°C and the pellets were resuspended in a small volume (50 - 100µl) of 50mM Tris pH7.4.

5.2.2 Bioassays

To ascertain whether yeast virus preparations contained infectious HaSV particles, droplet-feed bioassays were carried out on 24-hour-old *H. armigera* larvae. These larvae were obtained from a laboratory colony, which was maintained as described by Teakle and Jensen

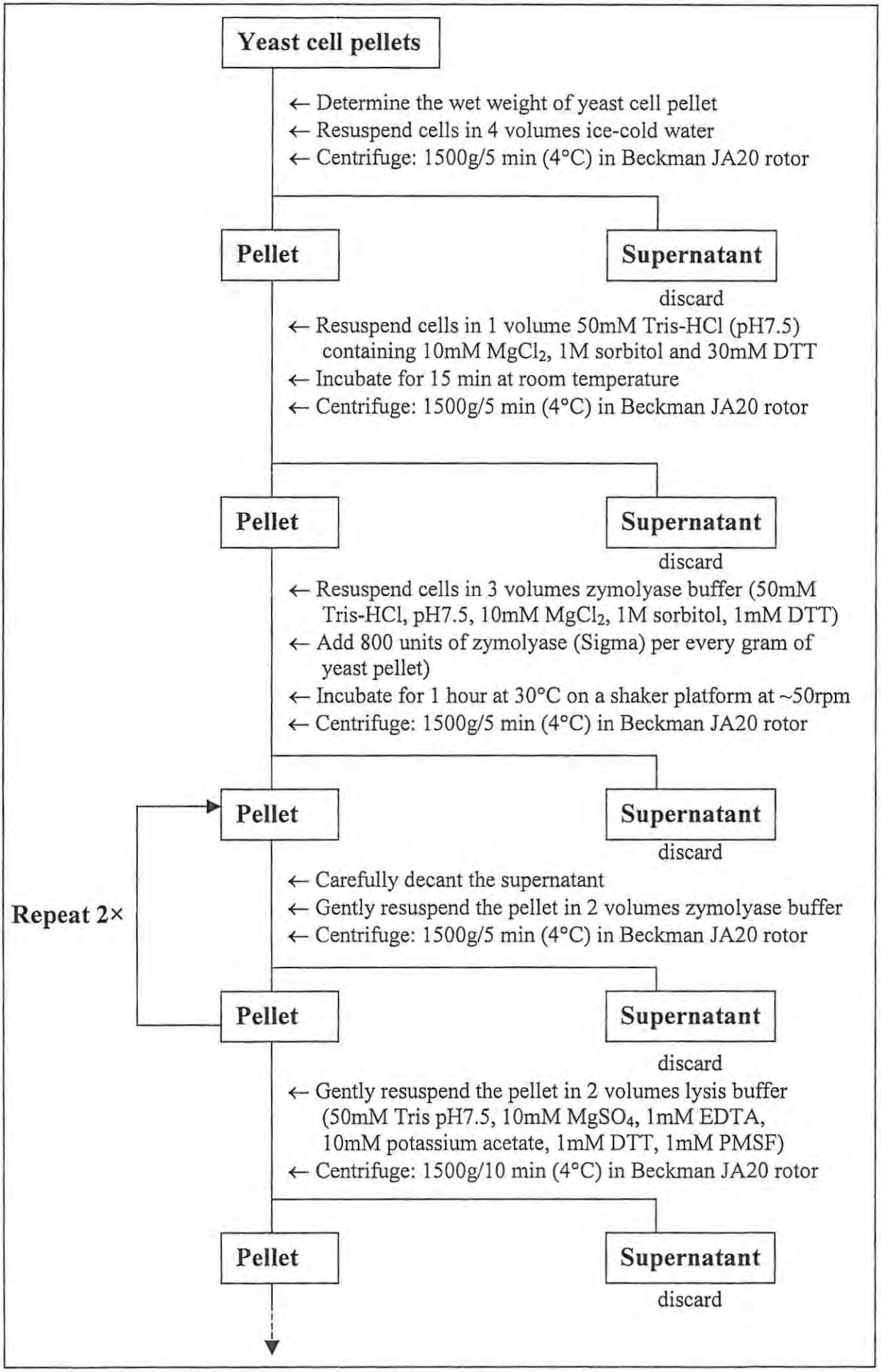

Figure 5.1 Flow diagram for the purification of HaSV particles from yeast by way of zymolyase treatment

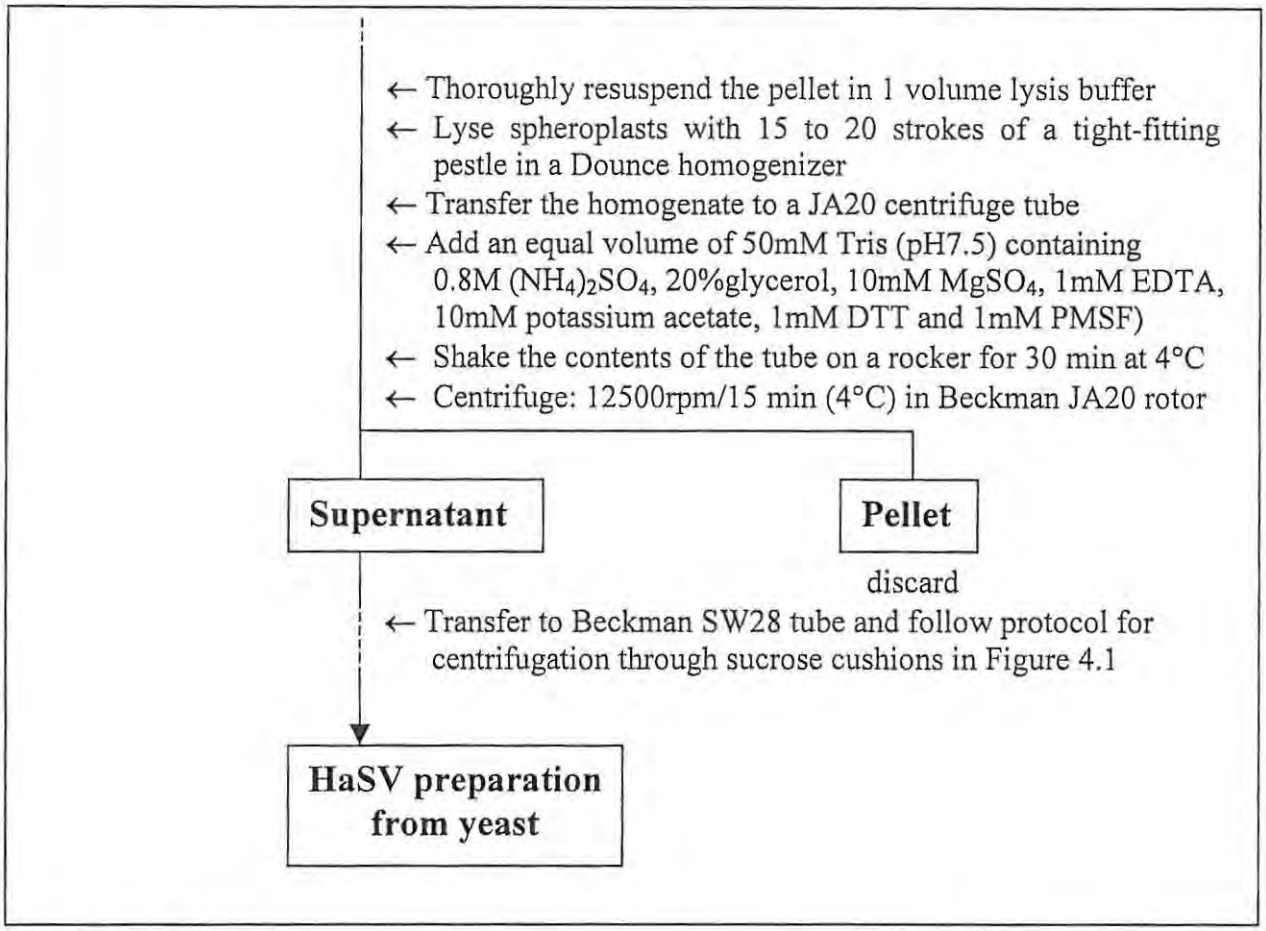

Figure 5.1 Continued...

(1985) at the CSIRO Division of Entomology in Canberra, Australia. Prior to the assay, $1/10^{th}$ volume of food colouring was added to virus preparations, droplets of which were arranged in a circle with a diameter of approximately 3 cm on a piece of wax paper. The coloured droplets were approximately 0.5 cm apart. The neonates were kept on a dry piece of filter paper in a desiccator for a few hours prior to the assay, and transferred to the centre of the wax paper. The insects were consequently forced to migrate past the virus specimens toward the periphery of the wax paper. Proof for ingestion of the viral specimens came from the detection of digestive tracts that had the same colour as that of the food colouring.

The insects were thereafter transferred to jelly trays (Nu-trend containers, Jacksonville, Florida, USA) containing soybean-wheat germ diet (Appendix 9) and sealed with Mylar™ (Dupont, Wilmington, Denver, USA). The larvae were maintained at 30°C throughout the test and response was assessed by scoring larval development at 5 and 7 days post infection. A description of the developmental stages of *H. armigera* used for the scoring of the bioassays is provided in Appendix 10.

5.2.3 RNA extractions

For total yeast RNA extractions, 200ml yeast cell cultures were grown to midlog phase at 30°C in SMM containing 2% glucose, centrifuged for 10 min at 4000rpm in a Beckman JA20 rotor and resuspended in SMM containing 2% galactose. The cells were then grown for a further 4h at 30°C and spun down as described above. RNA was extracted from the resultant pellets as described in Section A8.4 (Appendix 8). Total RNA extractions from *H. armigera* larvae were obtained according to the protocol described by Gordon *et al.* (2001). RNA was purified from HaSV and yeast virus preparations as described in Section 4.2.5, with the exception that it was treated with RQ1 RNAse-free DNase (Promega) prior to the addition of phenol. RNA within the various extracts was quantitated using a Gene Quant RNA/DNA calculator (Pharmacia Biotech).

5.2.4 *In vitro* transcription

A short supply of HaSV necessitated the generation of RNA1 and RNA2 transcripts for positive controls in RNA analyses. These transcripts were synthesized by means of in *vitro* transcription with T7 RNA polymerase (Promega) according to the supplier's protocol. The T7 promoter precedes the sequences of HaSV *RNA1* and *RNA2* in the plasmids pBJ33R1HC (Figure A2.1, panel B, Appendix 2) and pBJ33R2HC (Figure A2.1, panel C, Appendix 2), respectively. Accordingly, pBJ33R1HC was linearized by *Hind* III and used as a template for the synthesis of a 5536 nucleotide RNA1 transcript. Similarly, pBJ33R2HC was linearized by *Stu* I and used as a template for the synthesis of a 1747 nucleotide RNA2 transcript.

5.2.5 Northern analyses

RNA was subjected to denaturing agarose gel electrophoresis in the presence of formaldehyde according to Sambrook *et al.* (1989) and visualized by UV illumination. The RNA was transferred overnight to Zeta-Probe membranes (BIO-RAD) by capillary blotting (Sambrook, *et al.*, 1989) and fixed to the membranes by UV illumination for 3 min. The membranes were washed twice for 20 min in 2 x SSC (Sambrook *et al.*, 1989), dried between two pieces of filter paper and stored in plastic bags at room temperature. Pre-hybridizations and hybridizations on the Zeta-Probe membranes were carried out according to the formamide protocol described by the manufacturer (BIO-RAD).

For the detection of RNA1, P^{32}-labelled RNA probes were prepared by *in vitro* transcription using T3 RNA polymerase (Promega) as instructed by the supplier. Accordingly, the plasmid pBCR1dA (Figure A2.1, panel A, Appendix 2), which carries the T3 promoter followed by the complementary sequence to the 5' proximal region of HaSV RNA1, was linearized with *Afl* II

and used as a template for the synthesis of a 1347 nucleotide RNA probe. For the detection of *P71* mRNA and RNA2, P^{32}-labelled probes were prepared using the random primed DNA labelling kit from Roche. A 1954 bp *Bam* HI fragment was excised from the plasmid pAV3 (Figure 2.3), gel purified by means of the Gene Clean kit (BIO101) and used as a template for the synthesis of random priming probes. Both the RNA1- and RNA2-specific probes were purified using Sephadex G-50 columns (Roche).

5.2.6 RT-PCR analyses

The Superscript™ One-Step RT-PCR system (GibcoBRL) was used for the specific amplification of various HaSV RNA1 and RNA2 cDNA fragments from yeast and *H. armigera* RNA extracts (thermal cycling programme: Programme 4 in Appendix 5). The HVR1B5P / HVB11VF2, HVB11VF6 / HVB35XF1 and HB35F2C / HVR1Cla primer pairs were used for the detection of RNA1, while the HR236F3 / H3R1B primer pair was used for the detection of RNA2 (Appendix 4). Reverse transcriptase was omitted from certain reactions to ensure that the amplified products were not the result of genomic DNA contamination.

The primers RNA1F4 and RNA1 R7 (Appendix 4) were used in RT-PCR for the detection of encapsidated RNA1 transcripts. These reactions were performed on HaSV preparations from yeast through the application of the Titan™ One Tube RT-PCR System (Roche). A similar programme to Programme 3 (Appendix 5) was used for thermal cycling, with the exception that the annealing temperature was reduced from 50°C to 45°C. PCR analyses (using the Expand™ High Fidelity PCR System from Roche) were performed on these RNA extracts to ensure that amplified products were not the result of genomic DNA contamination.

5.2.7 Use of pAV13HC and pAV13HC (G+) vectors in expression experiments

pAV13HC (a defective plasmid that lacks the 5'-most nucleotide of *RNA1*) and pAV13HC (G+) (a plasmid in which this error was repaired) were used for the expression of *RNA1* in *S. cerevisiae* (Figure 2.1 and Table 2.2). pAV13HC was used in experiments that led to: (a) the detection of RNA1, RNA2 and *P71* mRNA in total yeast RNA (Section 5.3.1) and (b) the production of a virus preparation (denoted BZ23 in Figure 5.7, panel C) that was used in a droplet feed bioassays (Section 5.3.5). pAV13HC (G+) was used for the remainder of the work described in this chapter, which include: (a) studies on the effect of the expression of *RNA1* on the yield of yeast-produced VLPs (Section 5.3.2), (b) the majority of virus preparations from cells co-expressing *P71*, *RNA1* and *RNA2* (Section 5.3.3) and (c) RT-PCR analysis of RNA encapsidated by yeast-produced HaSV particles (Section 5.3.4).

5.3 Results

5.3.1 Detection of RNA1, RNA2 and *P71* mRNA in total yeast RNA

To test whether the co-expression of *P71*, *RNA1* and *RNA2* results in the production of viral genomic RNA transcripts and *P71* mRNA in yeast, expression experiments were carried out with JRY188 cells, with or without the chromosomal copy of *P71,* which were transformed with either or both of the *RNA1* and *RNA2* expression vectors. Henceforth, cells with these various combinations will be identified according to the names that are listed in Table 5.1.

Table 5.1 Names designated to different yeast-derived preparations

Name of preparation	Yeast Strain	Plasmids	Phenotype
JRY188	JRY188	None	His^-, Leu^-, Trp^-, Ura^-
JRY188::*P71*	3#20.1	None	$P71^+$, His^-, Trp^-, Ura^-
JRY188::*P71; R1*	3#20.1	pAV13HC[1] or pAV13HC (G+)[1]	$P71^+$, $RNA1^+$ His^-, Trp^-,
JRY188::*P71; R2*	3#20.1	pAV14HPTrp[2]	$P71^+$, $RNA2^+$, His^-, Ura^-
JRY188::*P71; R1, R2*	3#20.1	pAV13HC[1] or pAV13HC (G+)[1] + pAV14HPTrp	$P71^+$, $RNA1^+$, $RNA2^+$, His^-
JRY188::*R1*	JRY188	pAV13HC	$RNA1^+$, His^-, Leu^-, Trp^-
JRY188::*R2*	JRY188	pAV14HPTrp	$RNA2^+$, His^-, Leu^-, Ura^-
JRY188::*R1,R2*	JRY188	pAV13HC + pAV14HPTrp	$RNA1^+$, $RNA2^+$, His^-, Leu^-

[1] Figure 2.1
[2] Figure 2.2

i Northern analyses

After induction with galactose, total RNA was extracted from yeast strains that carried chromosomal and episomal copies of expression cassettes for *RNA1*, *RNA2* and *P71* (Table 5.1). These RNA extracts were analyzed on formaldehyde agarose gels, blotted onto nucleic acid bonding membranes and probed for the presence of RNA1 and RNA2 transcripts as well as *P71* mRNA (Figure 5.2). To ensure the analysis of equivalent amounts of RNA on each Northern blot, the concentration of RNA in these extracts was determined

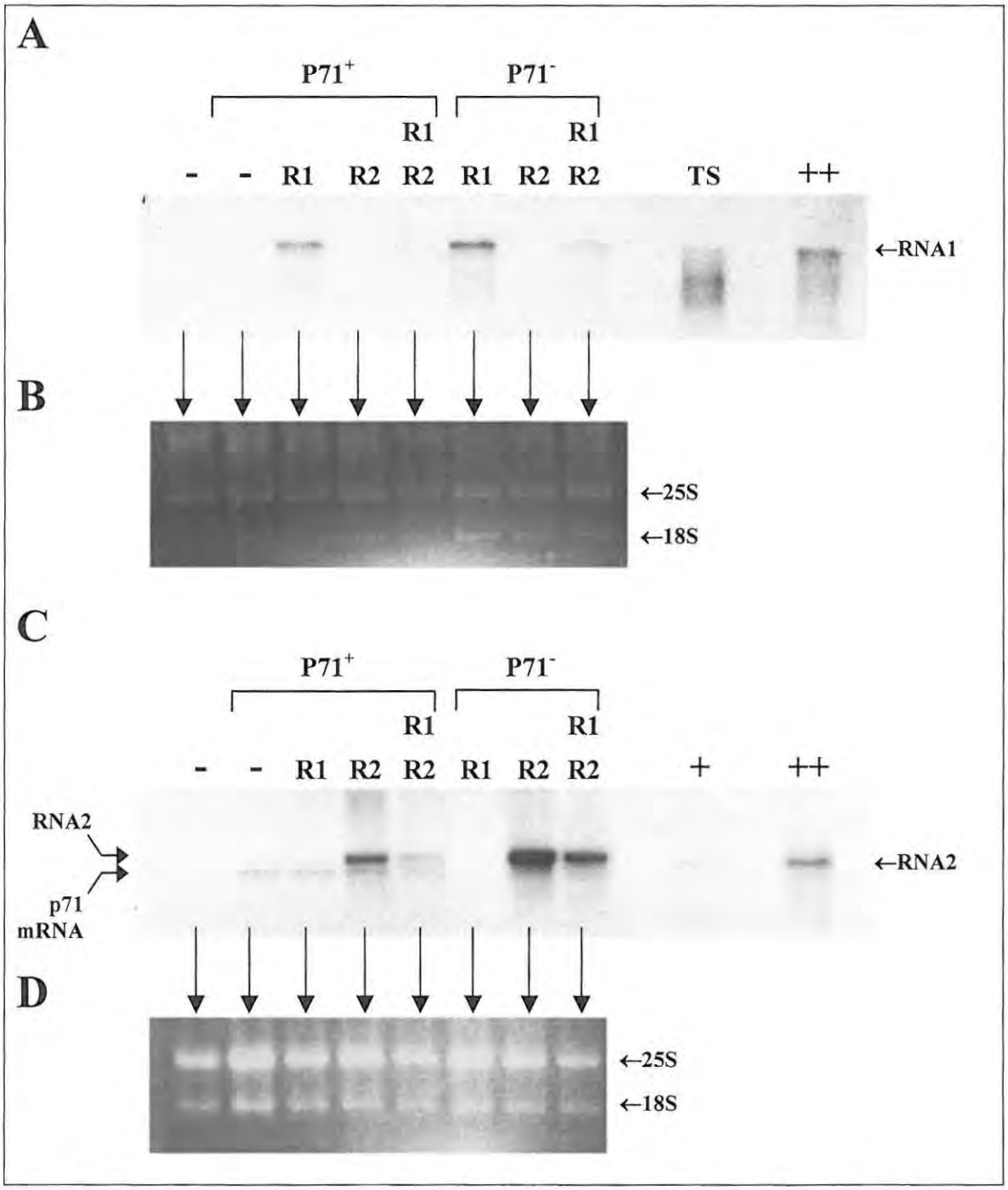

Figure 5.2 Northern analyses of total RNA extracts from yeast cells expressing HaSV gene constructs probed for RNA1 (panel **A**) and RNA2 (panel **C**). Bands for **28S** and **18S** rRNA in the formaldehyde agarose gels below each Northern blot (panels **B** and **D**) indicate that equivalent amounts of RNA were loaded in each well. Total RNA was extracted from **P71**$^{+}$ or **P71**$^{-}$ cells that were transformed with plasmids carrying *RNA1* (**R1**), *RNA2* (**R2**) or *RNA1* and *RNA2* (**R1 R2**). Bands representing RNA1, RNA2 and *P71* mRNA are indicated. 10ng and 1ng HaSV RNA labeled ++ and +, respectively, and an RNA1 sense transcript that was prepared by *in vitro* transcription (**TS**) were run as positive controls.

spectophotometrically. This was verified by RNA UV illumination of ethidium bromide stained gels (Figure 5.2, panels B and D), which revealed that the band intensities for 25S and 18S rRNA in the different lanes were equivalent.

RNA1 transcripts, which were similar in size to HaSV RNA1, were exclusively detected in RNA extracts from yeast cells expressing *RNA1* (Figure 5.2, panel A). On the other hand, RNA2-specific probes hybridized to two RNA species of distinct molecular weights that were present in some of the yeast RNA extracts (Figure 5.2, panel C). The one molecule had a similar molecular weight to HaSV RNA2 and was only present in RNA extracts from yeast cells expressing *RNA2*. Conversely, the other RNA molecule had a lower molecular weight than HaSV RNA2 and was only present in RNA extracts from yeast cells expressing *P71*. The RNA2-specific random priming probes, which were synthesized from a complementary sequence to RNA2 spanning the *P71* ORF, therefore hybridized to *P71* mRNA and RNA2 transcripts within the various RNA extracts. Thus the expression of the HaSV genomic transcripts and *P71* mRNA in yeast was detected on these blots.

The HaSV genomic RNA levels in extracts from cells transformed with both pAV13HC and pAV14HPTrp (Table 5.1) were lower than those for cells transformed with only one of these expression vectors (Figure 5.2, panels A and C). This trend was observed for the expression of *RNA1* and *RNA2* in $P71^{+}$and $P71^{-}$ cells. The level of chromosomally expressed *P71* mRNA, however, seemed to be unaffected by the presence, or absence, of one or both of these expression vectors (Figure 5.2, panel C). As a result of this, RNA2 appeared to be more abundant than *P71* mRNA for JRY188::*P71; R2* cells, while similar levels of these RNAs were detected for JRY188::*P71; R1*, *R2* cells.

ii RT-PCR analyses

Four primer pairs were used for the amplification of RNA1 and RNA2 cDNA fragments from yeast RNA extracts; three were specific for RNA1 sequences (PP1, PP2 and PP3) and one was specific for RNA2 sequences (PP4) (Figure 5.3, panel A and Figure 5.4, panel A). PP3-dependent amplification is dependent on the binding of the antisense primer (HVR1Cla) to the utmost 3' nucleotides of yeast-derived RNA1 transcripts. Likewise, PP1-dependent amplification is dependent on the binding of the sense primer (HVR1B5P) to a sequence complementary to that of the 5'end of RNA1. The detection of RT-PCR products for PP1 and PP3 would therefore indicate that most of the 5' and 3' nucleotides of yeast-derived RNA1 transcripts were present.

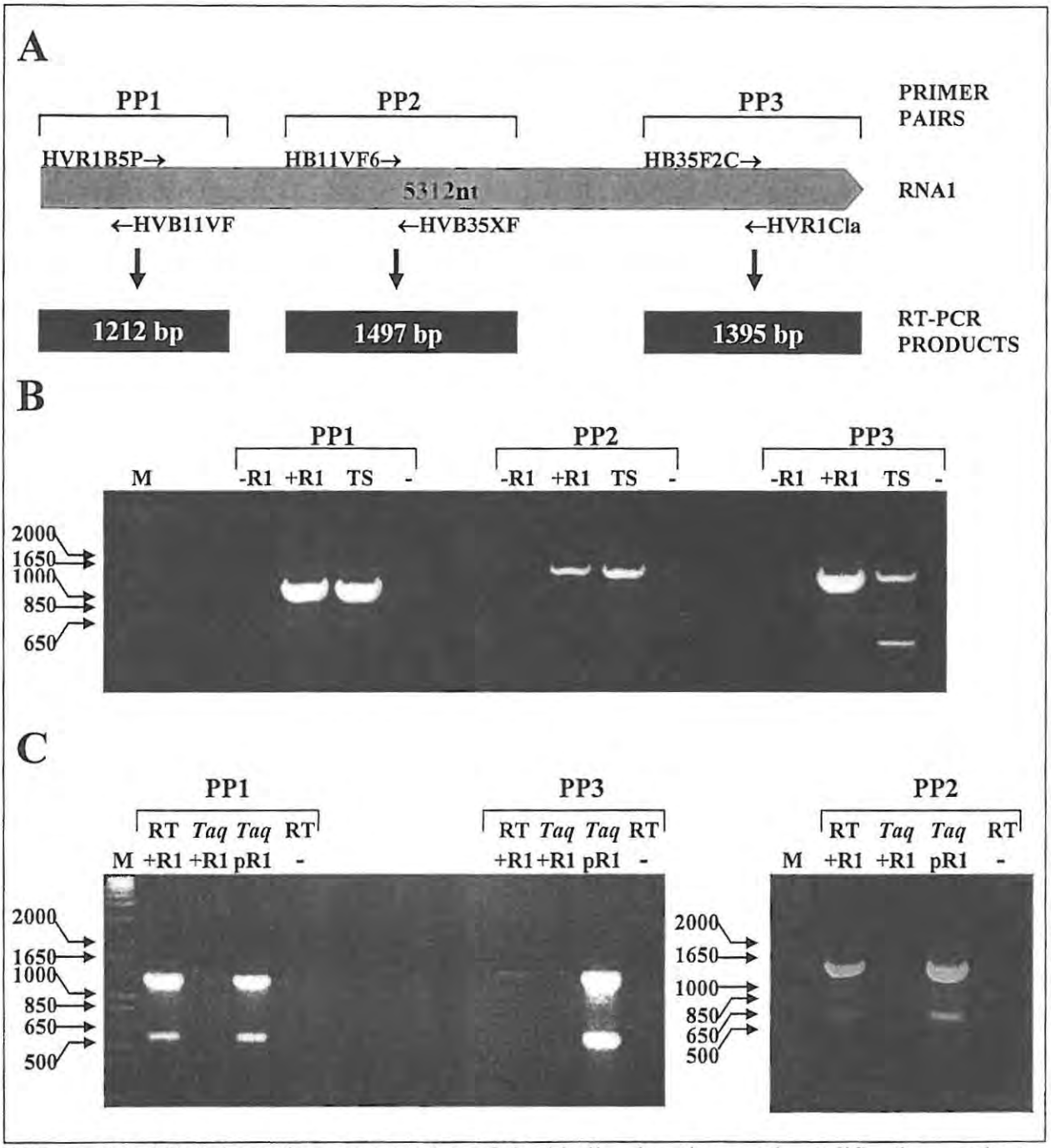

Figure 5.3 (**A**) Schematic representation of the binding locations and amplification products upon RT-PCR analysis using the HVR1B5P / HVB11VF2 (**PP1**), HVB11VF6 / HVB35XF1 (**PP2**) and HB35F2C / HVR1Cla (**PP3**) primer pairs. (**B**) RT-PCR on RNA extractions from JRY188 (**-R1**) and JRY188::*R1* (**+R1**) cells using the primer pairs PP1, PP2 and PP3. RNA1 sense transcripts that were prepared by *in vitro* transcription (**TS**) were used as positive controls for these reactions, while negative controls (-) contained all the required constituents except for an RNA template. (**C**) RT-PCR (**RT**) and PCR (***Taq***) on RNA extractions from JRY188::*R1* (**+R1**) cells using the primer pairs PP1, PP2 and PP3 to determine if the amplified products in panel **B** were not the result of genomic DNA contamination. pAV13HC (**pR1**) (Figure 2.1) was used as a DNA template for PCR positive controls. Negative controls for RT-PCR (-) contained all the required constituents except for an RNA template. The 1Kb Plus DNA Ladder (Promega) was used as a molecular weight marker (**M**) for each of these gels.

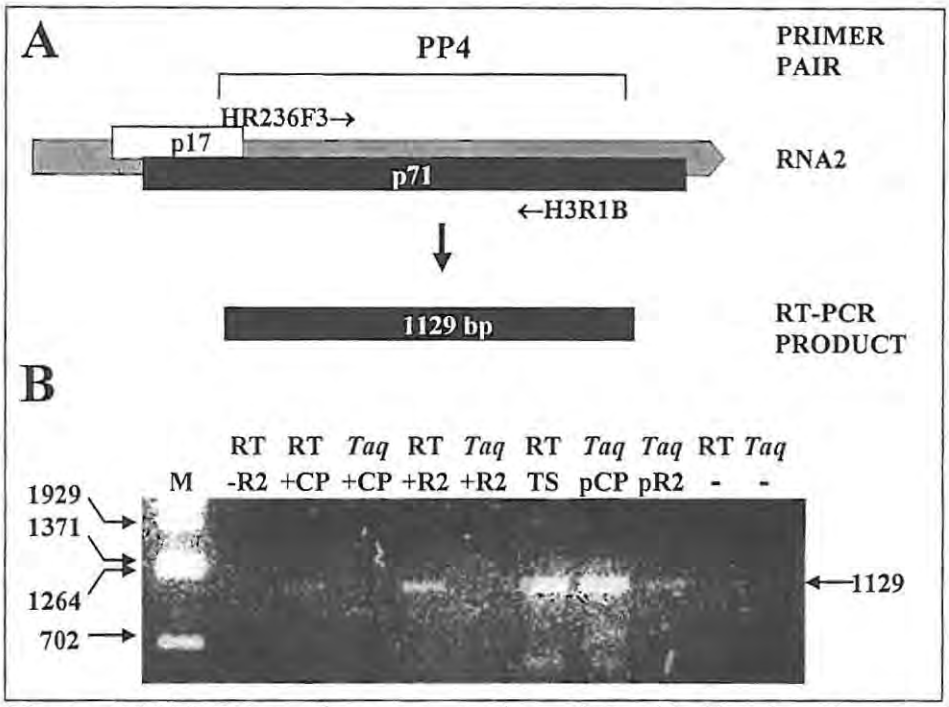

Figure 5.4 (**A**) Schematic representation of the binding locations and amplification product upon RT-PCR analysis using the HR236F3 / H3R1B (PP4) primer pair. (**B**) RT-PCR (**RT**) on RNA extractions from JRY188 (**-R2**), JRY188::*P71* (**+CP**) and JRY188::*R2* (**+R2**) cells using the PP4 primer pair. PCR (***Taq***) was performed on these RNA extracts to ensure that amplified products were not the result of genomic DNA contamination. An RNA2 sense transcript that was prepared by *in vitro* transcription (**TS**) was used as a positive control for RT-PCR, while pAV3 (**pCP**) (Figure 2.3) and pAV14HPTrp (**pR2**) (Figure 2.2) were used as DNA templates for PCR positive controls. Negative controls for RT-PCR and PCR (**-**) contained all the required constituents except for RNA and DNA templates, respectively. A *BstE*II digest of lambda-DNA was used as a molecular weight marker (**M**).

RT-PCR analyses on RNA extracts from JRY188::*R1* cells led to the amplification of cDNA fragments with similar sizes to that expected for each of the three primer pairs (Figure 5.3, panel B). No RT-PCR products were obtained from reactions that were performed on RNA from JRY188 cells. Furthermore, amplified products were not detected for PCR, indicating that these products were not the result of genomic DNA contamination in the RNA isolates (Figure 5.3, panel C). Similar results were obtained for the RT-PCR analysis of RNA extracts from JRY188::*R2* and JRY188::*P71* cells (Figure 5.4, panel B). 1129 bp fragments were amplified from these RNA extracts, as expected for the PP4 primer pair (Figure 5.4, panel A). Reactions on RNA extracts from JRY188 cells did not produce bands corresponding to this size. Furthermore, no bands were detected if reverse transcriptase was omitted from these reactions, proving that the amplified products were not a result of genomic DNA contamination. These analyses confirmed the Northern analyses (Figure 5.2) in demonstrating

that RNA1 and RNA2 transcripts, as well as *P71* mRNA, were detected in total RNA extracts from yeast.

5.3.2 The effect of yeast-expressed RNA1 transcripts on VLP preparations

A direct comparison was drawn between VLP preparations from JRY188::*P71* and JRY188::*P71*; *R1* cells to determine whether the expression of *RNA1* had an effect on the yield of yeast-produced VLPs. This comparative study also tested whether the inability of the VLPs to mature was due to a lack of encapsidated RNA1. Accordingly, VLP preparations from JRY188::*P71* and JRY188::*P71; R1* cells were subjected to CsCl density gradient ultracentrifugation, fractionated and subjected to Western analysis. There was a similar distribution of p71 throughout the CsCl density gradient fractions from these preparations (Figure 5.5, panels A and B). The co-expression of *RNA1* did not result in the production of p64 in any of the CsCl fractions (Figure 5.5, panel B). Therefore, the presence of RNA1 had no significant effects on VLP yield and maturation, and acid-maturation was still required for the preparation of mature VLPs from yeast.

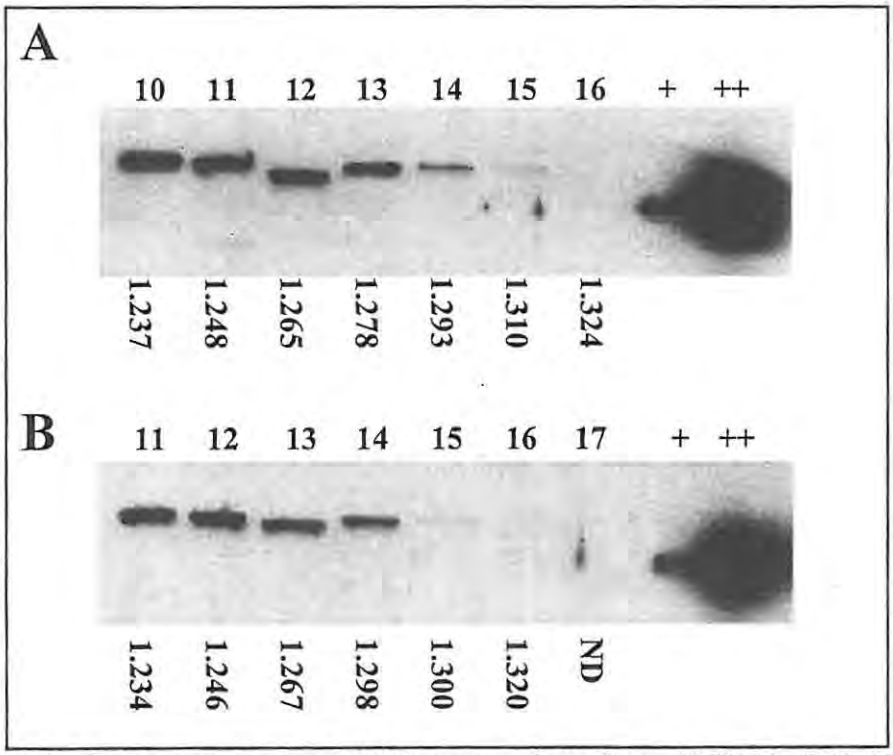

Figure 5.5 Western analysis of VLP preparations from JRY188::*P71* (**A**) and JRY188::*P71*; *R1* (**B**) cell cultures, each with a total volume of 1.5*l*. Yeast pellets were subjected to the sucrose cushion centrifugation purification procedure described in Figure 4.1. Accordingly, solutions buffered at a pH of 7.4 were used throughout the protocol. 20µl (out of a total volume of 400µl) of each of the dialyzed CsCl fractions were separated by SDS-PAGE. The buoyant densities (in g/ml) of these fractions are shown below each figure. (+) and (++) denote 0.1 and 1ng wild type HaSV, respectively.

5.3.3 Virus preparations from JRY188::*P71*; *R1*, *R2* cells

To determine whether infectious HaSV virions could be prepared from yeast, virus preparations were performed on JRY188::*P71*; *R1*, *R2* cells, which were induced for the expression of *P71*, and HaSV *RNA1* and *RNA2*. Two different protocols were followed for the extraction of virus particles from these cells: glass bead homogenization and zymolyase treatment.

i Preparation of mature HaSV by way of glass bead homogenization

The protocol described for the preparation of VLPs in the previous chapter (Figure 4.1) was modified by the inclusion of a pH reduction step prior to CsCl density gradient ultracentrifugation. The reasoning behind the introduction of pH reduction before CsCl density gradient ultracentrifugation was that the stable matured particles would be more resilient to this harsh purification technique than the unstable immature particles. This protocol had the potential for an improved yield of VLPs and vps to previous protocols in which the particles were only matured after CsCl gradient centrifugation.

Western analysis of virus preparations, in the presence (Figure 5.6, panel B) or absence (Figure 5.6, panel A) of a pH reduction step, demonstrated that all the p71-containing species in CsCl density gradient fractions became insoluble upon a reduction in pH. Other proteins, which interacted with the anti-HaSV antibodies, were also lost to the pellet fractions subsequent to pH reduction. These included a 69kDa protein (Fraction 14 in Figure 5.6, panel A), which was described as a Type II protein species (Figure 4.5), and proteins with molecular weights smaller than 71kDa (Figure 5.6, panel A), the latter probably representative of proteolytic breakdown products. Western analysis of preparations that were subjected to a reduction in pH demonstrated that the anti-HaSV antibodies exclusively detected a protein with a slightly lower electrophoretic mobility than that of p64 and a buoyant density of 1.330g/ml (Figure 5.6, panel B). The concentration of this protein was less than 3×10^7 vp/ml as estimated from the band intensity of the 0.1ng HaSV positive control. Taken that this protein band represented HaSV viral or subviral particles, this translates into a very low yield of approximately 10^7 HaSV particles from a 1.5*l* yeast cell culture. A second virus preparation from JRY188::*P71*; *R1*, *R2* cells produced similar results, with the exception that the density of the fraction containing an equivalent protein interacting with anti-HaSV antibodies was 1.292 g/ml (results not shown).

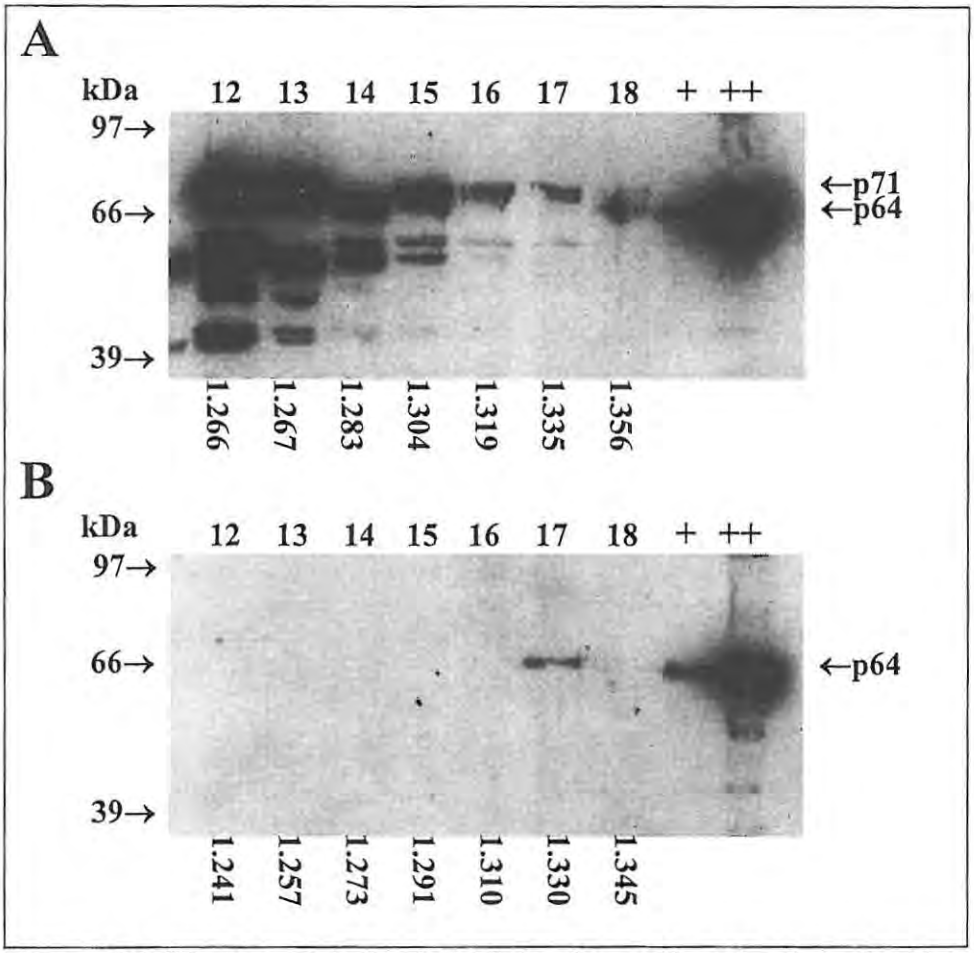

Figure 5.6 Western analysis of CsCl density gradient fractions for virus preparations from 1.5*l* JRY188::*P71*; *R1*, *R2* cell cultures that were either not acid matured (**A**) or acid matured (**B**) prior to centrifugation. The sucrose cushion centrifugation purification procedure for the preparation of mature HaSV particles (Section 5.2.1i) was followed for the fractions in panel **B**. A similar protocol was followed for the fractions in panel **A**, with the exception that the pH reduction step was omitted. 80µl (out of a total volume of 400µl) of each of the dialyzed fractions were TCA precipitated and separated by SDS-PAGE. The respective buoyant densities (in g/ml) of these fractions are shown below each figure. (+) and (++) denote 0.1 and 1ng wild type HaSV, respectively.

ii Preparation of mature HaSV by way of zymolyase treatment

A potential disadvantage of the glass bead homogenization procedure is that it is a harsh technique that could lead to the denaturation of proteins (Dunn and Wobbe, 1997). A gentler technique for cell lysis was tested to determine if the low yield of HaSV particles was due to physical damage of unstable HaSV provirus particles during glass bead homogenization. This technique included a step in which cells were converted to spheroplasts by zymolyase treatment (Figure 5.1), followed by the addition of a buffer containing 0.8M ammonium sulphate (which induced cell lysis through osmotic shock) and homogenization with a Dounce homogenizer.

A virus preparation was performed on JRY188::*P71*; *R1*, *R2* cells, which were induced for the expression of the HaSV components and subjected to this cell lysis technique. Two protein bands with similar relative mobilities to that of p64 were detected at a density of 1.308g/ml in the resultant CsCl fractions (Figure 5.7, panel A). An estimation of the amount of virus particles represented by each of these two bands indicated that the use of this cell lysis technique did not result in an improved yield over that of glass-bead homogenization. The possibility that one of these bands represented p64, however, suggested that mature HaSV particles could be purified from yeast by the use of this cell lysis technique. This was confirmed by Western blots of a subsequent virus preparation, in which CsCl was removed from the CsCl density gradient fractions by means of ultracentrifugation, instead of dialysis (Figure 5.7, panel B).

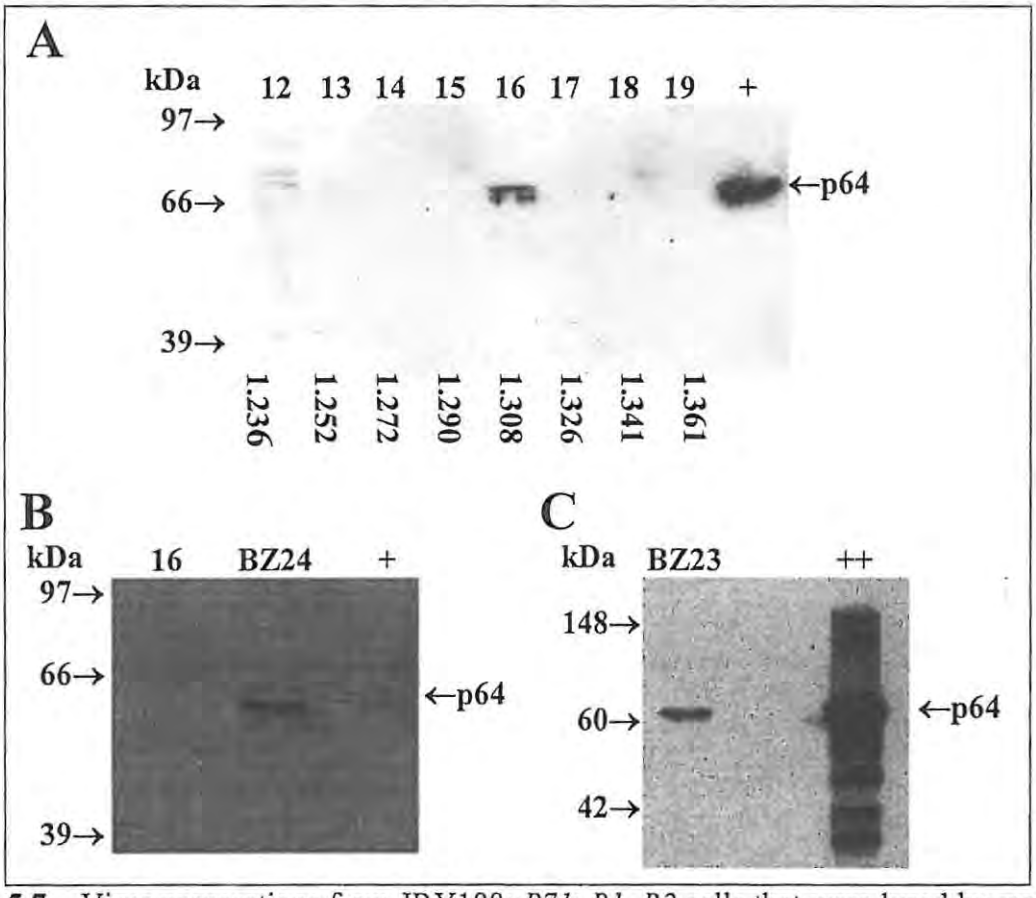

Figure 5.7 Virus preparations from JRY188::*P71*; *R1*, *R2* cells that were lysed by zymolyase treatment, followed by osmotic shock and Dounce homogenization (described in Figure 5.1). (**A**) Western analysis of CsCl density gradient fractions that were obtained from a 3*l* culture. 100µl (out of a total volume of 400µl) of each of the dialyzed fractions were TCA precipitated and separated by SDS-PAGE. (**B**) Western analysis of equivalent amounts of fraction 16 (**16**) in panel A and a preparation in which CsCl was removed by means of ultracentrifugation (**BZ24**) instead of dialysis. (**C**) Western analysis of a virus preparation (**BZ23**) that was purified from a 0.5l culture using the same protocol as what was used for the preparation of BZ24 (panel B). 2µl (out of a total volume of 20µl) of this preparation was loaded on the SDS-PAGE gel. (+) and (++) denote 0.1 and 2ng wild type HaSV, respectively.

Not only did this preparation demonstrate the presence of matured HaSV particles (sample labelled "BZ24" in Figure 5.7, panel B); it also showed that a greater part of the yeast-derived HaSV particles were lost to the purification procedure during dialysis. As a result of a variable sensitivity for detection by Western analysis, p64 was detected in the same dialysed CsCl fraction in one blot (sample labelled "16" in Figure 5.7, panel A) and not in another (sample labelled "16" in Figure 5.7, panel B). However, in the latter blot, this protein was clearly detected for an equivalent amount of a preparation that was subjected to ultracentrifugation (sample labelled "BZ24" in Figure 5.7, panel B).

5.3.4 RT-PCR analysis of encapsidated RNA

To determine if the yeast-derived HaSV particles were capable of the specific encapsidation of HaSV RNA transcripts that were expressed *in trans* with *P71*, RNA was extracted from a virus preparation from JRY188::*P71*; *R1*, *R2* cells. This RNA extract was subjected to RT-PCR analysis using primers specific for the amplification of a 492bp fragment from HaSV RNA1. A faint band of this size was detected for this extract (Figure 5.8), indicating that RNA1 transcripts were encapsidated by yeast-derived HaSV particles. This RT-PCR product was not amplified from yeast genomic DNA, since it was not detected for a reaction in which reverse transcriptase was left out.

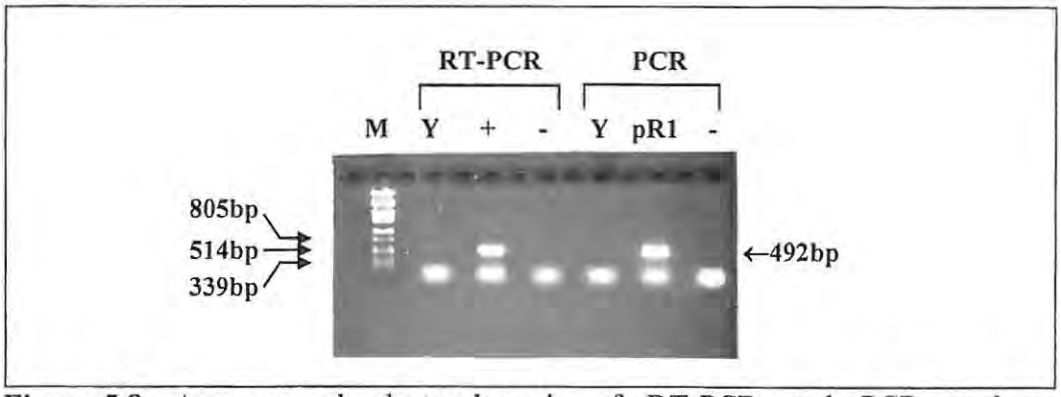

Figure 5.8 Agarose gel electrophoresis of RT-PCR and PCR analyses (indicated by square brackets) of RNA extracts from a yeast-derived virus preparation (**Y**) and wild-type HaSV RNA (+) through the use of primers that were specific for RNA1. RNA was extracted from 100µl of fraction 17 (Figure 5.6, panel B) and resuspended in 10µl DEPC-treated water subsequent to ethanol precipitation. 1µl of this extract was added to each reaction mix. pAV13HC (**pR1**) (Figure 2.1) was used as a positive control for PCR, while negative controls (-) for RT-PCR and PCR analyses contained all the required constituents, but an RNA or DNA template was left out, respectively. The expected sizes of RT-PCR and PCR products with the RNA1F4 / RNA1R7 primer pair are indicated on the right-hand side of the gel. A *Pst*I digest of lambda-DNA was used as a molecular weight marker (**M**).

5.3.5 Droplet feed bioassays on *H. armigera* larvae

The infectivity of yeast-derived HaSV particles was assessed by means of a droplet feed bioassay, in which the larval development of *H. armigera* larvae exposed to yeast-derived HaSV particles was scored. The particles were purified from JRY188::*P71*; *RNA1*, *RNA2* cells that were lysed by means of zymolyase-treatment (Figure 5.1). The detection of p64 on a Western blot provided evidence for the presence of mature HaSV particles within this preparation (sample labelled "BZ23" in Figure 5.7, panel C).

The bioassay data demonstrated that 36% of the larvae remained in the first three larval instar stages after 7 days upon ingestion of the yeast-derived HaSV, while only 8% of the control larvae remained in these larval stages after this period in time (Table 5.2). The larvae also showed a stronger response to the yeast-derived HaSV than to the 10^7vp/ml HaSV positive control, indicating that the concentration of this sample should be in the range of 10^7 – 10^8vp/ml. This virus particle concentration is compatible with estimations for the amount of p64 detected on Western blots (Figure 5.7, panels B and C).

Table 5.2 Droplet feed bioassay of HaSV particles produced in JRY188::*P71*; *R1*, *R2* cells

Sample	*n*	Proportion of treated larvae in respective developmental stages* (%)							
		S/D	**E3**	**M3**	**L3**	**E4**	**M4**	**L4**	**In5**
-ve control	26	4			4		38	23	31
Yeast-derived HaSV	25		4	32		4	24	12	24
HaSV (10^7vp/ml)	24				17		38	13	33
HaSV (10^8vp/ml)	24	42	4	13	4		17	8	13
HaSV (10^9vp/ml)	18	67		11		22			
HaSV (10^{10}vp/ml)	23	96		4					

n, sample number

* S/D, stunted or dead; E3, early third; M3, mid third; L3, late third; E4, early fourth; M4, mid fourth; L4, late fourth; In5, fifth instar

Further proof that the yeast produced HaSV particles were responsible for growth retardation was obtained from the RT-PCR analysis of RNA extracts from the larvae that were used in this bioassay (performed by Amir Masoumi from the CSIRO Division of Entomology in Canberra, Australia). Total RNA was prepared from larvae that ingested yeast-derived HaSV particles as well as those which served as positive and negative controls (Table 5.2). RT-PCR with primers specific to an 1128 nucleotide region internal to the HaSV RNA2 was used to

detect the presence of HaSV in these animals. The results confirmed the presence of HaSV in the stunted larvae fed on yeast particles or HaSV, but not in the negative control (Figure 5.9).

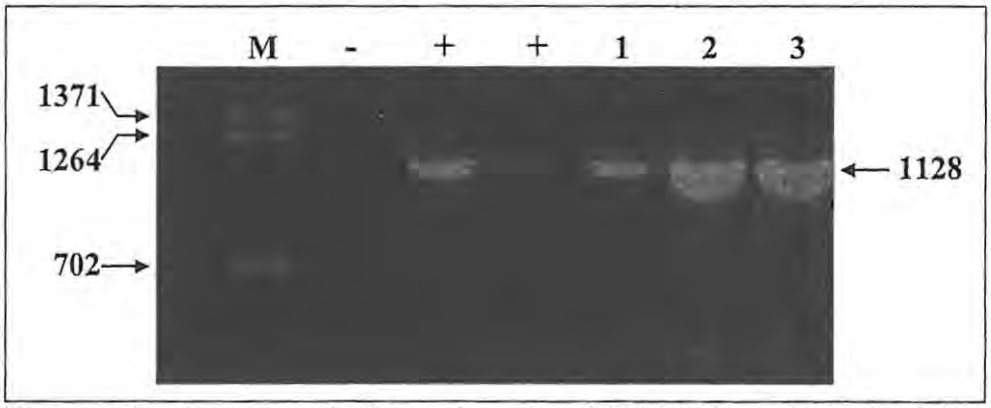

Figure 5.9 Agarose gel electrophoresis of RT-PCR products for RNA isolates from *H. armigera* larvae (**1 - 3**) fed on HaSV virus particles that were expressed in yeast. RT-PCR was also preformed on RNA isolates from two of the positive control larvae (+) and one of the negative control larvae (-) in the bioassay. The expected size of an RT-PCR product (in bp) with the HR236F3 / H3R1B primer pair is indicated on the right-hand side of the gel. A *BstE*II digest of lambda-DNA was used as a molecular weight marker (**M**). This experiment was carried out by Amir Masoumi (CSIRO Division of Entomology, Canberra, Australia).

Surface contamination bioassays performed by Rachel Blaine (ZENECA Agrochemicals Ltd., Jealott's Hill, UK) on yeast-derived HaSV preparations supported the results that were obtained for the above-described bioassay (Duncan, R., 1998). JRY188::*P71*, *RNA1*, *RNA2* cells were either induced overnight, or for 4 hours, at 30°C for the expression of HaSV, and lysed by zymolyase treatment. The mean weight of *H. armigera* larvae fed on a crude virus preparation from cells that were induced for 4 hours (0.018g, SEM ±0.003, $n = 50$) was significantly less than that of larvae fed on virus preparations from cells that were induced overnight (0.028g, SEM ±0.003, $n = 50$). A mean weight of 0.038 (SEM±0.005, $n = 50$) was obtained for negative control larvae that ingested a water control. The larvae that were tested in these bioassays were unfortunately not analysed for the presence of HaSV.

5.4 Discussion

5.4.1 HaSV genomic RNA and *P71* mRNA levels in yeast

RNA1 and RNA2 transcripts, with similar sizes to the HaSV genomic RNAs, were detected in total RNA extracts from yeast cells that were transformed with *RNA1* and *RNA2* expression vectors (Figure 5.2, panels A and C). In addition, mRNA was detected in cells that carried a chromosomal copy of the *P71* expression module (Figure 5.2, panel C). RT-PCR with primers specific for RNA1 5' and 3'ends demonstrated that most of the nucleotides at the 5' and 3'ends of yeast-derived RNA1 transcripts were present (Figure 5.3, panels A and B). An identical expression cassette to that of *RNA1* was used for the expression of *RNA2* (Figure 2.5). It is therefore highly likely that similar results would have been obtained for corresponding RT-PCR analyses on yeast-expressed RNA2 transcripts.

The level of RNA1 or RNA2 production was dependent on whether one or both of the RNA expression vectors were transformed into the cells (Figure 5.2, panels A and C). The *P71* mRNA level remained constant irrespective of the presence, or absence, of one or both of these expression vectors (Figure 5.2, panel C). This indicated that the decreased production of RNA1 and RNA2 transcripts could not be attributed to a depletion of factors that were required for P_{GAL1}-driven transcription. It is more likely that the cellular regulation of a specific copy number for *ARS/CEN* vectors (1 or 2 per cell) led to the reduction of RNA1 and RNA2 transcripts in cells that were transgenic for both *RNA1* and *RNA2* (Clark and Carbon, 1980). The copy number of an expression vector for a particular RNA transcript would be halved upon the introduction of an expression vector for another RNA transcript, resulting in a twofold reduction in the expression of each RNA transcript.

The production of HaSV RNA1 transcripts (which encode the viral replicase) did not result in a detectable level of viral RNA replication. The co-expression of *RNA1* and *RNA2* would have led to a much higher level of HaSV RNA transcripts if replication occurred. It was recently demonstrated that a functional FHV replication system in yeast amplified FHV RNA1 transcripts 40- to 150-fold above the levels produced by P_{GAL1}-directed transcription from 2μ-based vectors (Price *et al.*, 2000). Instead, yeast cells that were induced for the co-production of HaSV RNA1 and RNA2 transcripts produced fewer RNA2 transcripts than those induced for the production of RNA2 alone (Figure 5.1, panel C).

These results do, however, not exclude the possibility that HaSV replication occurs in yeast, because a much longer time course for DNA-induced replication (4 days for FHV replication

in yeast) than that used for these experiments (4 hours) is required to determine if this is the case (Price *et al.*, 2000). However, the lack of detectable HaSV replication in various insect cell lines (Bawden *et al.*, 1999) and plant protoplasts (Gordon *et al.*, 2001) makes it unlikely that HaSV replication could be maintained in the yeast expression system that was used in this study.

5.4.2 The purification of HaSV particles

In the previous chapter, it was proposed that the low yield of HaSV VLPs could be attributed to a shortage of sufficient amounts of viral RNA for encapsidation. Vlp preparations from JRY188::*P71* and JRY188::*P71*; *R1* cells, however, demonstrated that the co-expression of *RNA1* did not seem to have a significant effect on VLP production (Figure 5.5). It is probable that the increase in the cellular concentration of encapsidatable RNA was not sufficient for a detectable increase in VLP production. RNA2 was present at a higher concentration than *P71* mRNA in JRY188::*P71*, *RNA2* cells, but at a similar concentration to that of *P71* mRNA in JRY188::*P71*; *RNA1*, *RNA2* cells (Figure 5.2, panel C). It could therefore be assumed that RNA2 was present at roughly double the concentration of *P71* mRNA in JRY188::*P71*, *RNA2* cells. There was probably a similar increase in the concentration of RNA1 transcripts in JRY188::*P71*; *RNA1* cells as compared to JRY188::*P71* cells. It is possible that this slight increase in encapsidatable RNA transcripts did not have a significant effect on the yield of the yeast-expressed HaSV particles.

The protocol described for the purification of VLPs from JRY188::*P71* cells (Figure 4.1) was modified for that from JRY188::*P71*; *RNA1*, *RNA2* cells by the addition of a pH reduction step prior to CsCl density gradient centrifugation. Western analysis of resultant CsCl density gradient fractions showed the presence of a protein with a slightly lower electrophoretic mobility than that of p64 (Figure 5.6, panel B). A number of lines of evidence indicated that, despite its lower electrophoretic mobility, the identity of this protein was yeast-expressed p64. (i) It is highly likely that the chemical composition of the yeast-derived preparation (e.g. the presence of CsCl) could have influenced the mobility of its protein constituents. (ii) Evidence for the pH-dependent maturation of JRY188::*P71*-derived procapsids was provided in the previous chapter (Figures 4.9 and 4.10). An identical protocol to the one that was used for JRY188::*P71*-derived procapsids was used for preparations from JRY188::*P71*; *RNA1*, *RNA2* cells, the only difference being that the pH-reduction step was introduced at an earlier stage in the protocol. It is therefore feasible to conclude that this protein, which clearly had a lower M_R than p71 and a comparable M_R to p64, was generated as a result of a pH-dependent

processing event analogous to the autoproteolysis of p71. (iii) The yeast-expressed protein was detected in CsCl density gradient fractions with similar densities to that of the published buoyant density of HaSV (Hanzlik *et al.*, 1993), suggesting that this protein was associated with HaSV viral or subviral particles. (iv) The detection of RNA1 in one of these fractions (Figure 5.8) supported the hypothesis that this protein was associated with yeast-expressed HaSV particles.

The detection of mature HaSV particles in virus preparations from zymolyase-treated cells was unexpected, since the pH was not reduced at any stage of this protocol (Figure 5.7). This implies that a reduction in pH subsequent to cell lysis was not responsible for the maturation of these particles. It is possible that a rapid increase in ionic strength could have been responsible for the *ex vivo* maturation of the HaSV particles. Canady *et al.* (2000) proposed that electrostatically driven structural rearrangements of arginine rich interior helical domains mediate the maturation of NωV procapsids. During osmotic shock, a buffer with an ammonium sulphate concentration of 0.8M lyses the cellular membranes of spheroplasts (Figure 5.1). The sudden increase in ionic strength during osmotic shock could therefore have had an effect on ionic interactions within the interior helical domains of the HaSV provirions, resulting in structural rearrangement and maturation cleavage. Results from other virus preparations, where maturation was not observed subsequent to fluctuations in ionic strength, oppose this explanation. These include the exclusive production of immature VLPs from cells that were lysed in a buffer containing 250 mM NaCl, and the lack of maturation in CsCl concentrations of approximately 1.8 M during CsCl gradient ultracentrifugation (Figure 4.3, panel C; Figure 4.5, panel A; Figure 4.10, panel A; Figure 5.5, panels A and B).

A more likely explanation is that maturation occurred *in vivo* as a result of a cellular response to zymolyase treatment. Apart from being suspended in a nutrient depleted solution during this treatment, the yeast cells would suffer extensive damage during spheroplast formation. Agrawal and Johnson (1995) demonstrated that the maturation of NωV procapsids in insect cells coincided with cellular death and the subsequent release of virus particles from the cell. This suggested that certain physiological processes within these dying cells initiated maturation. It is possible that zymolyase treatment brought about a similar response within yeast cells, which in turn initiated the maturation of HaSV particles.

The use of zymolyase treatment for cell breakage did not result in an improved yield of HaSV particles (Figure 5.6, panel A and Figure 5.7, panel A) but the removal of CsCl by way of

ultracentrifugation instead of dialysis brought about a significant increase in this yield (Figure 5.7, panel B).

5.4.3 Encapsidation and delivery of viral RNA by yeast-expressed HaSV particles

The low yield of mature HaSV particles necessitated the use of a sensitive RT-PCR technique to obtain proof for the encapsidation of genomic RNA. The amplification of a faint band with RNA1-specific primers demonstrated that RNA1 is encapsidated by the yeast-expressed particles (Figure 5.8). Further evidence for the encapsidation of genomic RNA strands came from the ability of yeast-expressed HaSV particles to cause impaired larval development when fed to *H. armigera* larvae in bioassays. A significant proportion of the larvae that ingested the yeast-expressed HaSV particles lagged one to two developmental stages behind uninfected larvae (Table 5.2). This type of a response is typical of larvae that were exposed to a low concentration of HaSV (Christian, P.D., Dorrian, S.J., Gordon, K.H.J. and Hanzlik, T.N., unpublished results). It is possible that the absence of the 5' most G nucleotide could have had an effect on the virulence of the yeast-derived particles in this bioassay, because it has been demonstrated that replicase enzymes have a limited tolerance for sequence variations at the 5' ends of viral RNAs (Boyer and Haenni, 1994). However, RT-PCR analysis of RNA extractions from these larvae provided evidence that the growth retardation response was elicited by an HaSV infection (Figure 5.9). These reactions also demonstrated that the yeast-expressed HaSV particles were able to deliver genomic RNA to its host cells.

The above-described bioassay results were in agreement with bioassays that were performed on a separate laboratory colony of *H. armigera*. The mean weight, in stead of the development, of larvae were scored in these bioassays, which showed that an HaSV preparation from yeast cells that were induced for 4 hours had a greater stunting effect that from cells that were induced overnight. These results were consistent with the observation that prolonged induction led to the proteolytic degradation of p71 (Chapter3).

There was a potential risk in the placement of *cis*-cleaving HC ribozymes behind the viral sequences in the expression vectors for *RNA1* and *RNA2*, because it could have inhibited the export of the HaSV RNA transcripts from the nucleus. This is due to the absence of poly-A tails, which are required for nuclear export (Huang and Carmichael, 1996). Proof for the encapsidation of RNA1 transcripts, however, demonstrated that at least a fraction of these transcripts were exported to the cytoplasm. The detection of a very low level of *P71* expression in cells that were transgenic for *RNA2* (Figure 3.15), also demonstrated that RNA transcripts were exported from the nucleus.

Gordon *et al.* (2001) demonstrated that the infectivity of HaSV RNA transcripts was sensitive to the presence of non-viral sequences at their 3' ends. It is thus very likely that the yeast-expressed RNA transcripts, which were exported to the cytoplasm for virion assembly, were cleaved, because it was demonstrated that the yeast-expressed HaSV particles were infectious (Table 5.2). A probable explanation for the export of these transcripts to the cytoplasm is that ribozyme catalysis could have been inhibited by nuclear localization (as demonstrated by Tsuchihashi *et al.*, 1993). Accordingly, most transcripts probably remained polyadenylated in the nucleus for efficient transport to the cytoplasm, where cleavage took place.

On the whole, these results provided proof for functional HaSV capsid expression in yeast. The capsids were able to encapsidate viral nucleic acid, assemble into virions, specifically bind to the viral host cell and deliver genomic nucleic acid to this cell. This occurred in the absence of detectable replication, indicating that the assembly of HaSV in the cytoplasm was entirely reliant on the transcription of *P71* mRNA and genomic RNA in the nucleus. At present, the only evidence for replication independent encapsidation of viral RNA, which were expressed in *trans* with a coat protein gene in yeast, was provided for BMV (Price *et al.*, 1999). This study is therefore the second example for this type of encapsidation in yeast, and the first for a tetravirus.

6 Conclusions

6 Conclusions

The principal objective of this research was to develop a yeast-based expression system for the production of HaSV. To achieve this, conditions for the expression of HaSV components in yeast needed to be optimized and methods for the purification of this virus from yeast designed. Following from this, a number of hypotheses were generated. This chapter aims to elucidate these hypotheses and other key factors encountered during this research.

6.1 Expression of *P71*

To ensure optimal expression, *P71* was expressed from chromosomal and episomal loci in two different strains of yeast. The highest level of expression was attained for chromosomal expression in JRY188 3#20.1 cells and episomal expression in INVScI cells, which were transformed with the 2μ-plasmid pAV3. Low episomal expression levels in JRY188 could have been due to the lack of genes for the stable propagation of 2μ-plasmids in its genome; while higher chromosomal expression levels for JRY188 3#20.1, as compared to INVScI 3#20.1, most probably reflected differences in the regulation of galactose metabolism between these strains.

It was discovered that induction time played an essential role in the expression of this protein, since prolonged induction periods resulted in the disappearance of p71 in yeast cell lysates. This disappearance could probably not be attributed to the looping out of the *P71* expression module from the chromosome through homologous recombination, because it was demonstrated that the *LEU2* selectable marker, which was used for the selection of the JRY188::*P71* strain, was not lost to the cell during induction. It is, however possible that recombination occurred at a position in the chromosomal selectable marker that led to the looping out of *leu2* together with the *P71* expression module.

Loss of the *P71* gene could not be attributed to the repression of P_{GAL1}-dependent transcription, because no difference was detected in the growth of $P71^+$ and $P71^-$ cells during induction. A reduced cell growth rate would have been expected for cells that could not catabolize galactose (their sole carbon source) due to the repression of the galactose utilization pathway. Alternative explanations include a reduced rate of p71 synthesis or an increased rate of p71 degradation. Evidence for the complete depletion of detectable p71 levels indicated that proteolytic degradation was at least partly responsible for the disappearance of this protein in yeast cell lysates.

A large fraction of the yeast-expressed p71 was shown to be insoluble, which is indicative of the aggregation of these proteins within the yeast cell. There was only a minor increase in the solubility of this protein when cells were grown under conditions that led to a reduced rate of *P71* expression. It is therefore not certain whether the insolubility of yeast-expressed p71 was due to the improper folding of p71 polypeptides in yeast, or the tendency of non-host-produced capsid proteins to accumulate into insoluble protein aggregates.

6.2 Assembly and maturation of yeast-expressed HaSV VLPs

To determine whether p71 assembled into VLPs in yeast, virus preparations were carried out on cells that were induced for the expression of *P71*. It was found that PMSF was an essential constituent in buffers used during the lysis of yeast cells, since it protected soluble p71 fractions against proteolytic degradation. Analyses on yeast-derived VLP preparations were indicative of a very low yield of VLPs from yeast. A small fraction of the total expressed p71 had a similar buoyant density to that of HaSV. An even smaller fraction of the total expressed p71 could undergo pH-dependent cleavage into p64. A number of hypotheses could be proposed from these results:

First, the detection of maturation provided evidence that the expression of *P71* was sufficient for the assembly of HaSV procapsids in yeast. RT-PCR analyses on VLP preparations, however, failed to provide conclusive evidence for the specific encapsidation of *P71* mRNA in yeast. This was probably due to the low amount of VLPs ($\leq 10^7$ VLPs) in these preparations.

Second, these results were the first evidence of a pH-dependence for the maturation of HaSV procapsids. Cleavage of p71 was not detected after a one week storage period at 4°C, in agreement with the theory that a drop in pH is required for the initiation thereof (Canady *et al.*, 2000). It was detected when the pH of VLP preparations was dropped by the addition of 5 volumes of 70mM NaAc (pH 5).

Third, maturation was only detected for particles with an identical buoyant density to that of HaSV. Taken that the buoyant densities of virus particles are relative to their RNA contents, this result demonstrated that, as in nodavirus procapsids (Schneemann *et al.*, 1994), tetravirus procapsids are dependent on a certain complement of encapsidated RNA for maturation cleavage. The dependence on RNA for maturation was not only observed for VLPs that were derived from JRY188::*P71* cells, but also for HaSV preparations from JRY188::*P71*; *R1*, *R2* cells. Cheng *et al.* (1994) proposed that the close proximity of RNA molecules to the cleavage sites within nodavirus capsids could increase the rate of the cleavage reaction. The

phosphates of the RNA could polarize water molecules for the nucleophilic attack on the carbonyl group of the scissile peptide bond at each of the cleavage sites. During the tetraviral cleavage phase, autocatalytic cleavage events with similar mechanisms occur at similar geometrical locations to those of nodaviruses (Munshi *et al.*, 1996). It is therefore possible that the results obtained for the maturation of yeast-derived HaSV VLPs identified a similar role for tetraviral RNA during the cleavage phase.

Fourth, a certain complement of encapsidated RNA also seemed to be required for the assembly of stable procapsids. The majority of the p71 detected in VLP and virus preparations from JRY188::*P71* and JRY188::*P71*; *R1*, *R2* cells, respectively, were shown to be unstable, since it became insoluble subsequent to CsCl density gradient centrifugation and precipitated from solution upon a reduction in pH. The only capsid proteins (p71 or p64) that remained soluble prior to CsCl density gradient centrifugation and pH reduction were found in fractions with similar buoyant densities to that of HaSV. It was therefore demonstrated that the encapsidation of a certain complement of RNA was not only required for maturation, but also for the assembly of stable HaSV procapsids. These results are in agreement with a proposal by Agrawal and Johnson (1995) that the highly charged inner surfaces of tetravirus particles need to be neutralized by encapsidated RNA for the assembly of stable VLPs.

6.3 Expression of *RNA1* and *RNA2*

The *RNA1* and *RNA2* expression cassettes contained an exact fusion between P_{GAL1} and the 5' end of the viral RNA, and the ToRSV hairpin cassette ribozyme directly behind the last nucleotide of viral sequence. It was demonstrated that RNA transcripts with similar sizes to the HaSV genomic RNAs were expressed from these cassettes (through Northern blot analyses) and that most of the nucleotides at the 5' and 3' ends of yeast-derived RNA1 transcripts were present (through RT-PCR analyses). Similar results were expected for corresponding RT-PCR analyses on yeast-expressed RNA2 transcripts, because an identical expression cassette to that of *RNA1* was used for the expression of *RNA2*. It was also demonstrated that at least a fraction of the RNA transcripts were exported to the cytoplasm through (a) the detection of a very low level of *P71* expression in cells that were transgenic for *RNA2*, and (b) proof for the encapsidation and delivery of RNA transcripts.

6.4 Production of infectious HaSV particles from yeast

6.4.1 Development of protocols for the purification of HaSV from yeast

Two different protocols were developed for the purification of mature HaSV particles from yeast cells. In one protocol, the cells were mechanically ruptured by glass bead homogenization, and the provirions were matured by way of a reduction in pH. In the other, the cells were enzymatically converted to spheroplasts (by zymolyase) and then lysed by a combination of Dounce homogenization and osmotic shock. In both these protocols, purification was achieved through the application of sucrose cushion centrifugation and CsCl density gradient centrifugation. The application of ultracentrifugation was shown to be preferable to dialysis for the dual purposes of CsCl removal from, and concentration of, HaSV particles.

The purification of mature HaSV particles by way of the zymolyase-treatment protocol was an unexpected result because the pH was not reduced at any stage of this procedure. The maturation of these particles could either have occurred *ex vivo* or *in vivo*. *Ex vivo* maturation could have been the result of a rapid increase in ionic strength during osmotic shock, which involved the addition of 0.8 M ammonium sulphate to yeast spheroplasts. However, the addition of solutions with high NaCl (0.25 M) and CsCl (~1.8 M) concentrations to yeast cell lysates and VLP preparations, respectively, did not induce VLP maturation. A more likely explanation is that the maturation of these particles occurred *in vivo* as a result of a cellular response to the damaging effects of, or starvation effects during, zymolyase treatment. Stresses associated with this treatment could have triggered a physiological response that brought about the maturation of the HaSV particles.

Agrawal and Johnson (1995) demonstrated that NωV procapsids matured *in vivo* in baculoviral infected insect cells. Pulse-chase experiments revealed that maturation coincided with the death (and lysis) of these insect cells, suggesting that the cellular milieu in a dying cell could induce maturation. It is possible that these dying cells underwent apoptosis, based on a correlation between the rate of sloughing and the apoptotic activity in the sloughed cells in an HaSV-infected midgut (Hanzlik and Gordon, 1997). During apoptosis, mitochondrial membranes become progressively more leaky, resulting in a drop in the cellular pH (Shrode *et al.*, 1997). Apoptosis could therefore have been responsible for the pH-dependent maturation of the heterologously expressed NωV procapsids in the above-described experiment.

According to Madeo *et al.* (1997) an *S. cerevisiae* cell cycle gene mutant could show the phenotypic markers of apoptosis, i.e. DNA fragmentation, chromatin condensation and exposure of phosphatidyl serine at the outer layer of the cytoplasmic membrane. In yeast, reactive oxygen species (ROS), e.g. $O_2^{\bullet}$, H_2O_2 and $OH^{\bullet}$, function as the endogenous regulators of apoptosis (Madeo *et al.* 1999). ROS are normal byproducts of respiration. It has therefore been proposed that a specific modulation of the respiratory chain of yeast cells could produce an increased cellular concentration of ROS, which could serve as a trigger for apoptosis (Frölich and Madeo, 2000). Yeast cells could therefore be capable of "cellular suicide" under unfavourable conditions. An example of a potential advantage for cellular suicide would be the death of the majority of yeast cells in a nutrient depleted medium (as described by Longo *et al.*, 1997), which would spare the diminishing nutrients for healthier cells.

In the work described in this thesis, yeast cells were suspended in a nutrient depleted solution during zymolyase treatment and suffered extensive damage during spheroplast formation. Taken that tetraviral maturation could be dependent on apoptosis, it is therefore not unreasonable to propose that maturation could have been a direct result of apoptosis during zymolyase treatment.

6.4.2 Proof for concept of non-host-produced HaSV

The characterization of HaSV preparations was hindered by the very low yield of viral particles. This necessitated the use of numerous preparations from large volumes of yeast cultures to produce enough material for analyses. The detection and characterization of yeast-expressed HaSV particles was, in turn, reliant on the application of very sensitive techniques, such as immunoblotting, RT-PCR and droplet feed bioassays. A number of lines of evidence provided support for the concept of the non-host production of infectious HaSV particles from yeast:

First, p64-containing particles with identical buoyant densities to HaSV were purified from yeast that was transgenic for *P71*, *RNA1* and *RNA2*. Second, it was demonstrated that these particles contained genomic RNA transcripts, which were expressed in *trans* with *P71*. Third, the yeast-expressed particles caused impaired larval development when fed to *H. armigera* larvae from two separate laboratory colonies and fourth, the presence of HaSV in these larvae was detected by RT-PCR-analyses.

Proof for the encapsidation of viral genomic RNA, expressed *in trans* with a capsid protein gene in a yeast expression system, has only been reported for two other ssRNA+ viruses, BMV and FHV (Price *et al.*, 1999), which belong to the *Bromoviridae* and *Nodaviridae*

families, respectively. Proof for the expression of infectious ssRNA+ viruses in yeast has, in turn, only been reported for FHV (Price *et al.*, 1996, Price *et al.*, 1999). The work described in this thesis is therefore the first report on the expression of infectious tetravirus particles in yeast. Comparisons between the RNA2 levels in cells co-expressing *RNA1* and *RNA2* and those expressing *RNA2* alone, demonstrated that the expression of RNA1 did not result in any detectable levels of viral RNA replication. This suggests that the HaSV particles assembled in yeast in the absence of viral replication.

6.5 Future research

The principal objective of this project was achieved since it was shown that infectious HaSV particles could be assembled in yeast. However, a great deal of work still needs to be done to reach the ultimate goal, i.e. the development of an expression system for the large-scale production of this virus as a biopesticide. At the outset, this work should focus on: (a) alternative strategies for the expression of infectious HaSV particles in yeast, because it was demonstrated that a very low amount of HaSV was attained by the expression strategy that was used in this study, and (b) the characterization of the products of expression, including the viral components (p71, RNA1 and RNA2) and the virus or virus-like particles. The main objective of the latter studies would be to demonstrate that the heterologously expressed HaSV particles are biochemically equivalent to wild-type virions. This would be done to satisfy some of the stringent quality and safety standards for the commercial application of recombinant products (Eckart and Bussineau, 1996). If the yeast-derived particles are shown to be of sufficient quality, the expression system could be scaled up to a laboratory-scale fermentation process and the expression products could be tested in insect bioassays and small-scale field trials. Ultimately, these studies could lead to the development of a large-scale industrial fermentation process for HaSV, which has a great potential to become an effective biological control agent against *H. armigera*.

Proposed research, for the studies described in points (a) and (b) above, are presented in the remaining paragraphs of this dissertation:

6.5.1 The use of a dual promoter expression system for the production of HaSV

Genomic RNA is required for the assembly of nodavirus capsids and the nodaviral capsid protein precursors can therefore not assemble into empty VLPs, which are devoid of any RNA (Schneemann *et al.*, 1994). As a consequence, an excess of RNA is expressed in infected cells to ensure an optimal yield of virions (i.e. the expression of the capsid protein precursor is the rate-limiting step for nodavirus assembly) (Gallagher and Rueckert, 1988). According to

Bawden *et al.* (1999), tetravirus RNA replication most probably occurs exclusively in the early stages in an infected cell, while capsid protein precursor synthesis and particle assembly occurs later. It is therefore likely that capsid protein precursor synthesis is also the rate-limiting step for the assembly of tetraviruses.

This hypothesis is consistent with results for the baculoviral expression of the NωV capsid protein precursor (Agrawal and Johnson, 1995). The resultant VLPs were shown to be morphologically identical to wild-type virions and no empty VLPs were detected. The results obtained for the expression of *P71* (in this study) are also in agreement with this hypothesis, because they led to the proposal (explained above) that there was a requirement for a certain complement of encapsidated RNA for the assembly of stable HaSV procapsids. It is therefore highly probable that the low yield of virus and virus-like particles from yeast was due to a shortage of sufficient levels of RNA for encapsidation during assembly.

The amount of yeast-derived HaSV particles could possibly be increased though the implementation of a dual promoter expression system to reproduce the time-course for the synthesis of the viral RNAs and p71 in HaSV-infected cells. In such a system, the HaSV RNA1 and RNA2 transcripts would be produced up to a high cellular concentration prior to the induction of *P71* expression through the use of two different *S. cerevisiae* promoters. The transcription of the HaSV RNAs could either be under the control of a constitutive promoter, e.g. the glyceraldehyde-3-phosphate-dehydrogenase promoter (P_{GAPDH}) (Rosenberg *et al.*, 1990), or an inducible promoter, e.g. one of the galactose-inducible promoters (e.g. P_{GAL1}) (Johnston, 1987), the alcohol dehydrogenase 2 promoter (P_{ADH2}) (Price *et al.*, 1990) and the copper metallothionein promoter (P_{CUP1}) (Etcheverry, 1990). It is essential that an inducible promoter (other that the one used for the transcription of the viral RNAs) should be used for *P71* expression, because p71 was shown to be unstable in yeast (Chapter 3).

Based on this proposal, an *ARS/CEN* expression vector that places the transcription of HaSV RNA2 under the control of P_{ADH2} was constructed in our laboratory (Tomasicchio, 2001). The following strategy has been devised for a dual promoter expression system with P_{ADH2} (for *RNA2*) and P_{GAL1} (for *P71*):

- Grow a $P71^+$ yeast strain, which is transformed with above-described expression vector, to midlog phase in a medium with a high concentration of glucose (P_{GAL1} and P_{ADH2} are both tightly repressed by glucose) (Gancedo, 1998; Price *et al.*, 1990).
- Transfer the cells to a medium with a very low concentration of glucose for the induction of P_{ADH2} – dependent transcription of RNA2 and grow until an optimal level of cellular

RNA2 is detected (P_{ADH2} becomes derepressed to a high level upon the depletion of glucose, and a very low level of P_{GAL1} – dependent transcription is expected when cells are grown in a medium with depleted levels of glucose) (Gancedo, 1998; Price *et al.*, 1990).

- Add galactose to the medium for the P_{GAL1} - dependent expression of *P71*.

If it is demonstrated that this dual promoter expression system could lead to a significant increase in the amount of yeast-expressed VLPs, a similar expression system for the production of both of the viral RNA transcripts (using P_{ADH2}) and p71 (using P_{GAL1}) could be implemented for the production of HaSV particles.

6.5.2 The production of mature HaSV particles from apoptotic yeast cells

It has recently been demonstrated that an apoptotic response could be induced by the addition of low concentrations of H_2O_2 to yeast cell cultures (Madeo *et al*, 1999). The ability to induce apoptosis in yeast presents a unique opportunity to determine if apoptosis is indeed responsible for the maturation of tetraviral capsids. In this study, it was demonstrated that no mature HaSV particles were assembled in yeast that were lysed by glass bead homogenization and that *ex vivo* maturation was required for the production of infectious virus particles. Yeast cells, induced for the expression of HaSV, could therefore be treated with H_2O_2 (as described by Madeo *et al.*, 1999) to determine if the induction of apoptosis could circumvent the requirement for *ex vivo* maturation for the production of infectious HaSV particles.

6.5.3 The use of virus-free yeast strains for the production of HaSV

The purification of HaSV VLPs and virus particles from yeast was complicated by endogenous yeast virus particles, which co-purified with these particles in CsCl density gradient fractions (Chapter 4). These particles were tentatively identified as *S. cerevisiae* L-A virus particles, double-stranded RNA viruses with a similar diameter (40nm) to that of HaSV (Wickner, 1996). A yeast strain that is free from any endogenous viruses would be more suitable for the expression of HaSV. Two yeast strains, which lack any dsRNA viruses, have been acquired from Prof. Manfred J. Schmitt (Department of Microbiology, Universität des Saarlandes, Germany). Virus preparations from these strains could be subjected to TEM analysis in order to determine if the endogenous virus particles, which were visualized in our VLPs preparations, were in fact yeast double-stranded RNA viruses.

6.5.4 Analyses on yeast-expressed RNA1 and RNA2 transcripts

In this study, Northern analyses were used to demonstrate that RNA1 and RNA2 transcripts with similar sizes to that of the respective HaSV genomic RNAs were transcribed from yeast expression cassettes. These expression cassettes were, however, designed to transcribe

transcripts with natural 5' and 3' ends. More specific techniques like primer extension analyses (for the 5' ends) and RNase protection assays (for the 3' ends) could be used to determine if these transcripts are identical to the viral genomic RNAs.

Appendices

Appendix 1 Complete sequence of the HaSV genome

```
  1                                                  Met Tyr Ala Lys
  1  GUUCUGCCUC CCCCGGACGG UAAAUAUAGG GGAACA AUG UAC GCG AAA

  5  Ala Thr Asp Val Ala Arg Val Tyr Ala Ala Ala Asp Val Ala
 49  GCG ACA GAC GUG GCG CGU GUC UAC GCC GCG GCA GAU GUC GCC

 19  Tyr Ala Asn Val Leu Gln Gln Arg Ala Val Lys Leu Asp Phe
 91  UAC GCG AAC GUA CUG CAG CAG AGA GCA GUC AAG UUG GAC UUC

 33  Ala Pro Pro Leu Lys Ala Leu Glu Thr Leu His Arg Leu Tyr
133  GCC CCG CCA CUG AAG GCA CUA GAA ACC CUC CAC AGA CUG UAC

 47  Tyr Pro Leu Arg Phe Lys Gly Gly Thr Leu Pro Pro Thr Gln
175  UAU CCG CUG CGC UUC AAA GGG GGC ACU UUA CCC CCG ACA CAA

 61  His Pro Ile Leu Ala Gly His Gln Arg Val Ala Glu Glu Val
217  CAC CCG AUC CUG GCC GGG CAC CAA CGU GUC GCA GAA GAG GUU

 75  Leu His Asn Phe Ala Arg Gly Arg Ser Thr Val Leu Glu Ile
259  CUG CAC AAU UUC GCC AGG GGA CGU AGC ACA GUG CUC GAG AUA

 89  Gly Pro Ser Leu His Ser Ala Leu Lys Leu His Gly Ala Pro
301  GGG CCG UCU CUG CAC AGC GCA CUU AAG CUA CAU GGG GCA CCG

103  Asn Ala Pro Val Ala Asp Tyr His Gly Cys Thr Lys Tyr Gly
343  AAC GCC CCC GUC GCA GAC UAU CAC GGG UGC ACC AAG UAC GGC

117  Thr Arg Asp Gly Ser Arg His Ile Thr Ala Leu Glu Ser Arg
385  ACC CGC GAC GGC UCG CGA CAC AUU ACG GCC UUA GAG UCU AGA

131  Ser Val Ala Thr Gly Arg Pro Glu Phe Lys Ala Asp Ala Ser
427  UCC GUC GCC ACA GGC CGG CCC GAG UUC AAG GCC GAC GCC UCA

145  Leu Leu Ala Asn Gly Ile Ala Ser Arg Thr Phe Cys Val Asp
469  CUG CUC GCC AAC GGC AUU GCC UCC CGC ACC UUC UGC GUC GAC

159  Gly Val Gly Ser Cys Ala Phe Lys Ser Arg Val Gly Ile Ala
511  GGA GUC GGC UCU UGC GCG UUC AAA UCG CGC GUU GGA AUU GCC

173  Asn His Ser Leu Tyr Asp Val Thr Leu Glu Glu Leu Ala Asn
553  AAU CAC UCC CUC UAU GAC GUG ACC CUA GAG GAG CUG GCC AAU
```

Figure A1.1 RNA sequence of HaSV RNA1 (Genome sequence accession number: U18246). The amino acid sequence of the replicase gene is shown above the sequence.

```
 187  Ala Phe Glu Asn His Gly Leu His Met Val Arg Ala Phe Met
 595  GCG UUU GAG AAC CAC GGA CUU CAC AUG GUC CGC GCG UUC AUG

 201  His Met Pro Glu Glu Leu Leu Tyr Met Asp Asn Val Val Asn
 637  CAC AUG CCA GAA GAG CUG CUC UAC AUG GAC AAC GUG GUU AAU

 215  Ala Glu Leu Gly Tyr Arg Phe His Val Ile Glu Glu Pro Met
 679  GCC GAG CUC GGC UAC CGC UUC CAC GUU AUU GAA GAG CCU AUG

 229  Ala Val Lys Asp Cys Ala Phe Gln Gly Gly Asp Leu Arg Leu
 721  GCU GUG AAG GAC UGC GCA UUC CAG GGG GGG GAC CUC CGU CUC

 243  His Phe Pro Glu Leu Asp Phe Ile Asn Glu Ser Gln Glu Arg
 763  CAC UUC CCU GAG UUG GAC UUC AUC AAC GAG AGC CAA GAG CGG

 257  Arg Ile Glu Arg Leu Ala Ala Arg Gly Ser Tyr Ser Arg Arg
 805  CGC AUC GAG AGG CUG GCC GCC CGC GGC UCC UAC UCC AGA CGC

 271  Ala Val Ile Phe Ser Gly Asp Asp Asp Trp Gly Asp Ala Tyr
 847  GCC GUC AUU UUC UCC GGC GAC GAC GAC UGG GGU GAU GCG UAC

 285  Leu His Asp Phe His Thr Trp Leu Ala Tyr Leu Leu Val Arg
 889  UUA CAC GAC UUC CAC ACA UGG CUC GCC UAC CUA CUG GUG AGG

 299  Asn Tyr Pro Thr Pro Phe Gly Phe Ser Leu His Ile Glu Val
 931  AAC UAC CCC ACU CCG UUU GGU UUC UCA CUC CAU AUA GAA GUC

 313  Gln Arg Arg His Gly Ser Ser Ile Glu Leu Arg Ile Thr Arg
 973  CAG AGG CGC CAC GGC UCC AGC AUU GAG CUG CGC AUC ACU CGC

 327  Ala Pro Pro Gly Asp Arg Met Leu Ala Val Val Pro Arg Thr
1015  GCG CCA CCU GGA GAC CGC AUG CUG GCC GUC GUC CCA AGG ACG

 341  Ser Gln Gly Leu Cys Arg Ile Pro Asn Ile Phe Tyr Tyr Ala
1057  UCC CAA GGC CUC UGC AGA AUC CCA AAC AUC UUU UAU UAC GCC

 355  Asp Ala Ser Gly Thr Glu His Lys Thr Ile Leu Thr Ser Gln
1099  GAC GCG UCG GGC ACU GAG CAU AAG ACC AUC CUU ACG UCA CAG

 369  His Lys Val Asn Met Leu Leu Asn Phe Met Gln Thr Arg Pro
1141  CAC AAA GUC AAC AUG CUG CUC AAU UUU AUG CAA ACG CGU CCU

 383  Glu Lys Glu Leu Val Asp Met Thr Val Leu Met Ser Phe Ala
1183  GAG AAG GAA CUA GUC GAC AUG ACC GUC UUG AUG UCG UUC GCG

 397  Arg Ala Arg Leu Arg Ala Ile Val Val Ala Ser Glu Val Thr
1225  CGC GCU AGG CUG CGC GCG AUC GUG GUC GCC UCA GAA GUC ACC

 411  Glu Ser Ser Trp Asn Ile Ser Pro Ala Asp Leu Val Arg Thr
1267  GAG AGC UCC UGG AAC AUC UCA CCG GCU GAC CUG GUC CGC ACU
```

Figure A1.1 Continued...

```
 425  Val Val Ser Leu Tyr Val Leu His Ile Ile Glu Arg Arg Arg
1309  GUC GUG UCU CUU UAC GUC CUC CAC AUC AUC GAG CGC CGA AGG

 439  Ala Ala Val Ala Val Lys Thr Ala Lys Asp Asp Val Phe Gly
1351  GCU GCG GUC GCU GUC AAG ACC GCC AAG GAC GAC GUC UUU GGA

 453  Glu Thr Ser Phe Trp Glu Ser Leu Lys His Val Leu Gly Ser
1393  GAG ACU UCG UUC UGG GAG AGU CUC AAG CAC GUC UUG GGC UCC

 467  Cys Cys Gly Leu Arg Asn Leu Lys Gly Thr Asp Val Val Phe
1435  UGU UGC GGU CUG CGC AAC CUC AAA GGC ACC GAC GUC GUC UUU

 481  Thr Lys Arg Val Val Asp Lys Tyr Arg Val His Ser Leu Gly
1477  ACU AAG CGC GUC GUC GAU AAG UAC CGA GUC CAC UCG CUC GGA

 495  Asp Ile Ile Cys Asp Val Arg Leu Ser Pro Glu Gln Val Gly
1519  GAC AUA AUC UGC GAC GUC CGC CUG UCC CCU GAA CAG GUC GGC

 509  Phe Leu Pro Ser Arg Val Pro Pro Ala Arg Val Phe His Asp
1561  UUC CUG CCG UCC CGC GUA CCA CCU GCC CGC GUC UUU CAC GAC

 523  Arg Glu Glu Leu Glu Val Leu Arg Glu Ala Gly Cys Tyr Asn
1603  AGG GAA GAG CUU GAG GUC CUU CGC GAA GCU GGC UGC UAC AAC

 537  Glu Arg Pro Val Pro Ser Thr Pro Pro Val Glu Glu Pro Gln
1645  GAA CGU CCG GUA CCU UCC ACU CCU CCU GUG GAG GAG CCC CAA

 551  Gly Phe Asp Ala Asp Leu Trp His Ala Thr Ala Ala Ser Leu
1687  GGU UUC GAC GCC GAC UUG UGG CAC GCG ACC GCG GCC UCA CUC

 565  Pro Glu Tyr Arg Ala Thr Leu Gln Ala Gly Leu Asn Thr Asp
1729  CCC GAG UAC CGC GCC ACC UUG CAG GCA GGU CUC AAC ACC GAC

 579  Val Lys Gln Leu Lys Ile Thr Leu Glu Asn Ala Leu Lys Thr
1771  GUC AAG CAG CUC AAG AUC ACC CUC GAG AAC GCC CUC AAG ACC

 593  Ile Asp Gly Leu Thr Leu Ser Pro Val Arg Gly Leu Glu Met
1813  AUC GAC GGG CUC ACC CUC UCC CCA GUC AGA GGC CUC GAG AUG

 607  Tyr Glu Gly Pro Pro Gly Ser Gly Lys Thr Gly Thr Leu Ile
1855  UAC GAG GGC CCG CCA GGC AGC GGC AAG ACG GGC ACC CUC AUC

 621  Ala Ala Leu Glu Ala Ala Gly Gly Lys Ala Leu Tyr Val Ala
1897  GCC GCC CUU GAG GCC GCG GGC GGU AAA GCA CUU UAC GUG GCA

 635  Pro Thr Arg Glu Leu Arg Glu Ala Met Asp Arg Arg Ile Lys
1939  CCC ACC AGA GAA CUG AGA GAG GCU AUG GAC CGG CGG AUC AAA

 649  Pro Pro Ser Ala Ser Arg Thr Gln His Val Ala Leu Ala Ile
1981  CCG CCG UCC GCC UCG CGU ACG CAA CAU GUC GCC CUU GCG AUU
```

Figure A1.1 Continued...

```
 663  Leu Arg Arg Ala Thr Ala Glu Gly Ala Pro Phe Ala Thr Val
2023  CUC CGU CGU GCC ACC GCC GAG GGC GCC CCU UUC GCU ACC GUG

 677  Val Ile Asp Glu Cys Phe Met Phe Pro Leu Val Tyr Val Ala
2065  GUU AUC GAC GAG UGC UUC AUG UUC CCG CUC GUG UAC GUC GCG

 691  Ile Val His Ala Leu Ser Pro Ser Ser Arg Ile Val Leu Val
2107  AUC GUG CAC GCC UUG UCC CCG AGC UCA CGA AUA GUC CUU GUA

 705  Gly Asp Val His Gln Ile Gly Phe Ile Asp Phe Gln Gly Thr
2149  GGG GAC GUC CAC CAA AUC GGG UUU AUA GAC UUC CAA GGC ACA

 719  Ser Ala Asn Met Pro Leu Val Arg Asp Val Val Lys Gln Cys
2191  AGC GCG AAC AUG CCG CUC GUU CGC GAC GUC GUU AAG CAG UGC

 733  Arg Arg Arg Thr Phe Asn Gln Thr Lys Arg Cys Pro Ala Asp
2233  CGU CGG CGC ACU UUC AAC CAA ACC AAG CGC UGU CCG GCC GAC

 747  Val Val Ala Thr Thr Phe Phe Gln Ser Leu Tyr Pro Gly Cys
2275  GUC GUU GCC ACC ACG UUU UUC CAG AGC UUG UAC CCC GGG UGC

 761  Thr Thr Thr Ser Gly Cys Val Ala Ser Ile Ser His Val Ala
2317  ACA ACC ACC UCA GGG UGC GUC GCA UCC AUC AGC CAC GUC GCC

 775  Pro Asp Tyr Arg Asn Ser Gln Ala Gln Thr Leu Cys Phe Thr
2359  CCA GAC UAC CGC AAC AGC CAG GCG CAA ACG CUC UGC UUC ACG

 789  Gln Glu Glu Lys Ser Arg His Gly Ala Glu Gly Ala Met Thr
2401  CAG GAG GAA AAG UCG CGC CAC GGG GCU GAG GGC GCG AUG ACU

 803  Val His Glu Ala Gln Gly Arg Thr Phe Ala Ser Val Ile Leu
2443  GUG CAC GAA GCG CAG GGA CGC ACU UUU GCG UCU GUC AUU CUG

 817  His Tyr Asn Gly Ser Thr Ala Glu Gln Lys Leu Leu Ala Glu
2485  CAU UAC AAC GGC UCC ACA GCA GAG CAG AAG CUC CUC GCU GAG

 831  Lys Ser His Leu Leu Val Gly Ile Thr Arg His Thr Asn His
2527  AAG UCG CAC CUU CUA GUC GGC AUC ACG CGC CAC ACC AAC CAC

 845  Leu Tyr Ile Arg Asp Pro Thr Gly Asp Ile Glu Arg Gln Leu
2569  CUG UAC AUC CGC GAC CCG ACA GGU GAC AUU GAG AGA CAA CUC

 859  Asn His Ser Ala Lys Ala Glu Val Phe Thr Asp Ile Pro Ala
2611  AAC CAU AGC GCG AAA GCC GAG GUG UUU ACA GAC AUC CCU GCA

 873  Pro Leu Glu Ile Thr Thr Val Lys Pro Ser Glu Glu Val Gln
2653  CCC CUG GAG AUC ACG ACU GUC AAA CCG AGU GAA GAG GUG CAG

 887  Arg Asn Glu Val Met Ala Thr Ile Pro Pro Gln Ser Pro Thr
2695  CGC AAC GAA GUG AUG GCA ACG AUA CCC CCG CAG AGU CCC ACG
```

Figure A1.1 Continued…

```
 901  Pro His Gly Ala Ile His Leu Leu Arg Lys Asn Phe Gly Asp
2737  CCG CAC GGA GCA AUC CAU CUG CUC CGC AAG AAC UUC GGG GAC

 915  Gln Pro Asp Cys Gly Cys Val Ala Leu Ala Lys Thr Gly Tyr
2779  CAA CCC GAC UGU GGC UGU GUC GCU UUG GCG AAG ACC GGC UAC

 929  Glu Val Phe Gly Gly Arg Ala Lys Ile Asn Val Glu Leu Ala
2821  GAG GUG UUU GGC GGU CGU GCC AAA AUC AAC GUA GAG CUU GCC

 943  Glu Pro Asp Ala Thr Pro Lys Pro His Arg Ala Phe Gln Glu
2863  GAA CCC GAC GCG ACC CCG AAG CCG CAU AGG GCG UUC CAG GAA

 957  Gly Val Gln Trp Val Lys Val Thr Asn Ala Ser Asn Lys His
2905  GGG GUA CAG UGG GUC AAG GUC ACC AAC GCG UCU AAC AAA CAC

 971  Gln Ala Leu Gln Thr Leu Leu Ser Arg Tyr Thr Lys Arg Ser
2947  CAG GCG CUC CAG ACG CUG UUG UCC CGC UAC ACC AAG CGA AGC

 985  Ala Asp Leu Pro Leu His Glu Ala Lys Glu Asp Val Lys Arg
2989  GCU GAC CUG CCG CUA CAC GAA GCU AAG GAG GAC GUC AAA CGC

 999  Met Leu Asn Ser Leu Asp Arg His Trp Asp Trp Thr Val Thr
3031  AUG CUA AAC UCG CUU GAC CGA CAU UGG GAC UGG ACU GUC ACU

1013  Glu Asp Ala Arg Asp Arg Ala Val Phe Glu Thr Gln Leu Lys
3073  GAA GAC GCC CGU GAC CGA GCU GUC UUC GAG ACC CAG CUC AAG

1027  Phe Thr Gln Arg Gly Gly Thr Val Glu Asp Leu Leu Glu Pro
3115  UUC ACC CAA CGC GGC GGC ACC GUC GAA GAC CUG CUG GAG CCA

1041  Asp Asp Pro Tyr Ile Arg Asp Ile Asp Phe Leu Met Lys Thr
3157  GAC GAC CCC UAC AUC CGU GAC AUA GAC UUC CUU AUG AAG ACU

1055  Gln Gln Lys Val Ser Pro Lys Pro Ile Asn Thr Gly Lys Val
3199  CAG CAG AAA GUG UCG CCC AAG CCG AUC AAU ACG GGC AAG GUC

1069  Gly Gln Gly Ile Ala Ala His Ser Lys Ser Leu Asn Phe Val
3241  GGG CAG GGG AUC GCC GCU CAC UCA AAG UCU CUC AAC UUC GUC

1083  Leu Ala Ala Trp Ile Arg Ile Leu Glu Glu Ile Leu Arg Thr
3283  CUC GCC GCU UGG AUA CGC AUA CUC GAG GAG AUA CUC CGU ACC

1097  Gly Ser Arg Thr Val Arg Tyr Ser Asn Gly Leu Pro Asp Glu
3325  GGG AGC CGC ACG GUC CGG UAC AGC AAC GGU CUC CCC GAC GAA

1111  Glu Glu Ala Met Leu Leu Glu Ala Lys Ile Asn Gln Val Pro
3367  GAA GAG GCC AUG CUG CUC GAA GCG AAG AUC AAU CAA GUC CCA

1125  His Ala Thr Phe Val Ser Ala Asp Trp Thr Glu Phe Asp Thr
3409  CAC GCC ACG UUC GUC UCG GCG GAC UGG ACC GAG UUU GAC ACC
```

Figure A1.1 Continued…

```
1139  Ala His Asn Asn Thr Ser Glu Leu Leu Phe Ala Ala Leu Leu
3451  GCC CAC AAU AAC ACG AGU GAG CUG CUC UUC GCC GCC CUU UUA

1153  Glu Arg Ile Gly Thr Pro Ala Ala Ala Val Asn Leu Phe Arg
3493  GAG CGC AUC GGC ACG CCU GCA GCU GCC GUU AAU CUA UUC AGA

1167  Glu Arg Cys Gly Lys Arg Thr Leu Arg Ala Lys Gly Leu Gly
3535  GAA CGG UGU GGG AAA CGC ACC UUG CGA GCG AAG GGU CUA GGC

1181  Ser Val Glu Val Asp Gly Leu Leu Asp Ser Gly Ala Ala Trp
3577  UCC GUU GAA GUC GAC GGU CUG CUC GAC UCC GGC GCA GCU UGG

1195  Thr Pro Cys Arg Asn Thr Ile Phe Ser Ala Ala Val Met Leu
3619  ACG CCU UGC CGC AAC ACC AUC UUC UCU GCC GCC GUC AUG CUC

1209  Thr Leu Phe Arg Gly Val Lys Phe Ala Ala Phe Lys Gly Asp
3661  ACG CUC UUC CGC GGC GUC AAG UUC GCA GCU UUC AAA GGC GAC

1223  Asp Ser Leu Leu Cys Gly Ser His Tyr Leu Arg Phe Asp Ala
3703  GAC UCG CUC CUC UGU GGU AGC CAU UAC CUC CGU UUC GAC GCU

1237  Ser Arg Leu His Met Gly Glu Arg Tyr Lys Thr Lys His Leu
3745  AGC CGC CUU CAC AUG GGC GAA CGU UAC AAG ACC AAA CAU UUG

1251  Lys Val Glu Val Gln Lys Ile Val Pro Tyr Ile Gly Leu Leu
3787  AAG GUC GAG GUG CAG AAA AUC GUG CCG UAC AUC GGA CUC CUC

1265  Val Ser Ala Glu Gln Val Val Leu Asp Pro Val Arg Ser Ala
3829  GUC UCC GCU GAG CAG GUC GUC CUC GAC CCU GUC AGG AGC GCU

1279  Leu Lys Ile Phe Gly Arg Cys Tyr Thr Ser Glu Leu Leu Tyr
3871  CUC AAG AUA UUU GGG CGC UGC UAC ACA AGC GAA CUC CUU UAC

1293  Ser Lys Tyr Val Glu Ala Val Arg Asp Ile Thr Lys Gly Trp
3913  UCC AAG UAC GUG GAG GCU GUG AGA GAC AUC ACC AAG GGC UGG

1307  Ser Asp Ala Arg Tyr His Ser Leu Leu Cys His Met Ser Ala
3955  AGU GAC GCC CGC UAC CAC AGC CUC CUG UGC CAC AUG UCA GCA

1321  Cys Tyr Tyr Asn Tyr Ala Pro Glu Ser Ala Ala Tyr Ile Ile
3997  UGC UAC UAC AAU UAC GCG CCG GAG UCU GCG GCG UAC AUC AUC

1335  Asp Ala Val Val Arg Phe Gly Arg Gly Asp Phe Pro Phe Glu
4039  GAC GCU GUU GUU CGC UUU GGG CGC GGC GAC UUC CCG UUU GAA

1349  Gln Leu Arg Val Val Arg Ala His Val Gln Ala Pro Asp Ala
4081  CAA CUG CGC GUG GUG CGU GCC CAU GUG CAG GCA CCC GAC GCU

1363  Tyr Ser Ser Thr Tyr Pro Ala Asn Val Arg Ala Ser Cys Leu
4123  UAC AGC AGC ACG UAU CCG GCU AAC GUG CGC GCA UCG UGC CUU
```

Figure A1.1 Continued...

```
1377  Asp His Val Phe Glu Pro Arg Gln Ala Ala Ala Pro Ala Gly
4165  GAC CAC GUC UUC GAG CCC CGC CAG GCC GCC GCC CCG GCA GGU

1391  Phe Val Ala Thr Cys Ala Lys Pro Glu Thr Pro Ser Ser Leu
4207  UUC GUU GCG ACA UGU GCG AAG CCG GAA ACG CCU UCU UCA CUU

1405  Thr Ala Lys Ala Gly Val Ser Ala Thr Thr Ser His Val Ala
4249  ACC GCG AAA GCU GGU GUU UCU GCG ACU ACA AGC CAC GUU GCG

1419  Thr Gly Thr Ala Pro Pro Glu Ser Pro Trp Asp Ala Pro Ala
4291  ACU GGG ACU GCG CCC CCG GAG UCU CCA UGG GAU GCA CCU GCA

1433  Ala Asn Ser Phe Ser Glu Leu Leu Thr Pro Glu Thr Pro Ser
4333  GCC AAC AGC UUU UCG GAG UUA UUG ACA CCG GAG ACC CCG UCC

1447  Thr Ser Ser Ser Ala Val Ile Val Phe Ile Gly Leu Leu Tyr
4375  ACA UCA UCC UCG GCC GUC AUC GUC UUC AUC GGA CUC CUC UAC

1461  Ile Val Trp Lys Val Ala Gln Trp Trp Arg His Arg Lys Arg
4417  AUC GUG UGG AAG GUC GCU CAG UGG UGG AGA CAC CGC AAG AGG

1475  Thr Glu Asp Leu Asn Ser Arg Lys Pro Pro Ser Gln Asp Arg
4459  ACA GAA GAC UUG AAC AGC AGA AAG CCG CCU UCG CAA GAC AGG

1489  Gln Ser Arg Ser Ser Glu Cys Leu Asp Arg Ser Gly Glu Arg
4501  CAA UCA CGC UCG UCU GAA UGU CUG GAC AGA AGC GGA GAA AGG

1503  Thr Gly Ser Ser Leu Thr Ala Pro Thr Ala Pro Ser Pro Ser
4543  ACA GGC AGU UCG UUA ACU GCC CCC ACU GCU CCG AGC CCC UCA

1517  Phe Ser Phe Ser Glu Arg Ala Arg Leu Ala Thr Gly Pro Thr
4585  UUC UCA UUU UCG GAA AGA GCU CGA CUG GCG ACC GGG CCG ACU

1531  Val Ala Ala Ala Thr Ser Pro Ser Ala Thr Pro Ser Cys Ala
4627  GUC GCC GCU GCG ACA UCA CCU UCG GCA ACC CCA UCC UGC GCC

1545  Thr Asp Gln Val Ala Ala Arg Thr Thr Pro Asp Phe Ala Pro
4669  ACG GAC CAG GUU GCC GCG AGG ACC ACG CCG GAC UUU GCG CCU

1559  Phe Leu Gly Ser Gln Ser Ala Arg Ala Val Ser Lys Pro Tyr
4711  UUC CUG GGU UCC CAG UCU GCC CGU GCU GUC UCG AAG CCG UAC

1573  Arg Pro Pro Thr Thr Ala Arg Trp Lys Glu Val Thr Pro Leu
4753  CGG CCC CCC ACG ACU GCC CGU UGG AAA GAA GUC ACC CCG CUC

1587  His Ala Trp Lys Gly Val Thr Gly Asp Arg Pro Glu Val Arg
4795  CAC GCG UGG AAG GGC GUG ACC GGA GAC CGA CCG GAA GUC AGG

1601  Glu Asp Pro Glu Thr Ala Ala Val Val Gln Ala Leu Ile Ser
4837  GAG GAC CCG GAG ACA GCG GCG GUC GUC CAG GCU CUG AUC AGC
```

Figure A1.1 Continued...

```
1615  Gly Arg Tyr Pro Gln Lys Thr Lys Leu Ser Ser Asp Ala Ser
4879  GGC CGU UAU CCU CAG AAG ACG AAG CUU UCC UCC GAC GCA UCC

1629  Lys Gly Tyr Ser Arg Thr Lys Gly Cys Ser Gln Ser Thr Ser
4921  AAA GGC UAC UCA AGA ACU AAG GGA UGC UCA CAA UCC ACC UCU

1643  Phe Pro Ala Pro Ser Ala Asp Tyr Gln Ala Arg Asp Cys Gln
4963  UUU CCU GCC CCG AGU GCG GAU UAC CAG GCC CGC GAC UGC CAG

1657  Thr Val Arg Val Cys Arg Ala Ala Ala Glu Met Ala Arg Ser
5005  ACA GUC CGA GUC UGC CGC GCC GCU GCA GAG AUG GCG CGC UCA

1671  Cys Ile His Glu Pro Leu Ala Ser Ser Ala Ala Ser Ala Asp
5047  UGU AUU CAC GAG CCG UUG GCU UCA UCU GCC GCC AGU GCC GAC

1685  Leu Lys Arg Ile Arg Ser Thr Ser Asp Ser Val Pro Asp Val
5089  UUG AAG CGC AUA CGC UCU ACC UCG GAC UCU GUU CCC GAU GUA

1699  Lys Ile Ser Lys Ser Ala
5131  AAG AUC AGC AAG AGC GCA UGAAGGAACA AAAUUAGUUU CCUUGUUCGU

5179  AAACAAGGUG GUCCCUCCCA UUGAGGUAAA GACUCUGGUG AGUCCUCAAC

5229  GUUACUCGUU GAGUCUGCUG CGGUUCGAUU CCAUUCCCAA GCAGCAAAGG

5279  GUGCGCAACU AGUACGGCGC CCCCUGGGAU ACCA
```

Figure A1.1 Continued…

```
  1  GUUUUUCUUU CUUUACCAAG UGUGGUAAAA UUUAAACAAA GAAGAAAACC

 51  AGGACCGUAA CCCGGCCCUU ACACACCUCG AGUCCGUGAC CACCGGAUUA

101  UACGUCGCCC ACCACACGGC GCCUUUUCCG ACCACUCUCG AGAGUCGUUG

151  GGAGUUUCGU CCGUGACCAC CCGGUUGGCA GUCGACAGAC GCUUCCGGAC

201  CACUAGAACC UCCUCGAGCG ACGCACACAC AGCACACACA CCGCCUUAGC

251  UGCACCUACG GCAGCGUUGA UAGCGCGGAU UUAUGAGCGA GCACACCAUC

301  GCCCACUCCA UCACAUUACC ACCCGGUUAC ACCCUUGCCC UAAUACCCCC

  1                    Met Gly Asp Ala Gly Val Ala Ser Gln
351  UGAACCUGAA GCAGG AUG GGA GAU GCU GGA GUG GCG UCA CAG

 10  Arg Pro His Asn Arg Arg Gly Thr Arg Asn Val Arg Val Ser
393  CGA CCU CAC AAC CGU CGC GGA ACC CGU AAC GUU CGG GUC AGC

 24  Ala Asn Thr Val Thr Val Asn Gly Arg Arg Asn Gln Arg Arg
435  GCC AAC ACC GUC ACC GUC AAU GGU AGA AGA AAC CAA CGG CGU

 38  Arg Thr Gly Arg Gln Val Ser Pro Pro Asp Asn Phe Thr Ala
477  CGG ACC GGA AGG CAA GUU UCU CCC CCU GAC AAU UUC ACC GCU

 52  Ala Ala Gln Asp Leu Ala Gln Ser Leu Asp Ala Asn Thr Val
519  GCU GCA CAA GAC CUC GCG CAA AGC CUU GAC GCC AAC ACC GUC

 66  Thr Phe Pro Ala Asn Ile Ser Ser Met Pro Glu Phe Arg Asn
561  ACU UUC CCC GCU AAC AUC UCU AGC AUG CCC GAA UUC CGG AAU

 80  Trp Ala Lys Gly Lys Ile Asp Leu Asp Ser Asp Ser Ile Gly
603  UGG GCC AAG GGA AAG AUC GAC CUC GAC UCC GAU UCC AUC GGC

 94  Trp Tyr Phe Lys Tyr Leu Asp Pro Ala Gly Ala Thr Glu Ser
645  UGG UAC UUC AAG UAC CUU GAC CCA GCG GGU GCU ACA GAG UCU

108  Ala Arg Ala Val Gly Glu Tyr Ser Lys Ile Pro Asp Gly Leu
687  GCG CGC GCC GUC GGC GAG UAC UCG AAG AUC CCU GAC GGC CUC

122  Val Lys Phe Ser Val Asp Ala Glu Ile Arg Glu Ile Tyr Asn
729  GUC AAG UUC UCC GUC GAC GCA GAG AUA AGA GAG AUC UAU AAC

136  Glu Glu Cys Pro Val Val Thr Asp Val Ser Val Pro Leu Asp
771  GAG GAG UGC CCC GUC GUC ACU GAC GUG UCC GUC CCC CUC GAC

150  Gly Arg Gln Trp Ser Leu Ser Ile Phe Ser Phe Pro Met Phe
813  GGC CGC CAG UGG AGC CUC UCG AUU UUC UCC UUU CCG AUG UUC
```

Figure A1.2 RNA sequence of HaSV RNA2 (Genome sequence accession number: L37299). The amino acid sequence of the capsid precursor protein gene is shown above the sequence.

```
 164  Arg Thr Ala Tyr Val Ala Val Ala Asn Val Glu Asn Lys Glu
 855  AGA ACC GCC UAC GUC GCC GUA GCG AAC GUC GAG AAC AAG GAG

 178  Met Ser Leu Asp Val Val Asn Asp Leu Ile Glu Trp Leu Asn
 897  AUG UCG CUC GAC GUU GUC AAC GAC CUC AUC GAG UGG CUC AAC

 192  Asn Leu Ala Asp Trp Arg Tyr Val Val Asp Ser Glu Gln Trp
 939  AAU CUC GCC GAC UGG CGU UAU GUC GUU GAC UCU GAA CAG UGG

 206  Ile Asn Phe Thr Asn Asp Thr Thr Tyr Tyr Val Arg Ile Arg
 981  AUU AAC UUC ACC AAU GAC ACC ACG UAC UAC GUC CGC AUC CGC

 220  Val Leu Arg Pro Thr Tyr Asp Val Pro Asp Pro Thr Glu Gly
1023  GUU CUA CGU CCA ACC UAC GAC GUU CCA GAC CCC ACA GAG GGC

 234  Leu Val Arg Thr Val Ser Asp Tyr Arg Leu Thr Tyr Lys Ala
1065  CUU GUU CGC ACA GUC UCA GAC UAC CGC CUC ACU UAU AAG GCG

 248  Ile Thr Cys Glu Ala Asn Met Pro Thr Leu Val Asp Gln Gly
1107  AUA ACA UGU GAA GCC AAC AUG CCA ACA CUC GUC GAC CAA GGC

 262  Phe Trp Ile Gly Gly Gln Tyr Ala Leu Thr Pro Thr Ser Leu
1149  UUU UGG AUC GGC GGC CAG UAC GCU CUC ACC CCG ACU AGC CUA

 276  Pro Gln Tyr Asp Val Ser Glu Ala Tyr Ala Leu His Thr Leu
1191  CCG CAG UAC GAC GUC AGC GAG GCC UAC GCU CUG CAC ACU UUG

 290  Thr Phe Ala Arg Pro Ser Ser Ala Ala Ala Leu Ala Phe Val
1233  ACC UUC GCC AGA CCA UCC AGC GCC GCU GCA CUC GCG UUU GUG

 304  Trp Ala Gly Leu Pro Gln Gly Gly Thr Ala Pro Ala Gly Thr
1275  UGG GCA GGU UUG CCA CAG GGU GGC ACU GCG CCU GCA GGC ACU

 318  Pro Ala Trp Glu Gln Ala Ser Ser Gly Gly Tyr Leu Thr Trp
1317  CCA GCC UGG GAG CAG GCA UCC UCG GGU GGC UAC CUC ACC UGG

 332  Arg His Asn Gly Thr Thr Phe Pro Ala Gly Ser Val Ser Tyr
1359  CGC CAC AAC GGU ACU ACU UUC CCA GCU GGC UCC GUU AGC UAC

 346  Val Leu Pro Glu Gly Phe Ala Leu Glu Arg Tyr Asp Pro Asn
1401  GUU CUC CCU GAG GGU UUC GCC CUU GAG CGC UAC GAC CCG AAC

 360  Asp Gly Ser Trp Thr Asp Phe Ala Ser Ala Gly Asp Thr Val
1443  GAC GGC UCU UGG ACC GAC UUC GCU UCC GCA GGA GAC ACC GUC

 374  Thr Phe Arg Gln Val Ala Val Asp Glu Val Val Val Thr Asn
1485  ACU UUC CGG CAG GUC GCC GUC GAC GAG GUC GUU GUG ACC AAC

 388  Asn Pro Ala Gly Gly Gly Ser Ala Pro Thr Phe Thr Val Arg
1527  AAC CCC GCC GGC GGC GGC AGC GCC CCC ACC UUC ACC GUG AGA
```

Figure A1.2 Continued...

```
 402  Val Pro Pro Ser Asn Ala Tyr Thr Asn Thr Val Phe Arg Asn
1569  GUG CCC CCU UCA AAC GCU UAC ACC AAC ACC GUG UUU AGG AAC

 416  Thr Leu Leu Glu Thr Arg Pro Ser Ser Arg Arg Leu Glu Leu
1611  ACG CUC UUA GAG ACU CGA CCC UCC UCU CGU AGG CUC GAA CUC

 430  Pro Met Pro Pro Ala Asp Phe Gly Gln Thr Val Ala Asn Asn
1653  CCU AUG CCA CCU GCU GAC UUU GGA CAG ACG GUC GCC AAC AAC

 444  Pro Lys Ile Glu Gln Ser Leu Leu Lys Glu Thr Leu Gly Cys
1695  CCG AAG AUC GAG CAG UCG CUU CUU AAA GAA ACA CUU GGC UGC

 458  Tyr Leu Val His Ser Lys Met Arg Asn Pro Val Phe Gln Leu
1737  UAU UUG GUC CAC UCC AAA AUG CGA AAC CCC GUU UUC CAG CUC

 472  Thr Pro Ala Ser Ser Phe Gly Ala Val Ser Phe Asn Asn Pro
1779  ACG CCA GCC AGC UCC UUU GGC GCC GUU UCC UUC AAC AAU CCG

 486  Gly Tyr Glu Arg Thr Arg Asp Leu Pro Asp Tyr Thr Gly Ile
1824  GGU UAU GAG CGC ACA CGC GAC CUC CCG GAC UAC ACU GGC AUC

 500  Arg Asp Ser Phe Asp Gln Asn Met Ser Thr Ala Val Ala His
1863  CGU GAC UCA UUC GAC CAG AAC AUG UCC ACC GCU GUG GCC CAC

 514  Phe Arg Ser Leu Ser His Ser Cys Ser Ile Val Thr Lys Thr
1905  UUC CGC UCA CUC UCC CAC UCC UGC AGU AUC GUC ACU AAG ACC

 528  Tyr Gln Gly Trp Glu Gly Val Thr Asn Val Asn Thr Pro Phe
1947  UAC CAG GGU UGG GAA GGC GUC ACG AAC GUC AAC ACG CCU UUC

 542  Gly Gln Phe Ala His Ala Gly Leu Leu Lys Asn Glu Glu Ile
1989  GGC CAA UUC GCG CAC GCG GGC CUC CUC AAG AAU GAG GAG AUC

 556  Leu Cys Leu Ala Asp Asp Leu Ala Thr Arg Leu Thr Gly Val
2031  CUC UGC CUC GCC GAC GAC CUG GCC ACC CGU CUC ACA GGU GUC

 570  Tyr Pro Ala Thr Asp Asn Phe Ala Ala Ala Val Ser Ala Phe
2073  UAC CCC GCC ACU GAC AAC UUC GCG GCC GCC GUU UCU GCC UUC

 584  Ala Ala Asn Met Leu Ser Ser Val Leu Lys Ser Glu Ala Thr
2115  GCC GCG AAC AUG CUG UCC UCC GUG CUG AAG UCG GAG GCA ACG

 598  Ser Ser Ile Ile Lys Ser Val Gly Glu Thr Ala Val Gly Ala
2157  UCC UCC AUC AUC AAG UCC GUU GGC GAG ACU GCC GUC GGC GCG

 612  Ala Gln Ser Gly Leu Ala Lys Leu Pro Gly Leu Leu Met Ser
2199  GCU CAG UCC GGC CUC GCG AAG CUA CCC GGA CUG CUA AUG AGU

 626  Val Pro Gly Lys Ile Ala Ala Arg Val Arg Ala Arg Arg Ala
2241  GUA CCA GGG AAG AUU GCC GCG CGU GUC CGC GCG CGC CGA GCG
```

Figure A1.2 Continued...

```
 640  Arg Arg Arg Ala Ala Arg Ala Asn
2283  CGC CGC CGC GCC GCU CGU GCC AAU UAGUUUGCUC GCUCCUGUUU

2327  CGCCGUUUCG UAAAACGGCG UGGUCCCGCA CAUUACGCGU ACCCUAAAGA

2377  CUCUGGUGAG UCCCCGUCGU UACACGACGG GUCUGCCGCG GUUCGAUUCC

2427  AUUCCCAAGC GGCAAGAAGG ACGUAGUUAG CUCUGCGUCC CUCGGGAUAC

2477  CA
```

Figure A1.2 Continued...

Appendix 2 Plasmids not generated in this study

TableA2.1 Plasmids used during this study that were acquired from other sources

Plasmid	Section Reference	Obtained from
pBCR1dA	5.2.5	Karl Gordon and Terry Hanzlik (CSIRO Entomology, Canberra, ACT, Australia)
pBJ33R1HC	5.2.4	Karl Gordon and Terry Hanzlik (CSIRO Entomology, Canberra, ACT, Australia)
pBJ33R2HC	5.2.4	Karl Gordon and Terry Hanzlik (CSIRO Entomology, Canberra, ACT, Australia)
pCR®2.1	2.2.4	Invitrogen
pDHVCAPB	2.2.4	Karl Gordon and Terry Hanzlik (CSIRO Entomology, Canberra, ACT, Australia)
pDHVStuR1HC	2.2.2	Karl Gordon and Terry Hanzlik (CSIRO Entomology, Canberra, ACT, Australia)
pDHVStuR2HP	2.2.3	Karl Gordon and Terry Hanzlik (CSIRO Entomology, Canberra, ACT, Australia)
pDHVR2HP	2.2.3	Karl Gordon and Terry Hanzlik (CSIRO Entomology, Canberra, ACT, Australia)
pKG3	2.2.3	Paul Keese, CAMBIA, Canberra, ACT, Australia
pKG4	2.2.2/2.2.3	Paul Keese, CAMBIA, Canberra, ACT, Australia
pKG5	2.2.3	Paul Keese, CAMBIA, Canberra, ACT, Australia
pKG6	2.2.2	Paul Keese, CAMBIA, Canberra, ACT, Australia
pYES2	2.2.4	Invitrogen
YIpLac128	2.2.4	Gietz and Sugino (1988)
YIpLac204	3.2.1	Gietz and Sugino (1988)
YIpLac211	3.2.1	Gietz and Sugino (1988)

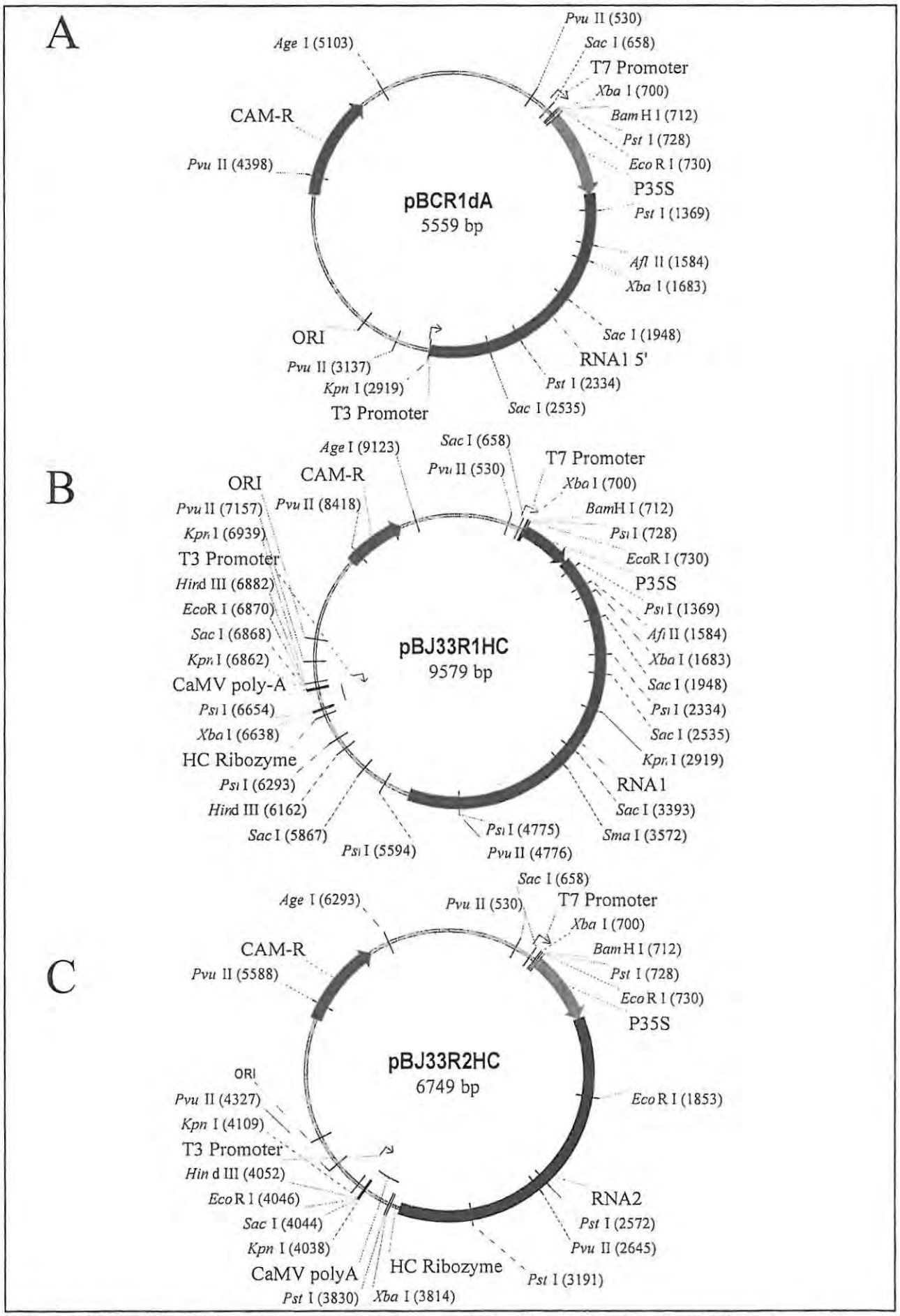

Figure A2.1 Plasmids that were used as templates for *in vitro* transcription from T3 or T7 promoters: pBCR1dA (panel **A**), pBJ33R1HC (panel **B**) and pBJ33R2HC (panel **C**).

Appendix 3 Plasmids constructed during this study

TableA3.1 Plasmids constructed during the course of this study

Plasmid	Section Reference	Constructed by
5.66/5(G+)	3.2.1	Rachel Blaine, Syngenta, Jealott's Hill Research Station, Berkshire, UK
pAV3	2.2.4	Author
pAV8F	2.2.2	Author
pAV10	2.2.2	Author
pAV11	2.2.3	Author
pAV13HC	2.2.2	Author
pAV14HP	2.2.3	Author
pAV14HPTrp	2.2.3/3.2.1	Author
pMJ2	3.2.1	Meesbah Jiwaji, Department of Biochemistry and Microbiology, Rhodes University, Grahamstown, South Africa
pMLY2	2.2.3	Michelle Williams (CSIRO Entomology, Canberra, ACT, Australia)
pMLY3	2.2.3	Michelle Williams (CSIRO Entomology, Canberra, ACT, Australia)
pVH1	2.2.2	Val Hodgson, Department of Biochemistry and Microbiology, Rhodes University, Grahamstown, South Africa
pVH4	2.2.2	Val Hodgson, Department of Biochemistry and Microbiology, Rhodes University, Grahamstown, South Africa
pVH5	2.2.3	Val Hodgson, Department of Biochemistry and Microbiology, Rhodes University, Grahamstown, South Africa
YIpLac204/5.66(G+)	3.2.1	Author
YIpLac204/HaSVRNA2	3.2.1	Author
YIpLacVCAPB320	2.2.4/3.2.1	Rachel Blaine, Syngenta, Jealott's Hill Research Station, Berkshire, UK

Appendix 4 Primers

Table A4.1 Primers used during the course of this study

Primer	Gene	Location	Direct/ Complement	Sequence
AV1	*RNA1**	1 to 25	D	GTTCTGCCTCCCCCGGACGGTAAAT
AV2	*RNA2**	1 to 25	D	GTTTTTCTTTCTTTACCAAGTGTGG
AV4	*PGAL1***	-25 to –1	C	TTTATTACATTTGAATAAGAAG
AV9	*RNA2**	1351 to 1368	C	CGTTTGTGGCGCCAGGTGA
H3R1B	*RNA2**	1985 to 2001	C	GCGCGAATTGGCCGAAA
HB11VF6	*RNA1**	1538 to 1554	D	GCCTGTCCCCTGAACAG
HB35F2C	*RNA1**	3917 to 3933	D	AGTACGTGGAGGCTGTGA
HR236F3	*RNA2**	873 to 889	D	GTAGCGAACGTCGAGAA
HVB11VF2	*RNA1**	1192 to 1212	C	CAAGACGGTCATGTCGACTAG
HVB35XF1	*RNA1**	3016 to 3035	C	AGCATGCGTTTGACGTCCTC
HVR1B5P	*RNA1**	1 to 18	D	GTTCTGCCTCCCCCGGAC
HVR1Cla	*RNA1**	5283 to 5312	C	TGGTATCCCAGGGGGCGCCGT
RNA1F4	*RNA1**	637 to 657	D	CACATGCCAGAAGAGCTGCTC
RNA1R7	*RNA1**	1109 to 1129	C	GGATGGTCTTATGCTCAGTGC
RNA2F3	*RNA2**	52 to 72	D	GGACCGTAACCCGGCCCTTAC
RNA2F6	*RNA2**	502 to 522	D	CTGACAATTTCACCGCTGC
RNA2R2	*RNA2**	530 to 550	C	GCGTCAAGGCTTTGCGCGAGG

* HaSV
** *S. cerevisiae*

Appendix 5 Thermal cycling programmes

Programme 1

1×	94°C for 90 sec
10×	94°C for 45 sec 40°C for 90 sec 68°C for 4 min
1×	68°C for 4 min

Programme 2

1×	94°C for 2 min
30×	94°C for 45 sec 55°C for 45 sec 72°C for 2 min
1×	72°C for 7 min

Programme 3

1×	50°C for 30 min 94°C for 2 min
10×	94°C for 15 sec 50°C for 30 sec 72°C for 1 min
20×	94°C for 15 sec 50°C for 30 sec 72°C for 1 min (+5 sec per cycle)
1×	72°C for 7 min

Programme 4

1×	55°C for 30 min 94°C for 2 min
40×	94°C for 15 sec 55°C for 30 sec 70°C for 2 min
1×	72°C for 10 min

Appendix 6 Yeast strains used in this study

Table A6.1 Yeast strains used in this study

S. cerevisiae strain	Genotype	Yip(s)
INVScI	*MATα, his3-Δ1, leu2, trp1-289, ura3-52*	
JRY188	*MATα, his3, leu2, trp1, ura3*	
INVScI 3#20.1	*MATα, his3-Δ1, P71::LEU2, trp1-289, ura3-52*	YIpLacVCAPB320
JRY188 3#20.1	*MATα, his3, P71::LEU2, trp1, ura3*	YIpLacVCAPB320
INVScI R2	*MATα, his3-Δ1, leu2, R2::TRP1, ura3-52*	YIpLac204HaSVRNA2
INVScI L+	*MATα, his3-Δ1,* ***LEU2****, trp1-289, ura3-52*	**YipLac128**
INVScI R2 L+	*MATα, his3-Δ1,* ***LEU2****, R2::TRP1, ura3-52*	YIpLac204HaSVRNA2 **YipLac128**
INVScI L+ T+	*MATα, his3-Δ1,* ***LEU2, TRP1****, ura3-52*	**YipLac128** **YIpLac204**
INVScI U+ T+ L+	*MATα, his3-Δ1,* ***LEU2, TRP1, URA3***	**YipLac128** **YIpLac204** **YIpLac211**
INVScI CAP T+ L+	*MATα, his3-Δ1,* ***LEU2, TRP1****, p71::URA3*	pMJ2 **YipLac128** **YIpLac204**
INVScI R2 U+ L+	*MATα, his3-Δ1,* ***LEU2****, R2::TRP1,* ***URA3***	YIpLac204HaSVRNA2 **YipLac128** **YIpLac211**
INVScI CAP R2 L+	*MATα, his3-Δ1,* ***LEU2****, R2::TRP1, p71::URA3*	pMJ2 YIpLac204HaSVRNA2 **YipLac128**

Green text denotes plasmids and genotypic markers carrying *P71*
Blue text denotes plasmids and genotypic markers carrying *RNA2*

Appendix 7 Preparation of media

YPD and SMM were prepared as described by Kaiser *et al.* (1994) as follows:

YPD:

Per liter: 10 g yeast extract
20g peptone
20g glucose
(supplemented with 20g agar for agar plates)

SMM:

Per liter: 1.7g yeast nitrogen base without amino acids and ammonium sulfate (Difco)
5g ammonium sulfate
20g glucose
(supplemented with 20g agar for agar plates)

Various supplements were added to the above medium to maintain selection of plasmid-containing strains. All the supplements (uracil, L-tryptophan, L-histidine and L-leucine) that were used in this study could be added to the medium prior to autoclaving. The stock and working concentrations of these supplements were as follows:

Supplement	**Stock concentration (g/ml)**	**Working concentration (mg/*l*)**
Uracil (Sigma)	0.2	20
L-Tryptophan (Sigma)	1	20
L-Histidine (Sigma)	1	20
L-Leucine (Sigma)	1	100

Appendix 8 General Methods

A8.1 Yeast protein extracts

The following method was adapted from Kaiser *et al.*, 1994:

- Add 30 µl ESB to every 2 OD units of yeast cell pellet and resuspend the pellet with a pipette.
- Boil the suspension for 3 min (the samples can be stored at -20°C after this).
- Add 0.1 g of 0.2 mm glass beads (Sigma) to every 30µl of sample.
- Vortex for 30 sec periods with 30 sec intervals and a total homogenization time of 3 min.
- Add 2.3 volumes of ESB and vortex briefly.
- Boil for 2 min and load on an SDS-PAGE gel.

ESB: 2% SDS
80mM Tris pH6.8
10% glycerol
1.5% DTT
0.1mg/ml bromophenol blue

A8.2 Preparation of acid-washed glass beads

Acid-washed glass beads were prepared as described by Treco (1997). The 0.2 mm beads (obtained from Sigma) were soaked in concentrated nitric acid for 1 hour, washed extensively with deionized water and dried in a baking oven.

A8.3 Yeast genomic DNA isolation

The following method, for the isolation of yeast genomic DNA, was taken from Kaiser *et al.*, 1994:

- Grow 10 ml yeast cultures to saturation in YPD a 30°C.
- Collect the cells by centrifugation for 2 min in a microfuge. Remove the supernatant and resuspend the cells in 0.5 ml of distilled water. Transfer the cells to a 1.5 ml Eppendorf tube and collect them by centrifugation for 5 seconds in a micofuge.
- Decant the supernatant and briefly vortex the tube to resuspend the pellet in the residual liquid.
- Add 0.2 ml of 2% Triton X-100, 1% SDS, 100mM NaCl, 10mM Tris-HCl (pH8), 1mM Na_2EDTA. Add 0.2ml of phenol:chloroform:isoamyl alcohol (25:24:1). Add 0.3g of acid-washed glass beads (with a diameter of ~0.2mm).
- Vortex for 3-4 min. Add 0.2 ml of 10mM Tris-HCL (pH8) containing 1mM Na_2EDTA (TE).
- Centrifuge for 5 minutes in a microfuge. Transfer the aqueous layer to a fresh tube. Add 1ml of 100% ethanol. Mix by inversion.

- Centrifuge for 5 min in a microfuge. Discard the supernatant. Resuspend the pellet in 0.4 ml of TE plus 3µl of a 10 mg/ml solution of RNase A (Roche), which was made DNase-free according to the protocol in Sambrook *et al.* (1989). Incubate for 5 min at 37°C. Add 10µl of 4M ammonium acetate plus 1 ml of 100% ethanol. Mix by inversion.
- Centrifuge for 2 min in a microfuge. Discard the supernatant. Air-dry the pellet and resuspend in 50µl of TE.

A8.4 Yeast total RNA extracts

The following method, for the isolation of total RNA from a 200 ml yeast culture, was adapted from Kaiser *et al.*, 1994:

- After induction, add 0.01g cycloheximide to each 200 ml culture and incubate (shaking) for a further 15 min at 30°C.
- Pellet the cells by centrifuging at 5000rpm for 5 min at 4°C in a precooled Beckman JA10 rotor. Decant the supernatants and resuspend the cells in 2.5 ml ice-cold LETS buffer.
- Add 5.5 g of 0.2 mm acid-washed glass beads and 3 ml ice-cold phenol (equilibrated with LETS buffer) to the smallest chamber of a Bead Beater (Biospec Products). Disrupt the cells, alternating 30 sec of disrupting with 30 sec on ice for a total of 5 min.
- Add 5 ml ice-cold LETS and separate the phases by centrifugation at 8000 rpm for 5 min at 4°C in a precooled Beckman JA20 rotor. Transfer the aqueous phase to a clean tube and extracted twice with 5 ml of phenol:chloroform:isoamyl alcohol (25:24:1) and once with chloroform (optional).
- Add $1/10^{th}$ volume of 5M LiCl to the resulting aqueous phase and leave the tubes overnight at -20°C to precipitate the RNA.
- Centrifuge the precipitated RNA at 16000 rpm for 10 min at 4°C in a precooled Beckman JA20 rotor. Resuspend the RNA pellets in 50 – 250 µl DEPC-treated H_2O.

LETS buffer: 0.1M LiCl
0.01M Na_2-EDTA
0.01M Tris-HCl (pH7.4)
0.2% SDS
0.1% DEPC

Appendix 9 Preparation of *Helicoverpa armigera* diet

Prepare the following mixtures:

A. 12g agar
   50g yeast

B. 86g soya flour
   60g wheat germ

C. 3g nipagen
   3g ascorbic acid
   1g sorbic acid

Fix the center of a piece of tubing, which has a diameter of 1 cm and is about 1 meter in length, into a peristaltic pump. Add 600ml hot water to mixture B and decant it into a blender. Add 400ml hot water to mixture A, boil for 5 min in a microwave, add to mixture B and blend until properly mixed. Add mixture C and blend further until it is dissolved in the suspension. Place the one end of the tubing into the diet, switch on the pump and aliquot the diet into the jelly trays using the other end as a nozzle. This procedure should be carried out swiftly, because the diet solidifies at room temperature.

Appendix 10 *Helicoverpa armigera* developmental stages

Table A10.1 Developmental stages of *Helicoverpa armigera* used in scoring of the bioassays (adapted from a table in a draft by Christian, P.D., Dorrian, S.J., Gordon, K.H.J. and Hanzlik, T.N. for submission to *J. Biol. Control.*).

Developmental Stage	Abbrev.	Weight in grams (±SD)	Description
Mid first instar	M1	0.30 (0.06)	Basal colour of upper parts yellow-brown to dark amber. Head capsule slightly narrower than body. Length approximately 1.5-3.5 mm.
Late first instar	L1	0.72 (0.11)	Basal colour of upper parts amber. Head capsule very narrow in relation to the body with distinct pale (almost white) marking behind the dark head capsule created by separation of the head capsule from the integument of the body. Length approximately 3.5 mm.
Early second instar	E2	1.14 (0.37)	Basal colour of upper parts very dark (nearly black). Head capsule nearly the same width as the body. Length approximately 3.5-4.0 mm
Mid second instar	M2	2.11 (0.87)	Basal colour of upper parts ranges from yellow-brown to dark amber. Head capsule slightly narrower than body. Length approximately 4.0-5.5 mm.
Late second instar	L2	4.38 (0.97)	Basal colour of upper parts amber. Head capsule very narrow in relation to the body with same distinct pale (almost white) marking behind the dark head capsule as L1. Length approximately 5.5 mm.
Early third instar	E3	5.20 (1.48)	Basal colour of upper parts very dark (nearly black). Head capsule nearly the same width as the body. Length approximately 5.5-6.5 mm.
Mid third instar	M3	11.61 (3.95)	Basal colour of upper parts ranges from yellow-brown to dark amber. Head capsule slightly narrower than body. Length approximately 6.5-13 mm.
Late third instar	L3	23.51 (4.63)	Basal colour of upper parts amber. Head capsule very narrow in relation to the body with same distinct pale (almost white) marking behind the dark head capsule as L1. Length approximately 13 mm.
Early fourth instar	E4	38.58 (13.71)	Basal colour of upper parts very dark (nearly black). Distinct "saddle" across the first and second abdominal segments formed by two large lateral spots. Length approximately 12-15 mm.
Mid fourth instar	M4	80.19 (27.18)	Basal colour ranges from slightly paler than E4 (black-brown) to dark amber. Gap in "saddle" (see E4) on first and second abdominal segments formed by pale median line. Length 13-18 mm
Late fourth instar	L4	134.86 (25.87)	Basal colour of the upper parts dark pink-brown to pale green-brown. Lateral and dorsal markings darkish brown (not black) with pale dorso-medial line. Gap in "saddle" (see E4) on first and second abdominal segments formed by pale median line. Head capsule very narrow and amber in colour with distinct pale marking behind the head capsule. Length approximately 18-23 mm.
Fifth instar	I5	455.47 (139.88)	Basal colour of the upper parts dark pink-brown to pale green-brown. Dorso-lateral markings ranging from black to dark brown. Length greater than 18 mm.
Pre-pupae	PP	434.06 (58.56)	Very similar discolouration to I5 but with distinct "compressed" appearance, much paler ventral colouration and very narrow head capsule. Length approximately 18-22 mm.

References

Aaziz, R. and Tepfer, M. (1999). Recombination in RNA viruses and in virus-resistant transgenic plants. *J. Gen. Virol.* **80**, 1339-1346.

Agrawal, D.K. and Johnson, J.E. (1992). Sequence and analysis of the capsid protein of *Nudaurelia capensis* omega virus, an insect virus with $T = 4$ icosahedral symmetry. *Virology* **190**, 806-814.

Agrawal, D.K. and Johnson, J.E. (1995). Assembly of the $T = 4$ *Nudaurelia capensis* omega virus capsid protein, post-translational cleavage, and specific encapsidation of its mRNA in a baculovirus expression system. *Virology* **207**, 89-97.

Ball, L.A. (1992). Cellular expression of a functional nodavirus RNA replicon from vaccinia virus vectors. *J. Virol.* **66**, 2335-2345.

Ball, L.A. and Johnson, K.N. (1998). Nodaviruses. In *The insect viruses*. (L.K. Miller and L.A. Ball, eds.), pp. 225-267. Plenum Press, London.

Ball, L.A. and Li, Y. (1993). *cis*-acting requirements for the replication of Flock House Virus RNA 2. *J. Virol.* **67**, 3544-3551.

Bawden, A.L., Gordon, K.H.J. and Hanzlik, T.N. (1999). The specificity of *Helicoverpa armigera* stunt virus infectivity. *J. Invertebr. Pathol.* **74**, 156-163.

Beckmann (1995). Beating the bollworm. *Rural research* **167**, 29-32.

Binder, M., Schanz, M., and Hartig, A. (1991). Vector-mediated overexpression of catalase A in the yeast *Saccharomyces cerevisiae* induces inclusion body formation. *Eur. J. Cell. Biol.* **54**, 305-312.

Boga, J. A. and Alonso, J. M. M. (1997). A single dose immunization with rabbit hemorrhagic disease virus major capsid protein produced in *Saccharomyces cerevisiae* induces protection. *J. Gen. Virol.* **78**, 2315-2318.

Bong, D.T., Janshoff, A., Steihnem, C. and Ghadiri, M.R. (2000). Membrane partitioning of the cleavage peptide in flock house virus. *Biophys. J.* **78**, 839-845.

Bong, D.T., Steinhem, C., Janshoff, A., Johnson, J.E. and Ghadiri, M.R. (1999). A highly membrane-active peptide in flock house virus: implications for the mechanism of nodavirus infection. *Chemistry and Biology* **6**, 473-481.

Boyer, J.-C. and Haenni, A.-L. (1994). Infectious transcripts and cDNA clones of RNA viruses. *Virology* **198**, 415-426.

Brooks, E.M., Hines, E., Bawden, A.L., Hanzlik, T.N. and Gordon, K.H.J. (1998). Midgut pathology induced by small RNA virus infection of lepidopteran larvae: Histological and immunolabeling techniques for light, confocal and electron microscopy. In *Techniques in Insect Immunology*. (A. Wiesner, G.B. Dunphy, V.J. Marmaras, L. Morishma, M. Sugumuran, and M. Yamakawa, eds.), pp. 289-304. SOS Publications, USA.

Canady, M.A., Tihova, M., Hanzlik, T.N and Johnson, J.E. (2000). Large conformational changes in the maturation of a simple RNA virus, *Nudaurelia capensis* ω Virus (NωV). *J. Mol. Biol.* **299**, 573-584.

Caponigro, G. and Parker, R. (1996). Mechanisms and control of mRNA turnover in *Saccharomyces cerevisiae*. *Microbiol. Rev.* **60,** 233-249.

Caspar, D. L. D. and Klug, A. (1962). Physical principles in the construction of regular viruses. *Cold Spring Harbor Symp. Quant. Biol.* **27**, 1-24.

Cheng, R.H., Reddy, V.S., Olson, H., Fisher, A.J., Baker, T.S. and Johnson, J.E. (1994). Functional implications of quasi-equivalence in a $T = 3$ icosahedral animal virus established by cryo-electron microscopy and X-ray crystal. *Structure* **2**, 271-282.

Chowrira, B.M., Pavco, P.A. and McSwiggen, J.A. (1994). *In vitro* and *in vivo* comparison of hammerhead, hairpin, and hepatitis delta virus self-processing ribozyme cassettes. *J. Biol. Chem.* **269**, 25856-25864.

Christian, P.D., Hanzlik, T.N., Dall, D.J. and Gordon, K.H.J. (1993). Insect viruses: new strategies for pest control. In *Molecular approaches to fundamental and applied entomology*. (J.G. Oakeshott and M.J. Whitten, eds.), pp. 128-163. Springer-Verlag, New York.

Cigan, A. M. and Donahue, T. F. (1987). Sequence and structural features associated with translational initiator regions in yeast - a review. *Gene* **59**, 1-18.

Clark, L. and Carbon, J. (1980). Isolation of a yeast centromere and construction of functional small circular chromosomes. *Nature* **257**, 504-509.

Cregg, J.M., Tschopp, J.F., Stillman, C., Siegel, R., Akong, M., Craig, W.S., Buckholz, R.G., Madden, K.R., Kellaris, P.A., Davies, G.R., Smiley, B.L., Cruze, J., Torregrossa, R., Velicelebi, G. and Thill, G.P. (1987). High-level expression and efficient assembly of hepatitis B surface antigen in the methylotrophic yeast *Pichia pastoris*. *Bio/Technology* **5**, 479-485.

Davies, R.G. (1988). Outlines of Entomology. pp.61-67. Chapman and Hall, London and New York.

Dawson, R.M.C., Elliott, D.C., Elliott, W.H. and Jones, K.M. (1987). Data for biochemical research. Oxford Science Publications, Great Britain.

Doherty, E. A. and Doudna, J.A. (2000). Ribozyme structures and mechanisms. *Annu. Rev. Biochem.* **69**, 597-615.

Duncan, R. (1998). HaSV report: January - September 1998. Report from ZENECA Agrochemicals, Jealott's Hill Research Station, Berkshire, UK.

Dunn, B. and Wobbe, C.R. (1997). Preparation of protein extracts from yeast. In *Current Protocols in Molecular Biology*. (F.M. Ausubel, R. Brent, R.E. Kingston, D.D. Moore, J.G. Seidman, J.A. Smith and K. Struhl., eds), vol. 2., unit 13.13. John Wiley and Sons, New York.

Dzianott, A. M. and Bujarski, J. J. (1989). Derivation of an infectious viral RNA by autocatalytic cleavage of *in vitro* transcribed viral cDNAs. *Proc. Natl. Acad. Sci. U.S.A.* **86**, 4823-4827.

Eckart, M.R. and Bussineau, C.M. (1996). Quality and authenticity of heterologous proteins synthesized in yeast. *Curr. Opin. Biotech.* **7**, 525-530.

Egli, C. M. and Braus, G. H. (1994). Uncoupling of mRNA 3' cleavage and polyadenylation by expression of a hammerhead ribozyme in yeast. *J. Biol. Chem.* **269**, 27378-27383.

Etcheverry, T. (1990). Induced expression using yeast copper metallothionein promoter. *Meth. Enzymol.* **185**, 319-329.

Finch, J.T., Crowther, R.A., Hendry, D.A. and Struthers, J.K. (1974). The structure of *Nudaurelia capensis* β virus: the first example of a capsid with icosahedral surface symmetry $T = 4$. *J. Gen. Virol.* **24**, 191-200.

Finley, D. (1992). The yeast ubiquitin system. In *The molecular and cellular biology of the yeast Saccharomyces.* (E.W. Jones, J.R. Pringle, and J.R. Broach, eds.), pp. 539-582. Cold Spring Harbor Laboratory Press, New York.

Fischer, B., Sumner, I. and Goodenough, P. (1993). Isolation, renaturation, and formation of disulfide bonds of eukaryotic proteins expressed in *Escherichia coli* as inclusion bodies. *Biotech. Bioeng.* **41**, 3-13.

Fisher, A. J. and Johnson, J. E. (1993). Ordered duplex RNA controls capsid architecture in an icosahedral animal virus. *Nature* **361**, 176-179.

Fraenkel-Conrat, H., Kimball, P.C. and Levy, J.A. (1988). Virology. Prentice-Hall, Inc., New Jersey.

Francki, R.I.B., Fauquet, C.M., Knudson, D.L. and Brown, F. (1991). Classification and Nomenclature of Viruses: Fifth Report of the International Committee on Taxonomy of Viruses. Springer-Verlag, Vienna.

Fricks, C.E. and Hogle, J.M. (1990). Cell-induced conformational change in poliovirus: externalization of the amino-terminus of VP1 is responsible for liposome binding. *J. Virol.* **64**, 1934-1945.

Frölich, K.,-U and Madeo, F. (2000). Apoptosis in yeast – a monocellular organism exhibits altruistic behaviour. *FEBS Lett.* **473**, 6-9.

Fuller, S.D. (1987). The $T = 4$ envelope of Sinbis virus is organized by interactions with a complimentary $T = 3$ capsid. *Cell* **48**, 923-934.

Gallagher, T.M. and Rueckert, R.R. (1988). Assemby-dependent maturation cleavage in provirions of a small icosahedral insect ribovirus. Journal of Virology **62**, 3399-3406.

Gancedo, J. M. (1998). Yeast carbon catabolite repression. *Microbiol. Mol. Biol. Rev.* **62**, 334-361.

Gietz, R.D. and Sugino, A. (1988). New yeast - *Escherichia coli* shuttle vector with *in vitro* mutagenized yeast genes lacking six-base pair restriction sites. *Gene* **74**, 527-534.

Gordon, K.H.J. and Hanzlik, T.N. (1998). Tetraviruses. In *The insect viruses*. (L.K. Miller and L.A. Ball, eds.), pp. 269-299. Plenum Press, London.

Gordon, K.H.J., Johnson, K.N. and Hanzlik, T.N. (1995). The larger genomic RNA of *Helicoverpa armigera* stunt tetravirus encodes the viral RNA polymerase and has a novel 3'-terminal tRNA-like structure. *Virology* **208**, 84-98.

Gordon, K.H.J., Williams, M.R., Baker, J.S., Gibson, J.M., Bawden, A.L., Millgate, A., Larkin, P.J. and Hanzlik, T.N. (2001). Replication-independent assembly of an insect virus (Tetraviridae) in plant cells. *Virology* **288**, 36-50.

Gordon, K. H. J., Williams, M. R., Hendry, D. A., and Hanzlik, T. N. (1999). Sequence of the genomic RNA of *Nudaurelia* β virus (*Tetraviridae*) defines a novel genome organization. *Virology* **258**, 42-53.

Hampel, A., Tritz, R., Hicks, M., and Cruz, P. (1990). 'Hairpin' catalytic RNA model: evidence for helices and sequence requirement for substrate RNA. *Nucleic. Acids. Res.* **18**, 299-304.

Hanahan, D. (1983). Studies on transformation of *Escherichia coli* with plasmids. *J. Mol. Biol.* **166**, 557.

Hanzlik, T.N., Dorrian, S.J., Gordon, K.H.J. and Christian, P.D. (1993). A novel small RNA virus isolated from the cotton bollworm, *Helicoverpa armigera*. *J. Gen.Virol.* **74**, 1805-1810.

Hanzlik, T.N., Dorrian, S.J., Johnson, K.N., Brooks, E.M. and Gordon, K.H.J. (1995). Sequence of RNA2 of the *Helicoverpa armigera* stunt virus (*Tetraviridae*) and bacterial expression of its genes. *J. Gen. Virol.* **76**, 799-811.

Hanzlik, T.N. and Gordon, K.H.J. (1997). The *Tetraviridae*. *Adv. Virus Res.* **48**, 101-168.

Hendry, D.A. and Agrawal, D.K. (1994). Tetraviruses. In *Encyclopedia of Virology*. (A. Granoff and R.G. Webster, eds), pp. 1416-1422. Academic Press, San Diego, CA.

Hendry, D.A., Hodgson, V., Clark, R. and Newman, J. (1985). Small RNA viruses co-infecting the pine emperor moth (*Nudaurelia cytherea capensis*). *J. Gen. Virol.* **66**, 627-632.

Hill, J., Donald, K.A.I.G. and Griffiths, J.E. (1991). DMSO-enhanced whole-cell yeast transformation. *Nucleic Acids Res.* **19**, 5791

Hiscox, J.A. and Ball, L.A. (1997). Cotranslational disassembly of flock house virus in a cell-free system. *J. Virol.* **71**, 7974-7977.

Hofmann, K.J., Cook, J.C., Joyce, J.G., Brown, D.R., Schultz, L.D., George, H.A., Rosolowsky, M., Fife, K.H. and Jansen, K.U. (1995). Sequence determination of Human Papillomavirus Type 6a and assembly of virus-like particles in *Saccharomyces cerevisiae*. *Virology* **209**, 506-518.

Hofman, O., Mould, R. and Brittain, T. (1995). Allosteric modulation of oxygen binding to the three human embryonic haemoglobins. *Biochem. J.* **306**, 367-370.

Horowitz, B., Eakle, K.A., Scheiner-Bobis, G., Randolph, G.R., Chen, C.Y., Hitzeman, R. and Farley, R.A. (1990). Synthesis and assembly of functional mammalian Na^+,K^+-ATPase in yeast. *J. Biol. Chem.* **265**, 4189-4192.

Hosur, M. V., Schmidt, T., Tucker, R. C., and Johnson, J. E. (1987). Structure of an insect virus at 3Å resolution. *Proteins* **2**, 167-176.

http://genome-www.stanford.edu/Saccharomyces

Huang, Y. and Carmichael, G.G. (1996). Role of polyadenylation in nucleocytoplasmic transport in mRNA. *Mol. Cell. Biol.* **16**, 1534-1542.

Ishikawa, M., Janda, M., Krol, M.A. and Ahlquist, P. (1997). *In vivo* DNA expression of functional brome mosaic virus RNA replicons in *Saccharomyces cerevisiae*. *J. Virol.* **71**, 7781-7790.

Jackson, R. J. and Standart, N. (1990). Do the poly(A) tail and 3' untranslated region control mRNA translation? *Cell* **62**, 15-24.

Janda, M. and Ahlquist, P. (1993). RNA-dependent replication, transcription, and persistence of brome mosaic virus RNA replicons in *S. cerevisiae*. *Cell* **72**, 961-970

James, H.A. and Turner, P.C. (1995). Ribozymes. *Essays Biochem.* **29,** 175-192.

Jazwinski, S.M. (1990). Preparation of extracts from yeast. *Meth. Enzymol.* **182**, 154-174.

Jiwaji, M. (1999). Optimization of *Helicoverpa armigera* stunt virus (HaSV) particle expression in the yeast *Saccharomyces cerevisiae*. Honours thesis. Rhodes University, South Africa.

Johnson, J.E. (1996). Functional implications of protein-protein interactions in icosahedral viruses. *Proc. Natl. Acad. Sci. U.S.A.* **93**, 27-33.

Johnson, J.E., Munshi, S., Liljas, L., Agrawal, D., Olson, N.H., Reddy, V., Fisher, A., McKinney, B., Schmidt, T. and Baker, T.S. (1994). Comparative studies of $T = 3$ and $T = 4$ icosahedral RNA insect viruses. *Arch. Virol. Suppl.* **9**, 497-512.

Johnson, J.E. and V. Reddy. (1998). Structural studies of nodaviruses and tetraviruses. In *The insect viruses*. (L.K. Miller and L.A. Ball, eds.), pp. 171-224. Plenum Press, London.

Johnston, M. (1987). A model fungal gene regulatory mechanism: the *GAL* genes of *Saccharomyces cerevisiae*. *Microbiol. Rev.* **51**, 458-476.

Johnston, M. and Davis, R. W. (1984). Sequences that regulate the divergent *GAL1-GAL10* promoter in *Saccharomyces cerevisiae*. *Mol. Cell. Biol.* **4**, 1440-1448.

Jones, E.W. (1991). Three proteolytic systems in the yeast *Saccharomyces cerevisiae*. *J. Biol. Chem.* **266**, 7963

Jore, J. P. M, Veldhuisen, G., Kottenhagen, M., Pouwels, P. H., Foriers, A. and Rombaut, B. (1994) Formation of poliomyelitis subviral particles in the yeast *Saccharomyces cerevisiae*. *Yeast* **10**, 907-922.

Juckes, I.R.M (1970). Viruses of the pine emperor moth. *Bull. S. Afr. Soc. Plant. Pathol. Microbiol.* **4**, 18.

Juckes, I.R.M (1979). Comparison of some biophysical properties of the Nudaurelia β and ε viruses. *J. Gen. Virol.* **42**, 89-94.

Kaiser, C., Michaelis, S. and Mitchell, A. (1994). Methods in yeast genetics. Cold Spring Harbor Laboratory Press, New York.

Kikuchi, Y. (1983). Yeast plasmid requires a *cis*-acting locus and two plasmid proteins for its stable maintenance. *Cell* **35**, 487-493.

Kozak, M. (1989). The scanning model for translation: an update. *J. Cell. Biol.* **108**, 229-241.

Laemmli, U.K. (1970). Cleavage of structural proteins during the assembly of the head of a bacteriophage T4. *Nature* **227**, 680-685.

Li, T.-C., Yamakawa, Y., Suzuki, K., Tatsumi, M., Razak, A., Uchida, T., Takeda, N. and Miyamura, T. (1997). Expression and self-assembly of empty virus-like particles of hepatitis E virus. *J. Virol.* **71**, 7207-7213.

Longo, V.D., Ellerby, L.M., Bredesen, D.E., Valentine, J.S. and Gralla, E.B. (1997). Human Bcl-2 reverses survival defects in yeast lacking superoxide dismutase and delays death of wild-type yeast. *J. Cell. Biol.* **137**, 1581-1588.

Lundblad, V. (1997). Yeast cloning vectors and genes. In *Current Protocols in Molecular Biology*. (F.M. Ausubel, R. Brent, R.E. Kingston, D.D. Moore, J.G. Seidman, J.A. Smith and K. Struhl., eds), vol. 2., unit 13.4. John Wiley and Sons, New York.

Macilwain, C. (1996). Bollworms chew hole in gene-engineered cotton. *Nature* **382**, 289

Madeo, F., Frölich, E. and Frölich, K.-U. (1997). A yeast mutant showing diagnostic markers of early and late apoptosis. *J. Cell Biol.* **139**, 729-734.

Madeo, F., Frölich, E., Ligr, M., Grey, M., Sigrist, S.J., Wolf, D.H. and Frölich, K.-U. (1999). Oxygen stress: a regulator of apoptosis in yeast. *J. Cell Biol.* **145**, 757-767.

Matthews, R.E.F. (1982). Classification and nomenclature of viruses. Fourth report of the international committee on taxonomy of viruses. *Intervirology* **17**, 1 – 160.

Meilhoc, E., Masson, J.-M. and Tessie, J. (1990). High efficiency transformation of intact yeast cells by electroporation. *Bio/Technology* **8**, 223-227.

Miller, L.K. (1988). Baculoviruses as gene expression vectors. *Annu. Rev. Microbiol.* **42**, 177-199

Miller, L.K. (1998). Ascoviruses. In *The insect viruses*. (L.K. Miller and L.A. Ball, eds.), pp. 91-103. Plenum Press, London.

Mintz, G.R. (1993). Technical note: an irreversible serine protease inhibitor. *Biopharm.* **6**, 34.

Miyanohara, A., Toh-e, A., Nozaki, C., Hamada, F., Ohtomo, N., and Matsubara, K. (1983). Expression of hepatitis B surface antigen gene in yeast. *Proc. Natl. Acad. Sci. U.S.A.* **80**, 1-5.

Munshi, S., Liljas, L., Cavarelli, J., Bomu, W., McKinney, B., Reddy, V. and Johnson, J.E. (1996). The 2.8Å Structure of a $T = 4$ animal virus and its implications for membrane translocation of RNA. *J. Mol. Biol.* **261**, 1-10.

Murphy, F.A., Fauquet, C.M., Bishop, D.H.L., Ghabrial, S.A., Jarvis, A.W., Martelli, G.P., Mayo, M.A. and Summers, M.D. (1995). Virus Taxonomy: Sixth Report of the International Committee on Taxonomy of Viruses. Springer-Verlag, Vienna

Nilsson, B. and Anderson, S. (1991). Proper and improper folding of proteins in the cellular environment. *Annu. Rev. Microbiol.* **45**, 607-635.

Olson, N.H., Baker, T.S., Johnson, J.E. and Hendry, D.A. (1990). The three-dimensional structure of frozen-hydrated *Nudaurelia capensis* β virus, a $T = 4$ virus. *J. Struct. Biol.* **105**, 111-122.

Olson, N.H., Kolatkar, P.H., Oliveira, M.A., Cheng, R.H., Greve, J.M., McClelland, A., Baker, T.S. and Rossmann, M.G. (1993). Structure of a human rhinovirus complexed with its receptor molecule. *Proc. Natl. Acad. Sci. U.S.A.* **90**, 507-511.

O'Reilly, D.R., Miller, L.K. and Luckow, V.A. (1992). Baculovirus expression systems. W.H. Freeman & Co., New York.

Philippe, R., Veyrunes, J.-C., Mariau, D., and Bergoin, M. (1997). Biological control using entemopathogenic viruses. Application to oil palm and coconut pests. *Plantations, Recherche, Développement* **1**, 39-45.

Polson, A., Stannard, L., and Tripconey, D. (1970). The use of haemocyanin to determine the molecular weight of *Nudaurelia cytherea capensis* β virus by direct particle counting. *Virology* **41**, 680-687.

Price, B. D, Rueckert, R. R., and Ahlquist, P. (1996). Complete replication of an animal virus and maintenance of expression vectors derived from it in *Saccharomyces cerevisiae*. *Proc. Natl. Acad. Sci. U.S.A.* **93**, 9465-9470.

Price, B. D, Roeder, M., and Ahlquist, P. (2000). DNA-directed expression of functional flock house virus RNA1 derivatives in *Saccharomyces cerevisiae*, heterologous gene expression, and selective effects on subgenomic mRNA synthesis. *J. Virol.* **74**, 11724-11733.

Price, B. D, Rueckert, R. R., Krol, M. A., and Ahlquist, P. (1999). Method of producing particles containing nucleic acid sequences in yeast. United States Patent 5869287

Price, V.L., Taylor, W.E., Clevenger, W., Worthington, M. and Young, E.T. (1990). Expression of heterologous proteins in *Saccharomyces cerevisiae* using the *ADH2* promoter. *Meth. Enzymol.* **185**, 308-318.

Pringle, F.M., Gordon, K.H.J., Hanzlik, T.N., Kalmakoff, J., Scottii, P.D. and Ward, V. (1999). A novel capsid expression strategy for *Thosea asigna* virus (*Tetraviridae*). *J. Gen. Virol.* **80**, 1855-1863.

Pringle, F.M., Kalmakoff and Ward, V. (2001). Analysis of the capsid processing strategy of *Thosea asigna* virus using baculovirus expression of virus-like particles. *J. Gen. Virol.* **82**, 259-266.

Roenhorst, J.W., Verduin, B.J.M. and Goldbach, R. (1989). Virus-ribosome complexes from cell-free translation systems supplemented with cowpea chlorotic mottle virus particles. *Virology* **168**, 138-146.

Romanos, M.A., Clare, J.J., Beesley, K.M., Rayment, F.B., Ballantine, S.P., Makoff, A.J., Dougan, G., Fairweather, N.F. & Charles, I.G. (1991). Recombinant *Bordetella pertussis* pertactin (P69) from the yeast *Pichia pastoris*: high-level production and immunological properties. *Vaccine* **9**, 901-906.

Romanos, M.A., Scorer, C.A. and Clare, J.J. (1992). Foreign gene expression in yeast: a review. *Yeast* **8**, 423-488.

Rombaut, B. and Jore, J.P.M. (1997). Immunogenic, non-infectious polio subviral particles synthesized in *Saccharomyces cerevisiae*. *J. Gen. Virol.* **78**,1829-1832.

Rose, A.B. and Broach, J.R. (1990). Propagation and expression of cloned genes in yeast: 2μm circle-based vectors. *Meth. Enzymol.* **185**, 234-279.

Rosenberg, S., Coit, D. and Tekamp-olson, P. (1990). Glyceraldehyde-3-phosphate-dehydrogenase-derived expression cassettes for constitutive synthesis of heterologous proteins. *Meth. Enzymol.* **185**, 341-351.

Rossmann, M. G. and Johnson, J. E. (1989). Icosahedral RNA virus structure. *Annu. Rev. Biochem.* **58**, 533-573.

Rueckert, R.R. (1996). *Picornaviridae*: the viruses and their replication. In *Virology* (B.N. Fields, D.M. Knipe, and P.M. Howley, eds.), Vol. 1, p. 609-654. Lippincott-Raven, Philadelphia.

Sambrook, J., Fritsch, E.F. and Maniatis, T. (1989). Molecular cloning, a laboratory manual. 2nd ed. Cold Spring Harbor Press, New York.

Schneemann, A., Dasgupta, R., Johnson, J.E. and Rueckert, R.R. (1993). Use of recombinant baculovirus in synthesis of morphological distinct virus-like particles of Flock House Virus, a Nodavirus. *J. Virol.* **67**, 2756-2763.

Schneemann, A., Gallagher, TM and Rueckert, R.R. (1994). Reconstitution of flock house provirions: a model system for studying structure and assembly. *J. Virol.* **68**, 4547-4556.

Schneemann, A. and Marshall, D. (1998). Specific encapsidation of nodavirus RNAs is mediated through the C terminus of capsid precursor protein alpha. *J. Virol.* **72**, 8738-8746.

Schneemann, A., Reddy, V., and Johnson, J. E. (1998). The structure and function of nodavirus particles: a paradigm for understanding chemical biology. *Adv. Virus Res.* **50**, 381-446.

Service, R. (1996). Arming plants with a virus. *Science* **271**, 145.

Shrode, L.D., Tapper, H. and Grinstein, S. (1997). Role of intracellular pH in proliferation, transformation, and apoptosis. *J. Bioenerg. Biomembr.* **29**, 393-399.

Sikorski, R.S. and Hieter, P. (1989). A system of shuttle vectors and yeast host strains designed for efficient manipulation of DNA in *Saccharomyces cerevisiae*. *Genetics* **122**, 19-27.

Smith, J.A. (1988). Quantitation of proteins. In *Current Protocols in Molecular Biology.* (F.M. Ausubel, R. Brent, R.E. Kingston, D.D. Moore, J.G. Seidman, J.A. Smith and K. Struhl, eds), vol. 2., unit 10.1. John Wiley and Sons, New York.

Smith, K.M. (1973). Insect viruses. In *Viruses and Invertebrates.* (Gibbs, A.J., ed), pp. 14-25. American Elsevier Publishing Company, Inc., New York.

Speed, M.A., Wang, D.I.C. and King, J. (1996). Specific aggregation of partially folded polypeptide chains: the molecular basis of inclusion body composition. *Nature Biotech.* **14**, 1283-1287.

Stearns, T., Ma, H. and Botstein, D. (1990). Manipulating yeast genome using plasmid vectors. *Meth. Enzymol.* **185**, 280-297.

Struthers, J. K. and Hendry, D. A. (1974). Studies of the protein and nucleic acid components of Nudaurelia capensis β virus. *J. Gen. Virol.* **22**, 355-362.

Teakle, R.E. and Jensen, J.M. (1985). *Heliothis punctigera*. In *Handbook of Insect Rearing.* (R. Singh and R.F. Moore, eds.), p. 312-322. Elsevier, Amsterdam.

Tiong, R. H. C. and Munroe, D. D. (1977). Microbial control of an outbreak of *Darna trima* (Moore) on an oil palm (*Elaeis gioneensis* Jacq) in Sarawak (Malasian Borneo). *Int. Dev. Oil Palm, Proc. Malays. Int. Agric. Oil Palm Conf.* 624-640.

Tomasicchio, M. (2001). Optimization of *Helicoverpa armigera* stunt virus virus-like particle production in *Saccharomyces cerevisiae*. Honours thesis in submission. Rhodes University, South Africa.

Towbin, H., Staehelin, T. and Gordon, J. (1979). Electrophoretic transfer of proteins from polyacrylamide gels to nitrocellulose sheets: procedure and some applications. *Proc. Natl. Acad. Sci. U.S.A.* **76**, 4350-4354.

Treco, D.A. (1997). Preparation of yeast RNA. In *Current Protocols in Molecular Biology.* (F.M. Ausubel, R. Brent, R.E. Kingston, D.D. Moore, J.G. Seidman, J.A. Smith and K. Struhl., eds), vol. 2., unit 13.12. John Wiley and Sons, New York.

Tsuchihashi, Z, Khosla, M., and Herschlag, D. (1993). Protein enhancement of hammerhead ribozyme catalysis. *Science* **262**, 99-102.

Valenzuela, P., A. Medina, and W.J. Rutter. (1982). Synthesis and assembly of hepatitis B surface antigen particles in yeast. *Nature* **298**, 347-350.

van den Heuvel, J. J., Planta, R. J., and Raue, H. A. (1990). Effect of leader primary structure on the translation efficiency of phosphoglycerate kinase mRNA in yeast. *Yeast* **6**, 473-482.

van Regenmortel, M.H.V., Fauquet, C.M., Bishop, D.H.L., Carstens, E.B., Estes, E.K., Lemon, S.M., Maniloff, J., Mayo, M.A., McGeoch, D.J., Pringle, C.R. and Wickner, R.B. (2000). Virus Taxonomy: Seventh Report of the International Committee on Taxonomy of Viruses. Academic Press, London.

Velmurugan, S., Ahn, Y.-T., Yang, X.-M., Wu, X.-L. and Jayaram, M. (1998). The 2μm plasmid stability system: analyses of the interactions among plasmid- and host-encoded components. *Mol. Cell. Biol.* **18**, 7466-7477.

Venter, P.A. (1998). Project report: Expression of HaSV in yeast, September 1998. Rhodes University Report to Syngenta, Jealott's Hill Research Station, Berkshire, UK.

Webb, B.A. (1998). Polydnaviruses. In *The insect viruses*. (L.K. Miller and L.A. Ball, eds.), pp. 105-139. Plenum Press, London.

Weik, R., Franck, A., Striedner, G., Raspor, P., Bayer, K. and Mattanovich, D. (1998). Recombinant expression of alliin lyase from garlic (*Allium sativum)* in bacteria and yeasts. *Planta Medica* **64**, 387-388.

Wickner, R.B. (1996). Double stranded RNA viruses of *Saccharomyces cerevisiae*. *Microbiol. Rev.* **60**, 250-265.

Wu, X.-L., Chen, P.-J., Mu, J.-J., Chi, W.-K., Kao, T.-L., Hwang, L.-H. and Chen, D.-S. (1997). Assembly of hepatitis delta virus-like empty particles in yeast. *Virology* **236**, 374-381.

Yafel, A.G., Kaplan, G., Racaniello, V.R. and Hoggle, J.M. (1993). Characterization of poliovirus alteration mediated by soluble cell receptors. *Virology* **236**, 501-505.

Yanisch-Perron, C., Viera, J. and Messing, J. (1985). Improved M13 phage cloning vectors and host strains: nucleotide sequences of the M13mp18 and pUC19 vectors. *Gene* **33**, 103.

Zlotnick, A., Reddy, V.S., Dasgupta, R., Schneemann, A., Ray, W.J., Rueckert R.R., and Johnson, J.E. (1994). Capsid assembly in a family of animal viruses primes an autoproteolytic maturation that depends on a single aspartic acid residue. *J. Biol. Chem.* **269**, 13680-13684.